NAVAL AIR ENGINEERING CENTER
LAKEHURST, N.J.
08733

REPORT NAEC-92-163

WEAR PARTICLE ATLAS
(REVISED)

Advanced Technology Office
Support Equipment Engineering Department
Naval Air Engineering Center
Lakehurst, New Jersey 08733

28 JUNE 1982

Final Technical Report
AIRTASK A03V3400/051B/2F41460000

APPROVED FOR PUBLIC RELEASE:
DISTRIBUTION UNLIMITED

Prepared for

Commander, Naval Air Systems Command
AIR-340E
Washington, DC 20361

NAEC-92-163

WEAR PARTICLE ATLAS
(REVISED)

Prepared by: Daniel P. Anderson
Daniel P. Anderson
Foxboro Analytical

Reviewed by: P. M. O'Donnell
P. M. O'Donnell
Advanced Technology Office (92A3)

Approved by: F. E. Evans
F. E. Evans
Support Equipment Engineering Superintendent

UNCLASSIFIED

SECURITY CLASSIFICATION OF THIS PAGE (When Data Entered)

REPORT DOCUMENTATION PAGE		READ INSTRUCTIONS BEFORE COMPLETING FORM
1 REPORT NUMBER NAEC-92-163	2. GOVT ACCESSION NO. AD A123 512	3. RECIPIENT'S CATALOG NUMBER
4 TITLE (and Subtitle) WEAR PARTICLE ATLAS (Revised)		5. TYPE OF REPORT & PERIOD COVERED Final Technical 6. PERFORMING ORG. REPORT NUMBER NAEC-92-163
7. AUTHOR(s) Daniel P. Anderson		8. CONTRACT OR GRANT NUMBER(s) N68335-80-C-0529
9. PERFORMING ORGANIZATION NAME AND ADDRESS Foxboro Analytical 78 Blanchard Road, P.O. Box 435 Burlington, MA 01803		10. PROGRAM ELEMENT, PROJECT, TASK AREA & WORK UNIT NUMBERS A03V3400/051B/2F41-460-000
11. CONTROLLING OFFICE NAME AND ADDRESS Naval Air Systems Command Code AIR-340E Washington, DC 20361		12. REPORT DATE 28 June 1982 13 NUMBER OF PAGES 194
14 MONITORING AGENCY NAME & ADDRESS(if different from Controlling Office) Naval Air Engineering Center Support Equipment Engineering Department Code 92A3 Lakehurst, NJ 08733		15. SECURITY CLASS. (of this report) Unclassified 15a. DECLASSIFICATION/DOWNGRADING SCHEDULE
16. DISTRIBUTION STATEMENT (of this Report) Approved for public release; distribution unlimited.		
17. DISTRIBUTION STATEMENT (of the abstract entered in Block 20, if different from Report)		
18. SUPPLEMENTARY NOTES (see reverse side)		
19. KEY WORDS (Continue on reverse side if necessary and identify by block number) (see reverse side)		
20 ABSTRACT (Continue on reverse side if necessary and identify by block number) (see reverse side)		

DD FORM 1 JAN 73 1473 EDITION OF 1 NOV 65 IS OBSOLETE
S/N 0102-LF-014-6601

UNCLASSIFIED

SECURITY CLASSIFICATION OF THIS PAGE (When Data Entered)

#18. Supplementary Notes

This report is a compendium of four contract efforts. Wear Particle Atlas I, Contract N00156-74-C-1682, covered the basics of ferrous wear debris analysis. Atlas II, Contract N68335-77-C-0585, covered other typical materials encountered in wear debris analysis. Atlas III, Contract N68335-79-C-1169, presented case history studies for illustrative purposes. All this material was technically updated and consolidated (via N68335-80-C-0529) resulting in this document, the Wear Particle Atlas (Revised).

#19. Key Words

bearing wear
condition monitoring
diesel engine wear
failure analysis
ferrography
gas turbine engine wear
wear
gear wear
grease-lubricated wear
hydraulic wear
machine diagnostics
oil analysis
oil-lubricated wear
wear atlas
oil sample
optical analysis
particle analysis
particle atlas
particle morphology
tribology
wear debris analysis
wear particle atlas

#20. Abstract

The Wear Particle Atlas (Revised) is a guide to wear particle identification containing photographs of typical wear particles found in used lubricating oil, illustrative case histories, and operational procedures for wear debris analysis.

Wear particle analysis supports identification of wear modes within a machine based on the quantity, morphology, and composition of particles present in a representative lubricant sample. Photomicrographs in this document facilitate technology transfer to the neophyte and act as a guide to the experienced analyst. Section 1.0 on Wear Particle Identification describes particle morphologies, distinguishes between ferrous and nonferrous materials, and illustrates typical particulate contamination.

Section 2.0, Case Histories, shows the potential utility of wear debris analysis and the progression of thought that goes into an analysis.

Section 3.0, Operational Procedures, details the methodologies used in wear debris analysis.

PREFACE

This work is based on experience gained over a period of about 10 years since the development of ferrography in 1971. The revised Wear Particle Atlas incorporates information published in 1976 in the Wear Particle Atlas, Volume 1, authored by E. Roderic Bowen and Vernon C. Westcott under the sponsorship of the Naval Air Engineering Center, Lakehurst, New Jersey, USA. The first Atlas was made possible by intensive research at several laboratories in this country as well as in the United Kingdom. Contracts from the Naval Air Engineering Center aimed to produce knowledge about the types of particles generated by various wear situations on actual machine mechanisms. This latter work included contracts at SKF Research Laboratories, Valley Forge, Pennsylvania; the Franklin Institute in Philadelphia, Pennsylvania; and the Naval Air Propulsion Center, Trenton, New Jersey. The work at the National Engineering Laboratory, East Kilbride, Scotland, Mr. Douglas Scott; the Admiralty Materials Laboratory, Holton Health, Poole, Dorset, England, Dr. Gerald Heath and Dr. Geoffrey Pocock; and the University College of Swansea, Wales, Professor Frederick Barwell; is recognized.

The analytical studies concerning X-ray analysis of particles on ferrograms performed at the National Bureau of Standards by Dr. William Ruff are gratefully acknowledged.

Contributions from the following, who have released material for use in this Atlas, are gratefully acknowledged:

R. C. Moore	Colorado Interstate Gas Company
Michael D. Perkins	Corpus Christi Army Depot
Nannaji Saka	Massachusetts Institute of Technology
Glenn R. Taylor	The Dow Chemical Company, Texas Division
— —	Solvay and Cie, S.A., Belgium
A. R. Jones	Eastern Airlines

Technical advice and support from the following Foxboro employees are acknowledged:

E. Roderic Bowen	Roger H. Rotondi
Raymond J. Dalley	Irma E. Ruggles
Richard D. Driver	Anthony P. Russell
Shirley M. Hodder	Vernon C. Westcott

The support and guidance of Mr. Peter M. O'Donnell of the Naval Air Engineering Center Advanced Technology Office (Code 92A3), technical liaison, is gratefully acknowledged. Special recognition is given to Mrs. P. Hamilton (Editor), also of NAVAIRENGCEN (Code 92A1C), whose talents contributed to this report.

This page left blank
intentionally.

TABLE OF CONTENTS

Section	Subject	Page
	PREFACE	1
	LIST OF FIGURES	5
	LIST OF TABLES	6
	INTRODUCTION	7
1.	PARTICLE IDENTIFICATION	8
	1.1 Rubbing Wear and Break-In Wear	10
	1.2 Cutting Wear	11
	1.3 Rolling Fatigue (Rolling Element Bearings)	17
	1.4 Combined Rolling and Sliding (Gear Systems)	21
	1.5 Severe Sliding Wear	22
	1.6 Nonferrous Metals	27
	1.6.1 White Nonferrous Metals	27
	1.6.2 Copper Alloys	28
	1.6.3 Lead/Tin Alloys	32
	1.7 Ferrous Oxides	33
	1.7.1 Red Oxides of Iron	33
	1.7.2 Black Oxides of Iron	34
	1.7.3 Dark Metallic-Oxides	37
	1.8 Lubricant Degradation Products and Friction Polymers	37
	1.8.1 Corrosive Wear Debris	37
	1.8.2 Friction Polymers	38
	1.8.3 Molybdenum Disulfide	41
	1.9 Contaminant Particles	42
	1.9.1 Contaminants in Unused Oil	42
	1.9.2 Contaminants in Unused Grease	42
	1.9.3 Road Dust	43
	1.9.4 Coal Dust	44
	1.9.5 Asbestos	44
	1.9.6 Machine Shop Air Contaminants	44
	1.9.7 Filter Materials	45
	1.9.8 Carbon Flakes	45
2.	CASE HISTORIES	49
	2.1 Diesel Engines	49
	2.1.1 Normally Operating Diesel Engines	50
	2.1.2 Cast Iron Wear	51
	2.1.3 Steel Wear	51
	2.1.4 Corrosive Wear	52
	2.1.5 Abrasive Wear	54

Section	Subject	Page
	2.1.6 Nonferrous Metal Wear	54
	2.2 Aircraft Gas Turbines	57
	2.2.1 Introduction	57
	2.2.2 Fleet Monitoring	58
	2.2.3 Military Oil Analysis Program	79
	2.3 Gears	93
	2.3.1 Overload on Gears	95
	2.3.2 Severe Sliding and Overload Due to Lubricant Deficiency	96
	2.3.3 Water in the Oil	99
	2.3.4 Abrasive Wear	100
	2.3.5 Spectrometer Warning/Normal Rubbing Wear	101
	2.3.6 Extending Service Until Scheduled Overhaul	101
	2.4 Natural Gas Fired Internal Combustion Engine	102
	2.4.1 Discussion of Preceding Analysis Report	102
	2.5 Journal Bearings	111
	2.6 Hydraulic Systems	113
	2.7 Splines/Fretting Wear	113
	2.8 Ballscrews	116
	2.9 Tapered Roller Bearing	120
3.	OPERATIONAL PROCEDURES	125
	3.1 Obtaining a Representative Sample	125
	3.1.1 Particle Behavior in a Machine	125
	3.1.2 Oil Sampling Techniques	133
	3.1.3 Sample Preparation and Sample Dilution	138
	3.2 Ferrographic Techniques	140
	3.2.1 Optical Examination of Ferrograms	140
	3.2.2 Ferrogram Analysis Report Sheet	144
	3.2.3 The Direct Reading (DR) Ferrograph	147
	3.2.4 Quantifying a Wear Situation	152
	3.2.5 Establishing a Condition-Monitoring Program	153
	3.2.6 Heating of Ferrograms	166
	3.2.7 Scanning Electron Microscopy and X-Ray Analysis	170
	3.2.8 Grease Analysis	174
	3.2.9 Precipitation of Nonmagnetic Particles	178
	3.2.10 Polarized Light	179
4.	REFERENCES	187
	INDEX	191

LIST OF FIGURES AND BLACK AND WHITE PHOTOS OTHER THAN PHOTOMICROGRAPHS ON FULL—PAGE LAYOUTS

Figure	Title	Page
1.1	Deposition Pattern on a Ferrogram	8
2.2.2.1	Cumulative Sum of D_L vs. Sample No. for Engine 10056	62
2.2.2.2	Cumulative Sum of D_L vs. Sample No. for Engine 10093	63
2.2.2.3	Cumulative Sum of D_L vs. Sample No. for Engine 10101	64
2.2.2.4	Cumulative Sum of D_S vs. Sample No. for Engine 10101	65
2.2.2.5	Cumulative Sum of D_L vs. Sample No. for Engine 10200	66
2.2.2.6	Cumulative Sum of D_L vs. Sample No. for Engine 10221	67
2.2.2.7	Cumulative Sum of D_S vs. Sample No. for Engine 10221	68
2.2.2.8	Cumulative Sum of D_L vs. Sample No. for Engine 10223	69
2.2.2.9	Cumulative Sum of D_L vs. Sample No. for Engine 10223 (expanded view)	70
2.2.2.10	Cumulative Sum of D_S vs. Sample No. for Engine 10223	71
2.2.2.11	Cumulative Sum of D_L vs. Sample No. for Engine 10231	72
2.2.2.12	Cumulative Sum of D_L vs. Sample No. for Engine 10536	73
2.2.3.1	Ferrogram Analysis Report Sheet, Ferrogram 4359	80
2.2.3.8	(B & W Photo) Overspeed Governor Shaft after Removal from a T53 Engine	81
2.2.3.9	Ferrogram Analysis Report Sheet, Ferrogram, 4204	82
2.2.3.13	(B & W Photo) Shaft Gear Bearing After Removal	85
2.2.3.14	Ferrogram Analysis Report Sheet, Ferrogram 4364	86
2.2.3.19	(B & W Photo) Worn Parts from T53 Engine	87
2.2.3.20	(B & W Photo) Worn Parts from T53 Engine	87
2.2.3.21	Ferrogram Analysis Report Sheet, Ferrogram 0017	88
2.2.3.26	(B & W Photo) Failed Bearing	91
2.2.3.27	Ferrogram Analysis Report Sheet, Ferrogram 4270	92
2.2.3.33	(B & W Photo) Bearing Removed from a UH-1H Transmission	93
2.3.1	Gear Failure	94
2.3.2	Gear System Operating Regimes	94
2.4.1	Report for Colorado Interstate Gas Company, Pages 1 through 6	105
2.5.1	Ferrogram Analysis Report Sheet, Ferrogram 0242	112
2.7.5	Topline Wear Curves	115
2.9.1	Ferrogram Analysis Report Sheet, Ferrogram 0566	121
3.1.1.1	Simplified Oil Path	125
3.1.1.2	Establishing Equilibrium Particle Concentration	128

LIST OF FIGURES AND BLACK AND WHITE PHOTOS (continued)

Figure	Title	Page
3.1.1.3	Establishing Equilibrium Particle Concentration	128
3.1.1.4	Comparison of Idealized Data	131
3.1.2.1	Settling Rate of Spherical Particles in Oil	135
3.1.3.1	Dilution Procedure	139
3.2.1.1	Light Path of Bichromatic Microscope	140
3.2.1.2	Taking a Ferrogram Reading	143
3.2.1.3	High Magnification Objective Lens	143
3.2.2.1	Ferrogram Analysis Report Sheet, Blank	144
3.2.3.1	Schematic of DR Ferrograph	147
3.2.3.2	Particle Deposition in the DR Ferrograph	151
3.2.5.1	Report for Solvay in its Entirety	154
3.2.6.1	Formation of Interference Colors	167
3.2.6.2	Visible Spectrum	167
3.2.10.1	Polarizer Arrangement in the Optical Microscope	180
3.2.10.2	Birefringent Particle in Crossed Polarizers	180

LIST OF TABLES

Table	Title	Page
1.6.1	Identification of White Nonferrous Metals	31
2.2.2.1	DR Readings for Last Taken Sample Before Removal	60
2.2.2.2	Baseline DR Readings for Several Engines	61
2.2.2.3	Abbreviations Used in Figures 2.2.2.1 through 2.2.2.12	61
3.1.1.1	Values of N (a_j, n) for X = 1	130
3.2.2.1	Distinction Between Free Metal Particles	145
3.2.2.2	Suggested Procedure for Analysis of a Ferrogram	149
3.2.6.1	Identification of Particles by Heat Treating Ferrograms	171
3.2.8.1	Types of Grease Selected for Investigation	175

INTRODUCTION

Wear particle analysis is a powerful technique for non-intrusive examination of the oil-wetted parts of a machine. The particles contained in the lubricating oil carry detailed and important information about the condition of the machine. This information may be deduced from particle shape, composition, size distribution, and concentration. The particle characteristics are sufficiently specific so that the operating wear modes within the machine may be determined, allowing prediction of the imminent behavior of the machine. Often, action may be taken to correct the abnormal wear mode without overhaul, such as when abrasive contamination indicates a change of oil and oil filter. Alternatively, timely overhaul can prevent costly secondary damage.

The Wear Particle Atlas provides information for the identification of various wear particle types, the description of wear modes that generate these particles, the consequence of these wear modes, and description of the techniques that facilitate wear particle analysis.

This Wear Particle Atlas is a revised and expanded edition of the Wear Particle Atlas, Volume I, published in 1976, which contains a description of various unoxidized ferrous particles and information on ferrographic techniques. The description of ferrous particles is presented in Section 1.0, paragraphs 1.1 to 1.5, in the revised Atlas with all the original photomicrographs and with only minor editorial changes to the text. The information on ferrographic techniques from the old Atlas is incorporated in Section 3.0, Operational Procedures, of the new Atlas which describes ferrographic techniques more completely and which discusses quantitative aspects of wear particles to permit interpretation of quantitative data. Paragraphs 1.6 to 1.9 have been added to the new Atlas to describe nonferrous metals, oxides, lubricant degradation products, and contaminants. Section 2.0 of the new Atlas presents cases that act as a teaching aid for those devoted to the practical application of wear debris analysis for mechanical system monitoring.

1. PARTICLE IDENTIFICATION

The particles described in this Atlas have been isolated for examination by ferrography,[1,2] although other separation techniques are possible for wear particle analysis. Ferrography uses a high gradient magnetic field to attract and hold particles from a fluid sample which flows down a specially prepared microscope slide/substrate inclined at a small angle to the horizontal. After the sample has been passed across the glass substrate, the substrate is washed with solvent to remove residual fluid. When the solvent dries, a ferrogram suitable for analysis results.

Figure 1.1 shows the deposition pattern on a ferrogram. Position along a ferrogram is referenced from the exit end. The entry, where the fluid first touches down on the substrate, is approximately 56 mm from the exit end where the sample flows off the substrate and is collected by a drain tube. The largest magnetic particles are deposited

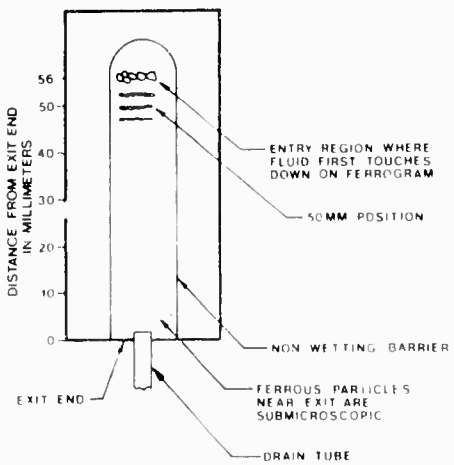

Figure 1.1 Deposition Pattern on a Ferrogram

at the entry region of the ferrogram because the magnetic force which attracts the particles is proportional to volume whereas the viscous resistance of the particles to motion in the fluid is proportional to surface area. If particle shape is the same, motion downward through the fluid as a function of size is governed by the ratio of the particle diameter cubed to the particle diameter squared. Therefore, the largest magnetic particles are deposited first. When the sample reaches the 50 mm position, magnetic particles larger than about 2 or 3 μm in major dimension have already been removed.

Ref. 1. Seifert, W.W., and Westcott, V.C. "A Method for the Study of Wear Particles in Lubricating Oil", Wear, 21 (1972) 22-42.

2 Bowen, E.R., Scott, D., Seifert, W.W. and Westcott, V.C. "Ferrography", Tribology International, 9 (3) (1976) 109-115.

Ferrous particles are at or below the lower limit of resolution (about 0.5 μm) of the optical microscope at the exit end of the ferrogram. Ferrous (magnetic) particles are deposited in strings which follow the field lines of the magnet assembly positioned below the ferrogram substrate. The strings are perpendicular to flow direction. The photomicrographs in this Atlas are presented with the flow direction from the top of the page to the bottom.

The particles described in paragraphs 1.1 through 1.5 are those primarily generated by steel or steel-based alloys. Other metals and alloys give similarly shaped particles, with only a slight difference being attributable to hardness and crystal structure of that material. These sections cover the free metal (similar to parent metal, not compounded) particles generated and are divided into the following five subsections:

1.1 Rubbing Wear and Break-In Wear
The usually normal benign wear of sliding surfaces.

1.2 Cutting Wear
Abnormal abrasive wear due to interpenetration of sliding surfaces.

1.3 Rolling Fatigue (Rolling Element Bearings and Gear Systems)
The fatigue wear of rolling contact bearings.

1.4 Combined Rolling and Sliding
The abnormal wear regimes of fatigue and scuffing as associated with gears.

1.5 Severe Sliding Wear
Excessive load and high speed wear of sliding surfaces.

The remainder of Section 1.0 describes nonferrous metal particles, ferrous oxides, lubricant degradation products, and contaminant particles.

Both optical and scanning electron microscopes have their advantages in particle analysis. The bichromatic microscope which utilizes both transmitted and reflected light can determine the degree of light attenuation and color of the particle. This information easily enables one to discern whether a particle is free metal or is a compound. Further analysis in polarized light yields information on the crystal structure of various compounds. See paragraph 3.2.1 on Optical Examination of Ferrograms.

The scanning electron microscope (SEM) is particularly useful in research where it is desired to photograph assemblies of particles requiring a large depth of focus. However, the SEM shows only the shape of the particles and does not, for example, distinguish between a translucent sand particle and a chunk of metal. Consequently, it is necessary to examine ferrograms with an optical microscope, or by other means, in order to obtain the maximum information about the particle's composition and source. The higher magnifications allowable with a SEM are occasionally useful but the maximum

of approximately 1000X obtained with an optical microscope is usually found to be adequate for wear particle analysis.

1.1 RUBBING WEAR AND BREAK-IN WEAR

Rubbing wear or normal wear particles are generated as the result of normal sliding wear in a machine.

During a normal break-in of a wear surface, a unique layer is formed at the surface. The break-in of a wear surface may be defined as the period of transition of the "as finished" surface to a smooth low wearing surface. Mechanical work at the surface breaks down the crystal structure of the metal resulting in a thin layer of short range crystalline order (approximately 30 nanometers) and about 1 μm thick for steel. The layer is known as the shear mixed layer.

The shear mixed layer exhibits super ductility and may flow along the surface a distance several hundred times its thickness. Its ability to flow when subjected to stress results in a very smooth wear track. As long as this layer is stable the surface will wear normally. If the removal rate is increased to the point that the layer is removed faster than it is generated, the wear rate increases and the maximum particle size changes from 5 to 15 μm to as much as 50 to 200 μm. See Section 1.5, Severe Sliding Wear.

Rubbing wear or normal wear particles are generated as the result of normal sliding wear in a machine and result from exfoliation of parts of the shear mixed layer.

Rubbing wear particles are platelets typically ranging in size from 15 μm down to 0.5 μm, or less, in major dimension. They have a smooth surface and range between 0.15 μm and 1 μm in thickness. The major dimension-to-thickness ratio varies from about 10:1 for the larger particles to about 3:1 for a 0.5 μm particle.

During break-in, rubbing wear particles in combination with other larger particles are seen. The larger particles are pieces of grinding ridges and other surface irregularities which break off in the process of smoothing the surface. During break-in the shear mixed layer covers over scratches and irregularities. Occasionally pieces of the layer cantilever over scratches and other depressions in the surface and break off. This is the source of some of the larger rubbing wear particles.

After a stable wearing surface is achieved, the shear mixed layer continues to exfoliate and supplies the normal rubbing wear particles.

Excessive quantities of particulate contamination, such as sand in a lubrication system, can increase the rubbing wear generation rate by more than an order of magnitude without completely removing the shear mixed layer. Although catastrophic failure is unlikely, such systems can wear out rapidly. In these cases, although all the wear debris may be principally rubbing wear, impending trouble may be forecast by the dramatically increased quantity of particles. The actual quantitative increase in wear

debris is dependent on the size, concentration, composition, and morphology of the contaminant. Components prone to this problem are those with opposing surfaces of roughly the same hardness, for example, diesel engine cylinder walls and piston rings. The particle analysis of such an oil sample will reveal the contaminant particles as well as the wear debris.

Figures 1.1.1 through 1.1.5 display normal rubbing wear as generated by a diesel engine. The photographs are taken at the same location with differing magnification. **Figure 1.1.1** displays the entry deposit at the top of the photograph. **Figures 1.1.3** and **1.1.4** show the largest particles present to be around 10 μm. Generally the maximum size of normal rubbing wear is approximately 15 μm.

Figure 1.1.6 is a photograph of the actual entry deposit. Some of the particles are oriented such that they can be seen to be thin platelets no more than 1 μm thick.

Figure 1.1.7 is a bichromatic view of **Figure 1.1.2.**

Figures 1.1.8 through 1.1.10 indicate the maximum ferromagnetic particle size at differing locations on a ferrogram. **Figure 1.1.8** displays the particles immediately after the entry point. Here the maximum particle size is that of the largest particles in the sample; in this case 15 μm.

Figure 1.1.9 is a photograph taken at 50 mm. The largest particles at this location are 2 μm. **Figure 1.1.10** is a photograph taken at 10 mm. The white particles seen in this photograph are, in fact, short strings of particles individually no larger than 0.2 μm.

It must be noted that these sizes are representative of ferromagnetic materials. Weakly magnetic particles are deposited further down the ferrogram. See paragraph 1.6 on Nonferrous Metals.

Figures 1.1.11 through 1.1.14 display particles typical of the break-in period for components having a ground or machined surface finish. During the break-in period, the ridges on the wear surface are flattened and form cornices along the ridge peaks. These cornices subsequently break away in the form of the long flat particles shown in the photograph. These particles are formed in decreasing quantity until the original finishing marks are covered over or worn away.

Figure 1.1.15 displays a few of the individual particles.

Figure 1.1.16 displays the smaller particles immediately after the entry deposit. Although not as wide, several of these particles still have the long, thin, straight-edged shape characteristic of the break-in process.

1.2 CUTTING WEAR

Cutting wear particles are generated as a result of one surface penetrating another. The effect is to generate particles much as a lathe creates machining swarf, except on a microscopic scale.

There are two ways of generating this effect. A relatively hard component can become misaligned or fractured, resulting in a hard sharp edge penetrating a softer surface. Particles generated this way are generally coarse and large, averaging 2 to 5 μm wide and 25 to 100 μm long.

Alternatively hard abrasive particles in the lubrication system, either as contaminants such as sand or wear debris from another part of the system, may become embedded in a soft wear surface (two body abrasion) such as a lead/tin alloy bearing. The abrasive particles protrude from the soft surface and penetrate the opposing wear surface. The maximum size of cutting wear particles generated in this way is proportional to the size of the abrasive particles in the lubricant. Again, very fine wire-like particles can be generated with thicknesses as low as 0.25 μm. Occasionally small particles, about 5 μm long by 0.25 μm thick, may be generated due to the presence of hard inclusions in one of the wearing surfaces.

The presence of abrasive contaminants in a lubrication system does not necessitate the generation of cutting wear, although the wear rate of the system may increase. Two wearing surfaces of comparable hardnesses, where particulate contaminant does not embed in one surface, will probably not generate cutting wear as a result of the presence of abrasive contaminants (see paragraph 1.1). This is a three body abrasion wear process.

Cutting wear particles are abnormal. Their presence and quantity should be carefully monitored. If the majority of cutting wear particles in a system are around a few micrometers long and a fraction of a micrometer wide, the presence of particulate contaminants should be suspected. If a system shows increasing quantities of large (50 μm long) cutting wear particles, a component failure is potentially imminent.

Figures 1.2.1 through 1.2.4 are views of the same location on a ferrogram made from an oil sample of a failing jet engine. As the majority of the cutting wear particles are large long strips, a component failure should be suspected. The absence of any abnormal contaminants reinforces this judgment.

Figures 1.2.5 and 1.2.6 are optical and scanning electron photographs of the same location. These photographs display the variation of size and shape possible with cutting wear.

Figures 1.2.7 through 1.2.9 display the heavy cutting wear generated as a consequence of abrasive contaminants (Arizona road dust) in a hydraulic system. The rock-like particles are the actual contaminants. Virtually all the remaining material on the ferrogram is metallic cutting wear.

Figures 1.2.10 through 1.2.12 are reflected white, bichromatic, and SEM photographs of the same cutting wear particle

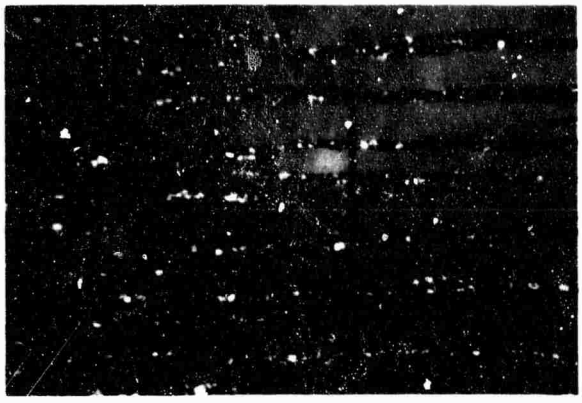

Fig. 1.1.1 Opt. M. 225X ⊢— 100μm —⊣

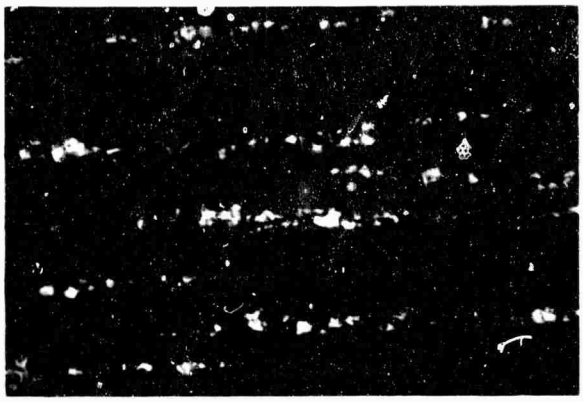

Fig. 1.1.2 Opt. M. 450X ⊢— 50μm —⊣

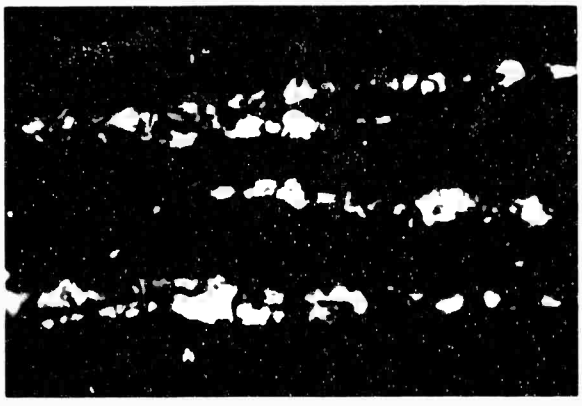

Fig. 1.1.3 Opt. M. 1000X ⊢— 20μm —⊣

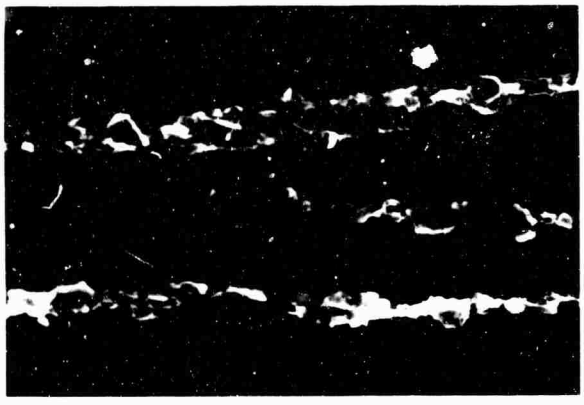

Fig. 1.1.4 S.E.M. 1000X ⊢— 20μm —⊣

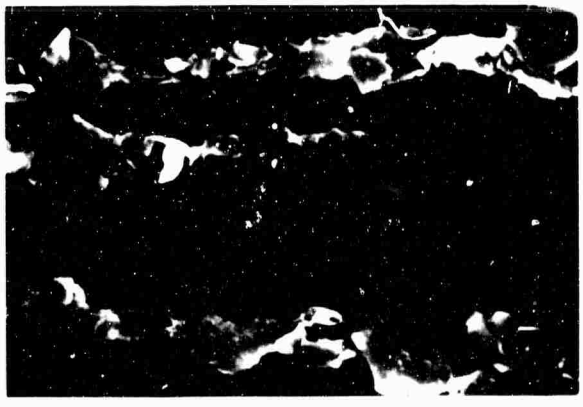

Fig. 1.1.5 S.E.M. 2500X ⊢— 10μm —⊣

Fig. 1.1.6 S.E.M. 2500X ⊢— 10μm —⊣

Fig. 1.1.7 Opt. M. 450X ⊢— 50μm —⊣

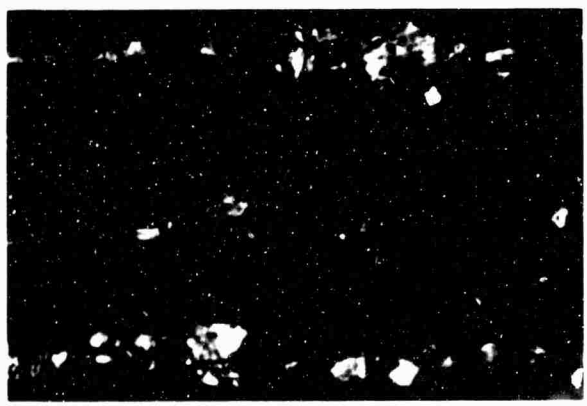

Fig. 1.1.8 Opt. M. 1000X ⊢— 20μm —⊣

Fig. 1.1.9 Opt. M. 1000X ⟵20μm⟶

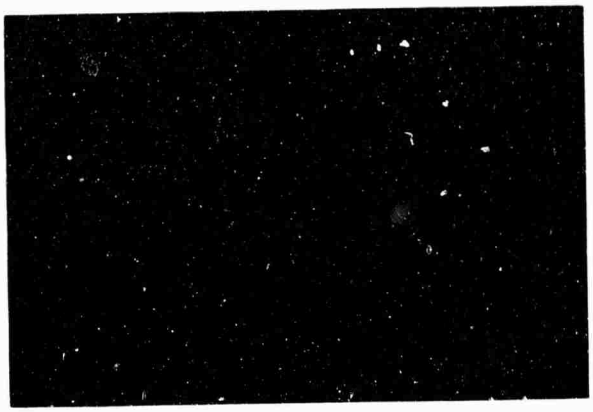

Fig. 1.1.10 Opt. M. 1000X ⟵20μm⟶

Fig. 1.1.11 Opt. M. 225X ⟵100μm⟶

Fig. 1.1.12 Opt. M. 450X ⟵50μm⟶

Fig. 1.1.13 Opt. M. 1000X ⟵20μm⟶

Fig. 1.1.14 S.E.M. 1000X ⟵20μm⟶

Fig. 1.1.15 Opt. M. 1000X ⟵20μm⟶

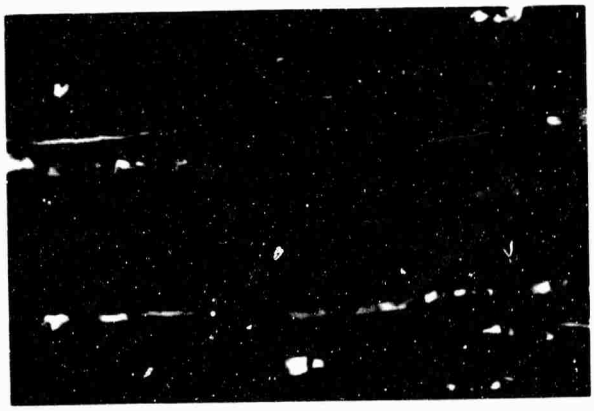

Fig. 1.1.16 Opt. M. 1000X ⟵20μm⟶

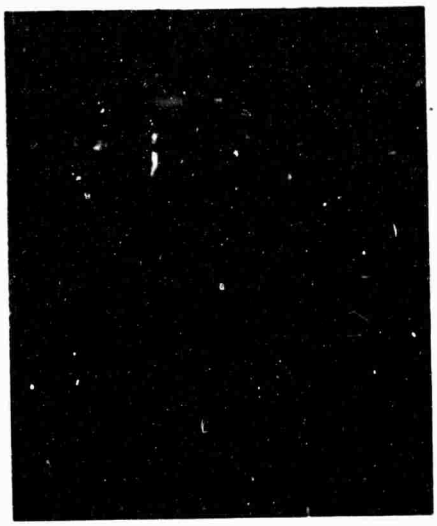

Fig. 1.2.1 Opt. M. 225X ⊢—— 100μm ——⊣

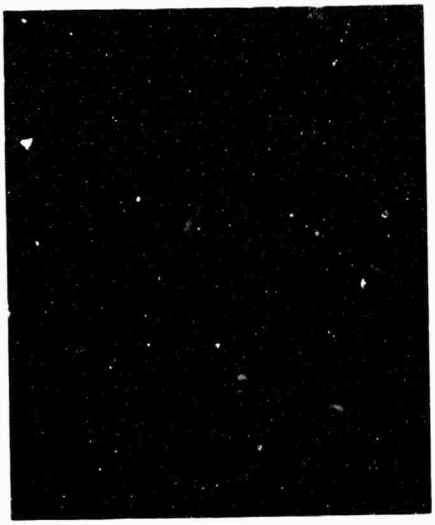

Fig. 1.2.2 Opt. M. 450X ⊢—— 50μm ——⊣

Fig. 1.2.3 Opt. M. 1000X ⊢—— 20μm ——⊣

Fig. 1.2.4 S.E.M. 1000X ⊢—— 20μm ——⊣

Fig. 1.2.5 Opt. M. 225X ⊢—— 100μm ——⊣

Fig. 1.2.6 S.E.M. 225X ⊢—— 100μm ——⊣

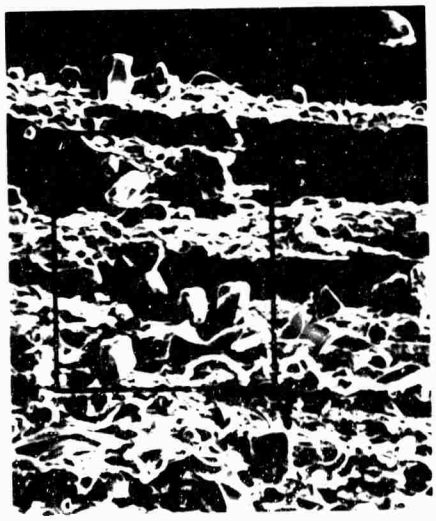

Fig. 1.2.7 S.E.M. 225X ⊢—— 100μm ——⊣

Fig. 1.2.8 S.E.M. 450X ⊢—— 50μm ——⊣

Fig. 1.2.9 S.E.M. 1000X ⊢—— 20μm ——⊣

Figures 1.2.13 and 1.2.14 are bichromatic and SEM photographs of fine cutting wear particles. The height of the largest particle is greater than the depth of focus of the optical microscope. The bent portion above the glass substrate cannot be brought into focus simultaneously with the substrate.

Figures 1.2.15 through 1.2.18 are SEM micrographs of a selection of cutting wear particles.

1.3 ROLLING FATIGUE (ROLLING ELEMENT BEARINGS)

This section deals primarily with particles generated as a result of rolling bearing fatigue. The particles associated with other bearing problems, such as roller end wear, skidding, and any other contact involving sliding are discussed in paragraphs 1.1 and 1.5.

Three distinct particle types have been associated with rolling bearing fatigue; namely, fatigue spall particles, spherical particles, and laminar particles.

Fatigue spall particles constitute the actual material removed as a pit or spall opens up. These particles reach a maximum size of 100 μm during the microspalling process. When the spalling becomes macroscopic and failure occurs, the particle size may increase still further. The initial abnormality can be deduced from the increasing quantity of particles larger than 10 μm. The fatigue particles are flat platelets with a major dimension-to-thickness ratio of approximately 10:1. They have a smooth surface and a random, irregularly shaped circumference. The ability to recognize these particles is very important as the quantity of wear debris that results in a serious loss of performance is much lower for bearings than for other devices.

The spherical particles associated with rolling bearing fatigue are generated in the bearing fatigue cracks. If generated, their presence gives an improved warning of impending trouble as they are detectable before any actual spalling occurs. It has been observed that bearings undergoing test at higher than normal loads and in clean lubrication systems have fatigued without generating any significant quantities of spheres. Consequently, in an abnormal wear situation, the possibility of rolling bearing fatigue should not be ruled out due to the absence of spherical debris. However, in many industrial systems monitored so far, rolling bearing fatigue spalling has been preceded by the generation of quantities of steel spheres having diameters ranging between one and five micrometers.[3,4] Fatiguing bearings have been estimated to generate several million spheres in the course of a failure.

Ref 3 Scott, D., and Mills, G. H. "Spherical Particles in Rolling Contact Fatigue", Nature (London), 241 (1973) 115-116

4 Scott, D., and Mills, G. H. "Spherical Debris - Its Occurrence, Formation, and Significance in Rolling Contact Fatigue", Wear, 24 (1973) 235-242

Rolling bearing fatigue is not the only source of spherical metallic particles. They are known to be generated by cavitation erosion and more importantly by welding or grinding processes. Spheres produced in fatigue cracks may be differentiated from those produced by other mechanisms through their size distribution. Rolling fatigue generates few spheres over 3 μm while the spheres generated by welding, grinding, and erosion are frequently over 10 μm. Lubricating oils, as supplied by manufacturers, frequently contain metal particles including metal spheres and other contaminant particles. Consequently, care must be taken to avoid confusing these contaminant spheres with those generated as the result of bearing fatigue.

Laminar particles are very thin free metal particles between 20 and 50 μm in major dimension with a thickness ratio of approximately 30:1. It is thought that laminar particles are formed by the passage of a wear particle through a rolling contact, possibly after adhering to a rolling element. The frequent occurrence of holes in these particles is in agreement with this explanation. Laminar particles may be generated throughout the life of a bearing, but at the onset of fatigue spalling, the quantity generated increases. Consequently, their increased presence, along with severe wear of uncertain origin, suggests a problem with a rolling contact bearing. Similarly, an increasing quantity of laminar particles together with quantities of spheres is taken as an indication of the presence of rolling bearing fatigue microcracks which in turn leads to spalling.

Figure 1.3.1 displays a typical distribution of particles during the normal running of rolling-element bearings.

Figures 1.3.2 through 1.3.5 display in increasing magnification particles generated by rolling-element bearing fatigue spalls. Note the smooth surfaces and irregular contours. Also, what appear to be micropits on the particle surfaces in the optical micrograph are in fact smaller pieces of wear debris.

Figures 1.3.6 through 1.3.8 display another sequence of increasing magnification photographs of rolling-element bearing fatigue particles. **Figure 1.3.6** clearly shows the relative absence of rubbing wear particles. This high ratio of large (20 μm) particles to small (2 μm) particles is typical of pure rolling-element fatigue. The relative absence of rubbing wear particles is seldom seen in oil samples of complete machines, because many other parts besides the bearing contribute wear particles.

Figures 1.3.9 and 1.3.10 display the irregular shape and size of a particle that rolling-element fatigue can generate.

Figures 1.3.11 through 1.3.13 are photographs of metallic spheres. They are much larger than the spheres normally generated by bearing fatigue. These spheres may be from an extraneous source. However, they serve the purpose of displaying the optical characteristics of these spheres. The curvature of the sphere causes light from above

Fig. 1.2.10 Opt. M. 1000X ⊢—20μm—⊣

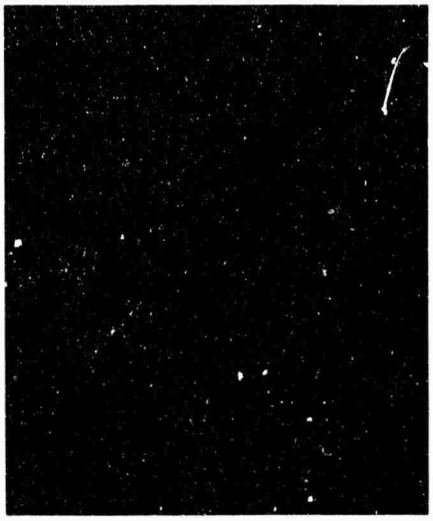

Fig. 1.2.11 Opt. M. 1000X ⊢—20μm—⊣

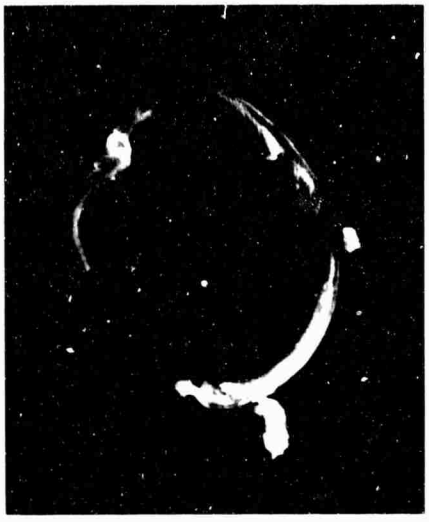

Fig. 1.2.12 S.E.M. 1000X ⊢—20μm—⊣

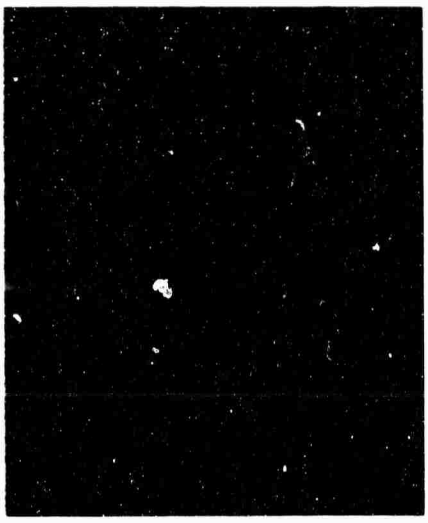

Fig. 1.2.13 Opt. M. 450X ⊢—50μm—⊣

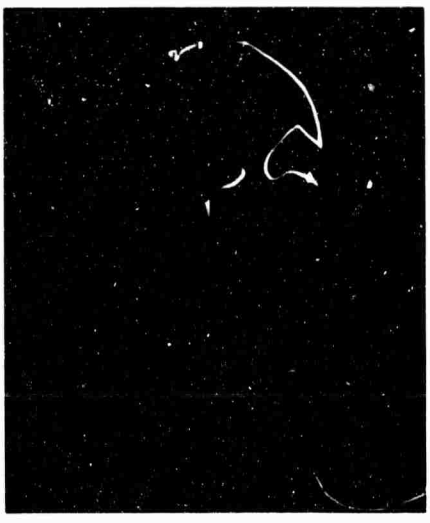

Fig. 1.2.14 S.E.M. 450X ⊢—50μm—⊣

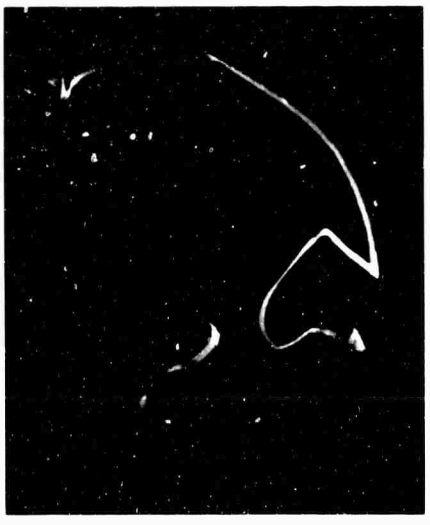

Fig. 1.2.15 S.E.M. 1000X ⊢—20μm—⊣

Fig. 1.2.16 S.E.M. 1000X ⊢—20μm—⊣

Fig. 1.2.17 S.E.M. 1000X ⊢—20μm—⊣

Fig. 1.2.18 S.E.M. 1000X ⊢—20μm—⊣

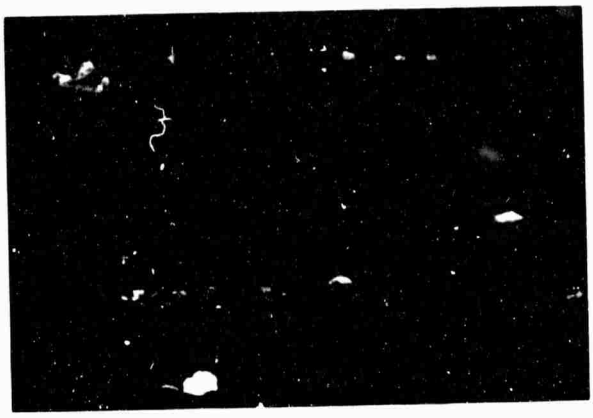

Fig. 1.3.1 Opt. M. 1000X ⊢—20μm—⊣

Fig. 1.3.2 Opt. M. 225X ⊢—100μm—⊣

Fig. 1.3.3 Opt. M. 450X ⊢—50μm—⊣

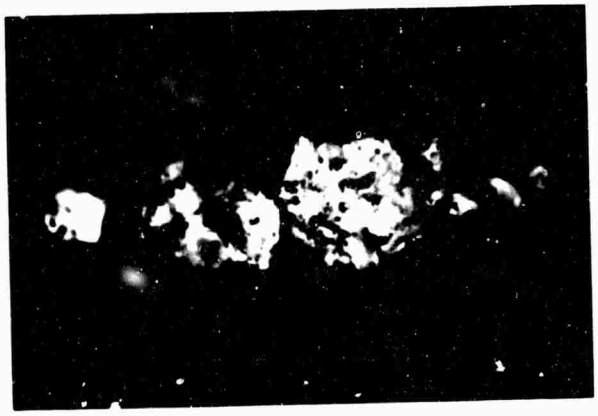

Fig. 1.3.4 Opt. M. 1000X ⊢—20μm—⊣

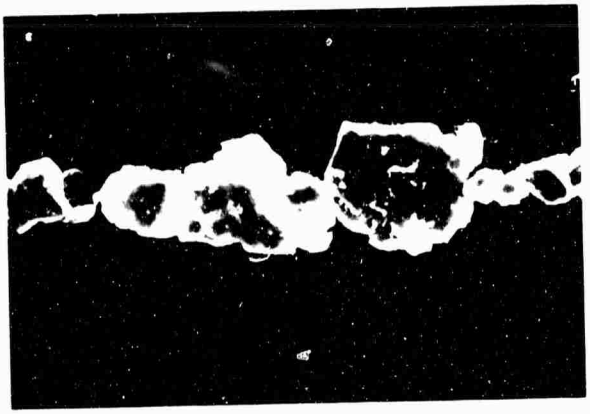

Fig. 1.3.5 S.E.M. 1000X ⊢—20μm—⊣

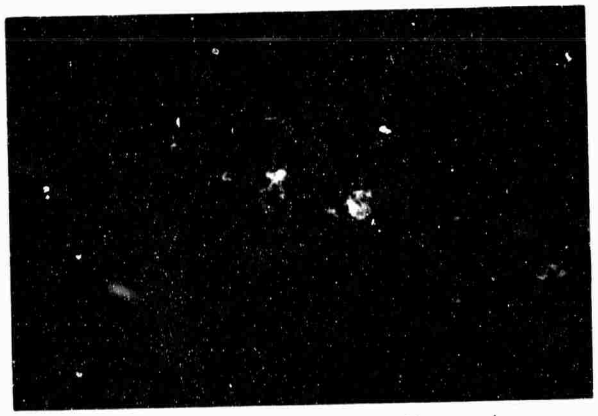

Fig. 1.3.6 Opt. M. 225X ⊢—100μm—⊣

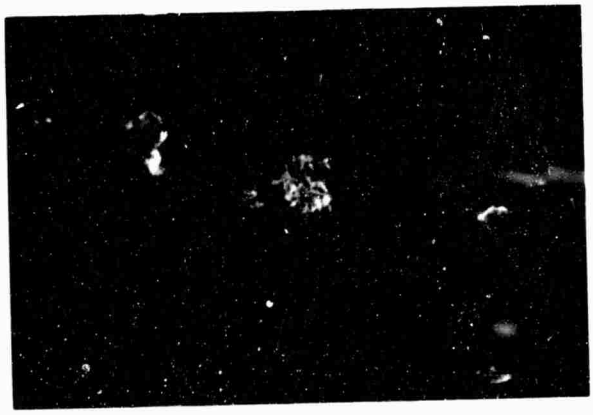

Fig. 1.3.7 Opt. M. 450X ⊢—50μm—⊣

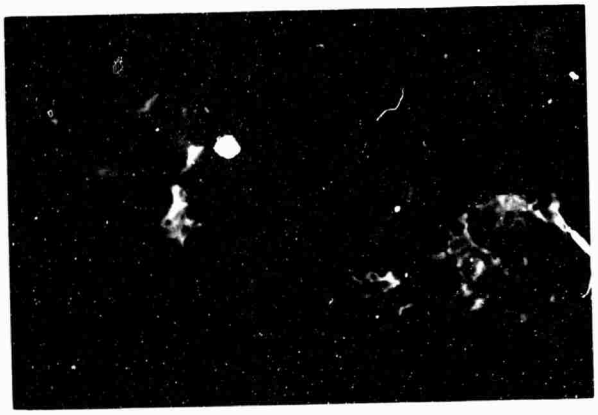

Fig. 1.3.8 Opt. M. 1000X ⊢—20μm—⊣

to be reflected off to the side and not directly back into the objective lens. An objective lens that accepts light from a wide angle is needed in order to show the spheres. Such a lens is called a high numerical aperture (NA) objective, the NA being the sine of the half angle. The numerical aperture should be 0.85 or higher for adequate observation of spheres. Because of the convex mirror effect of the spherical surface, an object inserted at the right point in the reflected light source beam will appear in focus on the spherical surface. **Figure 1.3.11** has a needle point inserted into the beam while **Figure 1.3.12** has a red filter partially inserted. The alternating light and dark bands on the particles is the image of the lamp filament. This characteristic of reflecting images enables the spheres to be readily identified in an optical microscope.

Figure 1.3.14 is a SEM photograph at a higher magnification of the previous example.

It should be noted that some lubrication systems can generate plastic spheres that are unrelated to the wear surfaces. The optical microscope can distinguish these by their ability to transmit light. In bichromatic illumination such spheres appear green while metal spheres appear red.

Figures 1.3.15 and 1.3.16 display a general view of spheres as generated by a fatiguing bearing. **Figure 1.3.17** is a SEM photograph at a higher magnification of the same spheres

Figures 1.3.18 through 1.3.20 display laminar particles as generated by rolling-element bearings. None of these particles are over 1 μm thick. Note the holes in the latter example, **Figures 1.3.19** and **1.3.20**.

1.4 COMBINED ROLLING AND SLIDING (GEAR SYSTEMS)

The modes of gear wear considered in this section are pitch line fatigue and scuffing or scoring. Overload wear, the infrequent result of very high loads at low speeds is classified as severe sliding wear; see paragraph 1.5. Similarly, the effects of abrasive contaminants in the lubricant are covered by paragraphs 1.1 and 1.2.

Fatigue particles from a gear pitch line have much in common with rolling-element bearing fatigue particles. They generally have a smooth surface and are frequently irregularly shaped. Depending on the gear design, the particles may have a major dimension-to-thickness ratio between 4:1 and 10:1. The chunkier particles result from tensile stresses on the gear surface causing the fatigue cracks to propagate deeper into the gear tooth prior to spalling.

A high ratio of large particles to small particles is also found as in rolling-element bearing fatigue.

Scuffing of gears is caused by too high a load and/or speed. Excessive heat generation breaks down the lubricant film and causes adhesion of the mating gear teeth. Roughening of the wear surfaces ensues with subsequent increase in wear rate. The regions of the gear teeth affected are between the pitch line and both gear root and tip.

Once initiated, scuffing usually affects each tooth on a gear, resulting in a large volume of wear debris.

Since there is a large variation in both sliding and rolling velocities at the wear contacts, there are corresponding variations in the characteristics of the particles generated. The ratio of large-to-small particles in a scuffing situation is small. All the particles tend to have a rough surface and a jagged circumference. Even the small particles may be discerned from rubbing wear by these characteristics. Some of the large particles have striations on their surface indicating a sliding contact. Because of the thermal nature of scuffing, quantities of oxide are usually present and some of the particles may show evidence of partial oxidation, that is, tan or blue temper colors. The degree of oxidation is dependent on the lubricant and the severity of scuffing.

Figures 1.4.1 through 1.4.4 are increasing magnification photographs of gear fatigue particles. A high ratio of large to small particles is evident and the surfaces of the large particles are smooth.

Figures 1.4.5 through 1.4.10 display four individual gear fatigue particles. **Figures 1.4.5, 1.4.6, 1.4.9,** and **1.4.10** show the irregular shape obtainable with gear fatigue while the particle in **Figures 1.4.7** and **1.4.8** is typical of the chunky type. This latter particle is 7 μm thick, giving a shape ratio of 5:1.

Figures 1.4.11 through 1.4.14 are photographs of a typical scuffing wear particle distribution. If **Figures 1.4.13** and **1.4.14** are compared with **1.1.3** and **1.1.4**, the difference between the smaller scuffing particle and rubbing wear becomes more apparent. The larger particles which show striations have probably been generated near the tip or root of the gear tooth where the sliding velocity is highest, while the particles with no striations may have been generated nearer the pitch line.

Figures 1.4.15 through 1.4.17 are individual scuffing wear particles. The dark parts on the particles in these optical photographs are the result of oxidation.

1.5 SEVERE SLIDING WEAR

Severe sliding wear commences when the wear surface stresses become excessive due to load and/or speed. The shear mixed layer then becomes unstable and large particles break away causing an increase in the wear rate. If the stresses applied to the surface are increased further, a second transition point is reached when the complete surface breaks down and a catastrophic wear rate ensues. The relationship between sliding wear particles and the generating surfaces is described in reference 5.

The ratio of large-to-small particles depends on how far the surface stress limit is exceeded. The higher the stress level, the higher the ratio becomes. If the stress level

---

Ref. 5. Reda, A.A., Bowen, E.R., and Westcott, V.C. "Characteristics of Particles Generated at the Interface Between Sliding Steel Surfaces", Wear, 34 (1975) 261-273.

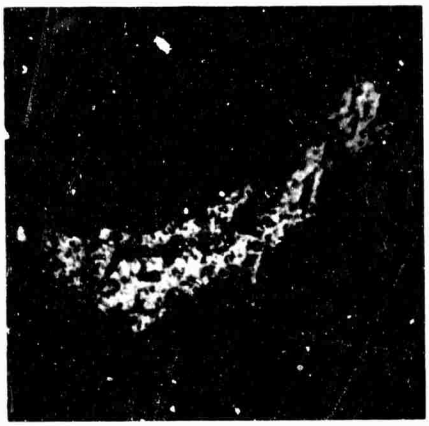

Fig. 1.3.9 Opt. M. 450X ⊢—50μm—⊣

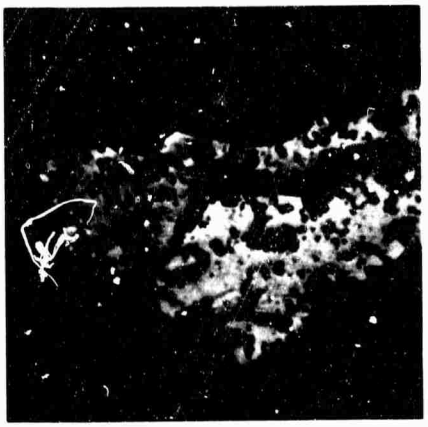

Fig. 1.3.10 Opt. M. 1000X ⊢—20μm—⊣

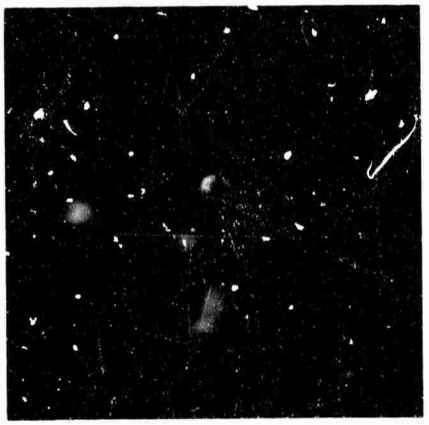

Fig. 1.3.11 Opt. M. 1000X ⊢—20μm—⊣

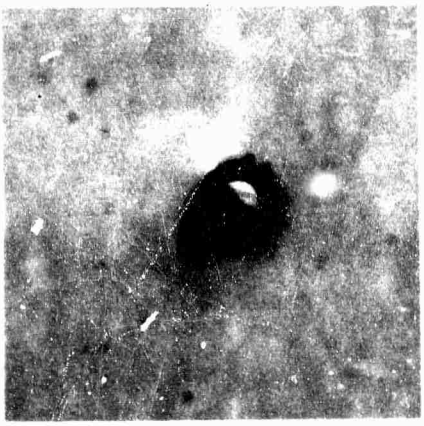

Fig. 1.3.12 Opt. M. 1000X ⊢—20μm—⊣

Fig. 1.3.13 S.E.M. 1000X ⊢—20μm—⊣

Fig. 1.3.14 S.E.M. 2500X ⊢——10μm——⊣

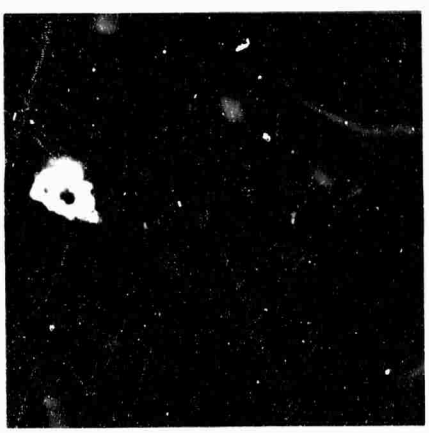

Fig. 1.3.15 Opt. M. 1000X ⊢—20μm—⊣

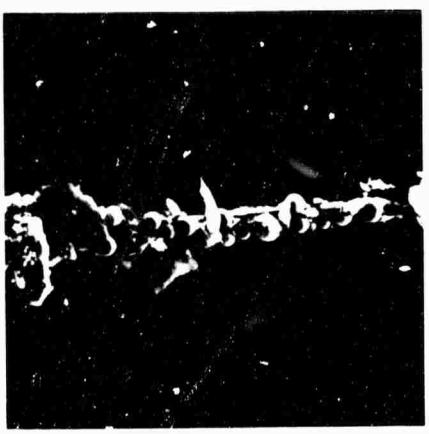

Fig. 1.3.16 S.E.M. 1000X ⊢—20μm—⊣

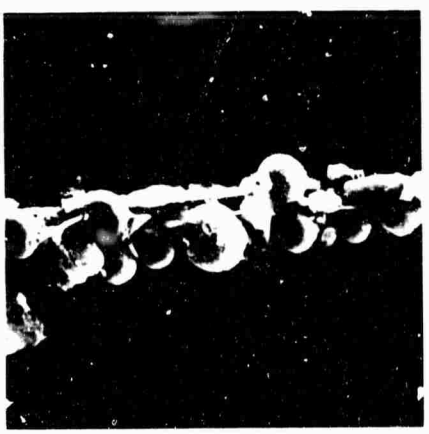

Fig. 1.3.17 S.E.M. 2500X ⊢——10μm——⊣

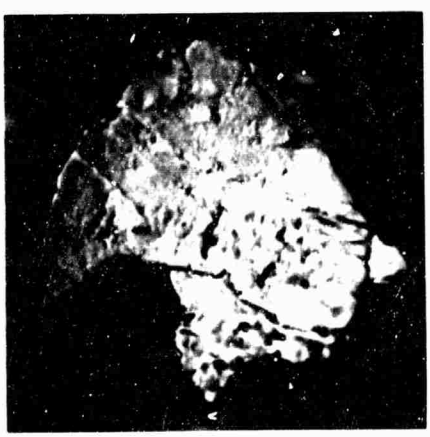

Fig. 1.3.18 Opt. M. 1000X ⊢—20μm—⊣

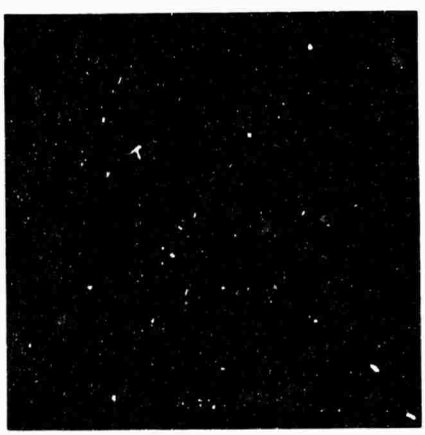

Fig. 1.3.19 Opt. M. 1000X ⊢—20μm—⊣

Fig. 1.3.20 Opt. M. 1000X ⊢—20μm—⊣

Fig. 1.4.1 Opt. M. 225X ⊢—100μm—⊣

Fig. 1.4.2 Opt. M. 450X ⊢— 50μm —⊣

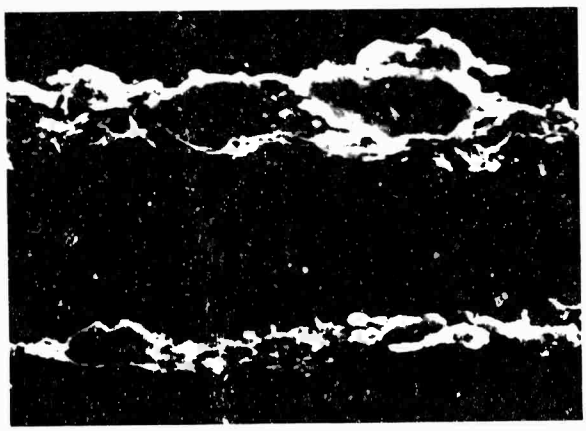

Fig. 1.4.3 S.E.M. 1000X ⊢— 20μm —⊣

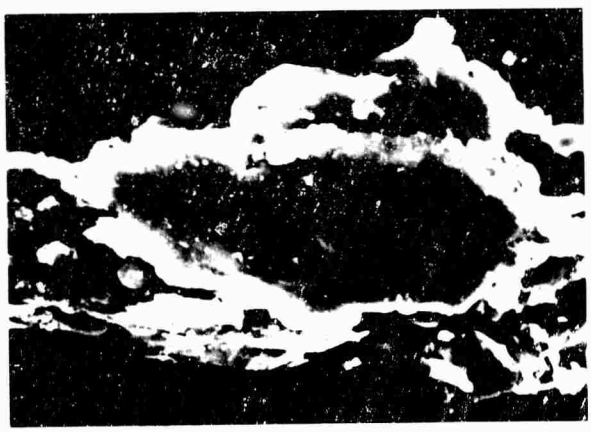

Fig. 1.4.4 S.E.M. 2500X ⊢——10μm——⊣

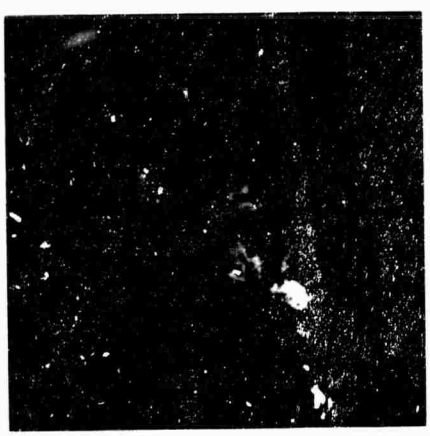

Fig. 1.4.5 Opt. M. 1000X ⊢—20μm—⊣

Fig. 1.4.6 S.E.M. 1000X ⊢—20μm—⊣

Fig. 1.4.7 Opt. M. 1000X ⊢— 20μm —⊣

Fig. 1.4.8 S.E.M. 1000X ⊢—20μm—⊣

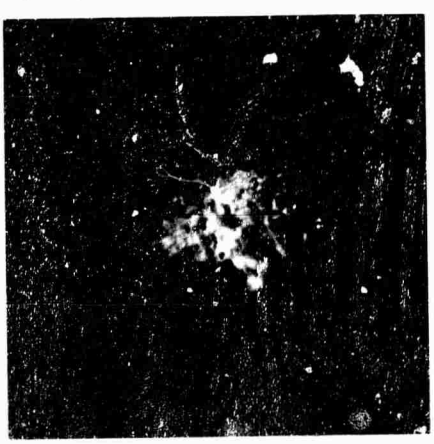

Fig. 1.4.9 Opt. M. 1000X ⊢— 20μm —⊣

Fig. 1.4.10 Opt. M. 1000X ⊢—20μm—⊣

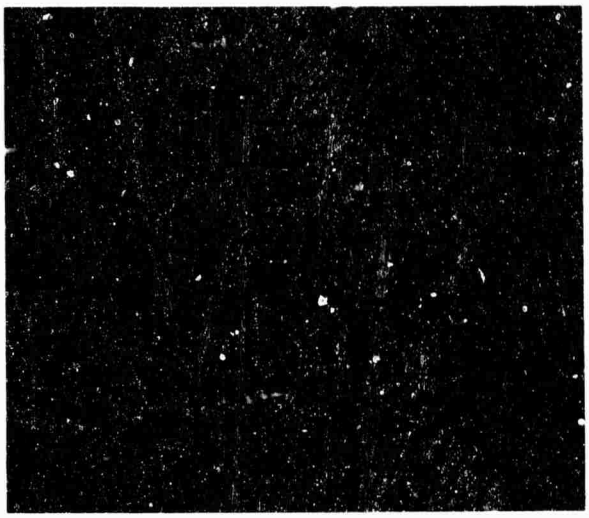

Fig. 1.4.11 Opt. M. 225X ⊢——100μm——⊣

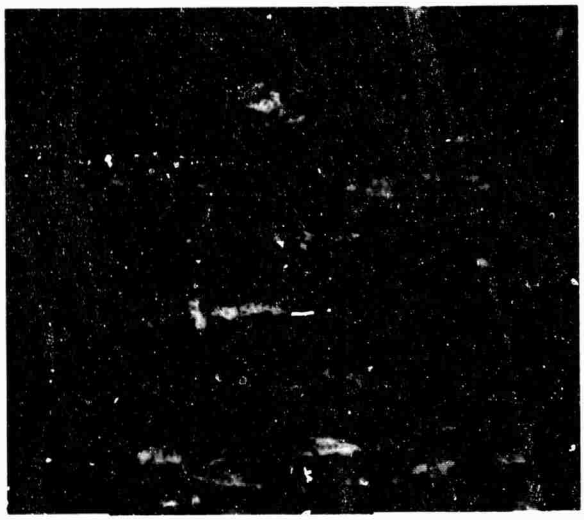

Fig. 1.4.12 Opt. M. 450X ⊢—— 50μm——⊣

Fig. 1.4.13 Opt. M. 1000X ⊢—— 20μm——⊣

Fig. 1.4.14 S.E.M. 1000X ⊢—— 20μm——⊣

Fig. 1.4.15 O t. M. 1000X ⊢—— 20μm——⊣

Fig. 1.4.16 Or t. M. 1000X ⊢—— 20μm——⊣

Fig. 1.4.17 Opt. M. 1000X ⊢—— 20μm——⊣

rises slowly, one may notice a significant increase in the quantity of rubbing wear prior to the development of any large severe wear particles.

Severe sliding wear particles range in size from 15 μm up. Some of these particles have surface striations as a result of sliding. They frequently have straight edges and their major dimension-to-thickness ratio is approximately 10:1. As the wear becomes more severe within this wear mode, the striations and straight edges on particles become more prominent.

Figures 1.5.1 through 1.5.4 are photographs of typical severe wear particles. The high ratio of large-to-small particles is indicative of stress levels far above that which the surface can tolerate.

Figures 1.5.5 through 1.5.7 are optical micrographs of individual severe sliding wear particles. The particle in **Figure 1.5.7** shows colors caused by surface heating resulting from a high sliding speed.

1.6 NONFERROUS METALS

Metal particles are recognized to be nonferrous by their nonmagnetic deposition pattern on ferrograms. Instead of lining up with the magnetic field to occupy a place in an orderly string of ferrous particles, a nonferrous particle will be deposited with random orientation, quite likely off, or between, strings of ferrous particles. **Figure 1.6.1** shows an aluminum particle deposited between strings of ferrous particles near the entry region of the ferrogram. Ferrous particles are oriented with their major dimension closely aligned with the direction of the string, whereas aluminum particles are randomly oriented. Nonferrous particles deposit along the entire length of the ferrogram, whereas ferrous particles larger than 2 or 3 μm in major dimension do not penetrate past the 50 mm position. Therefore, if a metal particle larger than a few micrometers is seen some distance down from the entry, it is nonferrous. **Figure 1.6.2** shows an aluminum particle deposited near the exit end of the ferrogram. Notice how small the ferrous debris is in the adjoining strings

1.6.1 White Nonferrous Metals

White nonferrous metal particles are virtually indistinguishable when examined with the optical microscope. All are white and lustrous unless coated with oxides or compounds.

Table 1.6.1 is presented as a guide to identifying white nonferrous metals when SEM X-ray analysis is unavailable. The first two columns summarize results of wet chemical analysis using either 0.1 N acid or 0.1 N base applied in small droplets onto a ferrogram heated to 90° C/195° F on a laboratory hot plate. Heating encourages the reaction and hastens evaporation of the acid or base solution. The size of the droplet delivered onto the ferrogram should be kept small since the liquid has a tendency to move particles so that locating a particle after treatment can be difficult. The last four columns of Table

1.6.1 describe the color changes the various nonferrous metals undergo when they are heat treated on a ferrogram to the temperatures indicated. Paragraph 3.2.6, Heating of Ferrograms, describes this technique in detail. Between wet chemistry and heat treatment, all the white nonferrous metals can be distinguished from one another with the exception of silver and chrome which behave similarly. If either silver or chrome is suspected, knowledge of the lubricant-wetted path (material survey data) in the system under scrutiny may resolve the question. Also, chrome particles usually are quite small because chrome is such a hard material. Softer metals tend to generate larger particles. Bear in mind that the test results given by Table 1.6.1 were obtained using commercially pure metals. Alloys, even when the alloying elements are present in fractions of a percent, can have much different physical properties and can, therefore, react differently to the identification procedures suggested in Table 1.6 1.

As a practical matter, aluminum is the most frequently encountered white nonferrous metal found on ferrograms. Magnesium, molybdenum, and zinc would not normally be found in an oil-wetted contact. Titanium is used in aircraft gas turbines, but more frequently in the gas path section of the engine than the oil-wetted path. Titanium parts in wear contacts must be well lubricated because of the tendency for titanium to gall. Chrome is used as a hard, wear resistant coating, and as an alloying element for steel. Parts are never fabricated from chrome because it is too brittle. Silver is occasionally used as an overlay in high quality bearings. Cadmium is sometimes used as a component in bearing alloy or as a coating.

1.6.2 Copper Alloys

Copper alloys are easily recognized by their characteristic reddish-yellow color. No other common metal is so colored, with the exception of gold, which is used only in exotic applications. However, other metal particles can display yellow or tan interference (temper) colors due to excessive heat during their generation which may cause them to be confused with copper alloy particles. See paragraph 3.2.6, Heating of Ferrograms. Tan ferrous particles will not be easily confused because of their magnetic deposition pattern on a ferrogram (copper is nonmagnetic). Other particles, such as titanium, austenitic stainless steel, or babbitt metal could be tan given the right formation conditions, but in most instances the color will not be as even as copper alloy and in any circumstances the color will not be as reddish as some copper alloys are. If some tan, temper colored, nonferrous metal particles are present of the type which could be mistaken for copper alloy, there should also be particles of the same metal which have not been affected and some which show further coloring (temper blue or purple). It is unlikely that any wear process will consistently temper all particles to the same color.

Copper alloys, themselves, will form temper colors when heat treated on a ferrogram or when subjected to heat during their formation. However, these color changes are not useful for identifying specific copper alloys because of the many possible alloys

Fig. 1.5.1 Opt. M. 225X ⟵100μm⟶

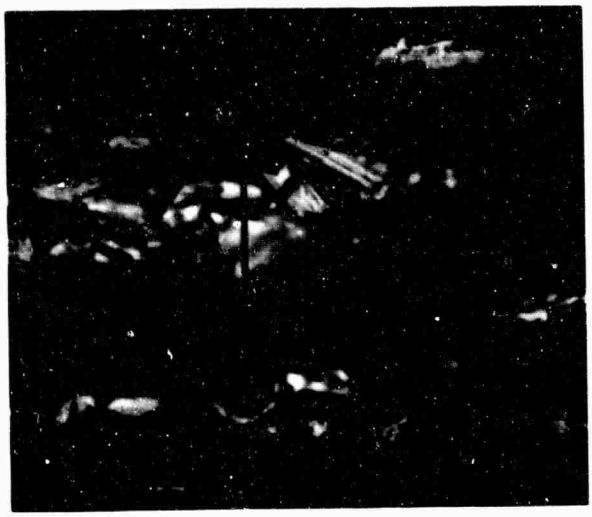

Fig. 1.5.2 Opt. M. 450X ⟵50μm⟶

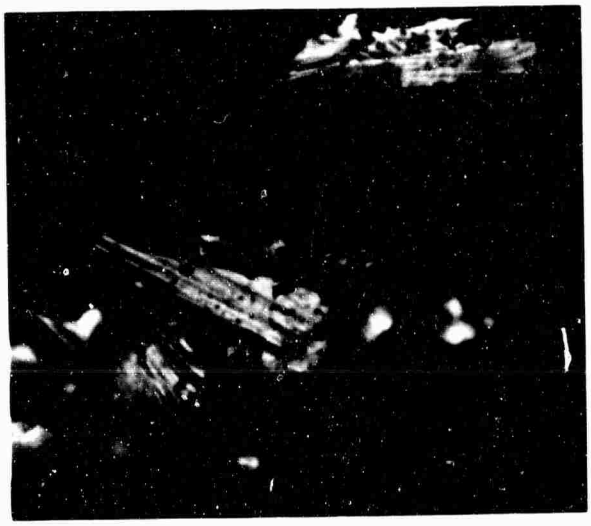

Fig. 1.5.3 Opt. M 1000X ⟵20μm⟶

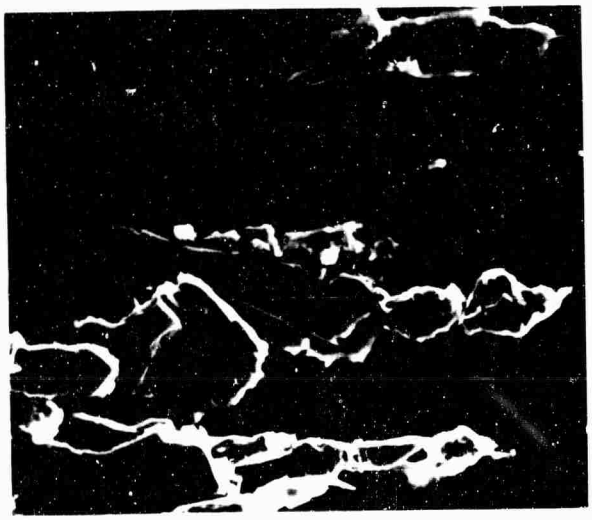

Fig. 1.5.4 S.E.M. 1000X ⟵20μm⟶

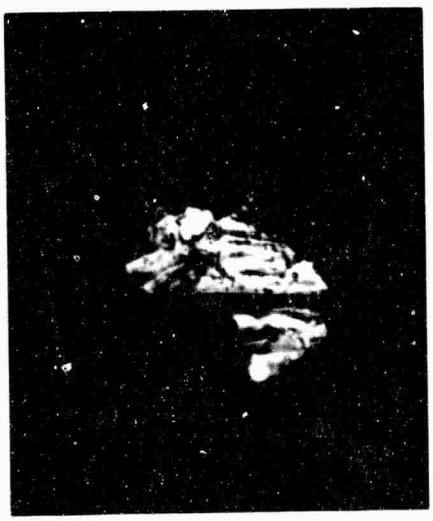

Fig. 1.5.5 Opt. M 450X ⟵50μm⟶

Fig. 1.5.6 Opt. M. 1000X ⟵20μm⟶

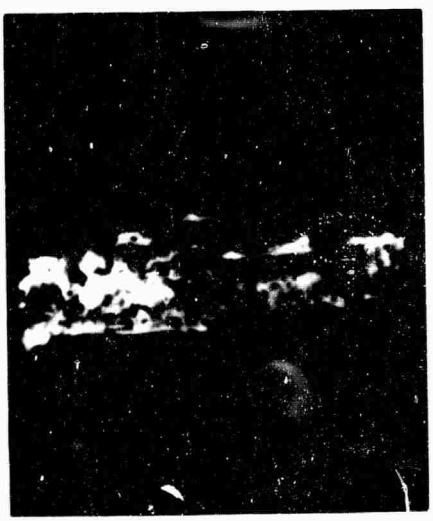

Fig. 1.5.7 Opt. M. 1000X ⟵20μm⟶

TABLE 1.6.1

IDENTIFICATION OF WHITE NONFERROUS METALS

	0.1 N HCl	0.1 N NaOH	330°C/625°F	400°C/750°F	480°C/900°F	540°C/1000°F
Al	sol	sol	N.C.	N.C	N.C.	N.C.*
Ag	insol	insol	N.C.	N.C.	N.C.	N.C.
Cr	insol	insol	N.C.	N.C.	N.C.	N.C.
Cd	insol	insol	tan	—	—	—
Mg	sol	insol	N.C.	N.C.	N.C.	N.C.
Mo	insol	insol	N.C.	tan with straw to some deep purple		—
Ti	insol	insol	N.C.	light tan	tan	deeper tan
Zn	sol	insol	N.C.	N.C.	tan	tan with blue
NOTE. Put ferrogram on 90°C/195°F hot plate. Add drop of acid or base. Leave ferrogram on hot plate until drop evaporates			Each test above is done by putting ferrogram on a hot plate of the specified temperature for 90 seconds.			

Abbreviations sol soluble
insol insoluble
N.C. no change

* may become brighter in some circumstances

and because the same alloy may have a different reaction depending upon grain structure, phase segregation, and previous plastic deformation caused by the wear process.

Figure 1.6..2.1 shows a copper particle deposited between strings of ferrous particles near the entry of a ferrogram. **Figure 1.6.2.2** shows the same view after heat treating the ferrogram to 330° C/625° F. **Figure 1.6.2.3** shows a copper particle obtained from a grease sample from a railroad axle rolling element bearing. Copper grounding brushes are used to prevent electropitting of the bearings. In this case the copper has partially oxidized to a dull gray color. Quite a few copper particles from this sample were entirely gray. The last three photographs show the range of surface colors possible for copper alloys depending upon their history.

1.6.3 Lead/Tin Alloys

It is unusual to encounter many free metal Pb/Sn alloy particles on ferrograms, probably because the metal is so ductile that it will smear rather than break to form particles. When Pb/Sn particles are found on ferrograms, it is likely that the particles will be oxidized. This is because Pb/Sn is extremely susceptible to oxidation at temperatures that are considered low in ferrous metallurgy. In fact, one failure mode encountered for journal bearings is an oxidative wear mode associated with poor lubrication and/or problems establishing or maintaining a hydrodynamic oil film when starting or stopping. Disassembly of a bearing with such a problem shows a "black scab' from Pb/Sn oxides.

Two other principal failure modes for Pb/Sn bearings are contamination and corrosive wear. Contamination is indicated by nonmetallic crystalline particles and cutting wear from the shaft. Corrosive wear causes a heavy deposit of very fine particles at the exit end of the ferrogram. Corrosive wear is most often encountered in internal combustion engines, most notably in diesels where sulfur in the fuel forms sulfuric acid, but in gasoline or gas-fired engines by the formation of organic acids as the crankcase oil oxidizes. These acids attack Pb Sn bearings as well as cause accelerated ring/piston wear. Lead is more susceptible to corrosion than tin.

In some journal bearing failures monitored by ferrography, copper alloy particles, which are extremely easy to recognize, are found in addition to oxidized Pb/Sn particles In these bearings, a thin layer of babbitt metal coats copper alloy, resulting in superior fatigue strength due to the copper alloy but with the desired surface properties of babbitt metal. Bearings constructed this way are particularly amenable to ferrographic analysis because if a number of copper alloy particles are found, it is reasonably certain that the bearing has been stripped Knowledge of the bearing design in the machine being monitored should be obtained in order to make a proper analysis.

In order to be able to recognize bearing alloys, old bearings should be obtained from some of the various machines being monitored Using fine emery paper or silicon

carbide paper, abrade some of the bearing metal, disperse it in filtered oil, and prepare a ferrogram. Observe what the metal looks like, then heat treat on a hot plate for 90 seconds up to 1000° F (the practical maximum temperature above which the ferrogram glass will most likely warp) in steps of about 100° F. Observe the babbitt particles after each heat treatment. Typically, oxidized Pb/Sn particles will have a multicolored, stippled appearance. At low magnification they will be blackish, but at 400x or 1000x, dots of blue and orange color will be seen on the surface (see **Figures 1.6.3.1** and **1.6.3.2**). Often the particles will be rather chunky, but sometimes they are flat with rounded edges where partial melting has taken place. **Figure 1.6.3.3** shows a Pb/Sn alloy particle obtained from a reciprocating aircraft engine. This photograph was taken prior to any heat treatment of the ferrogram.

Be aware that the melting temperature for the Pb/Sn alloy system is below the first heat challenge temperature (330° C/625° F) for distinguishing ferrous alloys on ferrograms. Therefore, if a free metal Pb/Sn particle is present on a ferrogram, the first heat treatment, normally done to distinguish low alloy steel from cast iron, will exceed the melting point. However, the Pb/Sn particle, instead of melting and pulling itself together into a globule by surface tension forces, will become grossly oxidized and have the multicolored, stippled appearance described above. This is due to the great affinity Pb/Sn alloys have for oxygen at elevated temperatures and is part of the reason why, if a pot of lead is melted on a stove, scale forms on the surface.

Figures 1.6.3.4 and 1.6.3.5 show a high tin babbitt particle before and after heat treating to 330° C/625° F. This particle was obtained from an oil sample taken from the bearing cavity of an 800 horsepower centrifugal fan in a power plant.

1.7 FERROUS OXIDES

Ferrous oxides are divided into two groups for purposes of identification, namely, red oxides and black oxides. The situation is actually more complicated due to the existence of three stoichiometric compounds, FeO, Fe_2O_3, and Fe_3O_4, as well as several crystalline forms of these compounds. However, as a general rule, red oxides, which are the final reaction product of iron and oxygen at room temperature, indicate moisture in the lubrication system, whereas black oxides indicate inadequate lubrication and excessive heat during particle generation.

1.7.1 Red Oxides of Iron

In work done to characterize regimes of wear between sliding steel surfaces[5], red oxides, which were determined to be hematite (αFe_2O_3) by X-ray diffraction analysis, were produced under poorly lubricated wear conditions. The particles were of two types. The first type is polycrystalline and appears orange in reflected white light (**Figure 1.7.1.1**) and appears saturated orange in polarized reflected light (**Figure 1.7.1.2**). This type is referred to as red oxide and is the common type of hematite

produced when water gets into an oil system. Red oxides are difficult to obtain under lubricated conditions but are common when water has entered the lubricant Red oxides are familiar to everyone as rust.

Water need not be in the oil sample at the time the sample is taken for red oxides to be present. If water had been in the oil at some previous time, red oxides could form and be present in a later sample. Usually, however, water will be present in the oil sample if many red oxides (especially large ones) are present.

Red oxides show varying color and appearance because (1) αFe_2O_3 is not the only crystalline form of Fe_2O_3; (2) in the presence of excess water hydrated iron oxide of various stoichiometry will occur; (3) in the presence of other elements or compounds red iron containing compounds occur; and (4) the size of the crystals in polycrystalline clusters will influence their appearance in polarized light.

The alpha hematite form of iron oxide, encountered as orange/red polycrystalline agglomerates, is paramagnetic and will, therefore, not deposit in a strongly magnetic manner so that large red oxide particles are found at all locations on a ferrogram.

The second type of red oxide particles produced under poorly lubricated wear conditions are flat, sliding wear particles which appear gray in white reflected light but are dull reddish-brown in white transmitted light. The surfaces of these particles are highly reflective so that even in bichromatic light (red reflected and green transmitted light) they can be mistaken for metal wear particles. Careful examination, however, shows that these particles are not as bright red in bichromatic light as are free metal particles, and in extremely thin sections some green light will penetrate from below. **Figure 1.7.1.3** shows several of these iron oxide particles in bichromatic light. **Figure 1.7.1.4** shows the same view in white reflected and green transmitted light, and **Figure 1.7.1.5,** taken with white transmitted light, shows these particles are reddish-brown. These flat iron oxide particles are clearly generated by a wear contact so that when these are present, either with or without polycrystalline red oxides, a poorly lubricated wear contact is indicated.

If an oil sample is analyzed and red oxides are found, it is a simple matter to test for water in the oil by placing a drop of oil on a hot plate at about 300° F. The water will sputter or sizzle if more than approximately 0.25% water is present.

1.7..2 Black Oxides of Iron

Black oxides of iron are associated with a more severe form of inadequately lubricated wear than are red oxides. X-ray diffraction analysis done in conjunction with work to characterize regimes of wear[6] identified black oxides as a nonstoichiometric compound containing a mixture of Fe_3O_4, αFe_2O_3, and FeO. Water in oil does not produce black oxides; rather, it produces red oxides.

Fig 1.6.1 Opt. M. 1000X ⊢— 20μm —⊣

Fig 1.6.2 Opt. M. 1000X ⊢— 20μm —⊣

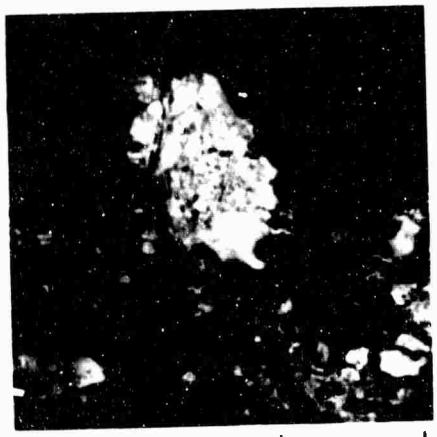

Fig 1.6.2.1 Opt. M. 1000X ⊢— 20μm —⊣

Fig 1.6.2.2 Opt. M. 1000X ⊢— 20μm —⊣

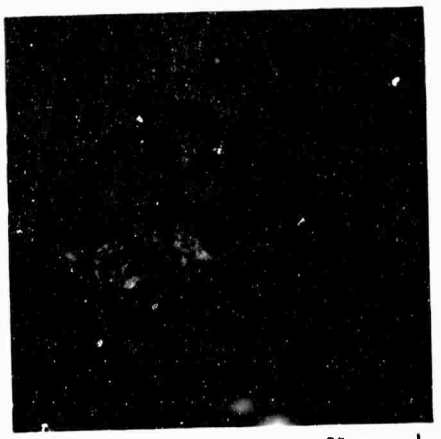

Fig. 1.6.2.3 Opt. M. 400X ⊢— 50μm —⊣

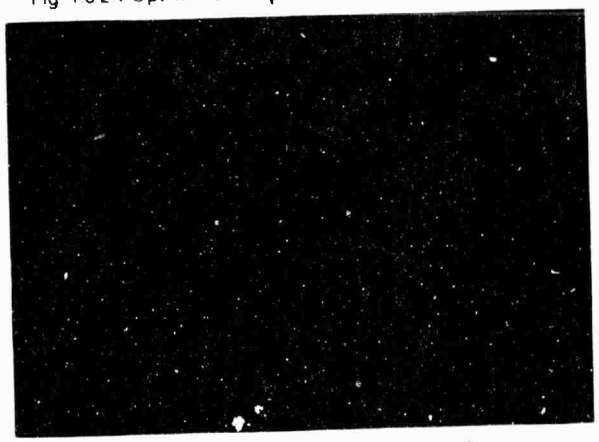

Fig 1.6.3.1 Opt. M. 400X ⊢— 50μm —⊣

Fig 1.6.3.2 Opt. M. 1000X ⊢— 20μm —⊣

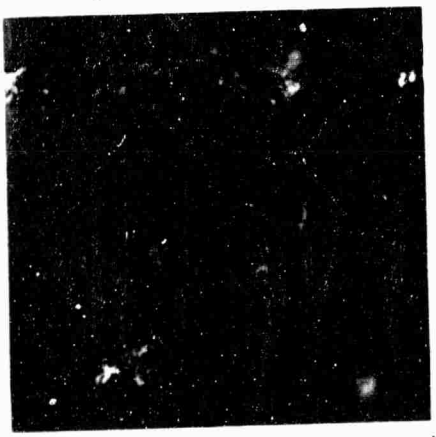

Fig 1.6.3.3 Opt. M. 1000X ⊢— 20μm —⊣

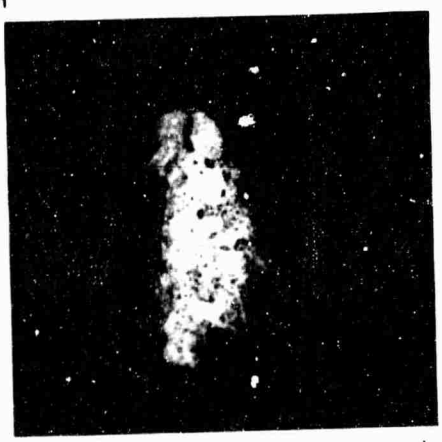

Fig 1.6.3.4 Opt. M. 400X ⊢— 50μm —⊣

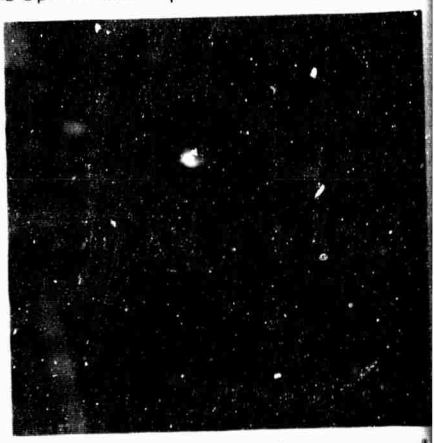

Fig 1.6.3.5 Opt. M. 400X ⊢— 50μm —⊣

Black oxide particles appear as clusters with a pebbled surface and have small dots of blue and orange color near the lower limit of resolution of the optical microscope. **Figures 1.7.2.1** and **1.7.2.2** show a black oxide agglomerate deposited at the entry region of a ferrogram prepared from an oil sample of a diesel engine undergoing severe cylinder scoring. The edges of black oxide particles will permit the transmittance of some light because of their nonmetallic structure. However, they do not shine brilliantly in polarized light because they are efficient light absorbers. **Figure 1.7.2.3** shows a field of view with black oxides and black-oxide-coated ferrous particles. Black oxides look similar to babbitt metal oxides since they have black, pebbled surfaces. However, Fe_3O_4, magnetite, is ferromagnetic so that black oxide agglomerates will deposit in a manner similar to other ferromagnetic materials.

1.7.3 Dark Metallo-Oxides

Partially oxidized ferrous wear particles are classified as dark metallo-oxides. These indicate the presence of heat during their generation and may indicate lubricant starvation. Large dark metallo-oxides are clearly an indication of catastrophic surface failure. Much smaller dark metallo-oxides, as are codeposited with strings of normal rubbing wear particles, may not indicate imminent failure. Nevertheless, the presence of any dark metallo-oxides is considered to be a sign of abnormal wear.

Figure 1.7.3.1 shows a string of wear particles comprised of normal rubbing wear particles and dark metallo-oxides. Both particle types deposit ferromagnetically. The dark metallo-oxides are dull gray whereas the free metal rubbing wear particles are white and lustrous. **Figure 1.7.3.2** shows the same view after heat treatment of the ferrogram to the first heat challenge temperature for the identification of ferrous alloys. See paragraph 3.2.6. Notice that the dark metallo-oxides remain unaffected whereas the free metal wear particles show blue or straw temper color depending upon their metallurgy. The dark metallo-oxides remain unaffected because these particles already had a thick oxide layer before heat treatment of the ferrogram. The blue or straw temper colors on the other particles are a result of the growth of a thin oxide layer, as explained in paragraph 3.2.6. In fact, it is not unusual to see particles oxidized to varying degrees from samples where the machine has been undergoing lubricant starvation. Some of the particles may show temper colors, others are dark metallo-oxides, and others are black oxides. **Figure 1.7.3.3**, from a diesel engine undergoing cylinder scoring, shows particles with varying degrees of oxidation.

1.8 LUBRICANT DEGRADATION PRODUCTS AND FRICTION POLYMERS

1.8.1 Corrosive Wear Debris

The three photographs presented in this section were obtained from a ferrogram prepared with oil from a diesel engine that was purposely subjected to a corrosive wear test. The effect of the test was to produce many fine particles, most of which are below the lower limit of resolution of the optical microscope; that is, the particulate matter

may be described as submicron. An unusual feature of the ferrograms obtained from this test is that the optical density reading (percent area covered) at the 10 mm position was greater than at the 50 mm position. Corrosive wear is indicated by a heavy deposit of fine particles at the exit end of the ferrogram.

Figure 1.8.1.1 shows a heavy deposit of fine particles at the exit end of a corrosive wear debris ferrogram. **Figures 1.8.1.2 and 1.8.1.3** are successively higher magnification views at the exit end. Notice that even at the highest magnification individual particles are not readily distinguishable.

This deposit was subjected to an area scan using an X-ray analyzer attached to a SEM with the result that the major metallurgical elements present were iron, aluminum, and lead.

1.8.2 Friction Polymers

Friction polymers are characterized by metal wear particles embedded in an amorphous matrix. They are thought to be created by overstress on a lubricant in a critical contact. Their structure is apparently a result of the polymerization of the oil molecules to form a large coherent structure. If an oil sample contains friction polymers, these polymers always have metal particles embedded within the amorphous structure. This observation indicates that friction polymers are formed in high stress zones of critical contact and that the presence of metal may be necessary to catalyze their formation.

The presence of friction polymers in an oil sample may or may not be worrisome depending upon circumstances. With the right oil, friction polymers are produced under the influence of heavy load. For certain applications, especially high performance gears such as in helicopter transmissions, the formation of friction polymers prevents scuffing that would otherwise occur. However, too many friction polymers are deleterious to machine health because (1) the viscosity of the oil will increase due to the presence of foreign bodies; and (2) the friction polymers can rapidly clog oil filters, causing them to bypass, thus allowing large contaminants and wear particles to reach working parts of the machine.

Friction polymers are encountered in oil from many types of equipment. The presence of friction polymers in an oil sample from a type of machine that usually does not produce them is interpreted to mean that overload has occurred. **Figures 1.8.2.1 and 1.8.2.2** show friction polymers generated by a steel-on-steel wear test with conditions of high load. Severe wear particles and cutting wear particles were also present on this ferrogram which are symptomatic of overload. Bichromatic illumination is the best way to view friction polymers because it highlights the metal wear particles (red), while showing the transparent (green) nature of the matrix.

Figures 1.8.2.3 and 1.8.2.4 show friction polymer from a traction transmission. This application, wherein power is transmitted by the tractive mating of two smooth steel

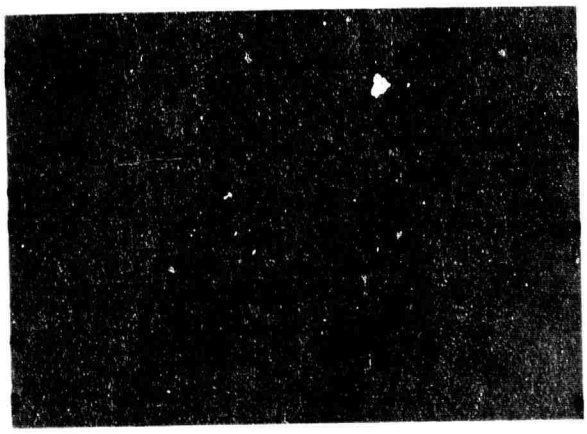

Fig. 1.7.1.1 Opt. M. 400X ⊢— 50μm —⊣

Fig. 1.7.1.2 Opt. M. 400X ⊢— 50μm —⊣

Fig. 1.7.1.3 Opt. M. 1000X ⊢— 20μm —⊣

Fig. 1.7.1.4 Opt. M. 1000X ⊢— 20μm —⊣

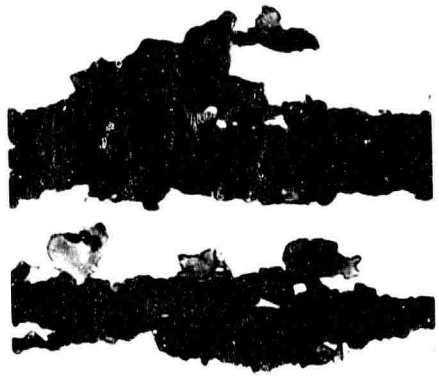

Fig. 1.7.1.5 Opt. M. 1000X ⊢— 20μm —⊣

Fig. 1.7.2.1 Opt. M. 400X ⊢— 50μm —⊣

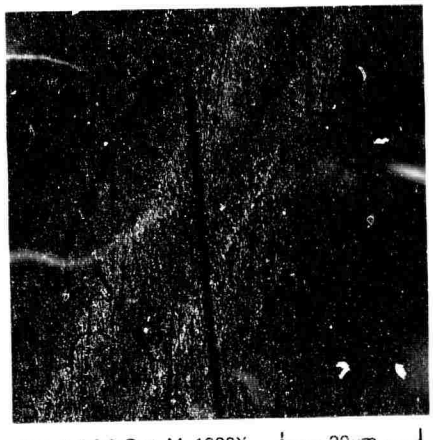

Fig. 1.7.2.2 Opt. M. 1000X ⊢— 20μm —⊣

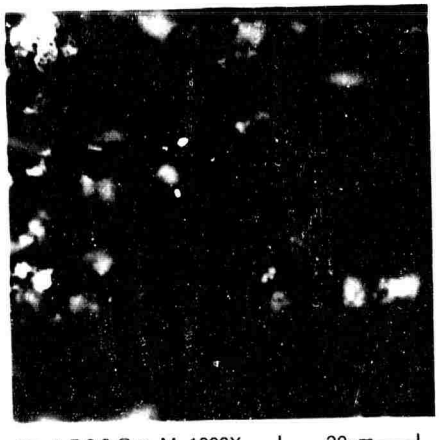

Fig. 1.7.2.3 Opt. M. 1000X ⊢— 20μm —⊣

Fig. 1.7.3.1 Opt. M. 1000X ⊢— 20μm —⊣

Fig. 1.7.3.2 Opt. M. 1000X ⊢— 20μm —⊣

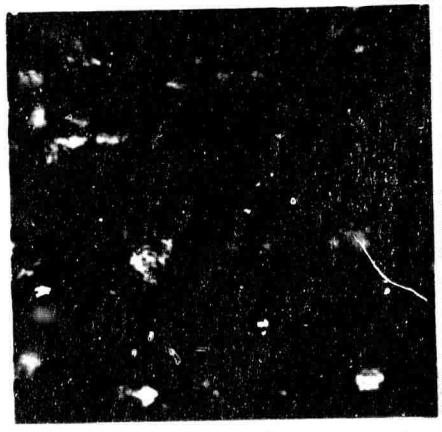

Fig. 1.7.3.3 Opt. M. 1000X ⊢— 20μm —⊣

Fig. 1.8.1.1 Opt. M. 100X ⊢— 200μm —⊣

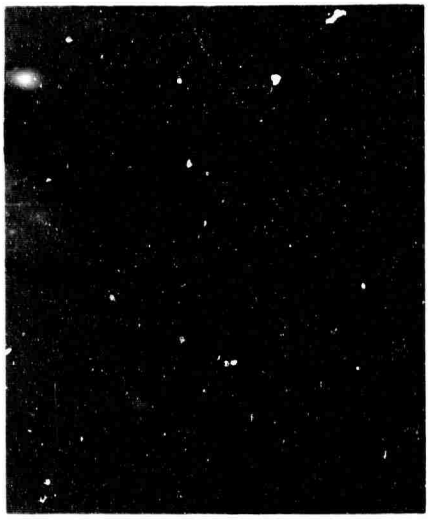

Fig. 1.8.1.2 Opt. M. 400X ⊢— 50μm —⊣

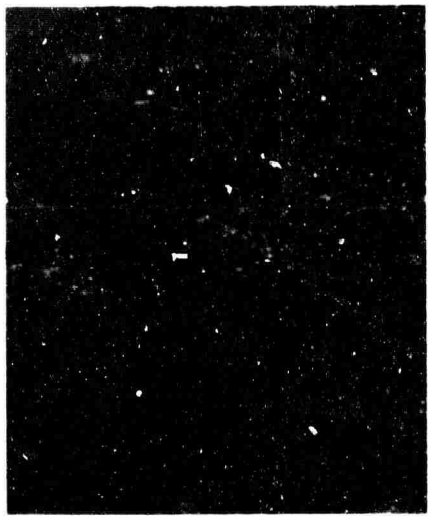

Fig. 1.8.1.3 Opt. M. 1000X ⊢— 20μm —⊣

Fig. 1.8.2.1 Opt. M. 400X ⊢— 50μm —⊣

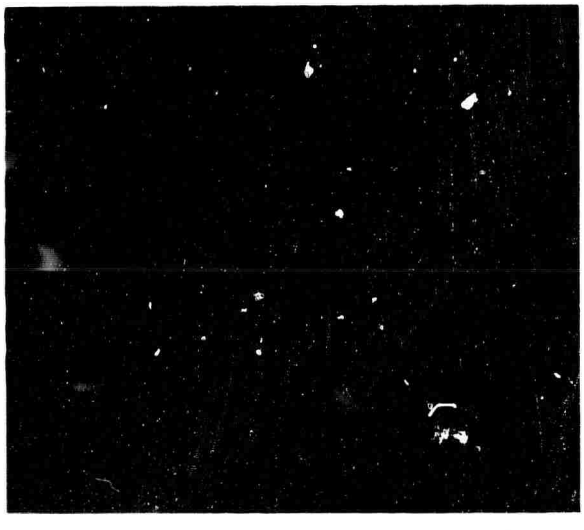

Fig. 1.8.2.2 Opt. M. 1000X ⊢— 20μm —⊣

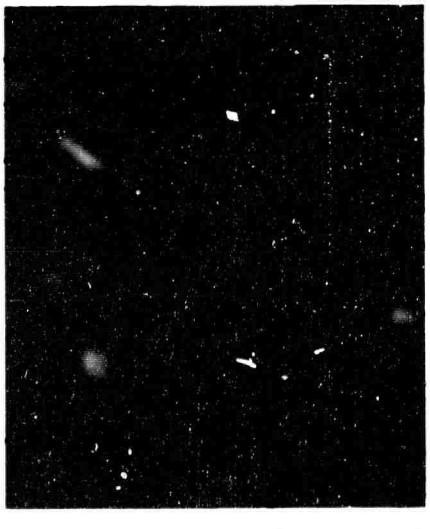

Fig. 1.8.2.3 Opt. M. 400X ⊢— 50μm —⊣

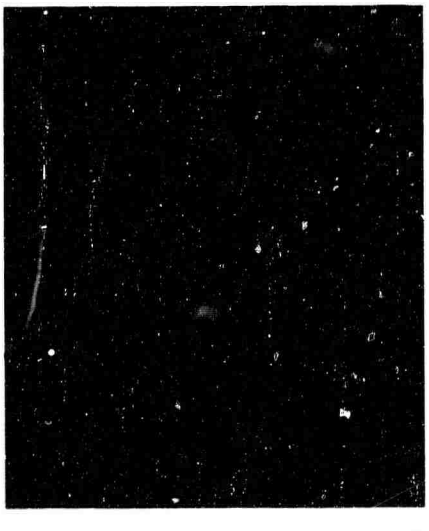

Fig. 1.8.2.4 Opt. M. 1000X ⊢— 20μm —⊣

Fig. 1.8.2.5 Opt. M. 1000X ⊢— 20μm —⊣

surfaces, may be one of the most demanding in regard to the formation of, or more correctly, the suppression of the formation of friction polymer. It is theorized that in a traction transmission, the lubricant, when st. .ssed in critical contact, forms a solid; but when the contact is relieved the lubricant reverses to a liquid. Evidence of irreversibility was found in the oil by the presence of many large friction polymers. **Figures 1.8.2.3 and 1.8.2.4** show the same view using bichromatic illumination at two different magnifications. **Figure 1.8.2.5** shows the same view as **Figure 1.8.2.4** in white reflected and green transmitted light. The large bright metal particles embedded in the friction polymer are aluminum, which is what the transmission case was made from.

Most friction polymers are quite resistant to heat degradation. Heat treatment to the first challenge temperature (330° C/625° F) for the classification of ferrous alloys, usually causes no discernible change to friction polymers. Even heat treatment to 480° C/900° F, which is devastating to most biologically formed organic materials, causes only partial volatilization of the amorphous friction polymer material which attests to the stability of these lubricant by-products. Friction polymers are also quite resistant to attack by organic solvents. Therefore, once friction polymers are formed in a lubrication system, they are not easily destroyed.

1.8.3 Molybdenum Disulfide

Molybdenum disulfide particles can cause confusion when they are present on a ferrogram because they look and behave much like nonferrous metal particles. However, once it is learned how to recognize MoS_2 particles, they are quite obvious. Molybdenum disulfide is used as a solid additive in oils and greases in applications where high temperature and high load are anticipated. It is an effective solid lubricant because it has high compressive strength to carry load but low shear strength, which causes it to be slippery. Because of the low shear strength MoS_2 particles show many shear planes and have straight edges with regular angles. **Figure 1.8.3.1** shows a typical MoS_2 particle. The color is a grayish-purple and is quite distinct from the white, lustrous appearance of nonferrous metals. Molybdenum disulfide particles cause confusion with nonferrous metals because they block light like metal particles although MoS_2 is a compound. Molybdenum disulfide is described as a semimetallic compound because of its metallic characteristics.

Figure 1.8.3.2 shows small MoS_2 particles deposited along the non-wetting barrier of a ferrogram. This ferrogram was prepared from an unused oil sample with MoS_2 additive. In this oil, the MoS_2 was much more finely dispersed than for the oil from which **Figure 1.8.3.1** was obtained. Molybdenum disulfide has a negative magnetic susceptibility so that, in its pure form, it should be repulsed by the magnetic field of the ferrograph. Deposition along the non-wetting barrier is evidence of its repulsion by the ferrograph. Presumably, for this sample, most of the MoS_2 was repelled by the magnetic field of the ferrograph and was rejected with the fluid as it flowed off the exit end of the ferrogram.

Figure 1.8.3.3 shows wear debris on a ferrogram made from used oil of the same type as described above. The ferrogram was heat treated to 330° C/625° F so that the steel particles turn blue. The MoS_2 particles remain unaffected (as they do to even the highest heat treatment temperature used for ferrograms), and are therefore easily distinguished from the ferrous wear particles. This ferrogram was prepared from a 1000:1 dilution whereas the ferrogram for **Figure 1.8.3.2**, made from unused oil, was undiluted. The used oil appears to contain many more MoS_2 particles, considering the dilution factor, than the unused oil. This is due to the intimate contact between the MoS_2 and the ferrous surfaces which magnetizes the MoS_2 to some degree. Also, for this sample, many friction polymers were present in which both ferrous particles and MoS_2 particles were embedded. The ferrous particles make the friction polymers sufficiently magnetic so that they are efficiently deposited on the ferrogram.

1.9 CONTAMINANT PARTICLES

1.9.1 Contaminants in Unused Oil

Most oil, taken clean from the can or drum, contains varying amounts of particulate matter. Certainly, any oil intended for diluting samples must be carefully filtered. Good results can be obtained by filtering through a surface-type filter with a pore size of about 0.4 μm. The damage to machinery resulting from clean oil contaminants depends mainly on how hard the contaminant particles are, how large they are, their quantity, and, of course, how critical the application is. Precision bearings, for example, could be ruined by the introduction of contaminated oil. However, many machines are protected by high efficiency filters between the tank and the machine where the introduction of particulates in the oil may only increase wear on the high pressure pump that delivers the oil from the tank, through the filter, to the machine. In this instance, contaminants are of minor significance as long as the concentration is not great enough to clog the filter and cause bypass flow.

Figure 1.9.1.1 shows the entry of a ferrogram prepared from synthetic polyester oil (MIL-L-23699) taken from a freshly opened can. The concentration of particles is several times the concentration normally found in used oil of this type from certain jet engines. **Figure 1.9.1.2** shows a higher magnification view of the entry, and **Figure 1.9.1.3** shows the same view in polarized reflected light. Among the particles found in this example are free metal particles, black and red oxides, and nonmetallic crystalline debris. All of these are potentially harmful due to their size and hardness.

1.9.2 Contaminants in Unused Grease

In general, grease is used only where it is impractical to have a circulating oil system. Grease is oil to which a filler has been added to increase viscosity to the point where the mixture is cohesive. When the grease is squeezed in service between two contacting machine parts, oil is released to lubricate the contact.

The particles in a grease sample may be scrutinized by dissolving the grease with a suitable solvent, then preparing a ferrogram. A mixture of toluol and hexane is effective at dissolving many commonly available greases. See paragraph 3.2.8.

Large, abrasive particles in grease may be more damaging than the same particles in oil because once the grease is applied, no opportunity exists for the contaminant particles to be removed; whereas in oil, the particles may be quickly removed by filtering.

Figure 1.9.2.1 shows some typical contaminant particles on a ferrogram prepared from about 1 cc of unused military aircraft grease (MIL-G-81322 B) suitable for lubricating splines. The concentration does not appear exceedingly high considering that 1 cc of used grease would provide hundreds to thousands times more particles. Many of the ferrous particles found in this grease were high alloy steel, suggesting they may be from the equipment that mixes the filler with oil to produce grease. **Figure 1.9.2.2** shows the entry view in white reflected light after heat treatment of the ferrogram to 480° C/900° F. Most of the ferrous particles have turned to a tan color, indicating high alloy (stainless) steel.

Figure 1.9.2.3 shows small fiber-shaped particles that are most likely a component of the filler. These fine particles were evenly deposited on the exit end of the ferrogram below about the 30 mm position.

1.9.3 Road Dust

This section presents photographs taken of a ferrogram which was prepared by dispersing AC Fine Test Dust, also known as Arizona Road Dust, in oil. The dust is prepared by General Motors AC Division at a Phoenix laboratory from locally obtained material. It is size classified and sold to many different laboratories for a variety of tests including filter efficiency tests, wear tests, and aerosol measurement tests. It may well be the most popular test dust available.

Arizona Road Dust is meant to be typical of what a car or off-road vehicle is exposed to. It contains mostly silica (SiO_2), but also contains a wide variety of other materials. Examination of the Road Dust ferrogram reveals quite a few dark metallo-oxide particles at the entry, but these are only a small fraction, certainly less than 1%, of the total. Red oxide (Fe_2O_3) particles are present as well.

Figure 1.9.3.1 shows a low magnification view of the road dust ferrogram. Ferromagnetic particles are aligned at the entry but most of the particles are not deposited in a strongly magnetic manner. **Figure 1.9.3.2** shows a view slightly downstream of the entry. Strings of ferromagnetic particles are seen aligned with the magnetic field of the ferrograph with the larger, siliceous particles randomly deposited. **Figure 1.9.3.3** shows the same view in polarized reflected light in which the nonmetallic material appears bright in an otherwise dark field.

1.9.4 Coal Dust

Figures 1.9.4.1 and 1.9.4.2 are illustrative of the oil contamination that can result from ingression of aerosols in an industrial environment. This oil sample was obtained from the diesel engine of a coal scraper operating at a strip mine. **Figure 1.9.4.1** was taken with bichromatic illumination. **Figure 1.9.4.2** shows the same view using white reflected and green transmitted light.

Coal dust, as it is found in the air at a mining operation, is a mixture of various components. Coal itself is rather soft and probably doesn't cause too much damage to oil lubricated parts. However, the dust contains quite a bit of silica in the form of quartz which is hard and abrasive, as well as other materials such as slate, iron oxides, and other minerals. These have the potential to do considerable damage. Therefore, machinery working in coal dust, and other industrial environments such as mining, ore extraction, cement production, quarrying, etc., should be protected against the ingression of contaminants into the oil system.

This sample was prepared by washing the ferrogram, after the oil had been passed along it, with methanol for a reasonably long time (15 cc was used), which dissolved some of the coal dust particles to expose the wear particles which were otherwise difficult to see. This can also be accomplished by adding a suitable solvent (alcohol is a good coal solvent) to a known quantity of oil sample and agitating the mixture in an ultrasonic bath to dissolve the unwanted particles.

1.9.5 Asbestos

Asbestos fibers may be distinguished from other common fibers, such as those used for filters, by their very fine size and by the fact that the fibers are capable of breaking or splitting to create even finer fibers. Even if asbestos is viewed at 1000x there will be individual fibers and splinters on larger fibers that will be at the lower limit of resolution of the microscope. Asbestos is the generic name of several mineral fibers. Crocidolite, as shown on **Figure 1.9.5.1**, is one type. However, chrysotile is the most commonly mined type in North America and is characterized by serpentine (curved) fibers. In spite of certain morphological differences, all asbestos is capable of becoming very finely divided.

Asbestos may be found in oil samples because it is used for brake linings, clutch plates, occasionally for special application filters, and insulation. Usually its presence in oil will be by ingression from air.

1.9.6 Machine Shop Air Contaminants

A glass slide smeared with petroleum jelly was left exposed for one work shift in a small machine shop with six workers. The slide was about 20 feet from the nearest operating machine. **Figure 1.9.6.1** shows the debris deposited on a ferrogram prepared from the

dissolved petroleum jelly. This provides some indication of the interference that could be caused if ferrograms are prepared near metal-working machinery. It also demonstrates that unprotected machinery is exposed to airborne contaminants which argues for closed sumps and proper air filters.

Most of the particles shown on **Figure 1.9 6.1** are ferrous and therefore could easily be misinterpreted as wear particles if lubricant was sampled from a machine working in that environment. Other contaminants, such as road dust or coal dust, can cause similar problems of interpretation because these dusts contain magnetic particles.

1.9.7 Filter Materials

Filters are used extensively in fuel, hydraulic, and lubrication systems to protect critical components from the ingression of harmful contaminant particles. Often filters will tear or shed so that filter fibers will be found in samples from these systems. The deposition of a few fibers on a ferrogram is not considered unusual or cause for concern, but if many fibers are present along with a higher than normal concentration of wear particles and contaminant particles, it may be suspected that holes have developed in the filter.

The most common filter media for routine applications such as gasoline and diesel engines is paper of various types. **Figure 1.9.7.1** shows cellulose in polarized transmitted light from a commonly used paper filter. Heat treatment will cause cellulose to char to a noticeable extent. It will usually shrivel somewhat, turn yellow, and become less bright in polarized light. Glass microfibers, **Figure 1.9.7.2**, are easily recognized by the fact that the center of the fibers do not disrupt polarized light but the edges are bright due to reflection and scattering of the polarized light. Synthetic fibers such as rayon, dacron, polyester, etc., show birefringent color effects in polarized light. **Figure 1.9.7.3** shows polyester fibers in polarized transmitted light. Synthetic fibers have smooth edges like fiberglass, but unlike cellulose.

1.9.8 Carbon Flakes

Figures 1.9.8.1 and 1.9.8.2 show carbon flakes from seal material at 200x and 400x magnification respectively. These particles are not contaminants; they are wear particles. These particles were deposited on a ferrogram made from an oil sample from a small swashplate type piston compressor with carbon seals. The spots of blue color visible on the 400x view are probably from fine steel particles embedded in the carbon.

This page left blank
intentionally.

Fig 1831 Opt M 1000X ⊢— 20μm —⊣

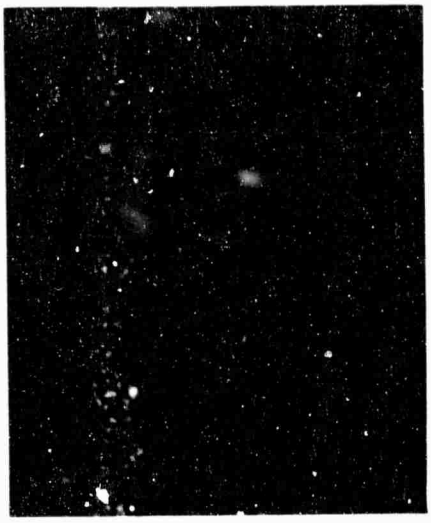

Fig 1832 Opt M 1000X ⊢— 20μm —⊣

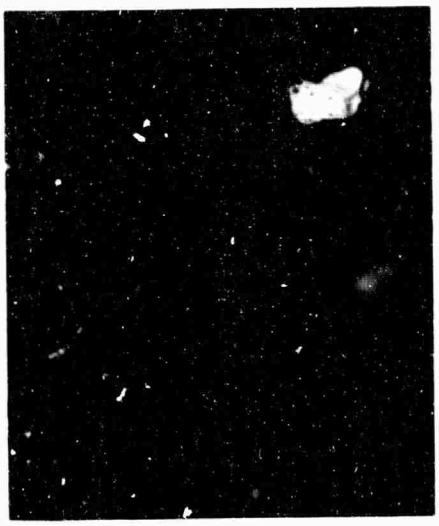

Fig 1833 Opt M 1000X ⊢— 20μm —⊣

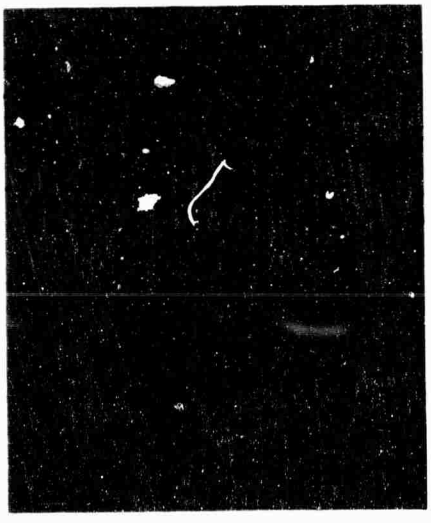

Fig 1911 Opt M 100X ⊢— 200μm —⊣

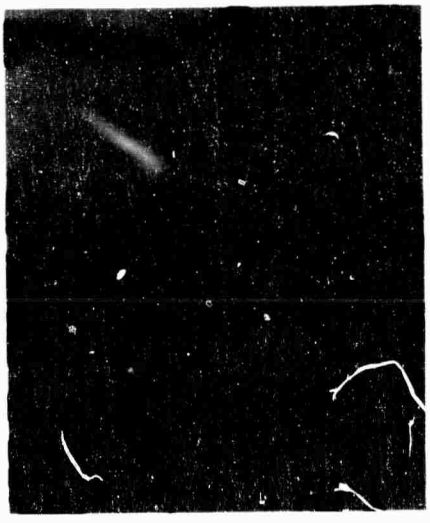

Fig 1912 Opt M 400X ⊢— 50μm —⊣

Fig 1913 Opt M 400X ⊢— 50μm —⊣

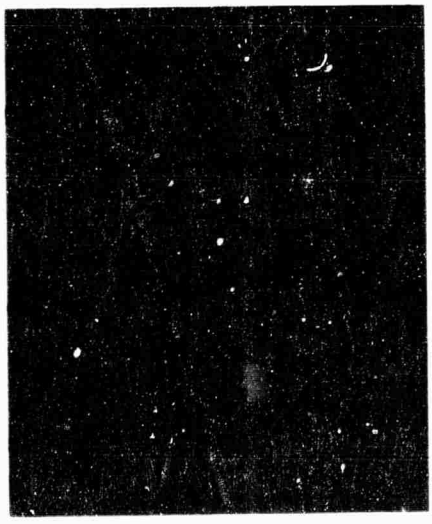

Fig 1921 Opt M 200X ⊢— 100μm —⊣

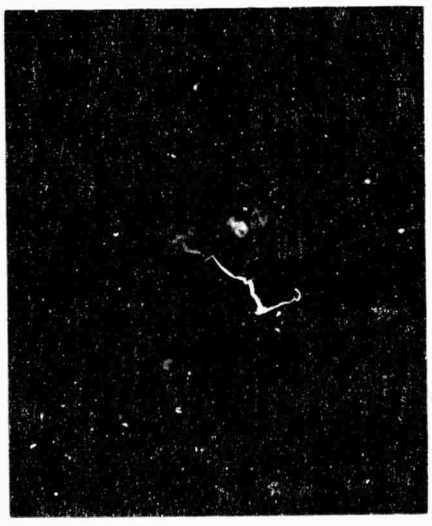

Fig 1922 Opt M 400X ⊢— 50μm —⊣

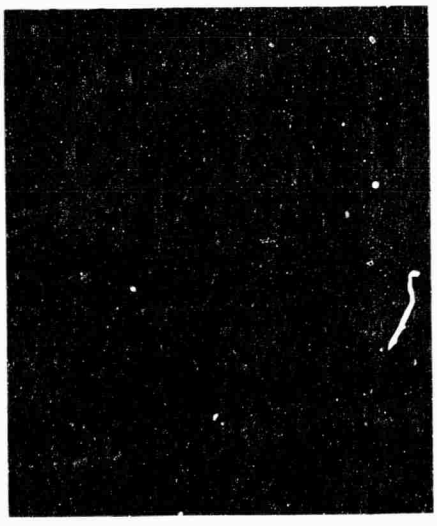

Fig 1923 Opt M 1000X ⊢— 20μm —⊣

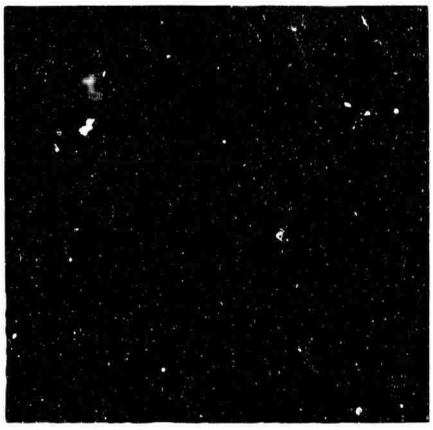

Fig. 1.9.3.1 Opt. M. 100X ⊢— 200μm —⊣

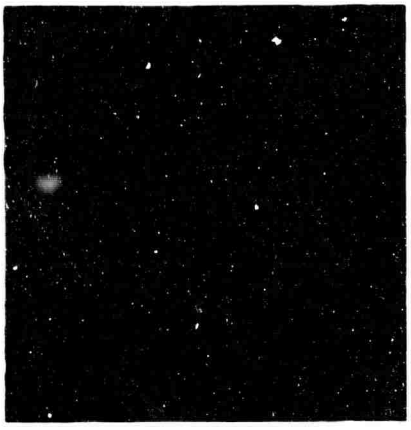

Fig. 1.9.3.2 Opt. M. 200X ⊢— 100μm —⊣

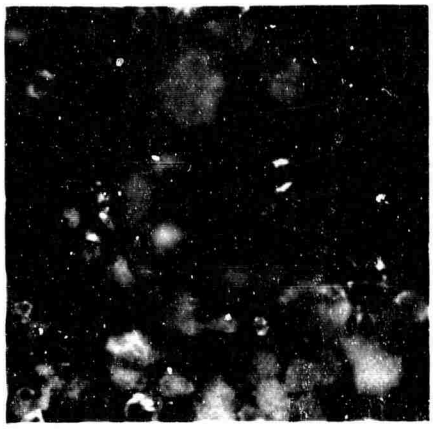

Fig. 1.9.3.3 Opt. M. 200X ⊢— 100μm —⊣

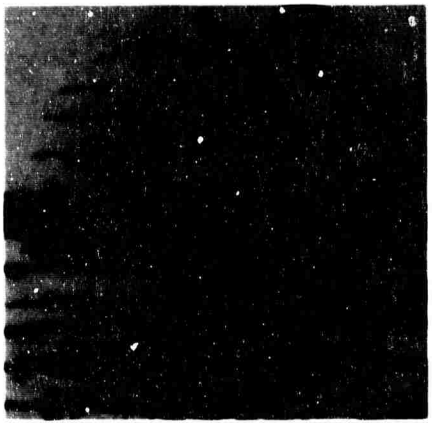

Fig. 1.9.4.1 Opt. M. 400X ⊢— 50μm —⊣

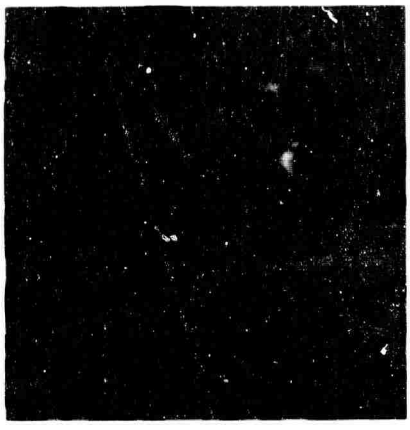

Fig. 1.9.4.2 Opt. M. 400X ⊢— 50μm —⊣

Fig. 1.9.5.1 Opt. M. 200X ⊢— 100μm —⊣

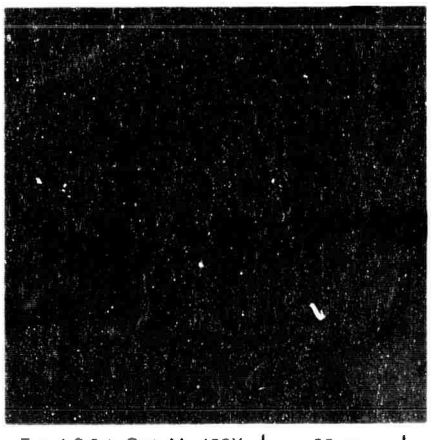

Fig. 1.9.6.1 Opt. M. 400X ⊢— 50μm —⊣

Fig. 1.9.7.1 Opt. M. 100X ⊢— 200μm —⊣

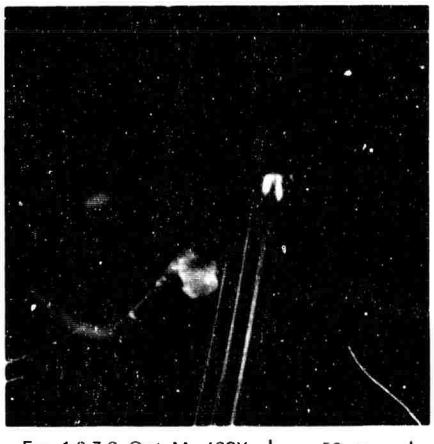

Fig. 1.9.7.2 Opt. M. 400X ⊢— 50μm —⊣

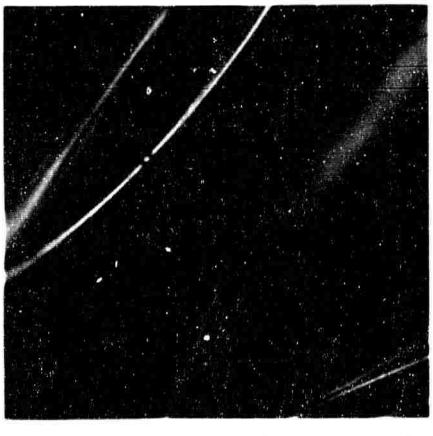

Fig. 1.9.7.3 Opt. M. 100X ⊢— 200μm —⊣

Fig. 1.9.8.1 Opt. M. 200X ⊢— 100μm —⊣

Fig. 1.9.8.2 Opt. M. 400X ⊢— 50μm —⊣

2. CASE HISTORIES

2.1 DIESEL ENGINES

Wear particle analysis for diesel engines, as for other oil lubricated equipment, provides important information regarding engine condition in three principal ways:

- A quantitative change in particle concentration and size distribution from established baseline values signals an abnormal wear mode;
- Examination of the particle morphology will reveal the wear mode such as severe sliding wear, lubrication starvation, contaminant induced wear, etc.; and
- The metallurgy of the particles may be determined by heat treatment of the ferrogram so that the part or parts in distress can be identified, or at least narrowed down to limited possibilities.[6,7] For diesels, heat treatment is used primarily to distinguish between low alloy steel and cast iron, which points mainly to crankshaft (steel) versus piston ring/cylinder (cast iron) wear problems. Although this generality is usually true, the possibilities are so varied that familiarity with the engine under scrutiny is necessary for specific conclusions.

In this section, examples of different types of wear problems detected by ferrography will be presented as follows:

(1) Cast iron wear — excessive piston ring/cylinder wall wear.

(2) Steel wear — crankshaft failure.

(3) Corrosive wear — typical wear debris from engine where the acid neutralizing additive was depleted.

(4) Abrasive wear — engine failure due to contaminant induced cutting wear.

(5) Nonferrous metal wear — presence of copper alloy particles precedes thrust washer failure.

First, however, a discussion of wear particles from normally operating diesel engines is given.

Ref. 6 Hofman, M.V., and Johnson, J.H. "The Development of Ferrography as a Laboratory Wear Measurement Method for the Study of Engine Operating Conditions on Diesel Engine Wear", Wear, 44 (1977) 183-199

7 Jones, M.H. "Ferrography Applied to Diesel Engine Oil Analysis", Wear, 56 (1979) 93-103.

2.1.1 Normally Operating Diesel Engines

Experience shows that normally running diesel engines often have oil that is quite clean in regard to wear metal particles, although the oil is completely black due to carbonaceous combustion products. These are repulsed by the magnetic field of the ferrograph and some washed away by the fixer. It is not unusual to use 10 ml of oil to prepare a ferrogram in order that a representative number of particles are deposited for examination. The ferrous particles on a ferrogram from an engine in good condition are mostly a mixture of steel and cast iron normal rubbing wear particles, the proportion varying depending on the specific machine. Only a few particles will be large enough to be classified as severe wear particles. Usually, a few small dark metallo-oxide particles will be present. Also, a light deposit of corrosive wear particles at the exit end of the ferrogram is typical.

Occasionally, large black nonmagnetic agglomerate particles are found on diesel oil ferrograms. These will be principally carbon, calcium, and sulfur. Fine ferrous wear particles may be in these agglomerates making them magnetic enough to be precipitated. The fine metal particles can sometimes be seen in the agglomerate particles, using the highest optical microscope magnification. The carbon and sulfur are from the diesel fuels and are introduced in the lubricating oil during the combustion process. The calcium is from calcium compounds added to the lubricating oil to neutralize the sulfuric acid produced when the fuel burns or when water contamination is present. Calcium and sulfur have been confirmed to be present in these particles by SEM X-ray analysis.

Carbon has too low an atomic number to be detected by energy dispersive X-ray analysis, but other workers have confirmed its presence in dark agglomerates using electron microprobe analysis.[8]

Carbon/calcium/sulfur compounds are not hard, so their presence is not considered harmful regarding wear. However, their presence is an indication that the dispersant additives in the oil are not functioning properly. The purpose of oil filters is not to capture soot, but to trap abrasive particles. Dispersants are incorporated in diesel engine oil to keep combustion products from agglomerating. Should they agglomerate, they have the potential to clog oil filters or to form sludge on engine parts.

Care must be taken not to confuse dark metallo-oxides with carbon/calcium/sulfur agglomerates. Dark metallo-oxides will line up with strings of magnetic particles on a ferrogram because they have ferrous cores. The black agglomerates will not behave in a strongly magnetic manner. The distinction is important because dark metallo-oxides are a clear sign of abnormal wear.

Ref 8 Davies, C B "Identifying Solid Particles in Used Lubricating Oils", Diesel and Gas Turbine Worldwide (Apr 1980)

2.1.2 Cast Iron Wear

Figure 2.1.2.1 shows the entry deposit at 400x of a ferrogram prepared from a medium speed marine diesel engine oil sample. This photograph was taken after heat treatment of the ferrogram to 330° C to distinguish between steel and cast iron. Notice that the particles display the straw temper color of cast iron where they do not appear black from oxide formation or from their tortuous shape. The fact that they are heavily oxidized and showed some spots of temper coloring even before heat treatment indicates a high temperature wear mode quite likely due to inadequate lubrication. Also, the number and size of the particles (many may be classified as severe wear particles) are much greater than normal, from which facts alone, an abnormal wear mode is inferred.

Figure 2.1.2.2 shows a 1000x view of a portion of the entry seen on **Figure 2.1.2.1**. A large severe wear particle which may be seen in the center of **Figure 2.1.2.1** shows spots of blue temper color. These spots should not cause the analyst to misidentify the particles as steel; a steel particle will turn all blue/purple, whereas cast iron often has a mottled blue/straw appearance due to composition inhomogeneities or variation in crystalline orientation. On the bottom of **Figure 2.1.2.2** and somewhat out of focus is a large dark metallo-oxide particle. The surface has a grayish-white appearance such as is seen after heat treating steel particles to 550° C. This appearance and the fact that it was unaffected by heat treatment of the ferrogram shows that it already had a thick oxide layer from the wear process from which it was generated.

Figure 2.1.2.3 shows two cast iron severe wear particles at 1000x magnification. Even the smaller particles are abnormal in that they are oxidized and have twisted, torn shapes with greater height than is usual for normal rubbing wear platelets.

Some weeks after this sample was taken, one of the cylinders froze due to the plugging of the oil line to that cylinder.

2.1.3 Steel Wear

Just as abnormal wear of cast iron parts can be detected by the predominant straw color of the particles on a ferrogram after heat treatment to the first heat challenge temperature, wear of steel parts can be readily detected by a predominant blue/purple temper color.

Figure 2.1.3.1 shows the entry at 400x magnification of a ferrogram prepared from a truck diesel engine oil. The shapes of the particles at the entry are equiaxed (chunky) and are therefore classified as fatigue chunks. The fact that the strings of finer wear particles to either side of the entry deposit are out of focus attests to the thickness of the particles at the entry deposit. These particles, in addition to being thick, had a twisted or gnarled morphology, and were, in part, covered with black oxide (dark metallo-oxides). **Figure 2.1.3.2** is a SEM view of the entry which better shows the

morphology of the particles. Heat treatment of the ferrogram to the first heat challenge temperature (330° C) revealed that the majority of the particles were low alloy steel as evidenced by their blue temper color. There were relatively few straw-colored cast iron particles. **Figure 2.1.3.3** shows two large steel cutting wear particles. Cutting wear particles this large are generated by a highly abnormal wear mode. On the basis of the presence of these various abnormal particles, a status of caution was issued for this engine, with emphasis on steel parts.

Less than two months later the crankshaft fractured. **Figure 2.1.3.4** shows a view just down from the entry at 400x magnification of a ferrogram prepared from the crankcase oil after the failure. Quite a few different abnormal particle types are represented, including fatigue chunks, spheres, severe wear, cutting wear, and dark metallo-oxide particles. Notice that, while not dominant, a certain number of straw colored cast iron particles are also present. This is not surprising, since as the crankshaft was undergoing heavy wear it is quite plausible that the induced vibrations and unstable rotation were transmitted to other parts of the engine. Problems in the gas path of gas turbine engines often result in increased wear particle concentration in the engine oil.

Quantitatively, the particle concentration for the post failure sample was much greater than for the first sample. The before fracture ferrogram was made using 10 ml of sample, whereas the after fracture ferrogram was made using 0.3 ml of sample. Therefore, the second sample had about 30 times the particle concentration as the first sample.

2.1.4 Corrosive Wear

Diesel fuel contains varying amounts of sulfur. In recent years, the amount of sulfur has increased because of the inability of refiners to obtain low sulfur crude. During combustion, sulfuric acid can be formed by the condensation of SO_3, sulfur trioxide gas. Condensation can be prevented by keeping the engine cooling system temperature as high as possible. As sulfur concentration increases, however, the dew point becomes higher and condensation is more likely. One manufacturer believes that corrosive wear will be four times worse if the fuel sulfur content increases from 0.5 to 1%.[9] Alkaline chemical additives are put into diesel engine lubricating oil to neutralize sulfur acids as well as to neutralize organic acids which can form as oil oxidation products. Reference 10 is recommended for a more detailed explanation of the role of additives in diesel engine oil. As acid is neutralized the alkaline additive is consumed. When it is depleted the engine is exposed to aggressive chemical attack causing severe wear, mostly to the piston rings and cylinder liners, although lead in bearings may also be attacked.

Ref 9 Caterpillar Service Letter, Caterpillar Tractor Co. (8 May 1979).

10 Hoffman, J G "Crankcase Lubricants for Four-Cycle Railroad and Marine Diesel Engines", Lubrication Engineering, V 35, No. 4 (Apr 1979) 189-197

To prevent corrosive wear, timely oil changes are necessary, especially when high sulfur fuel is used. It is a bit ironic that an older engine which consumes or leaks more oil than a new engine will be better protected from corrosive wear by virtue of the makeup oil, which contains neutralizing additives, that must be periodically added. Analytically, corrosive wear is readily detected by a low total base number combined with high wear metals concentration as reported by the emission spectrometer. Total base number (ASTM Procedure D2896) is a measure of the neutralizing capacity of an oil and relates to the amount of alkaline additive in the oil. Corrosive wear can be effectively controlled if total base number is not allowed to fall below a value of one.

Corrosive wear is quite readily detected by ferrography, although other oil analysis techniques, as mentioned above, also detect it easily. This is because corrosive wear generates dissolved metals and very fine debris. Ferrography, of course, is mostly concerned with larger particles generated by fatigue, abrasion, poor lubrication, overload, etc.

Corrosive wear will be indicated by the DR (direct reading) ferrograph by much higher than baseline concentration readings, although the ratio of large to small particles may be very close to one because of the absence of many large particles. Photomicrographs of corrosive wear debris are presented in paragraph 1.8.1 of this Atlas.

For one diesel engine test in which corrosive conditions were allowed to occur, it was found that the concentration of wear particles deposited on ferrograms increased by more than a factor of 100 compared to baseline. Also, as the test proceeded, the deposits of very fine particles at the exit end of the ferrogram (those classified as corrosive wear particles when using the ferrogram analysis report sheet) increased until they reached a certain concentration and then more or less leveled off. This is the behavior predicted by the particle equilibrium concentration model, but it is interesting to note that it appears to hold even for particles that are mostly submicron in size. Quantitatively, the ferrogram readings at the 10 mm position were as follows:

Sample	Dilution	% Area Covered at 10 mm	% Area Covered at 10 mm Normalized to 1 ml of Sample
Unused Oil	1:1	0.7	0.23
1	10:1	5.7	19.0
2	100:1	13.0	433.0
3	100:1	46.4	1547.0
4	100:1	39.5	1317.0
5	100:1	57.8	1927.0

2.1.5 Abrasive Wear

An oil sample along with the oil filter from a truck diesel engine were submitted for ferrographic analysis. This engine had failed much before its expected operating life. Sabotage by ingestion of abrasive contaminants was suspected. At first, a ferrogram from the oil sample was prepared which showed fine nonmetallic crystalline particles, fine ferrous wear particles, dark agglomerates, and small aluminum and copper alloy wear particles. The absence of large particles is typical of a corrosive wear mode, but in this case it was suspected that the large particles may have settled from the oil before the sample was taken. Therefore, the oil filter housing was opened and a piece of filter paper was ultrasonically scrubbed in oil to redisperse the particles. A ferrogram was prepared from a 100:1 dilution of this filter paper wash. The ferrogram showed heavy deposits of cutting wear particles consistent with abrasive wear.

Figure 2.1.5.1 shows the entry deposit at 400x magnification. **Figure 2.1.5.2** is a SEM photograph of the same view. **Figure 2.1.5.3** shows a typical field of view just downstream from the entry at 1000x. The cutting wear is all low alloy steel. Cutting wear from cast iron is not often observed, possibly because the typical cast iron structure is interspersed with carbon flakes which prevent long ribbons from being gouged out. Also, cast iron is usually more brittle than steel.

This analysis is instructive in several ways. The fact that the oil sample did not contain cutting wear or many large particles indicates that the sample was taken either after the engine had been shut down for a few days, allowing the largest particles to settle or, what appears more likely, the cutting wear mode had ceased because of the comminution (grinding up) of the abrasive contaminants. This second theory is supported by the presence of only very fine nonmetallic crystalline particles in the oil sample and the almost total absence of fine cutting wear particles which would not be expected to settle rapidly in still oil. Analysis of the filter, however, was able to give a wear history for the engine since the last filter change. Take note that the oil in which just a very small portion of the filter paper was washed, certainly the portion was less than 1% of the total area of the pleated paper filter element, had to be diluted by a factor of 100:1 to avoid making a ferrogram with too dense a deposit. The analysis of filter elements can provide significant information, especially for post-mortem analysis as was the case in the above example.

2.1.6 Nonferrous Metal Wear

An oil sample taken from a 12-cylinder General Motors Electromotive Division (EMD) series 645 engine used for marine propulsion showed a dramatic increase in wear particle concentration compared to the sample taken 2 weeks previously. The DR results are as follows:

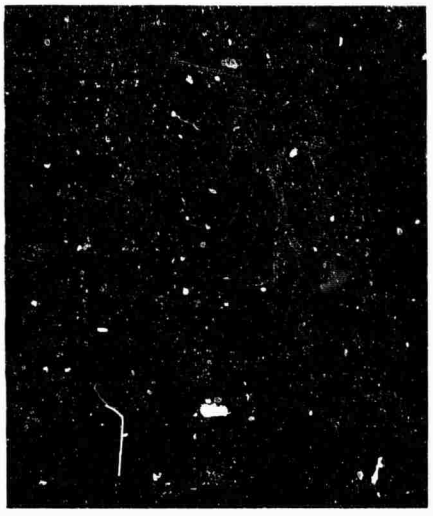

Fig 2.1.2.1 Opt. M. 400X — 50μm

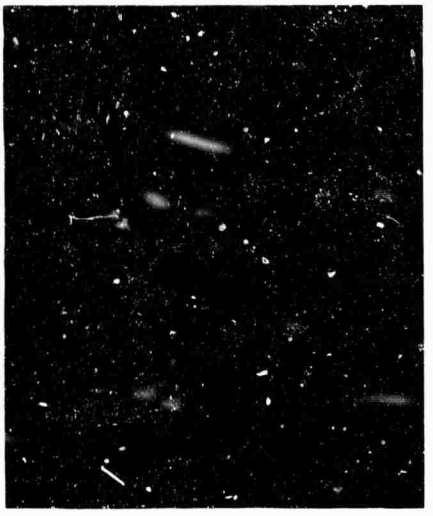

Fig 2.1.2.2 Opt. M. 1000X — 20μm

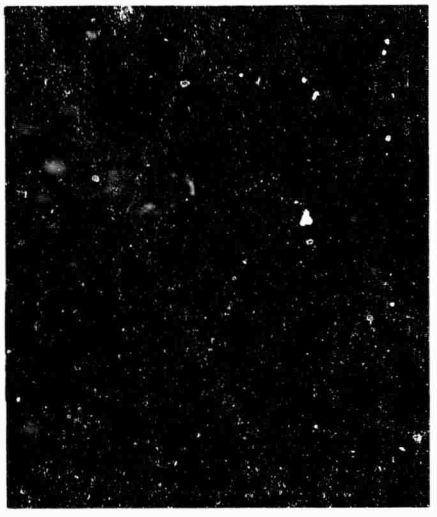

Fig 2.1.2.3 Opt. M. 1000X — 20μm

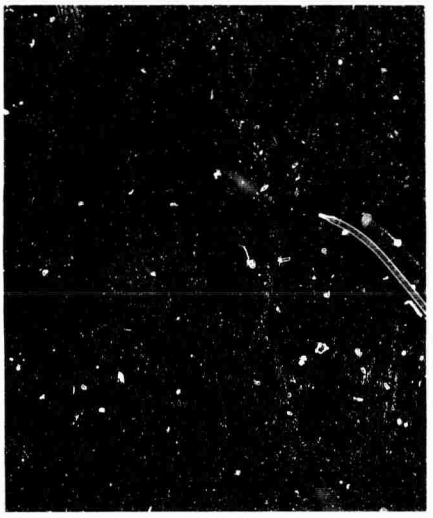

Fig 2.1.3.1 Opt. M. 400X — 50μm

Fig 2.1.3.2 S.E.M. 400X — 50μm

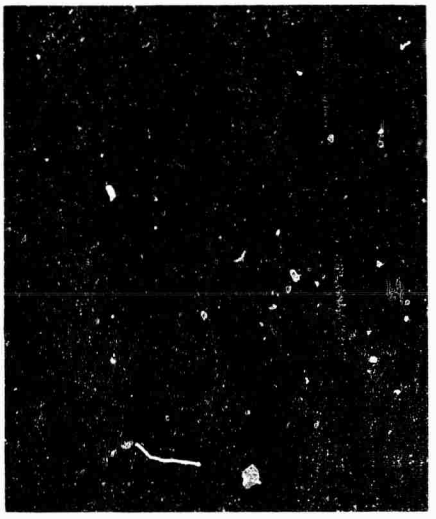

Fig 2.1.3.3 Opt. M. 1000X — 20μm

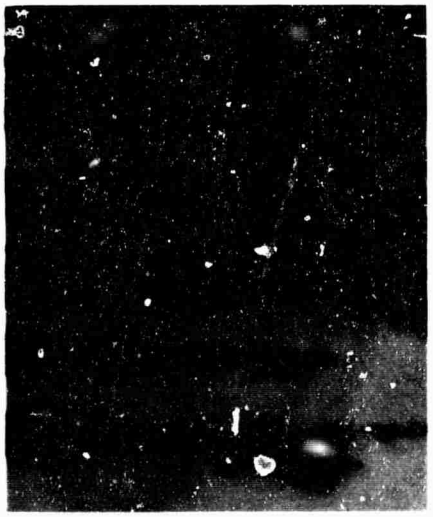

Fig 2.1.3.4 Opt. M. 400X — 50μm

Fig 2.1.5.1 Opt. M. 400X — 50μm

Fig 2.1.5.2 S.E.M. 400X — 50μm

	L*	S*
3 July 1980	1.4	1.5
17 July 1980	39.2	36.2

* L = large channel reading,
S = small channel reading

A ferrogram prepared from the second sample indicated a piston/cylinder failure was imminent based on the presence of many severe wear particles as well as many normal rubbing wear particles which were predominantly cast iron as determined by heat treatment of the ferrogram. Also of concern was the presence of many large, heat affected, copper alloy wear particles. **Figure 2.1.6.1** shows one of these particles. At the time of the analysis it was unclear whether the copper was from the bearings or from a copper thrust washer located between the piston carrier and the piston itself. On 30 July 1980, the ship entered a shipyard because of noise in the engine. Two cylinder heads were removed and signs of excessive wear and scoring of the piston skirt and cylinder liners were observed. Piston thrust washers cannot be visually observed without piston disassembly, but readings may be taken to check clearance to ascertain wear of the thrust washer. The copper particles were from a copper thrust washer which was greatly diminished in size and showed signs of excess heat.

2.2 AIRCRAFT GAS TURBINES

2.2.1 Introduction

Aircraft jet engines and aircraft-derivative jet engines are subject to various failure mechanisms. Some of these failure modes proceed very rapidly whereas others can be detected many hundreds of operating hours before a shutdown condition is reached. Most failures to gas turbines occur in the gas path. Some preliminary work on analyzing gas path particles[11] has been done, but much more must be done in order to obtain a representative sample for quantitative analysis and to characterize gas path particles so they may be successfully related to component deterioration. Gas path failures sometimes, but not always, cause an increase in wear particle size and concentration in the oil system due, most likely, to imbalance forces being transmitted to turbine bearings and other oil-wetted parts.

Usually more information is needed than that provided by the wear particles themselves, to pinpoint the cause of abnormal wear particle generation in gas turbines because of the complexity of the oil-wetted path. Typically, several cavities, housing bearings or gears, will be force lubricated with individual return lines to a tank from which the oil is pumped, passed through a filter and heat exchanger, from where the cycle is repeated.

Ref. 11. Scott, D., and Mills, G.H. "An Exploratory Investigation of the Application of Ferrography to the Monitoring of Machinery Condition from the Gas Stream", Wear, 48 (1978) 201-208

Magnetic chip detectors or magnetic plugs are often installed in the return lines from the various engine parts. These can help to pinpoint the source of generation in cases where particle metallurgy, as determined by heat treating ferrograms, is similar for various engine parts. However, chip detectors will not give a warning until the wear situation is so severe that extremely large particles are being generated. By this time, the opportunity for preventive maintenance may be lost. Other analytical techniques, such as spectrometric oil analysis or vibration analysis, may help to pinpoint the part(s) in distress but in most cases the engine will have to be inspected, perhaps by borescope, but most likely by disassembly. The oil analyst, in this instance, must be confident that a problem exists. Therefore, a number of techniques should be used to confirm initial results and a second sample should be taken and analyzed to make sure the first sample is not spurious. Wear particle analysis has the advantage that where abnormal particles are found the analyst can be reasonably certain that a problem exists. However, there is the potential disadvantage of too early a warning; the engine may be disassembled prematurely when it could run for many more hours without failure or causing secondary damage.

2.2.2 Fleet Monitoring

For a four-month period in 1976-1977, Eastern Airlines conducted a test program to evaluate ferrography.[12] Samples were collected every 50 operating hours from Rolls-Royce RB211 engines which power Eastern's L-1011 aircraft. DR ferrographic analysis was not performed as the samples were taken, but was performed at the end of the four-month period by the National Engineering Laboratory, Glasgow, Scotland. The analysis effort was directed mainly toward engines which had been removed during the sampling period. Of the 52 engines removed during the sampling period, the following were tested using the DR ferrograph:

(1) Single samples of 25 engines were tested. These were the last samples prior to engine removal.
(2) Single samples of 30 engines were tested. These samples were taken after test cell runs.
(3) Comprehensive samples were tested for 10 of the above 25 engines at increments of approximately 50 engine flight hours going back in operating history as much as 1000 hours.
(4) Comprehensive samples were tested for 3 engines which were not removed during the sampling period.

The object of this test program was to determine whether DR ferrography could give a timely removal alert based on 50 hour samples. In this exercise, two successive DR samples which were above baseline would constitute a removal alert.

Ref. 12 Blyskal, E.P. "RB 211 Ferrographic Analysis Investigation Status Report No. 1", Eastern Airlines, Engineering Report No. E-964 (18 Jul 1977)

Table 2.2.2.1 shows the DR readings for the last sample taken before removal for 25 engines along with the symptoms at the time of removal. Most of the removals were due to gas path failures and in most of these cases the DR readings were low. Several of the lubrication system failures were not wear related and therefore the DR readings for those engines were also low. **Table 2.2.2.2** gives baseline DR readings as determined from the straight portions of the wear history curves for various engines monitored in this study. These curves, **Figures 2.2.2.1 to 2.2.2.12**, present the DR history for some of the 13 engines which were comprehensively analyzed. **Table 2.2.2.3** lists the abbreviations used on **Figures 2.2.2.1 through 2.2.2.12.** Some curves, mostly those which showed no abnormalities, were omitted to save space. The readings on these graphs are plotted cumulatively as a function of operating time. For this type of plot, each new reading is added to the sum of the previous readings and that sum is plotted for the number of operating hours at which the sample was taken. This method will result in the plotting of a straight line if the readings are the same and the time interval between samples is the same. What has been done on these curves is that the distance along the time axis has been kept constant for each reading in spite of different time intervals between samples. These graphs, then, show readings plotted at equal intervals with the time the sample was taken noted at those intervals. If the readings increase, then the slope of the resulting curve will also increase, thus signaling the onset of abnormal wear.

Only 9 engines are included in the DR baseline data table because 4 of the comprehensively analyzed engines did not have straight sections, representing normal operation, in their DR curves. From **Table 2.2.2.2** it appears that the baseline for the L reading is between 5 and 10. Study of the DR curves presented for the 13 extensively analyzed engines shows that the L reading is much more responsive to incipient failure than is the S reading. In fact, the S channel has practically no response in most instances. This lack of increase in the S reading appears to be more pronounced for this engine than for many other types of equipment.

Of the 13 engines which were comprehensively tested, 3 ran properly during the test interval and were not removed. The DR ferrograph gave no indication that they should be removed.

These engines are as follows:

Engine	Comments
10057	No failure in this engine, and no DR trend indicating removal.
10072	No failure in this engine, and no DR trend indicating removal.
10064	No failure in this engine, and no DR trend indicating removal, although there was one anomalous sample at 557 operating hours. The next taken sample returned to baseline.

TABLE 2.2.2.1

DR READINGS FOR LAST TAKEN SAMPLE BEFORE REMOVAL

Engine No.	Notes	L	S	Symptoms
044		6.1	2.0	Takeoff compressor stall
051		5.7	2.5	Turbine damage
054		6.0	2.8	Vibration
056	*L	11.6	1.0	LP location bearing failure
066		14.7	2.3	Vibration
067		6.5	2.8	Turbine deterioration
093	*LA	49.1	5.1	Compressor stalls, minor LP bearing damage
101	*LA	25.0	6.4	Sheared starter
113		15.6	3.4	Turbine problem
134		4.4	3.3	Stalling
200	*A	20.2	4.4	Turbine deterioration
207	L	3.3	2.8	High oil consumption
210		6.4	1.4	Compressor stalls
221	*LA	72.2	2.2	Turbine deterioration, drain line failure
223	*LA	44.3	10.3	LP location bearing failure
224		5.4	1.8	Compressor stalls
229		12.7	3.6	Internal fire
231	*	37.9	3.9	Turbine damage
232	*L	18.2	5.0	Turbine damage, cracked gearbox bearing
245	*L	6.4	1.9	High oil consumption
249		7.0	4.5	LLP (life-limited part)
261		6.2	3.2	Cause not stated
364		10.7	2.9	LLP (life-limited part)
527		10.3	2.4	Cause not stated
536	*A	36.7	4.7	Turbine deterioration

* Engines analyzed comprehensively

L Lube system problems

A Removal alert based on DR trend would have been given.

LP Low Pressure

TABLE 2.2.2.2

BASELINE DR READINGS FOR SEVERAL ENGINES

	DR Readings	
Engine	L	S
10057	7.9	2.8
10072	6.7	3.6
10064	6.0	2.5
10245	8.5	1.8
10232	7.7	2.3
10231	7.2*	1.7
10093	8.6*	5.2
10223	9.9*	3.0*
10101	5.1*	3.4*
Average	7.5	2.9

* The wear history curves for these data points are included in this Atlas.

TABLE 2.2.2.3

Abbreviations Used in Figures 2.2.2.1 through 2.2.2.12

BRG	bearing
FOD	foreign object damage
HP/IP	high pressure intermediate pressure
HPT	high pressure turbine
I/C	intermediate compressor
IFSD	in-flight shutdown
LP	low pressure
TSLSV	time since last service
D_L	large reading, direct-reading ferrograph
D_S	small reading, direct-reading ferrograph

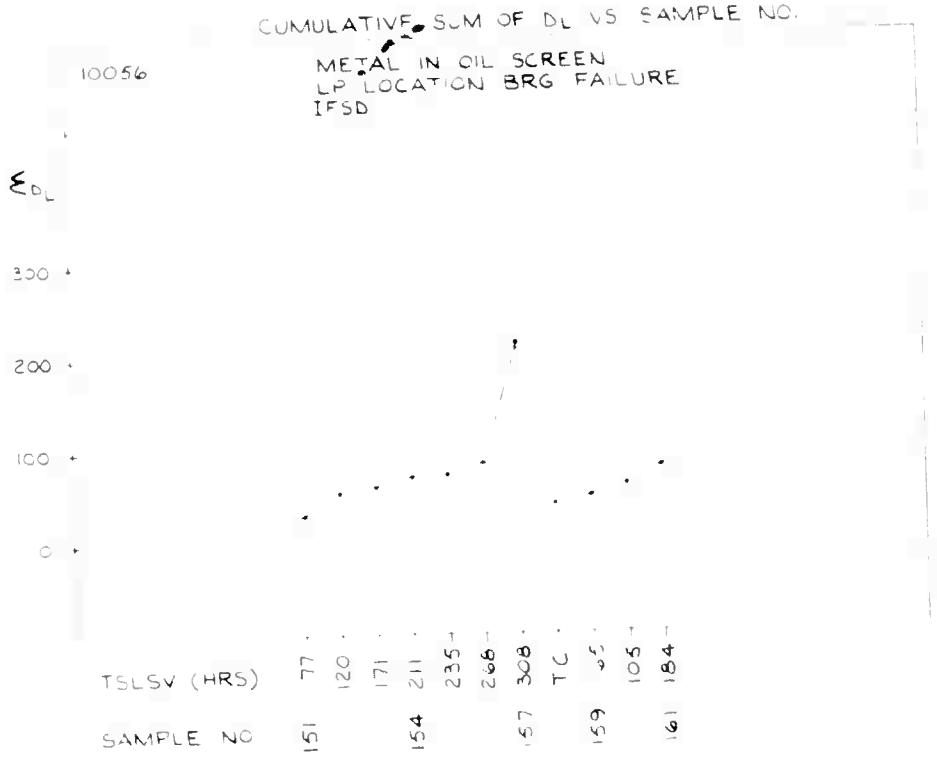

Figure 2.2.2.1 Cumulative Sum of D_L vs. Sample No. for Engine 10056

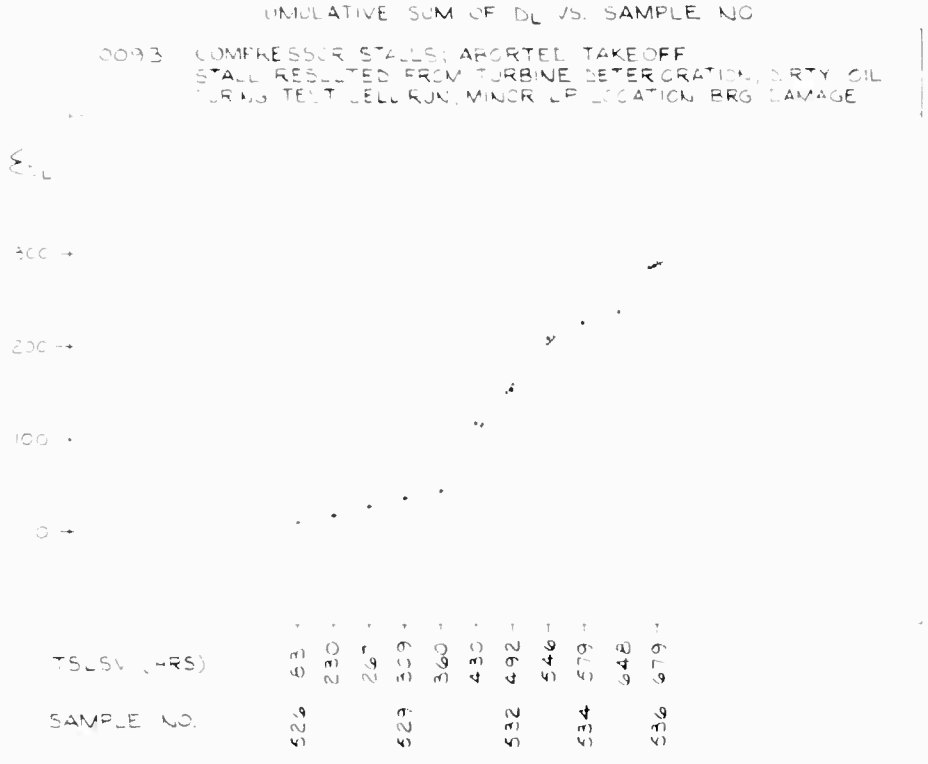

Figure 2.2.2.2 Cumulative Sum of D_L vs. Sample No. for Engine 10093

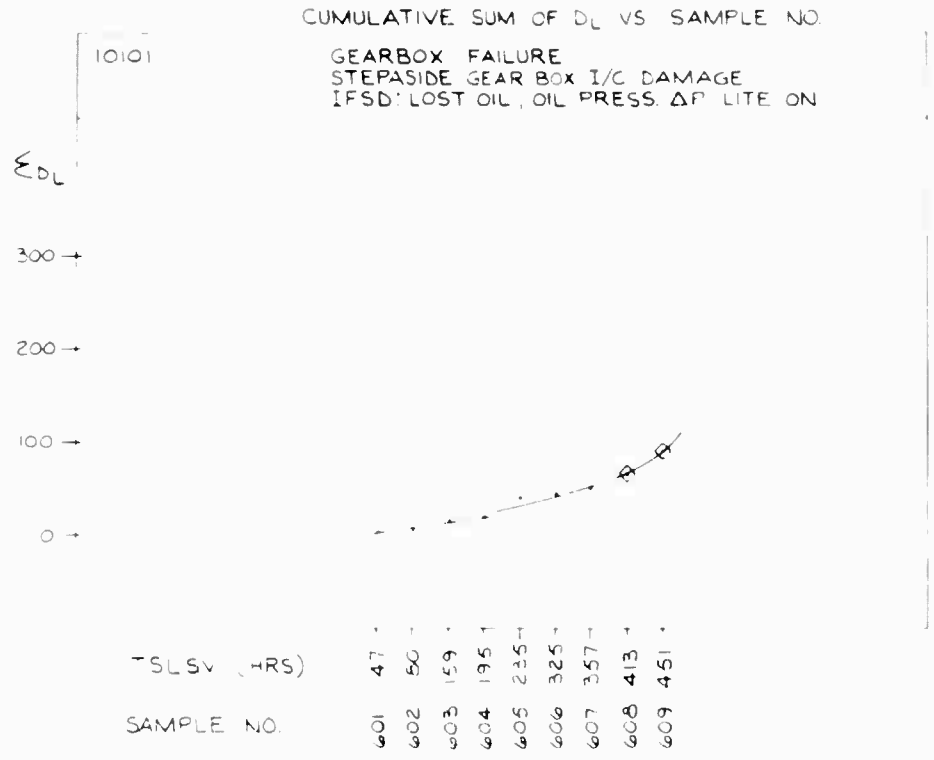

Figure 2.2.2.3 Cumulative Sum of D_L vs. Sample No. for Engine 10101

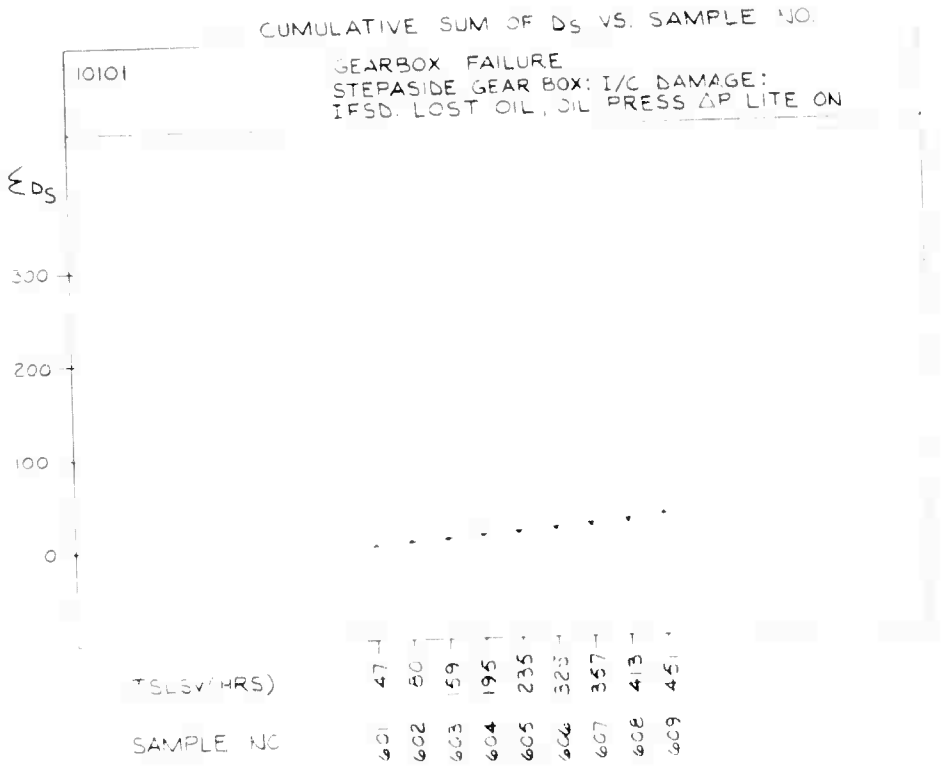

Figure 2.2.2.4 Cumulative Sum of D_S vs. Sample No. for Engine 10101

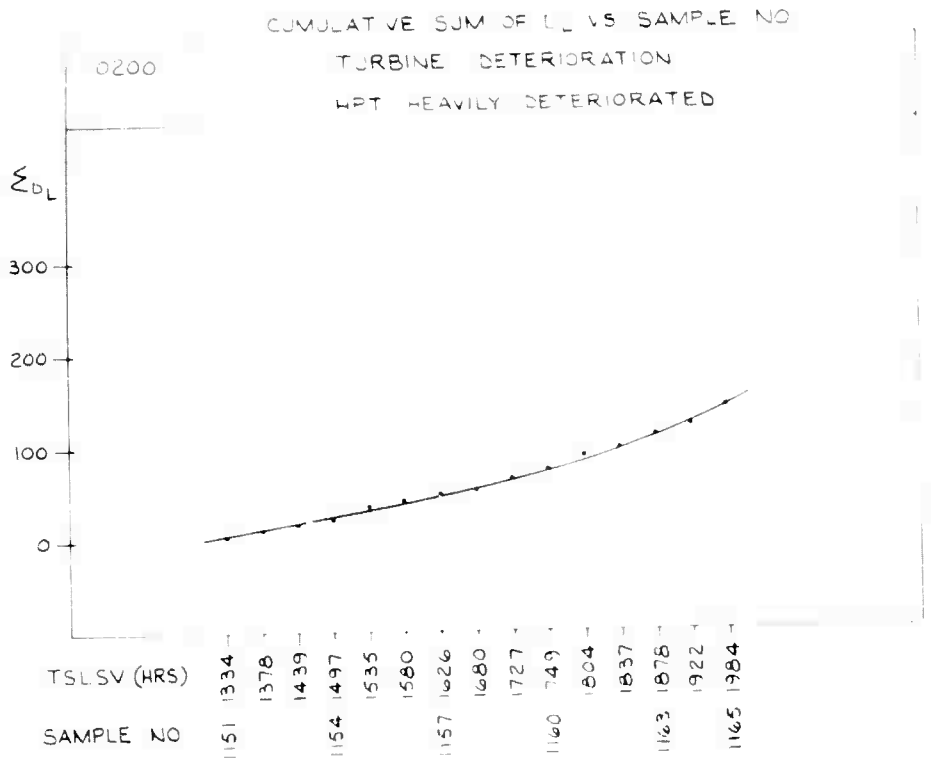

Figure 2.2.2.5 Cumulative Sum of D_L vs. Sample No. for Engine 10200

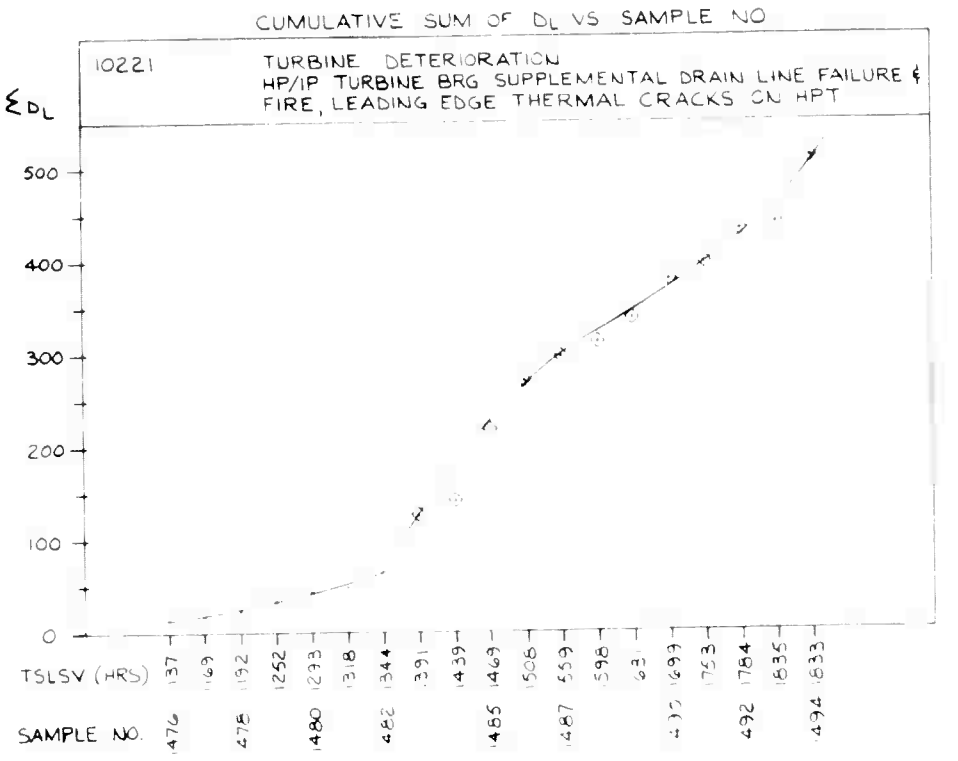

Figure 2.2.2.6 Cumulative Sum of D_L vs. Sample No. for Engine 10221

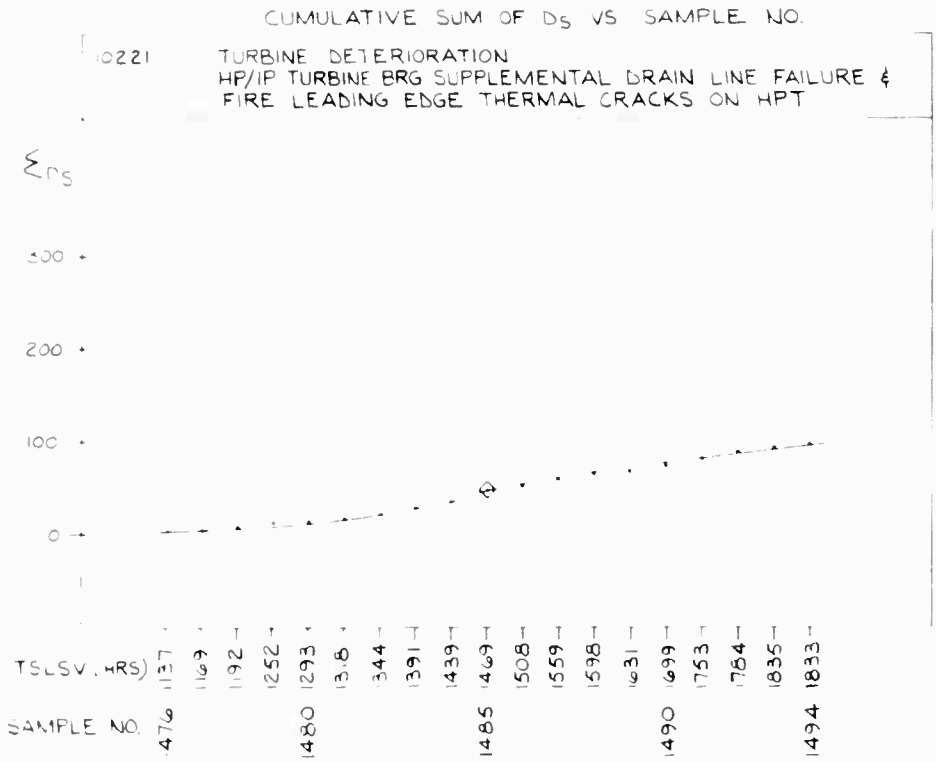

Figure 2.2.2.7 Cumulative Sum of D_S vs. Sample No. for Engine 10221

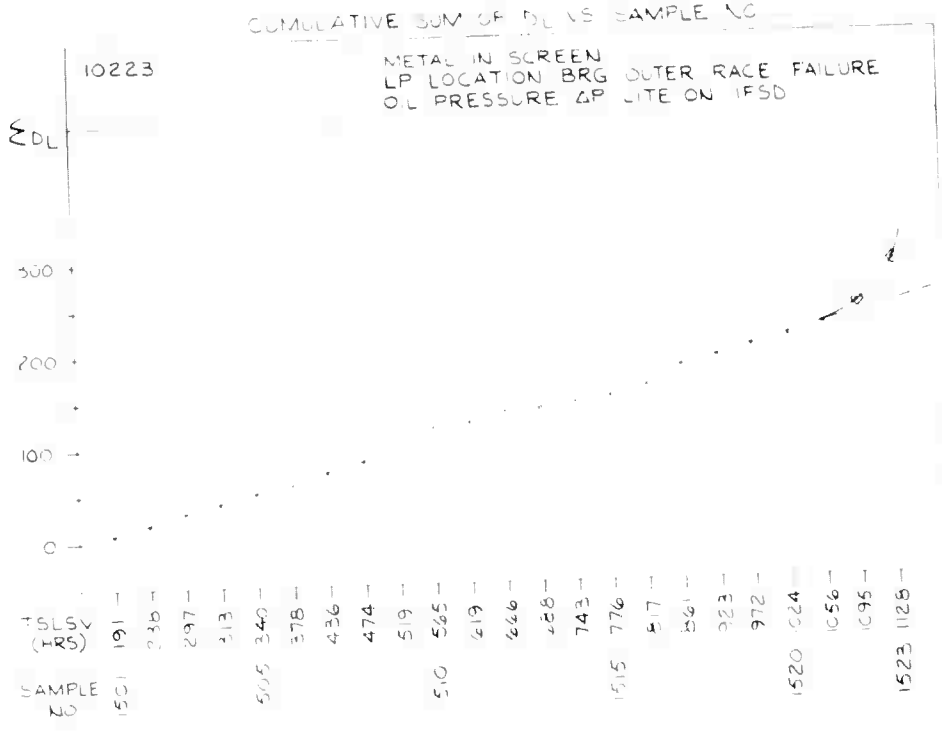

Figure 2.2.2.8 Cumulative Sum of D_L vs. Sample No. for Engine 10223

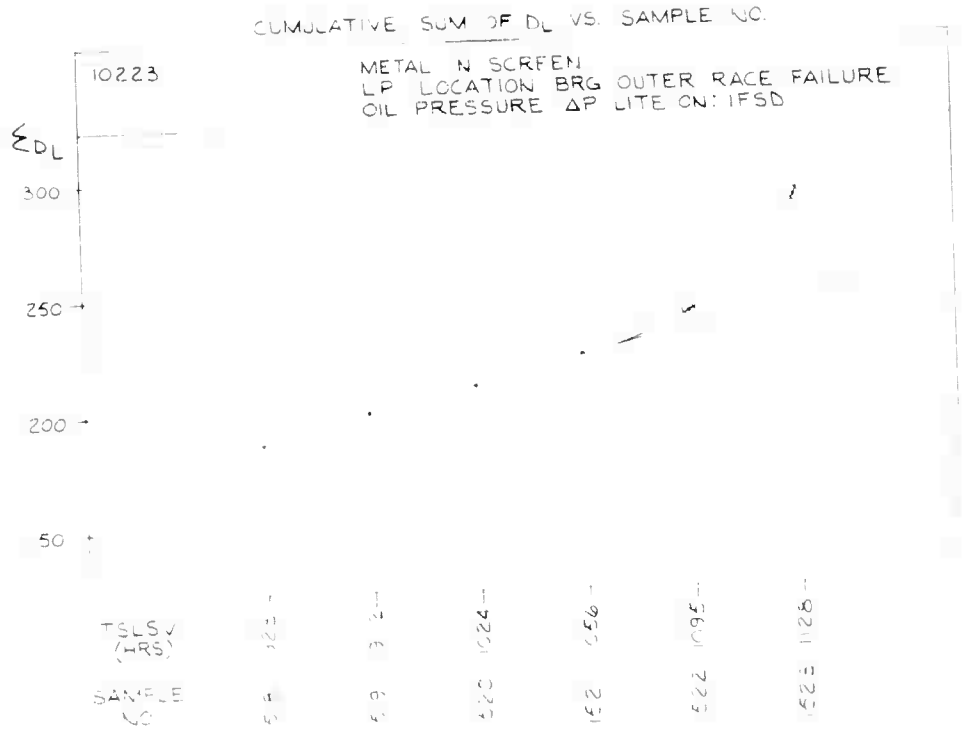

Figure 2.2.2.9 Cumulative Sum of D_L vs. Sample No. for Engine 10223 (expanded view)

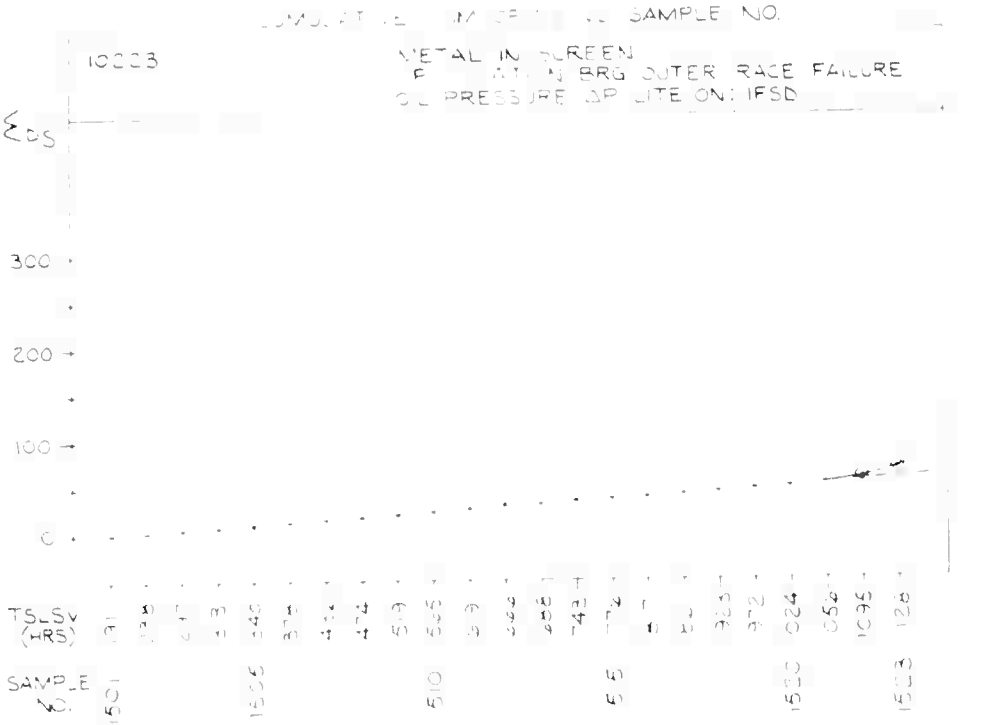

Figure 2.2.2.10 Cumulative Sum of D_S vs. Sample No. for Engine 10223

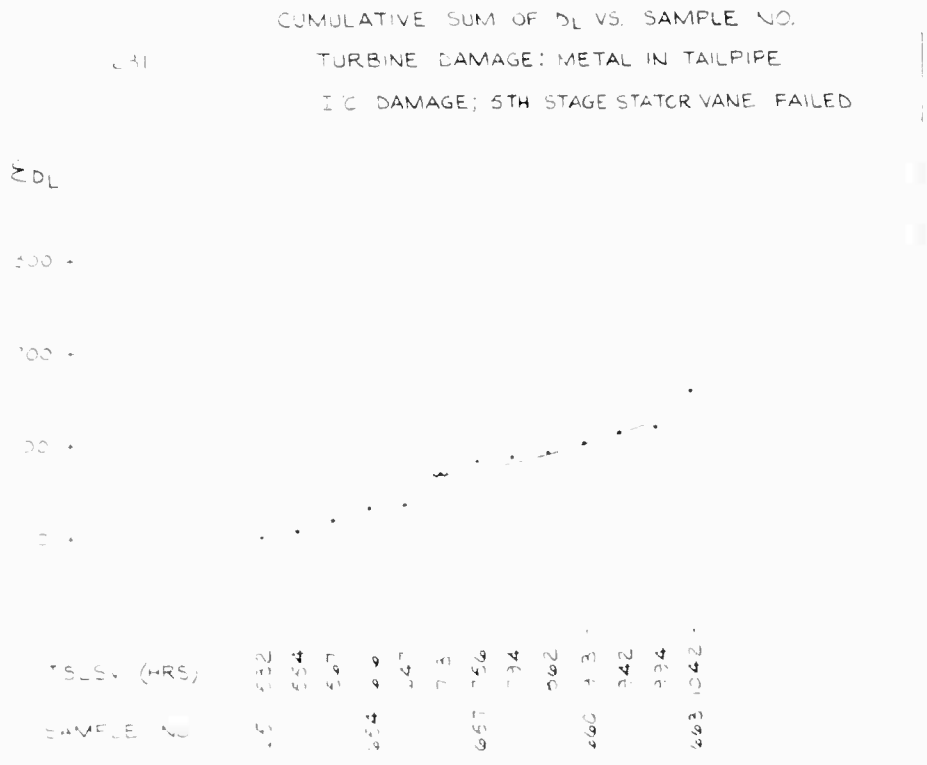

Figure 2.2.2.11 Cumulative Sum of D_L vs. Sample No. for Engine 10231

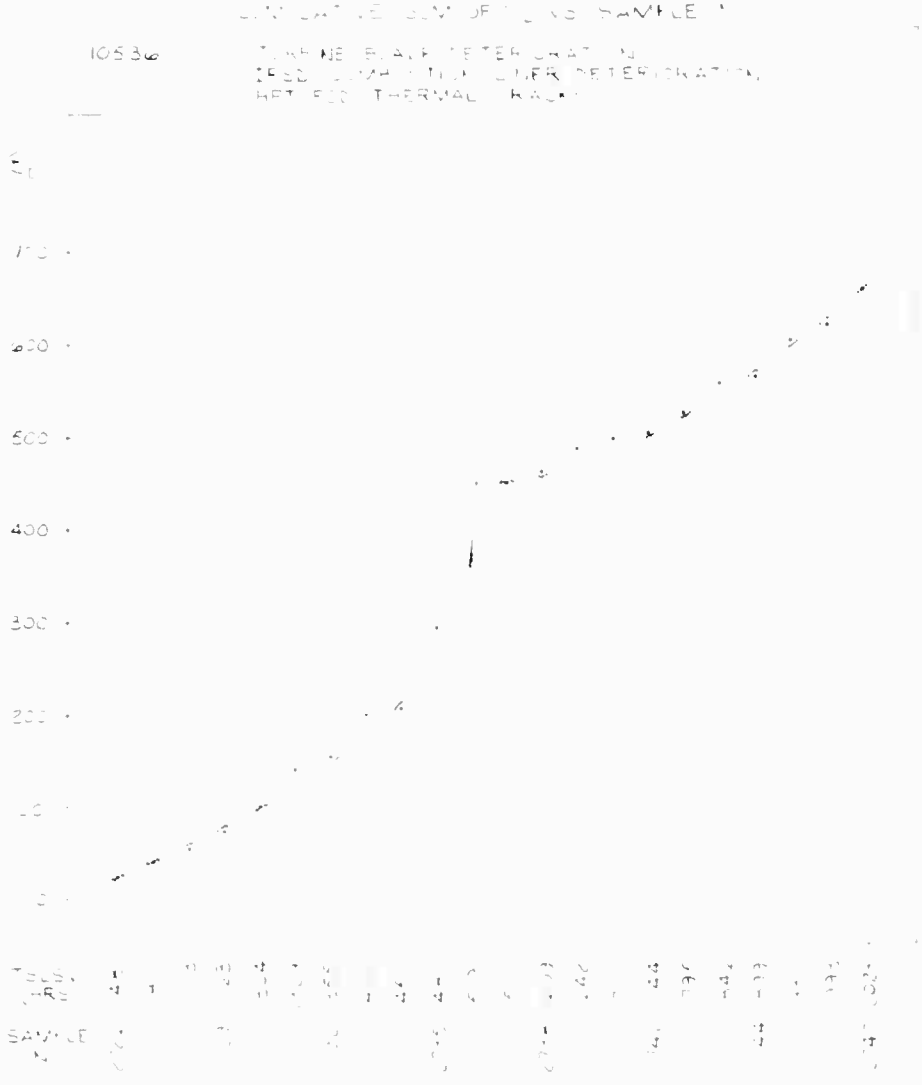

Figure 2.2.2.12 Cumulative Sum of D_L vs. Sample No. for Engine 10536

Ten of the 13 engines were removed for overhaul due to failure. Three of the 10 showed no DR trend indicating removal. These were:

Engine	Comments
10245	This engine was removed for high oil consumption due to failure of the HP/IP turbine bearing support oil tube. No DR trend was observed even though high oil consumption was reported when the last few samples were taken. This is not unexpected since the failure was not to a wearing part.
10232	This engine was shut down in flight due to a cracked step-aside gearbox housing. On-wing inspection revealed turbine damage/deterioration so the engine was removed. No DR trend was observed and no removal alert given, although the sample before removal (L = 18.2, S = 5.0) was about twice baseline. Again, failure was not to an oil-wetted wearing component.
10056	An in-flight shutdown caused this engine to be removed. **Figure 2.2.2.1** shows the DR history for this engine. Disassembly revealed an LP location bearing failure. Metal was found in the oil screen. A sample taken after engine removal showed a dramatically high DR reading (labeled at 308 hours on the Engine 10056 plot) but the previously taken sample (40 hours before shutdown) was not abnormally high. Although the DR did not show a trend indicating removal just prior to failure, closer examination of the DR data, shown later in this section, indicates that Samples 151 and 152, which are some 200 operating hours before the shutdown failure, are quite high. **Figure 2.2.2.13** shows the entry at low magnification of a ferrogram prepared from Sample 151. Many large free metal particles are seen in this bichromatic light view. **Figure 2.2.2.14** shows the entry region in polarized light. Both reflected and transmitted light sources were used in their fully polarized modes to highlight the many nonmetallic crystalline particles present. **Figures 2.2.2.15 and 2.2.2.16** show different views of the entry at 400x magnification after heat treating the ferrogram to the first heat challenge temperature (330° C). Present are many large cutting wear particles, large spheres, dark metallo-oxides, and severe wear particles. These, along with the nonmetallic crystalline particles, are indicative of heavy abrasive wear. Heat treatment shows that not only low alloy steel parts such as the bearings are made of, but other parts were being worn. This is consistent with an abrasive wear mode which indiscriminately wears all the engine components. Although this wear mode abated to a great degree, it may be

<table>
<tr><th>Engine</th><th>Comments</th></tr>
<tr><td>10056
(Cont)</td><td>that the heavy abrasive wear mode initiated subsurface deformation and cracking in the bearing which later led to the in-flight failure.

Figure 2.2.2.17 shows the entry view at low magnification of a ferrogram made from Sample 157 taken at the Eastern Service Center after engine removal. The particles on this ferrogram are huge by comparison to normal wear particles. Looking at the DR data for this engine, it appears that a removal alert would have been appropriate after Sample 152, since this was the second sample much above baseline. Unfortunately, it is impossible to know whether removal of the engine after Sample 152 would have resulted in replacement of the bearing that failed 200 or so hours later. The DR data for Engine 10056 is as follows.
<table>
<tr><th>Sample No</th><th>Date</th><th>Cum. Hrs.</th><th>L</th><th>S</th></tr>
<tr><td>151</td><td>10 20 76</td><td>77</td><td>28 1</td><td>5.5</td></tr>
<tr><td>152</td><td>12 1 76</td><td>120</td><td>24 5</td><td>5.7</td></tr>
<tr><td>153</td><td>12 8 76</td><td>171</td><td>6.4</td><td>3.7</td></tr>
<tr><td>154</td><td>12 12 76</td><td>211</td><td>9 3</td><td>2.5</td></tr>
<tr><td>155</td><td>12 15 76</td><td>235</td><td>3.0</td><td>1 0</td></tr>
<tr><td>156</td><td>12 19 76</td><td>268</td><td>11 6</td><td>1 0</td></tr>
<tr><td>*157</td><td>1 14 77</td><td>308</td><td>131 0</td><td>29 3</td></tr>
<tr><td>**158</td><td>2 12 77</td><td>0</td><td>39 9</td><td>16 0</td></tr>
<tr><td>159</td><td>3 2 77</td><td>65</td><td>6 2</td><td>5 0</td></tr>
<tr><td>160</td><td>3 6 77</td><td>105</td><td>11.9</td><td>2.1</td></tr>
<tr><td>161</td><td>3 16 77</td><td>184</td><td>18 1</td><td>0.1</td></tr>
</table>
* after removal
** test cell</td></tr>
</table>

Of the 7 remaining engines, 6 would have been given removal alerts based on sampling every 50 hours. The seventh engine (10231) would not have been given a removal alert although the sample before removal was high. These engines are as follows.

<table>
<tr><th>Engine</th><th>Comments</th></tr>
<tr><td>10093</td><td>This engine was removed for engine stalling due to turbine deterioration. Some minor LP location bearing damage was also found upon disassembly. A removal alert would have been given at 492 operating hours, nearly 200 hours before removal. Figure 2.2.2.18 shows the entry region at low magnification for Sample 526 taken well before a significant shift in the L reading trend. For comparison, Figure 2.2.2.19 shows the</td></tr>
</table>

Engine	Comments
10093 (Cont)	entry region for Sample 536 just before removal. The same view is shown on SEM **Figure 2.2.2.20. Figure 2.2.2.21** shows some of the particles at higher magnification, and SEM **Figure 2.2.2.22** better shows the heavy cutting wear in this view **Figure 2.2.2.2** shows the DR data for this engine.
10101	This engine was removed as a result of an in-flight shutdown due to loss of oil. Inspection revealed a step-aside gearbox failure and damage to one of the compressor stages. The first indication of trouble appears to be at 235 hours although the sample after that returned to baseline readings. A removal alert would have been given 2[illegible] days before in-flight shutdown based on the 413-hour and 451-hour samples both being above normal. **Figures 2.2.2.3 and 2.2.2.4** show the DR history for this engine. Note that the DR small channel readings did not respond to this failure.
10200	This engine was removed for turbine deterioration. In this case, there appears to be a sufficient gradual increase in the L reading slope to provide a removal alert some 100 hours before removal. **Figure 2.2.2.5** shows the data
10221	The failure of the HP IP turbine bearing supplemental drain line and subsequent internal oil fire caused this engine to be removed. Turbine deterioration was found after removal. A removal alert would probably have occurred at 1469 operating hours, some 400 hours before failure. **Figures 2.2.2.6 and 2.2.2.7** show the data
10223	This engine was removed after an in-flight shutdown due to an oil pressure LP light being on. Metal was found in the oil system screen and upon disassembly, an LP location bearing outer race failure was found. A removal alert, based on two successive high readings, would have been given about 6 operating hours before shutdown which probably would not have allowed for sufficient sample processing time for the alert to have resulted in engine removal. A monitoring strategy that requires another sample to be taken immediately after it is learned that the previous sample is abnormal would give more warning time. Assuming that the first sample is processed in 10 operating hours, an additional 40 hours could be gained for the removal alert. **Figures 2.2.2.8, 2.2.2.9, and 2.2.2.10** show the DR data for this engine
10231	This engine was removed for turbine damage. **Figure 2.2.2.11** shows the cumulative plot of the DR data for this engine. Although the sample before removal was quite high (L 37.9, S 3.9), and there was a slight upward

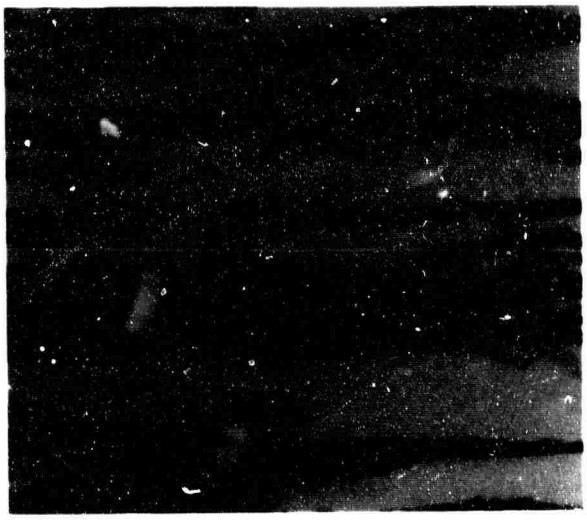

Fig 2 1 5 3 Opt M 1000X ⊢—20μm—⊣

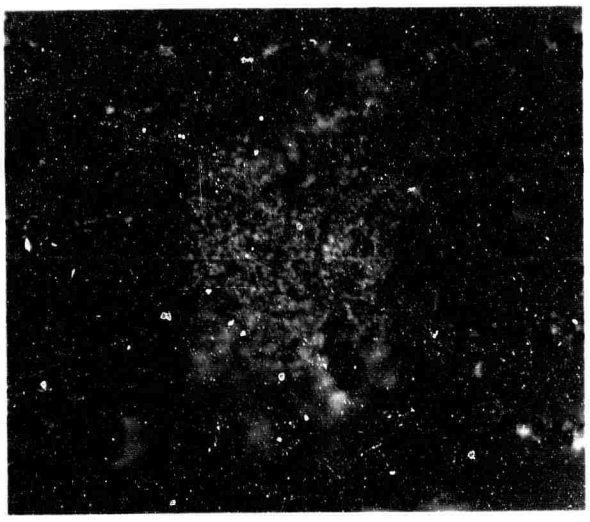

Fig 2 1 6 1 Opt M 400X ⊢—50μm—⊣

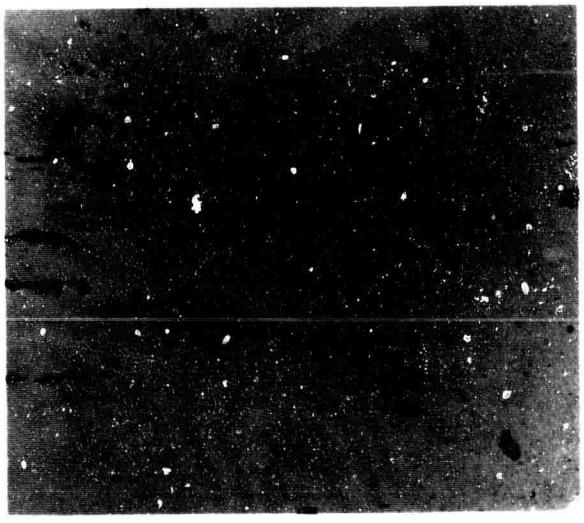

Fig 2 2 2 13 Opt M 100X ⊢— 200μm —⊣

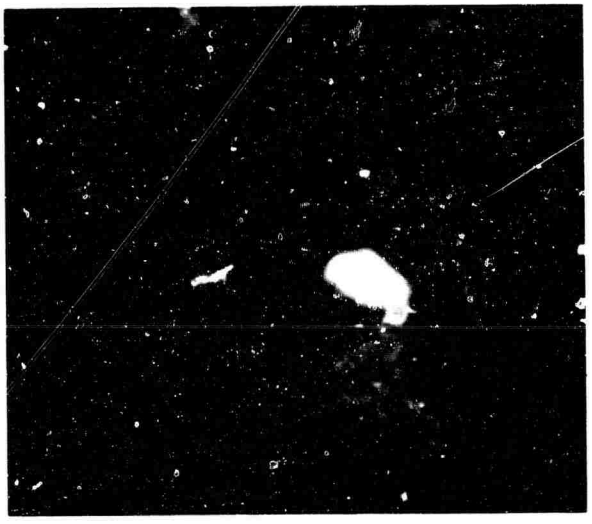

Fig 2 2 2 14 Opt M 100X ⊢—200μm—⊣

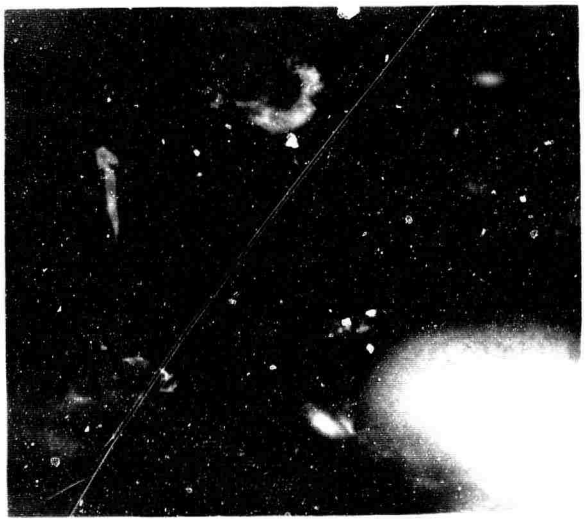

Fig 2 2 2 15 Opt M 400X ⊢—50μm—⊣

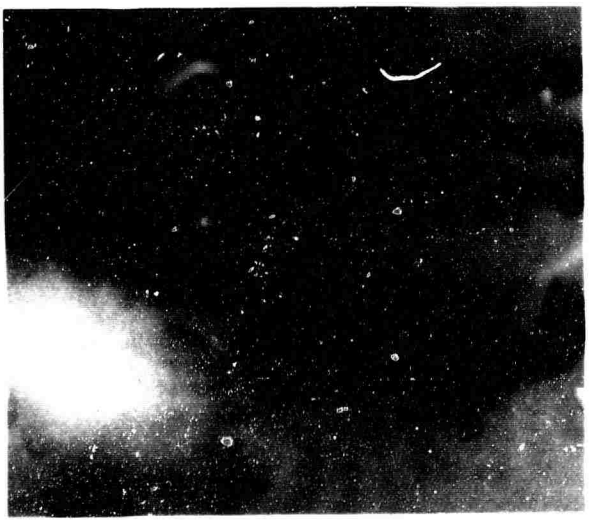

Fig 2 2 2 16 Opt M 400X ⊢—50μm—⊣

Engine	Comments
10231 (Cont)	increase in the slope of the L reading curve for some hours prior to the last sample, it is concluded that no removal alert would have been given.
10536	This engine incurred an in-flight shutdown. Disassembly revealed various gas path problems including turbine blade deterioration and combustion liner deterioration. The removal alert would probably have been given at 1329 operating hours, 709 hours before failure. This example raises the question as to whether such an early removal was worth losing 700 engine operating hours, even though an in-flight shutdown could have been prevented. **Figure 2.2.2.12** shows the DR data for this engine.

2.2.3 Military Oil Analysis Program

The examples in this section were obtained from the oil analysis laboratory at the Corpus Christi Army Depot where thousands of oil samples are processed each month. The primary instrument used for analysis at that laboratory, as is the case for all military oil analysis laboratories, is the rotating disc atomic emission spectrometer which provides a rapid determination of the wear metals content in an oil sample. However, this instrument is not efficient at detecting large particles (above several micrometers) for several reasons.[13] For the cases described in this section, the oil analysis laboratory used ferrography as a secondary check before a decision was made to recommend maintenance action. In each instance, an abnormality was first signaled by either a chip detector light or metal on a magnetic plug. Also, in each instance, spectrometric oil analysis reported that iron concentration was within acceptable limits. However, when each of these samples was analyzed ferrographically, enough ferrous wear particles were present to confirm an abnormal wear mode. Subsequent teardown then revealed the specific problem causing the generation of the wear debris. Following are five examples from the Corpus Christi Army Depot oil analysis laboratory.

(1) **Figure 2.2.3.1** is the ferrogram analysis report sheet for a T53 engine which showed metal on a magnetic plug when it was inspected. Ferrographic analysis revealed that the principal abnormal particles were severe wear particles and cutting wear particles. **Figure 2.2.3.2** shows the entry deposit of Ferrogram 4359 at low (100x) magnification using bichromatic light. Comparison with

Ref. 13 Eisentraut, K.J., Thornton, T.J., Rhine, W.E., Constandy, S.B., Brown, J.R., and Fair, P.S., "Comparison of the Analysis Capability of Plasma Source Spectrometers vs. Rotating Disc Atomic Emission and Atomic Absorption Spectrometry for Wear Particles in Oil - Effect of Wear Metal Particle Size", presented at the 1st International Symposium on Oil Analysis, Erding, Germany (4-6 Jul 1978).

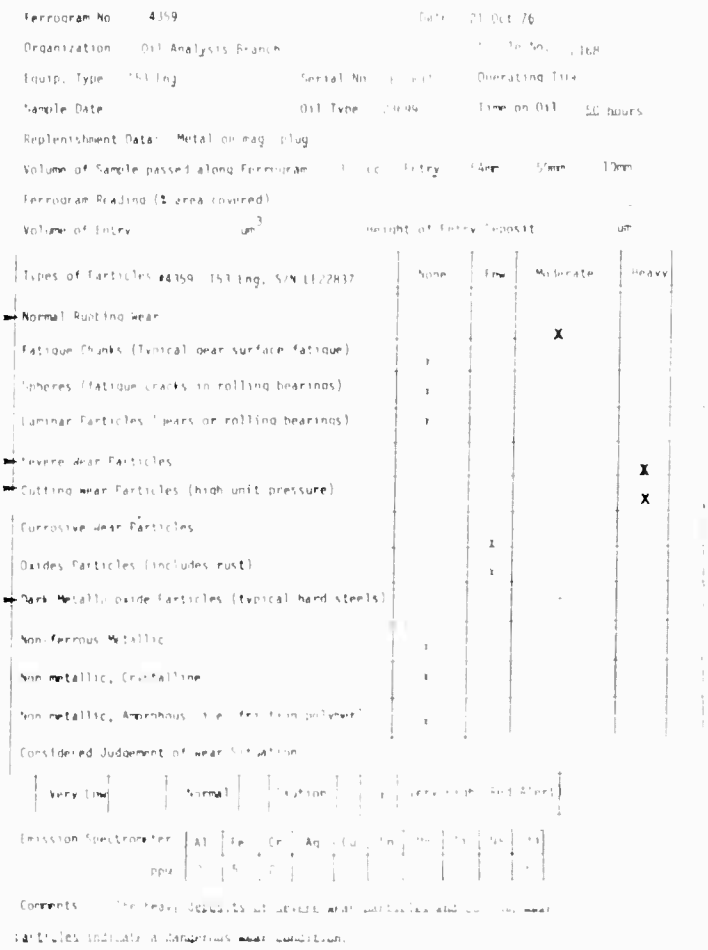

Ferrogram No 4359 Date 21 Oct 76

Organization Oil Analysis Branch

Equip. Type T53 Eng Serial No Operating Time

Sample Date Oil Type Time on Oil 50 hours

Replenishment Data: Metal on mag plug

Volume of Sample passed along Ferrogram cc Entry 4mm 5mm 10mm

Ferrogram Reading (% area covered)

Volume of Entry μm^3 Height of Entry Deposit μm

Types of Particles #4359 T53 Eng. S/N LE/2837	None	Few	Moderate	Heavy
Normal Running Wear			X	
Fatigue Chunks (Typical gear surface fatigue)	x			
Spheres (fatigue cracks in rolling bearings)	x			
Laminar Particles (wears on rolling bearings)	x			
Severe Wear Particles				X
Cutting Wear Particles (high unit pressure)				X
Corrosive Wear Particles		x		
Oxides Particles (includes rust)		x		
Dark Metallic Oxide Particles (typical hard steels)			-	
Non-ferrous Metallic	x			
Non metallic, Crystalline	x			
Non metallic, Amorphous (i.e. fibers from polymers)	x			

Considered Judgement of wear Situation

Very Low		Normal		Extreme		Very Severe Bad Alert

Emission Spectrometer	Al	Fe	Cr	Ag	Cu	Sn	Mo	Ti	Si	Ni
ppm		5	2							

Comments The heavy deposits of severe wear particles and [illegible] wear particles indicate a dangerous wear condition.

Figure 2.2.3.1 Ferrogram Analysis Report Sheet, Ferrogram 4359

Figure 2.2.3.3 which is the entry deposit of a ferrogram made from an oil sample from a T53 with a normal operating history shows that this engine was operating quite abnormally. **Figure 2.2.3.4** shows some of the largest particles from the normally operating engine in bichromatic light at 400x magnification. These are insignificant in comparison to the particles found on Ferrogram 4359. **Figure 2.2.3.5** shows some of the finer wear particles at 1000x magnification from the abnormal sample. Fine cutting wear particles and dark metallo-oxides are present along with normal rubbing wear particles. Some of these particles show blue or straw temper color (the ferrogram was not heat treated), attesting to high temperature during their generation. **Figure 2.2.3.6** shows a severe wear particle with spots of temper color at 1000x magnification and **Figure 2.2.3.7** shows a cutting wear particle that has turned a blue temper color, also at 1000x magnification. Engine inspection revealed a misaligned overspeed governor drive shaft and gearbox gearshaft. Grinding marks were found on the fuel control gearshaft. **Figure 2.2.3.8** shows the overspeed governor shaft after removal.

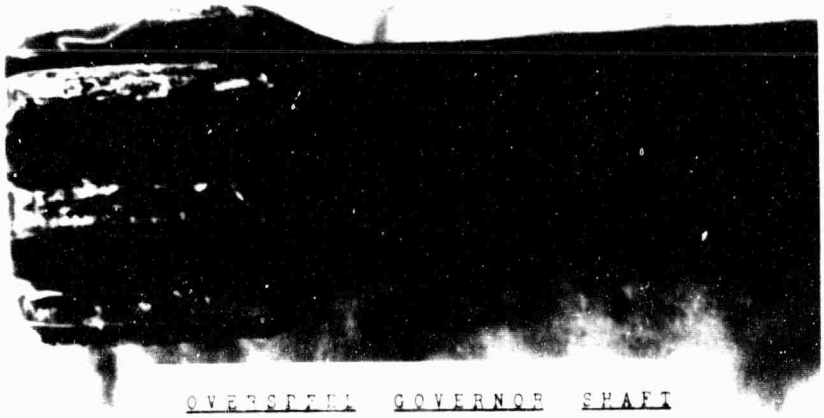

OVERSPEED GOVERNOR SHAFT
REMOVED FROM A T53-L13 ENGINE
EXPERIENCING ABNORMAL
CUTTING WEAR

Figure 2.2.3.8 (B & W Photo) Overspeed Governor Shaft after Removal from a T53 Engine

(2) **Figure 2.2.3.9** is the ferrogram analysis report sheet for another T53 oil sample which showed many dark metallo-oxides along with other abnormal particles present to a lesser extent. On these sheets from this laboratory "DMO" is the abbreviation for dark metallo-oxide. **Figure 2.2.3.10** shows the entry at low magnification. Once again, comparison with **Figure 2.2.3.3** representing the normal condition, shows that this engine is in distress. **Figure 2.2.3.11** shows a string of dark metallo-oxides with a large sphere partially covered by a large, out-of-focus nonmetallic crystalline particle. **Figure 2.2.3.12** shows a large severe wear particle at 1000x magnification. Also present are a few smaller dark metallo-oxides. **Figure 2.2.3.13** shows the oil/air separator shaft gear bearing after teardown. Both the rolling elements and the races are heavily spalled.

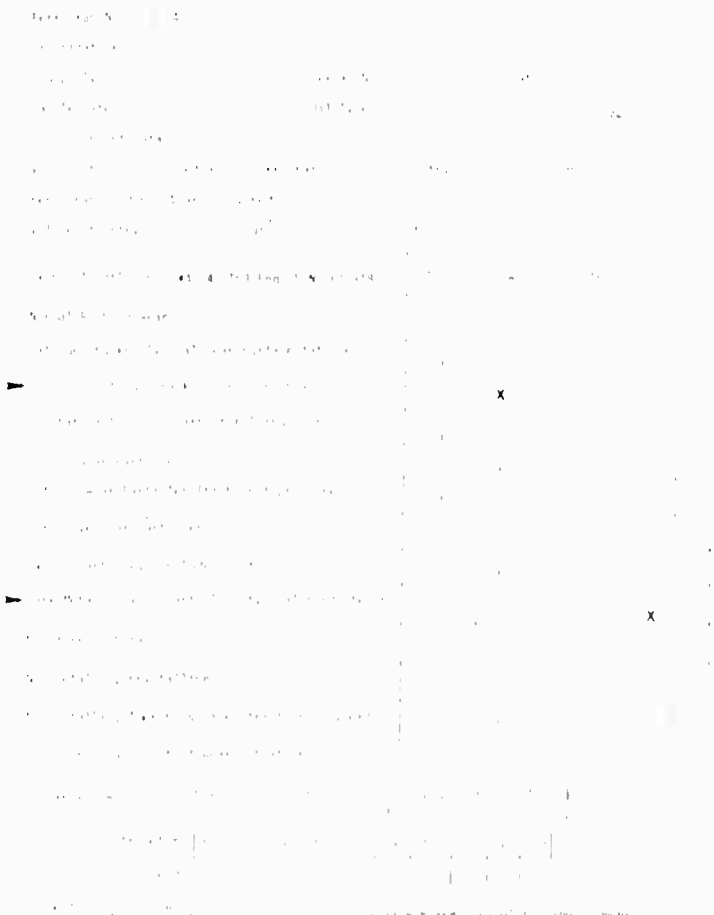

Figure 2.2.3.9 Ferrogram Analysis Report Sheet, Ferrogram 4204

Fig. 2.2.2.17 Opt. M. 100X ⊢— 200μm —⊣

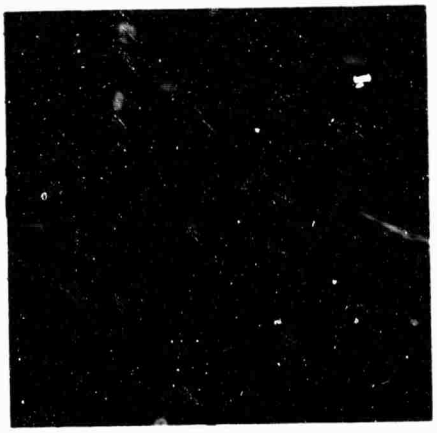

Fig. 2.2.2.18 Opt. M. 100X ⊢— 200μm —⊣

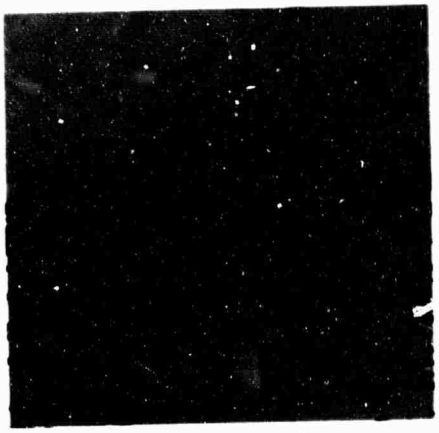

Fig. 2.2.2.19 Opt. M. 100X ⊢— 200μm —⊣

Fig. 2.2.2.20 S.E.M. 100X ⊢— 200μm —⊣

Fig. 2.2.2.21 Opt. M. 400X ⊢— 50μm —⊣

Fig. 2.2.2.22 S.E.M. 400X ⊢— 50μm —⊣

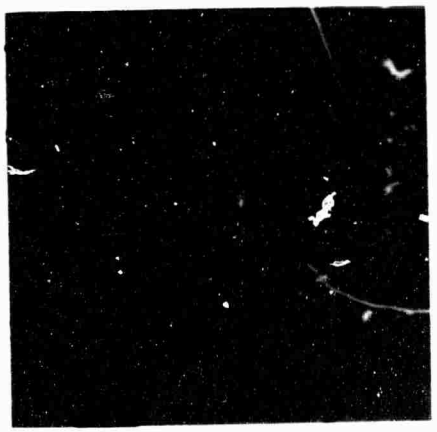

Fig. 2.2.3.2 Opt. M. 100X ⊢— 200μm —⊣

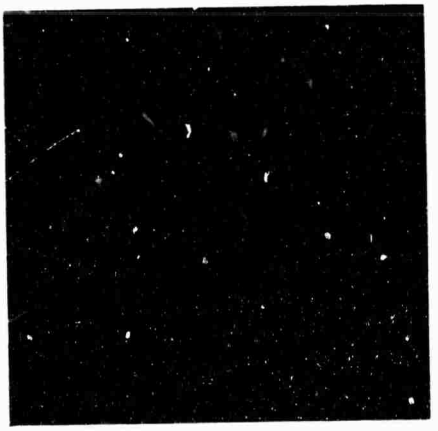

Fig. 2.2.3.3 Opt. M. 100X ⊢— 200μm —⊣

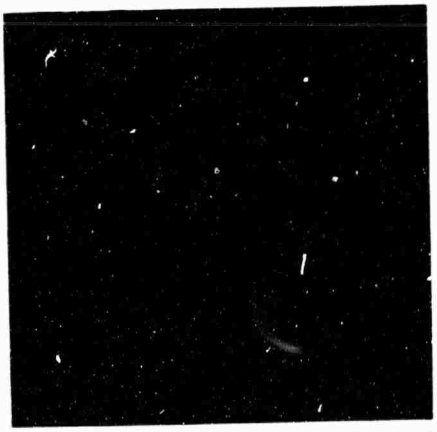

Fig. 2.2.3.4 Opt. M. 400X ⊢— 50μm —⊣

Fig. 2.2.3.5 Opt. M. 1000X ⊢— 20μm —⊣

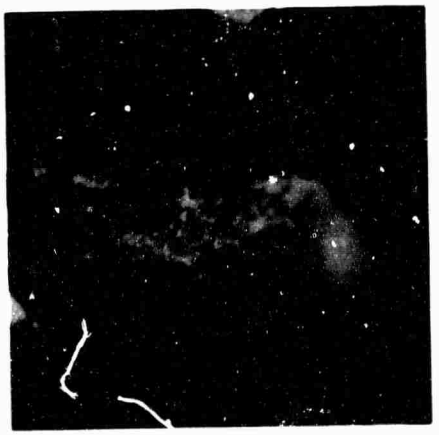

Fig. 2.2.3.6 Opt. M. 1000X ⊢— 20μm —⊣

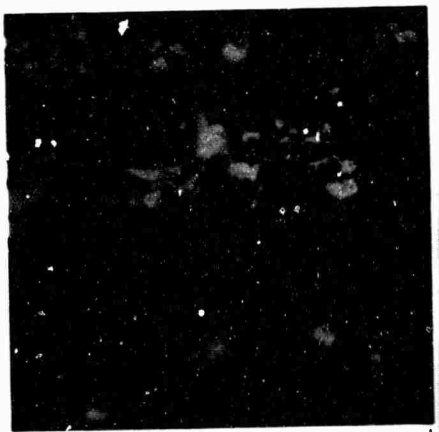

Fig. 2.2.3.7 Opt. M. 1000X ⊢— 20μm —⊣

Figure 2.2.3.13 (B & W Photo) Shaft Gear Bearing After Removal

(3) **Figure 2.2.3.14** is the ferrogram analysis sheet from another T53 engine in distress. **Figure 2.2.3.15** shows the entry at low magnification. **Figure 2.2.3.16** shows the largest particles at the entry at 400x in bichromatic illumination. Notice the several large spheres present which are typical of a grinding type wear mode. **Figure 2.2.3.17** shows part of this view at 1000x using white reflected and green transmitted light. **Figure 2.2.3.18** shows a typical view of the particles on this ferrogram just downstream from the entry at 1000x magnification. The dark metallo-oxides should be classified as more than "few" on the ferrogram analysis report sheet (**Figure 2.2.3.14**) considering their relative abundance on this ferrogram. Many dark metallo-oxides may be seen on **Figure 2.2.3.18**, quite a few of which are out of focus. **Figures 2.2.3.19** and **2.2.3.20** show some of the badly worn parts from this engine which include a fretted #2 bearing, an excessively worn spur gearshaft, a deeply grooved starter spacer, and a deeply grooved driven gear.

(4) **Figure 2.2.3.21** is the ferrogram analysis sheet for a T63 engine removed for suspected abnormal bearing wear. **Figure 2.2.3.23** is the entry view at low magnification of Ferrogram 0017 which may be compared with **Figure 2.2.3.22** which is a low magnification entry view of a ferrogram prepared from an oil sample from a normally operating T63 engine. A properly operating T63

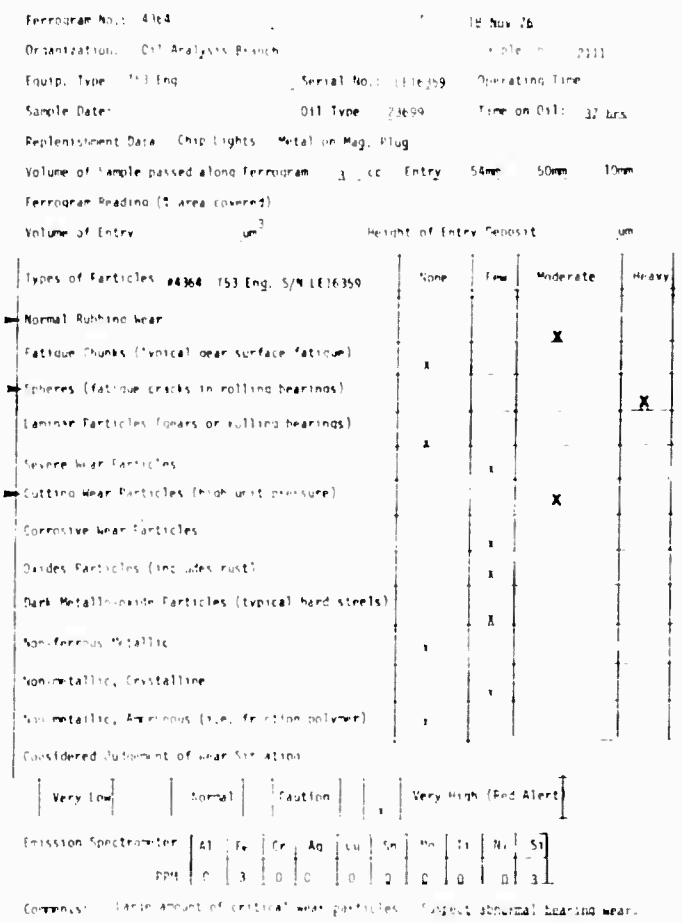

Ferrogram No.: 4364 19 Nov 76

Organization: Oil Analysis Branch Sample No. 2111

Equip. Type T53 Eng Serial No.: LE16359 Operating Time

Sample Date: Oil Type 23699 Time on Oil: 37 hrs

Replenishment Data Chip Lights Metal on Mag. Plug

Volume of Sample passed along Ferrogram 3 cc Entry 54mm 50mm 10mm

Ferrogram Reading (% area covered)

Volume of Entry μm^3 Height of Entry Deposit μm

Types of Particles #4364 T53 Eng. S/N LE16359	None	Few	Moderate	Heavy
Normal Rubbing Wear			X	
Fatigue Chunks (Typical gear surface fatigue)	X			
Spheres (fatigue cracks in rolling bearings)				X
Laminar Particles (gears or rolling bearings)	X			
Severe Wear Particles		X		
Cutting Wear Particles (high unit pressure)			X	
Corrosive Wear Particles		X		
Oxides Particles (inc oides rust)		X		
Dark Metallo-oxide Particles (typical hard steels)		X		
Non-ferrous Metallic	X			
Nonmetallic, Crystalline		X		
Nonmetallic, Amorphous (i.e. fibrous polymer)	X			

Considered Judgement of wear Situation

Very Low	Normal	Caution	X	Very High (Red Alert)

Emission Spectrometer	Al	Fe	Cr	Ag	Cu	Sn	Mo	Ti	Ni	Si
PPM	0	3	0	0	0	2	0	0	0	3

Comments: Large Amount of critical wear particles. Suggest abnormal bearing wear.

Figure 2.2.3.14 Ferrogram Analysis Report Sheet, Ferrogram 4364

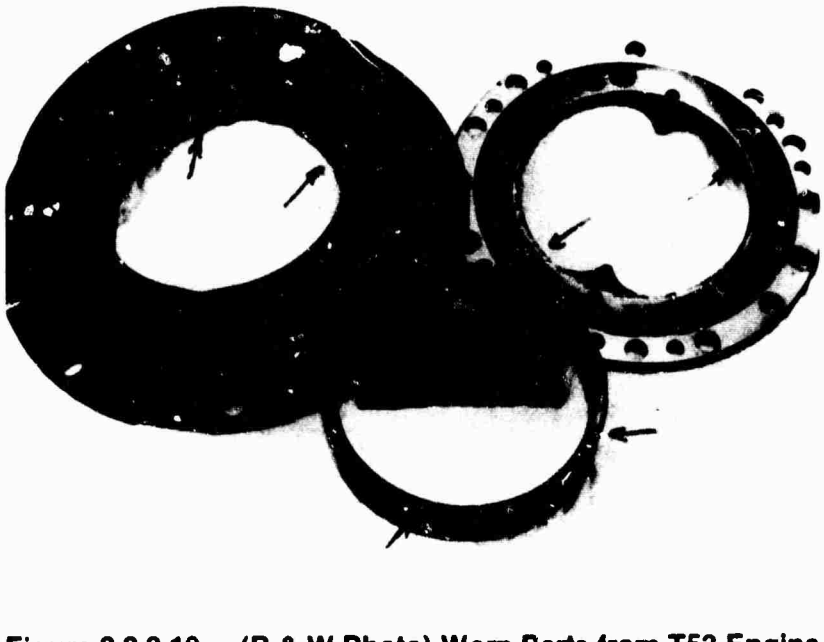

Figure 2.2.3.19 (B & W Photo) Worn Parts from T53 Engine

Figure 2.2.3.20 (B & W Photo) Worn Parts from T53 Engine

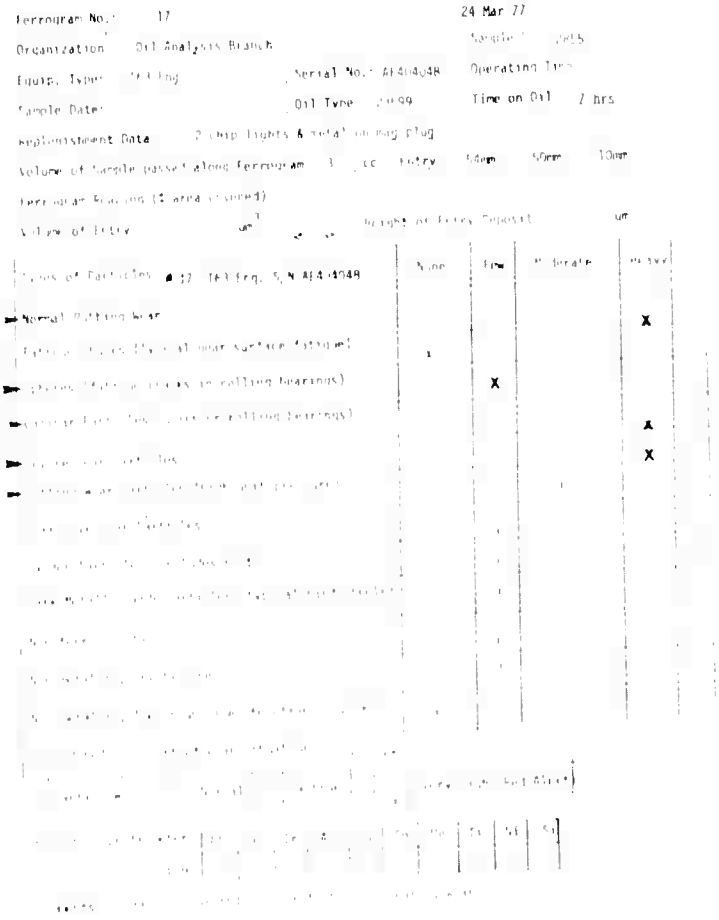

Figure 2.2.3.21 Ferrcgram Analysis Report Sheet, Ferrogram 0017

Fig. 2.2.3.10 Opt. M. 100X ⊢— 200μm —⊣

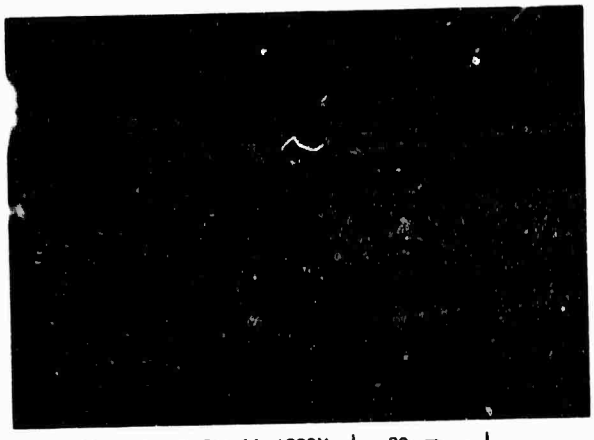

Fig. 2.2.3.11 Opt. M. 1000X ⊢— 20 μm —⊣

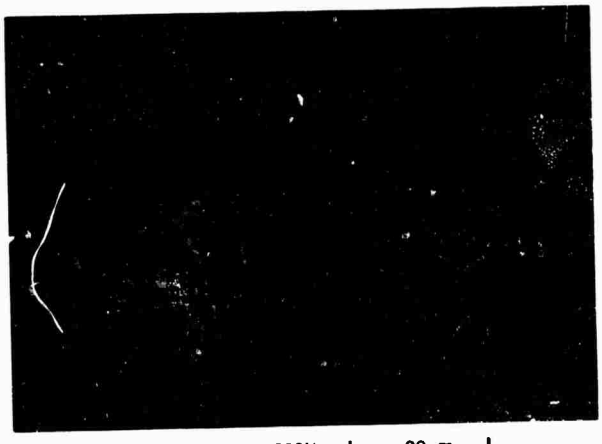

Fig. 2.2.3.12 Opt. M. 1000X ⊢— 20μm —⊣

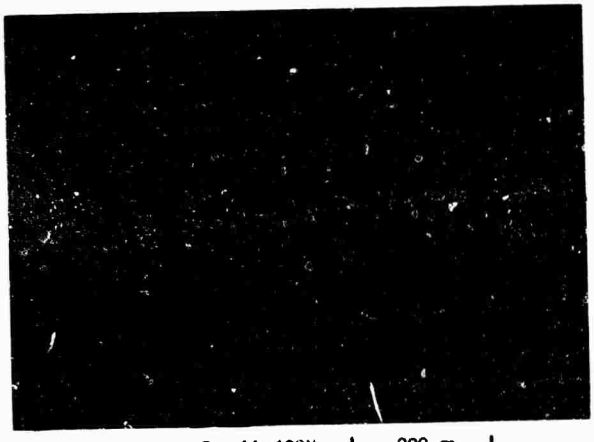

Fig. 2.2.3.15 Opt. M. 100X ⊢— 200μm —⊣

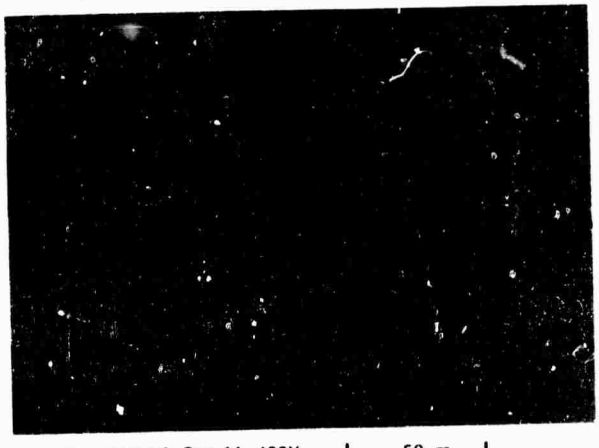

Fig 2.2.3.16 Opt. M. 400X ⊢— 50μm —⊣

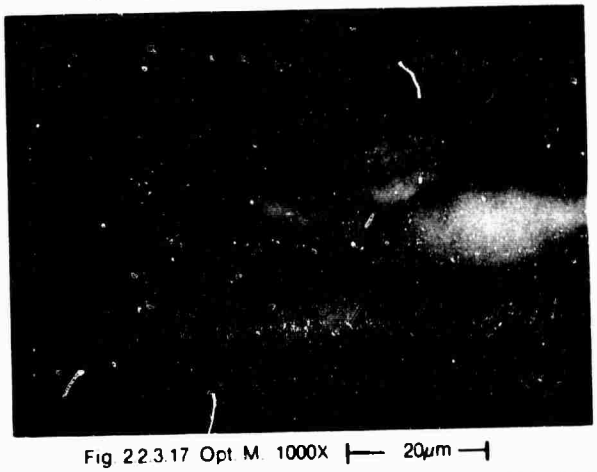

Fig 2.2.3.17 Opt. M. 1000X ⊢— 20μm —⊣

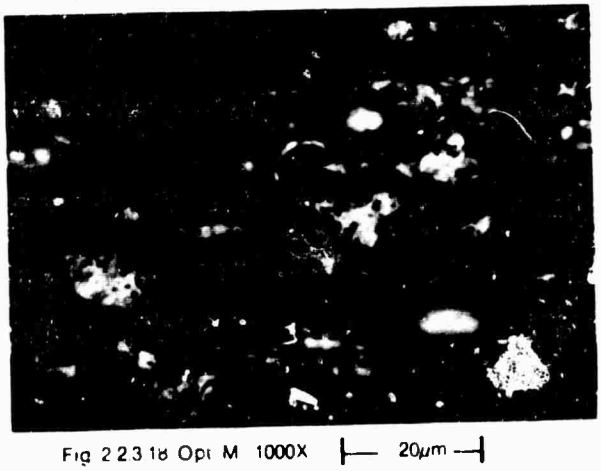

Fig 2.2.3.18 Opt. M. 1000X ⊢— 20μm —⊣

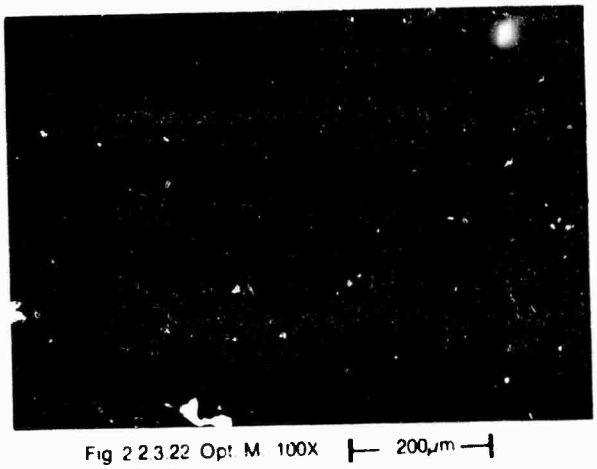

Fig 2.2.3.22 Opt. M. 100X ⊢— 200μm —⊣

(4) Continued

engine generates very few ferrous wear particles which is also true of the T53 engine discussed in this Section. On the other hand, RB211 engines discussed in paragraph **2.2.2** generate somewhat more particles during normal operation. **Figure 2.2.3.24** is a 400x view of some of the largest particles on the ferrogram for the abnormal wear situation. This cluster of particles may be seen on the top of **Figure 2.2.3.22**. The number of particles belonging to the laminar particle category was overstated.

Although some laminar particles are present, most of the particles are too thick to be so classified and should be categorized as severe wear particles. Notice on **Figure 2.2.3.24** the background is out of focus, indicating that the large severe wear particles are at least several micrometers thick. **Figure 2.2.3.25** shows a 1000x magnification view of some of these severe wear particles. Plenty of blue and straw temper color as well as some dark metallo-oxides are present, attesting to high heat and/or lubricant starvation during particle generation. **Figure 2.2.3.26** shows the failed bearing assembly which appears to be grossly spalled although the underlying cause for this failure is not known.

Figure 2.2.3.26 (B & W Photo) Failed Bearing

(5) **Figure 2.2.3.27** is the ferrogram analysis report sheet for a UH-1H helicopter transmission oil sample. **Figure 2.2.3.28,** the low magnification entry view, shows that there is an extremely high wear particle concentration for this unit compared to a normally operating one, **Figure 2.2.3.29**. **Figure 2.2.3.30** shows that the types of wear particles present are severe wear particles, spheres, cutting wear particles, but predominantly dark metallo-oxide particles. **Figure 2.2.3.31** shows a copper alloy wear particle which is probably from the bearing cage. Copper spheres were also found; one is shown on **Figure 2.2.3.32**. **Figure 2.2.3.33** shows the failed support bearing removed from the helicopter transmission. It was also reported that a pinion gear had failed.

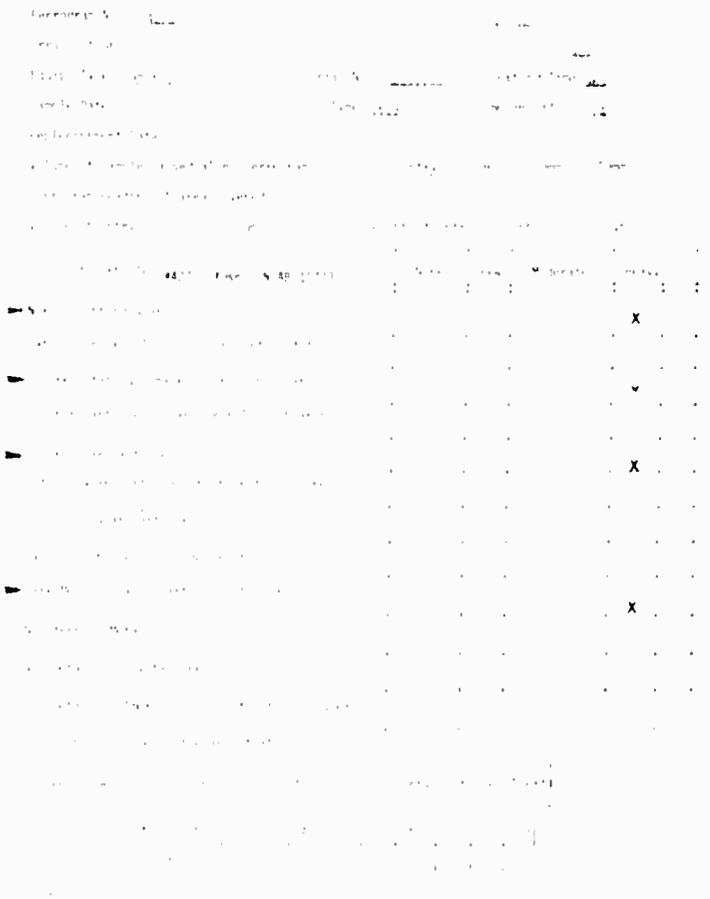

Figure 2.2.3.27 Ferrogram Analysis Report Sheet, Ferrogram 4270

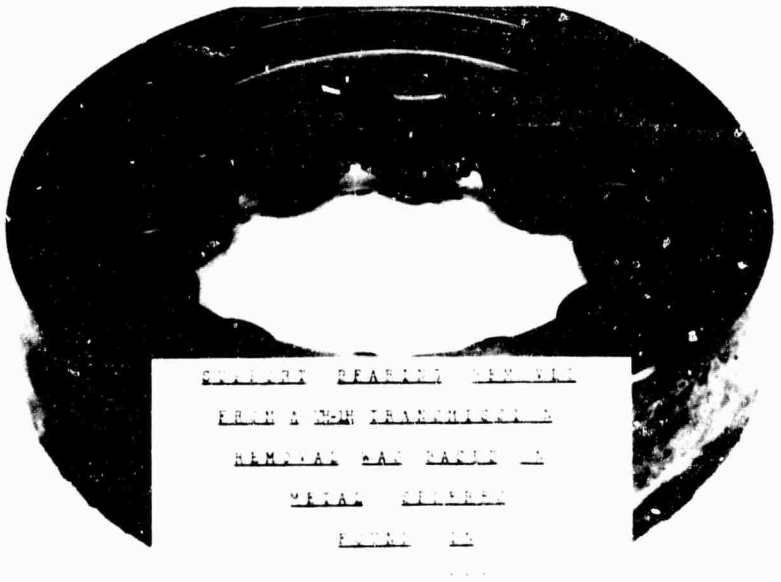

Figure 2.2.3.33 (B & W Photo) Bearing Removed from a UH-1H Transmission

2.3 GEARS

Figure 2.3.1 shows two wear patterns that may occur in gear systems where combined rolling and sliding takes place. See paragraph 1.4. At the pitch line, the contact is rolling so the particles will be similar to rolling contact fatigue particles. The contact has an increasing sliding component as the root or tip is approached. Therefore, the particles will show signs of sliding, such as striations and a greater ratio of major dimension to thickness, if they are from this part of the tooth.

Figure 2.3.2 shows idealized gear system operating regimes as a function of speed and load. To the left of the overload wear curve, where heavy loads are carried at low speed, wear occurs because the oil film is broken. At higher speeds allowable load increases because the oil film survives for this shorter time of contact. Above the fatigue spalling line, wear is governed by the strength of the gear material. It is not that the lubricant is inadequate, but that the load is transmitted through the oil film. If the load is excessive, fatigue particles from the gear pitch line will be generated. If the load is greater still, there is the chance that a tooth will break. Choice of lubricant has little effect in this case, since this event is governed primarily by material selection and load. If speed is increased, the wear regime will be to the right of the scoring or scuffing line. Particles of this type are shown in paragraph 1.4 and are characterized by oxidation and

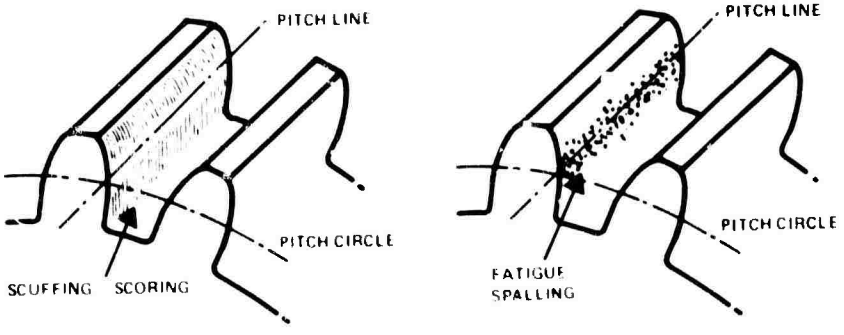

Figure 2.3.1 Gear Failure

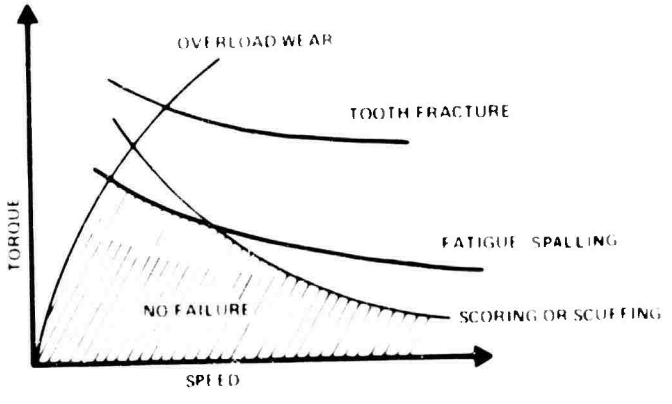

Figure 2.3.2 Gear System Operating Regimes

evidence of sliding due to the breakdown of the lubricant film and consequent thermal effects. See the chapter on gears in reference (14) for further details about gear lubrication.

In this section, the following examples of wear situations investigated by ferrography will be presented:

(1) Overload on gears due to design deficiency.

(2) Combined severe sliding and overload due to ineffective lubrication corrected by EP additive.

(3) Water in the oil.

(4) Abrasive wear.

(5) False warning by emission spectrometer, 3000 ppm Fe content - only normal rubbing wear present.

(6) Extending service until scheduled overhaul - monitoring of a compressor gear train.

2.3.1 Overload on Gears

Figure 2.3.1.1 shows the entry at low magnification in bichromatic light of a ferrogram made from oil from a reduction gearbox which drives an agitator in a chemical process plant. Notice the heavy entry deposit and the many large metal particles which reflect red light back into the optical train of the microscope. From this first impression of the ferrogram, it is clear that an abnormal wear situation exists because of the many large particles. **Figure 2.3.1.2** shows a SEM photograph of the same view.

Figure 2.3.1.3 shows the entry view at 400x in bichromatic illumination. The large particles, which range in size up to about 80 μm in major dimension, are all of one type. They are free metal platelets which do not show surface striations or signs of surface oxidation. **Figure 2.3.1.4**, a SEM photograph of the same view as **Figure 2.3.1.3**, clearly shows that the particle surfaces are very smooth. The lack of surface striations implies that sliding velocities during generation of the particles were low. The absence of oxide particles or surface oxidation on the metal particles rules out any difficulties due to high speed, high operating temperature, or poor lubrication. The major dimension to thickness ratio of these particles is about 10:1 as determined from measuring several particles.

These larger particles fit the discription of gear fatigue particles as described in paragraph 1.4 and are similar to fatigue particles generated by rolling bearings. In this

---

Ref 14 "Standard Handbook of Lubrication Engineering" sponsored by the American Society of Lubrication Engineers (1968), McGraw-Hill Book Company

case, though, it was considered unlikely (as subsequent events were to confirm) that these particles were from a rolling element because a fatiguing bearing rarely generates this much debris. In fact, it is inherently difficult to detect bearing failure when gears are in the same system because the particles are similar but the quantity produced by the gears will usually be much greater.[15] Therefore, it was judged at the time that the most probable source of difficulty was either:

(a) Gear tooth overload (not scuffing or scoring) or

(b) Gear tooth fatigue combined with rubbing wear.

Six months after the ferrographic analysis was made, the gearbox failed. The chemical company was able to convince the manufacturer of the gearbox that a design error had been made with evidence based partly on the wear particle analysis. This resulted in significant financial savings to the chemical company.

2.3.2 Severe Sliding and Overload Due to Lubricant Deficiency

Figure 2.3.2.1 shows the entry view in bichromatic light at low magnification of a ferrogram made from an oil sample obtained from a process industry reduction gearbox. As for the overload case presented in paragraph 2.3.1, cursory examination of the ferrogram at low magnification using bichromatic light makes it immediately obvious that an abnormal wear mode is ongoing because of the many large metal particles present.

This sample, however, differed from that discussed in paragraph 2.3.1 in that many of the severe wear particles showed striation marks, indicating that sliding was involved during their generation. Striation marks may be seen on some of the larger particles even at the low magnification of 100x. Notice also the huge (by wear particle standards) size of some of these particles. Also present, although not as plentiful as the sliding wear particles, were large free metal platelets with smooth surfaces and irregular edges, such as are typical of rolling element bearing fatigue or gear tooth pitch line fatigue. Therefore, the wear particles appear to be generated at the pitch line as well as at the tips and roots of the gear teeth. Present to a lesser extent were large cutting wear particles and some copper alloy particles. **Figure 2.3.2.2** shows the entry deposit in polarized reflected light which emphasizes the presence of large, flat, red oxide agglomerates that may be described as scale; the significance of these particles in relation to the wear situation was not ascertained. Examination of the ferrogram at 1000x magnification shows that the free metal wear particles are virtually free of oxidation, such as temper coloring; it can be safely assumed that the abnormal wear was not due to speed induced scuffing or scoring as represented on the right side of the gear system operating regimes diagram (Figure 2.3.2).

Ref. 15 Pocock, G., and Courtney, S.J. "Ferrography as a Health Monitor and a Design Aid for the Development of Helicopter Gearboxes", Paper 80-I.C-6B-4, San Francisco (Aug 1980).

Fig 2.2.3.23 Opt M 100X — 200μm

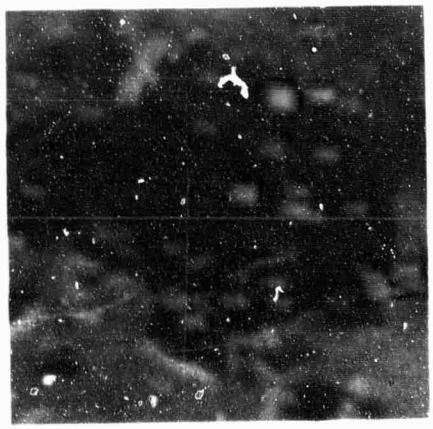

Fig 2.2.3.24 Opt M 400X — 50μm

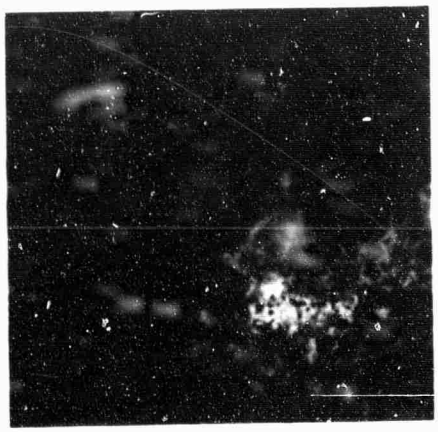

Fig 2.2.3.25 Opt M 1000X — 20μm

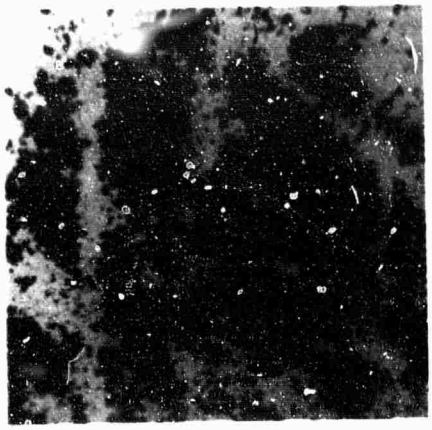

Fig 2.2.3.28 Opt M 100X — 200μm

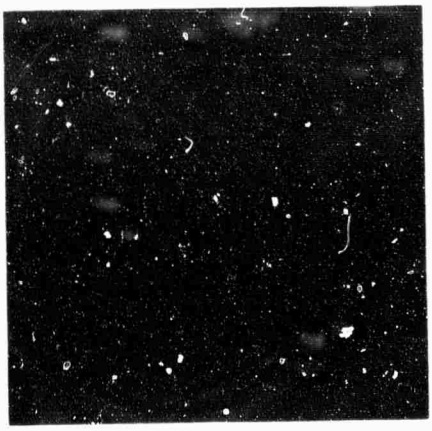

Fig 2.2.3.29 Opt M 100X — 200μm

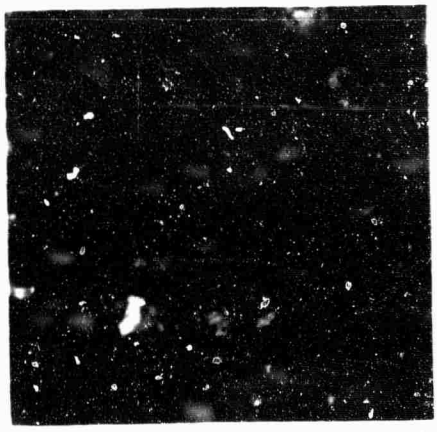

Fig 2.2.3.30 Opt M 400X — 50μm

Fig 2.2.3.31 Opt M 400X — 50μm

Fig 2.2.3.32 Opt M 1000X — 20μm

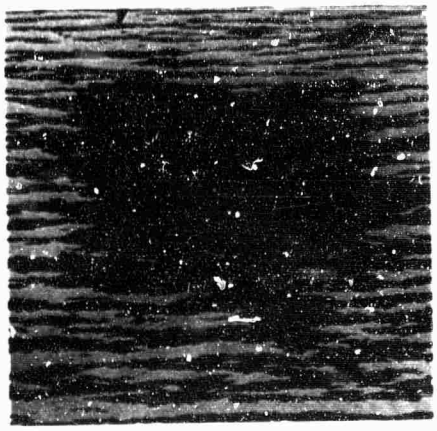

Fig 2.3.1.1 Opt M 100X — 200μm

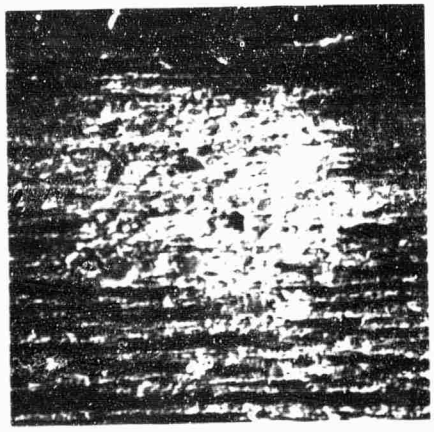

Fig 2.3.1.2 S.E.M. 100X — 200μm

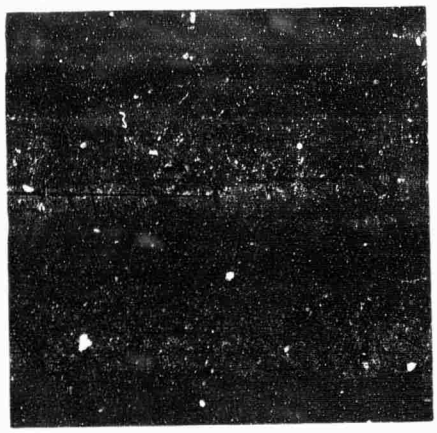

Fig 2.3.1.3 Opt M 400X — 50μm

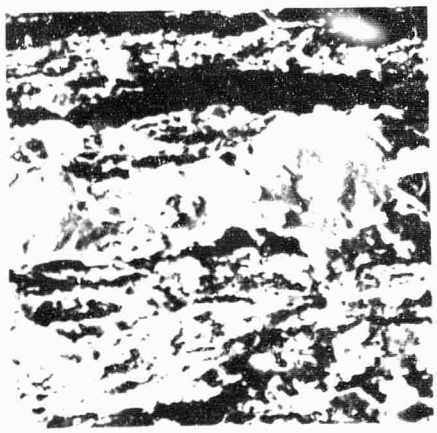

Fig 2.3.1.4 S.E.M. 400X — 50μm

At the time this sample was analyzed, it was reported to the operator of the gearbox that the considered judgment of the wear situation was very high (red alert) due to the presence of steel and cast iron severe wear particles. Following the report, inspection of the gearbox revealed that the gear teeth were heavily worn, especially at the tips where the case had been worn away. The fact that the case had been worn away explains the presence of both steel and cast iron particles in this sample. What is often done in the manufacture of gears, particularly for industrial applications, is that a gear will be case hardened; that is, it will be made of steel and then heated in a carbon atmosphere so that carbon will diffuse into outer layers of the gear. Subsequent quenching and temporing of the gear makes the outer case with the high carbon content hard, but leaves the steel core soft. This results in a hard, wear resistant surface with a tough, shock-resistant core to prevent tooth breakage. When examining a heat treated ferrogram from such a gear, the particles will range from blue to straw color depending on their carbon content. As can be seen on **Figure 2.3.2.3** both straw and blue temper colored particles are present. The low alloy steel particles (blue) are consistent with the finding that the case had worn away at the tips of the teeth, exposing softer steel. Notice that the steel particles show striation marks, indicating a sliding contact.

The problem was solved satisfactorily by using a gearbox oil with EP additive which arrested the excessive wear. EP additives have the ability to move the overload wear curve in **Figure 2.3.2** to the left so that, for this case, an operating regime formerly outside the no failure envelope is now within it.

2.3.3 Water in the Oil

The ferrographic analysis report which is presented in its entirety in paragraph 3.2.5, Establishing a Condition-Monitoring Program, serves as a good example of what wear particles look like when water gets in the oil. The samples were taken from a 1200 kW turbine driven reduction gearbox which had just been overhauled. A baseline had been established after 5 days operation. Notice there are practically no oxides or crystalline particles on the ferrogram prepared from that sample. The only reservation the analyst had was that a certain number of dark metallo-oxides were found at the entry deposit. The sample taken after 1 month of operation, however, reflected a much deteriorated wear situation. Notice the many red oxides as well as the tortuous morphology of the metal particles, many of which were oxide coated. **Figure 2.3.3.1** shows the entry of that ferrogram in polarized reflected light. Water in the lubricant not only causes an oxidative attack, but the load carrying ability of the lubricant is compromised so that large abnormal wear particles are generated.

Figure 2.3.3.2 shows the entry in polarized reflected light of a ferrogram prepared from an oil sample from a reduction gearbox used to drive an agitator in a pharmaceutical manufacturing plant. The agitator motor and gearbox are roof mounted with the

impeller drive shaft coming down from the ceiling to the mixing tank inside the plant. In this case, water has entered the gearbox, which is splash lubricated, and is causing an abnormally high wear rate. Many red oxides, which are characteristic of water attack, are present. Practically no free metal wear particles were found in this sample which could likely be the result of oxidative attack caused by the water during the two-week storage time before the ferrogram was prepared.

The sample resulted in the following DR readings,

L	S
40.6	2.6

which gives an unusually high ratio of large-to-small particles.

This size distribution differs drastically from the nearly equal ratio of large-to-small particles found in the example of corrosive wear in a diesel engine (paragraph 2.1.4). This difference is due to the fact that there were practically no large particles in the diesel oil; the wear mode was one of active corrosive attack on the oil-wetted surfaces, whereas in this case it is hypothesized that the water compromised the load carrying capacity of the lubricant, causing a severe wear mode.

As mentioned in paragraph 1.7.1., water in oil, at least in concentrations above a few tenths of a percent, may be easily detected by placing a drop of oil on a hot plate heated to about 150 to 200° C. If water is present it will boil, causing the oil drop to sputter.

In this case, the oil sample was cloudy because the water had formed an emulsion and it sputtered vigorously when a drop was put on the hot plate.

2.3.4 Abrasive Wear

Figure 2.3.4.1 is the entry view of one of the ferrograms described in paragraph 3.2.5, Establishing a Condition-Monitoring Program, in which a baseline of wear was established by taking one sample from each of several machines. This ferrogram, made from Sample 1, shows heavy strings of ferrous wear particles as well as many large nonmetallic crystalline particles. Compared with a baseline sample, this ferrogram deposit is extremely heavy. Closer examination, **Figure 2.3.4.2,** shows that large cutting wear particles dominate the ferrogram. **Figure 2.3.4.3** is a SEM photograph of the same view. **Figure 2.3.4.4** shows a large cutting wear particle at 1000x magnification. **Figure 2.3.4.5** is a SEM photograph of the same view. Because there are many nonmetallic crystalline particles, the assumption was made that the cutting wear was due to abrasive contamination, and a recommendation was made to change the oil and oil filter and to examine the machine for possible means of ingression of contaminants.

Another sample was submitted a month later from that machine and wear levels had returned to baseline.

2.3.5 Spectrometer Warning/Normal Rubbing Wear

In this case, a spectrometer gave a value of 3000 ppm for the iron content of an oil sample taken from an enclosed railroad gearbox. Although the spectrometer reading was unusually high, a ferrogram prepared from this oil revealed primarily normal rubbing wear particles. Subsequent inspection of the gearbox showed it to be in satisfactory condition. The oil was changed and it was put back in service.

This case illustrates the usefulness of wear particle analysis to confirm or deny indications given by another analytical method. The iron concentration of the oil was so high because in an enclosed environment particles were continually being ground into smaller bits adding to the population that would remain easily suspended. Acidic oil oxidation products may have played a role as well. As explained in paragraph 3.1.1 on equilibrium particle concentration, it is expected that spectrometer readings will increase in a situation where the same oil is used for an extended period without adding makeup oil.

2.3.6 Extending Service Until Scheduled Overhaul

In October 1979, the overall vibration level on a steam turbine driven centrifugal air compressor began increasing. Vibration monitoring showed that a problem was developing within the compressor. By December, vibration monitoring was being conducted daily. The goal was to keep the compressor running until mid-January when a plant shutdown was planned. S' alignment and wheel balance are important in this compressor because of high ro nal speed. A turbine driven bull gear which operates at 3450 rpm turns 2 pinion gears on shafts, each of which have blower wheels on both ends. The low speed pinion turns at 22,000 rpm, and the high speed pinion turns at 33,000 rpm, in this 4-stage compressor.

An oil sample was submitted in early December 1979, for ferrographic analysis to obtain another opinion on the seriousness of the vibrations in the compressor. **Figure 2.3.6.1** shows the entry view at low magnification of a ferrogram prepared from 10 ml of this sample. Although a baseline for this piece of equipment had not been previously established, the absence of a high concentration of large particles was a favorable indication. **Figure 2.3.6.2** shows the string of largest ferrous particles at the entry. Notice that the morphology of the particles is quite abnormal, with large cutting wear particles present. Also, temper colors were present on some of the ferrous severe wear particles, indicative of excessive heat during generation. Since this gearbox operates at such high speed, it may be assumed that the operating regime would be towards the scuffing/scoring region of **Figure 2.3.2.** Heat treatment showed the ferrous particles to be low alloy steel, consistent with the gear material. Also noted were red/blackish nonmetallic crystalline particles. In spite of the presence of a certain number of abnormal wear particles, the wear situation was given a status of caution rather than very high (red alert) due to the relatively low concentration of particles in the sample.

On 13 January 1980, the compressor was shut down and a factory consultant was on hand for inspection and repair. It was found that the bull gear and high-speed pinion showed irregular wear, and the high-speed shaft bearings (Pb/Sn) were found to be fretting on their back pads. The bull gear showed both spalling and what appeared to be a cutting type wear. The wear was primarily on one side of the pitch line of the teeth covering 1/3 to 1/2 the surface. This is consistent with a scuffing or scoring wear mode.

The bull gear, high-speed pinion gear, and high-speed shaft bearings were replaced and the machine was trial run with the result that the high-speed shaft showed unacceptably high vibration. This was due to imbalance in the fourth stage wheel which had to be rebalanced at the factory. Imbalance in the fourth stage wheel may have caused the initial high vibration and abnormal gear wear.

2.4 NATURAL GAS FIRED INTERNAL COMBUSTION ENGINE

Analytically, a natural gas fired diesel engine is the same as a diesel engine except that it is less complicated because black agglomerates (carbon-calcium-sulfur compounds) and corrosive wear debris should not be present. The following report, done for Colorado Interstate Gas Company, successfully predicted ring/cylinder scoring based on rather subtle, but identifiable, differences between the wear particles found in 3 samples from 3 different engines. **Figure 2.4.1** presents the summary, text, and ferrogram analysis sheets from that report. The photomicrographs called out in the text of the report are not reproduced in the Atlas, but several photomicrographs are included from these samples and are called out in paragraph 2.4.1.

2.4.1 Discussion of Preceding Analysis Report

Figures 2.4.1.1 and 2.4.1.2 are photographs of the first page of the preceding report showing the entry region for Unit #2 which had the highest DR readings. Notice that the strings of ferrous wear particles are quite small. The high DR reading is due to the nonmetallic crystalline debris present which appears not to be having an adverse effect on the engine since very few abnormal wear particles are present. If the crystalline contaminants were injurious, cutting wear would be present. Perhaps the sample bottle was contaminated or the contaminants were inadvertently introduced when the sample was taken. In contrast, the entry view, **Figure 2.4.1.3** for Unit #6, shows much thicker strings of ferrous wear particles which are partially oxidized cast iron severe wear particles. **Figure 2.4.1.4** shows some of these particles at 400x after heat treatment to the first test temperature (330° C) to reveal straw temper color. **Figure 2.4.1.5** shows some cast iron wear particles at 1000x. **Figure 2.4.1.6** shows the entry view for Unit #1. The strings on this ferrogram appear quite benign in comparison with the particles from Unit #6.

Fig. 2.3.2.1 Opt. M. 100X ⊢— 200μm —⊣

Fig. 2.3.2.2 Opt. M. 100X ⊢— 200μm —⊣

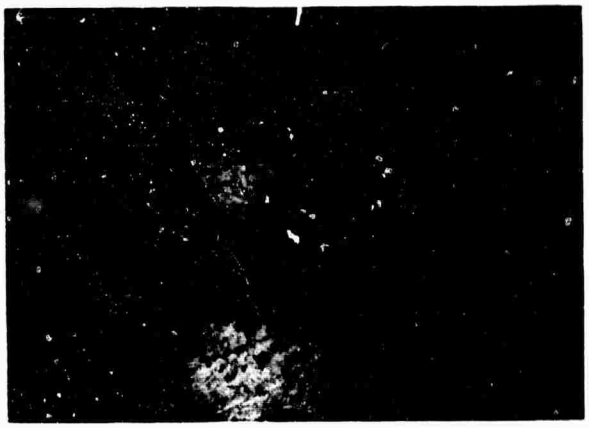

Fig. 2.3.2.3 Opt. M. 400X ⊢— 50μm —⊣

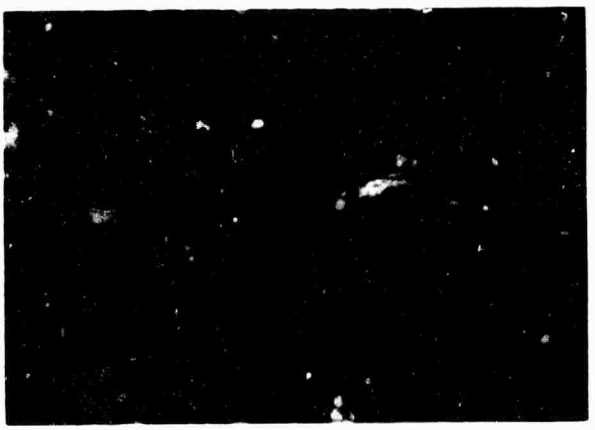

Fig. 2.3.3.1 Opt. M. 100X ⊢— 200μm —⊣

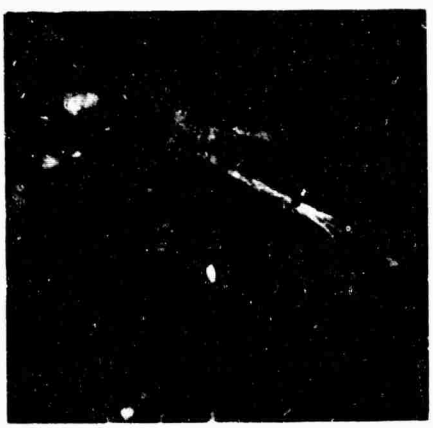

Fig. 2.3.3.2 Opt. M. 100X ⊢— 200μm —⊣

Fig. 2.3.4.1 Opt. M. 100X ⊢— 200μm —⊣

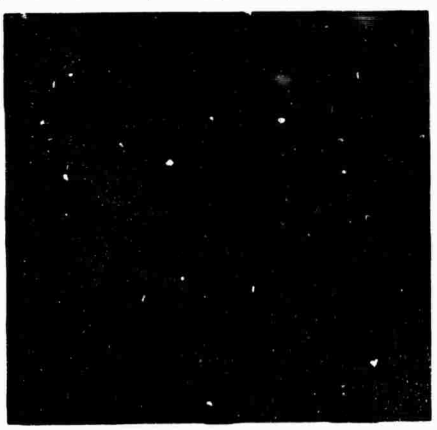

Fig. 2.3.4.2 Opt. M. 400X ⊢— 50μm —⊣

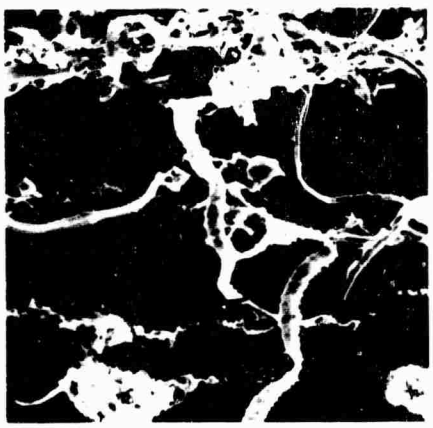

Fig. 2.3.4.3 S.E.M. 400X ⊢— 50μm —⊣

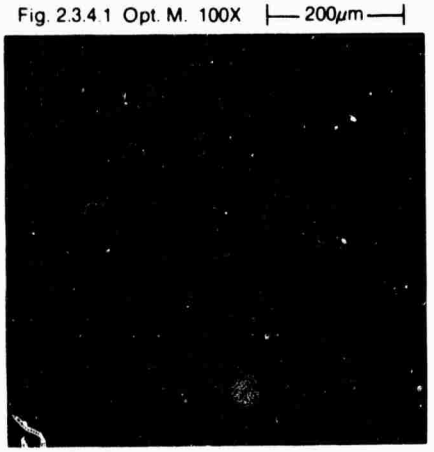

Fig. 2.3.4.4 Opt. M. 1000X ⊢— 20μm —⊣

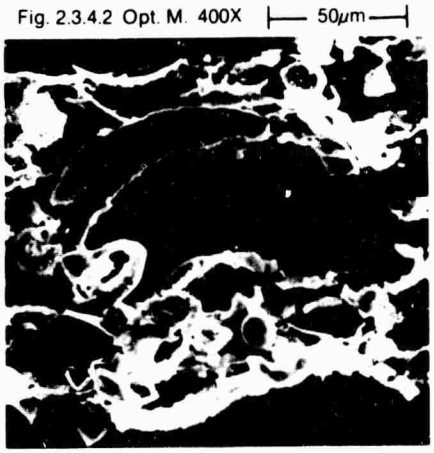

Fig. 2.3.4.5 S.E.M. 1000X ⊢— 20μm —⊣

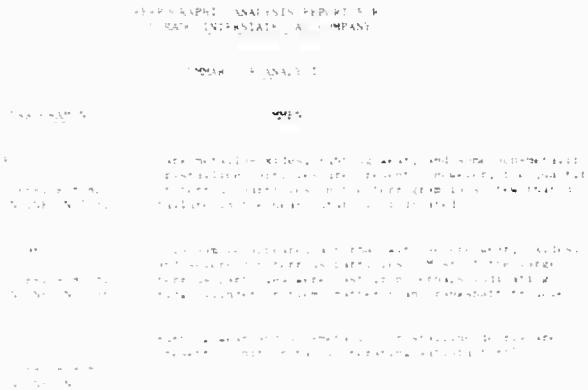

TEXT OF ANALYSIS REPORT

Ferrographic analysis of three oil samples submitted by Colorado Interstate Gas Company, which came from three different natural gas fueled internal combustion engines, revealed that two of the three engines appeared to be operating satisfactorily, but one engine (Superior 8GTB25, Engine Unit #6) appeared to be in an abnormal wear mode. Lacking previous samples from these engines makes it more difficult to judge engine conditions because a baseline has not been established. Nevertheless, in two of the three cases the quantity and size of the wear particles found were so low that the engine condition is considered normal. However, Sample #2 appears to have problems with a cast iron part, most likely one or several cylinders.

Ferrogram analysis report sheets are included in this report which detail the types and relative quantities of the particles present. Also included are photomicrographs which show examples of some of the various particles found in the samples. Photo - F0330-1, F0249-1 and F0311-1 are overall views of the entry deposit (where the sample oil first touches down on the ferrogram) at low magnification (100x) taken with white reflected and green transmitted light. Additional photos with the same illumination are taken at 400x magnification to better show the wear particles found. For example, photomicrograph F0250-1 is a 400x magnification view of the entry showing severe wear and dark metallic-oxide particles which could not be seen at 100x magnification.

Heat treatment of the ferrogram allows easy distinction of the ferrous particles into broad alloy classes. Low alloy steel turns blue at 625°F 330°C, medium alloy steel or cast iron turns a straw color at 525°F 310°C, and high alloy steels are only slightly affected at 625°F 310°C. Analysis of the resulting temper colors of the particles on ferrograms F0330 and F0311 subjected to heat treatment on a laboratory hotplate reveals about 70% of the ferrous particles are low alloy steel. The remaining 30% of the ferrous particles are either medium alloy steel or cast iron. Heat treatment of ferrogram F0249 showed that most of the largest wear particles are cast iron. A short paper "The Use of Temper Colors in Ferrography" is appended which gives details on the heat treating of ferrograms to identify various alloys.

Page 1

Page 2

105

NAEC-92-163

Figure 2.4.1 Report for Colorado Interstate Gas Company, Pages 1 through 6

[illegible] ANALYSIS REPORT (Continued)

The [illegible] Reading Ferrograph [illegible] was used to obtain quantitative information. The results were:

Sample 1	Sample 2	Sample 3
[illegible]	11.[illegible]	[illegible]
[illegible]	[illegible]	[illegible]

[illegible] sample [illegible] method. Sample #1 was found to [illegible] high readings although [illegible] The baseline for this type of [illegible] establishing a [illegible] ferrograms for [illegible]

Page 3

FERROGRAM ANALYSIS REPORT SHEET

Ferrogram Number: 0330 — Date: 12 May 1986

Origination: Colorado Interstate Gas Co. — Sample No.: 1

Equipment Type: Superior [illegible] — Equipment Serial No.: Unit #2

Sample Date: — Total Operating Hours:

D.R. Reading (per ml) L: [illegible] S: [illegible] — Oil Type:

Time on Oil:

Volume of Undiluted Sample to Make Ferrogram: 1[illegible] ml

Ferrogram Reading % area covered: Entry 20.1; 50mm [illegible]; 10mm 14.5

TYPES OF PARTICLES	NONE	FEW	MODERATE	HEAVY
Normal Rubbing Wear Particles		X		
Severe Wear Particles				
Cutting Wear Particles	X			
Chunks				
Laminar Particles	X			
Spheres				
Dark Metallic Oxide Particles		X		
Red Oxide Particles				
Corrosive Wear Debris	X			
Non Ferrous Metal Particles	X			
Non Metallic Birefringent: Inorganic			X	
Non Metallic Birefringent: Organic				
Non Metallic, Amorphous				
Friction Polymers	X			
Fibers	X			
Other, Specify	X			

Considered Judgment of Wear Situation: [X] Normal [ ] Watch [ ] Very High Red Alert

COMMENTS:

Although a moderate amount of non-metallic crystalline particles are present, these particles do not seem to be causing any damage by the fact that cutting wear particles or severe wear particles are not found on the ferrogram to any significant degree. Recommend change of oil and oil filter and check of air filter to eliminate non-metallic particles.

FORM [illegible]

Page 4

Figure 2.4.1 Report for Colorado Interstate Gas Company (Continued)

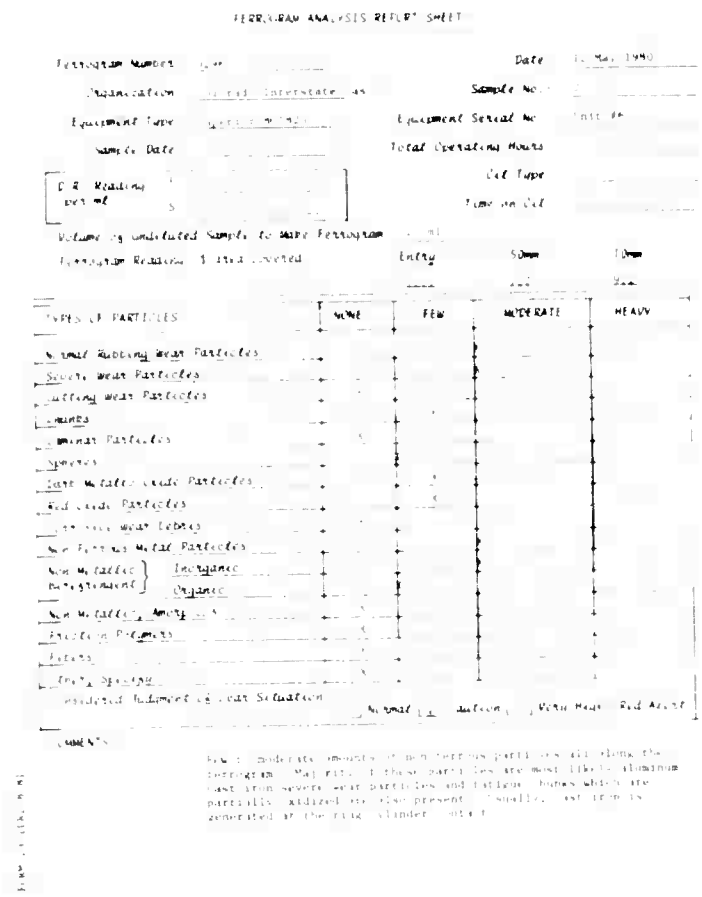

FERROGRAM ANALYSIS REPORT SHEET

Ferrogram Number: 0331 — Date: 12 May 1980

Organization: Colorado Interstate Gas Co. — Sample No.: 3

Equipment Type: Superior Bk825 — Equipment Serial No.: Unit #1

Sample Date: — Total Operating Hours:

D.R. Reading (per ml) L: 1.7 S: 1.1 — Oil Type:

Time on Oil:

Volume of Undiluted Sample to Make Ferrogram: 10 ml

Ferrogram Reading (% area covered): Entry 4.2 — 5.0mm 1.9 — 1.0mm 1.7

TYPES OF PARTICLES	NONE	FEW	MODERATE	HEAVY
Normal Rubbing Wear Particles		X		
Severe Wear Particles	X			
Cutting Wear Particles	X			
Chunks	X			
Laminar Particles	X			
Spheres		X		
Dark Metallic Oxide Particles		X		
Red Oxide Particles	X			
Corrosive Wear Debris	X			
Non Ferrous Metal Particles		X		
Non Metallic Birefringent: Inorganic	X			
Non Metallic Birefringent: Organic	X			
Non Metallic, Amorphous	X			
Friction Polymers	X			
Fibers	X			
Other, Specify				

Considered Judgment of Wear Situation: [X] Normal [ ] Caution [ ] Abnormal [ ] Severe

COMMENTS

The ferrous debris appears benign in this sample.

FORM 2 JWATEL 8 81

Page 6

FERROGRAM ANALYSIS REPORT SHEET

Ferrogram Number: — Date: 12 May 1980

Organization: Colorado Interstate Gas Co. — Sample No.: 2

Equipment Type: Superior Bk825 — Equipment Serial No.: Unit #1

Sample Date: — Total Operating Hours:

D.R. Reading (per ml) L: 1.7 S: 1.1 — Oil Type:

Time on Oil:

Volume of Undiluted Sample to Make Ferrogram: ml

Ferrogram Reading (% area covered): Entry — 5.0mm — 1.0mm

TYPES OF PARTICLES	NONE	FEW	MODERATE	HEAVY
Normal Rubbing Wear Particles				
Severe Wear Particles				
Cutting Wear Particles				
Chunks				
Laminar Particles				
Spheres				
Dark Metallic Oxide Particles				
Red Oxide Particles				
Corrosive Wear Debris				
Non Ferrous Metal Particles				
Non Metallic Birefringent: Inorganic				
Non Metallic Birefringent: Organic				
Non Metallic, Amorphous				
Friction Polymers				
Fibers				
Other, Specify				

Considered Judgment of Wear Situation: [ ] Normal [ ] Caution [ ] Abnormal [ ] Severe

COMMENTS

Few : moderate amounts of non ferrous particles will plate the ferrogram. Majority of these particles are most likely aluminum cast iron severe wear particles and fatigue chunks which are partially oxidized are also present. Usually, cast iron is generated at the ring, cylinder, and p

FORM 2 JWATEL 8 81

Page 5

Figure 2.4.1 Report for Colorado Interstate Gas Company (Continued)

This page left blank
intentionally.

Fig. 2.3.6.1 Opt. M. 100X ⊢— 200μm —⊣

Fig. 2.3.6.2 Opt. M. 400X ⊢— 50μm —⊣

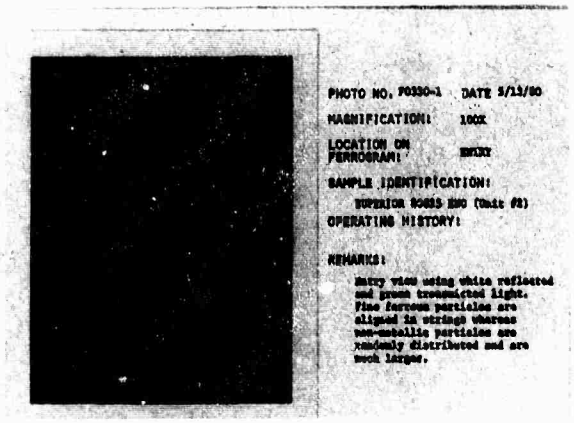

Fig. 2.4.1.1 Photoreduction of report

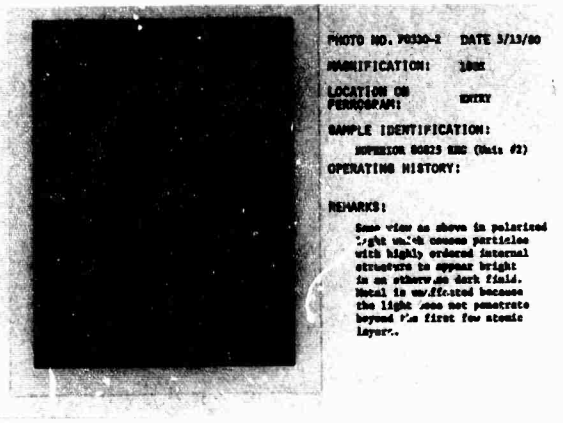

Fig. 2.4.1.2 Photoreduction of report

Fig. 2.4.1.3 Opt. M. 100X ⊢— 200μm —⊣

Fig. 2.4.1.4 Opt. M. 400X ⊢— 50μm —⊣

Fig. 2.4.1.5 Opt M. 1000X ⊢— 20μm —⊣

Fig. 2.4.1.6 Opt. M. 100X ⊢— 200μm —⊣

After the report had been submitted to Colorado Interstate Gas Company, two of the units, #2 and #6, were disassembled and inspected. The #2 unit was not in any severe distress and likely would have operated for a considerably longer time. The cylinders of the #6 unit were examined by use of a borescope and the decision to overhaul it was made at that time. Six of the eight cylinders were severely scuffed as were the piston rings. This unit could not have run any appreciable length of time without getting into some very severe problems.

Observations and other analyses indicated that the #1 unit is in no distress and that there was no reason to go into it as of October 1980. The samples were sent 11 April 1980 and the report was sent back to Colorado Interstate Gas Company on 21 May 1980, indicating that the cylinder scuffing problem was detected well in advance of when the engine was shut down.

2.5 Journal Bearings

Journal or plain bearings may be made of several different materials, the general requirement being that the bearing be softer than the rotating shaft it supports to prevent the shaft from wearing. Babbitt bearings are made from alloys of lead, tin, antimony, and often other metals. Being relatively soft, a babbitt bearing allows contaminant particles to become embedded, preventing abrasive wear to the shaft. Other common material choices for bearings are copper, brass, bronze, silver, and aluminum alloys. These materials are, in general, harder and are consequently less tolerant to abrasive contamination. These bearing materials, however, are more conducive to ferrographic analysis than babbitt bearings which have a tendency to smear rather then generate particles. Tests run on a lathe at Foxboro Analytical in which a lead babbitt metal slider was run with a heavy load against hard steel caused gross smearing of the babbitt metal. In spite of this extensive deformation, very few babbitt particles were found in the oil, although many steel particles were present. Examination of oil samples from journal bearing cavities and from other machines having journal bearings confirm that many babbitt particles are rarely present.

Another difficulty with detecting babbitt particles is that they are easily oxidized by exposure to heat. If the heat exposure, in an oxidizing atmosphere, is only of modest duration, the lead/tin particles will have a stippled appearance. Longer exposure at higher temperature will cause extensive oxidation so that the particles will no longer be metallic, but will be nonmetallic crystalline.

Babbitt metal bearings often have a copper alloy underlay to achieve good bonding to a steel backing. Once the babbitt overlay has been worn or smeared away, copper alloy particles will be generated which give a good indication that the bearing has deteriorated.

Figure 2.5.1 is the ferrogram analysis sheet for an oil sample taken from the inboard bearing cavity of a 500 HP blower motor. Subsequent disassembly of the unit showed heavy babbitt metal wear on the bearing thrust faces. It was necessary to recast the babbitt bearings. DR readings subsequent to reassembly were much reduced. **Figures 2.5.2 and 2.5.3** show a lead/tin alloy particle from the failed bearing before and after heat treating to the first ferrogram heat treatment temperature. Notice the many copper alloy particles present in these views. **Figures 2.5.4 and 2.5.5** show another Pb/Sn particle before and after heating. **Figure 2.5.6** shows a copper alloy particle further along the ferrogram. Notice the large oxide agglomerates in this view. The dominant features of this ferrogram were copper alloy severe wear particles and oxide particles. **Figure 2.5.7** shows a larger Pb/Sn particle which shows evidence of oxidation although the photo was taken before heat treatment of the ferrogram.

FERROGRAM ANALYSIS REPORT SHEET

Ferrogram Number: 242 — Date: 11 April 1980

Organization: Dow Chemical — Sample No.: 2733

Equipment Type: Motor Inboard Bearing — Equipment Serial No.: B-501C

Sample Date: — Total Operating Hours:

D.R. Reading (per ml) L: S: — Oil Type:

Time on Oil:

Volume of Undiluted Sample to Make Ferrogram: 1 ml

Ferrogram Reading (% area covered): Entry 1.1 — 50mm 16.2 — 10mm 61.1

TYPES OF PARTICLES	NONE	FEW	MODERATE	HEAVY
Normal Rubbing Wear Particles			X	
Severe Wear Particles			X	
Cutting Wear Particles		X		
Chunks			X	
Laminar Particles	X			
Spheres	X			
Dark Metallic-Oxide Particles			X	
Red Oxide Particles				X
Corrosive Wear Debris			X	
Non Ferrous Metal Particles		(copper alloy)		X
Non Metallic Background — Inorganic			X	
Non Metallic Background — Organic			X	
Non Metallic, Amorphous			X	
Friction Polymers	X			
Fibers	X			
Other, Specify	X			
Considered Judgment of Wear Situation	☐ Normal	☐ Caution	☒ Very High (Red Alert	

COMMENTS:

Lots of copper alloy wear particles. Some Pb/Sn particles are present. Bearing has probably worn away.

FORM 23-8(REL 8/81)

Figure 2.5.1 Ferrogram Analysis Report Sheet, Ferrogram 0242

2.6 HYDRAULIC SYSTEMS

Ferrography has been used extensively by the Fluid Power Research Center [16,17] to measure the quantity and to identify the type of wear debris in hydraulic system components as well as complete systems. An important result of their work is that hydraulic pump contaminant sensitivity tests in which pumps are subjected to hydraulic fluid loaded with various concentrations and size distributions of abrasive test dust may be conducted at much lower dust concentrations. This is because ferrography can accurately measure small quantities of wear debris, whereas previously, wear was measured by flow degradation of the pump. In order to do this, correlation between flow degradation and the amount of wear debris measured by the ferrograph was established. The advantage gained is that many more tests can be conducted on the same test pump before it wears out, thus saving significant expense.

Hydraulic system components that were exposed to hydraulic fluid with various concentration levels and sizes of test dust include a rotary mechanism, a linear mechanism, gear type pumps, and hydraulic cylinders. Results show the relation between wear as measured by the ferrograph and various test parameters such as dust concentration, dust size (particles above a certain size are removed so that the dust includes all particles up to a certain size), fluid pressure, and different designs of the same mechanism. An interesting result, although one known from previous studies, is that for the linear mechanism more wear occurs for dust with a maximum particle size near the spool clearance dimension than for much coarser or much finer dust at the same concentration. This is attributed to a wedging action of critical size particles that are close to the clearance dimensions.

The Fluid Power Research Center also did ferrographic analysis over substantial portions of the operating life for the following systems: (1) two complete vehicle hydraulic systems (agricultural tractors); (2) a vehicle hydraulic steering system; (3) a vehicle transmission lubrication system; and (4) an auxiliary hydraulic system on an agricultural tractor. Ferrogram readings as well as particle analysis data are presented in reference 16 for these systems.

2.7 Splines/Fretting Wear

The spline coupling is the modern version of a very old idea, namely, using a key and keyway to lock together a shaft and a hub. Today's spline uses multiple teeth (keys) with involute profiles which are integral with the shaft to transmit rotary power from the

---

Ref. 16. Fluid Power Research Center "Wear in Fluid Power Systems", Final Report to the Office of Naval Research, Contract No. N00014-75-C-1157 (Jun 1979).

17. Tessman, R.K., and Fitch, E.C. "Contaminant Induced Wear Debris for Fluid Power Components", Tribology 1978 — Materials Performance and Conservation, University College of Swansea, Wales (3-4 Apr 1978), Published by the I. Mech. E., Paper C45/78 (1978).

engine to various accessories such as pumps, generators, etc. Spline couplings are common to aircraft, although they are found in many types of machinery. Military aircraft can have 100 or more spline couplings in each plane.

Aircraft splines are particularly susceptible to fretting wear failure. Fretting is a wear mode that is caused by low amplitude reciprocating motion between two loaded surfaces in contact. Fretting occurs as a result of vibration or cyclic stressing. Aircraft splines are subjected to an inherently high vibration environment which is compounded by the fact that most splines are grease lubricated because of their inaccessibility. When the grease dries metal-to-metal contact occurs and fretting proceeds rapidly. Splines that are oil lubricated suffer much less from fretting wear problems,[18] but the complexities of forced lubrication are too great for the limited space and access in aircraft applications. Misalignment of the splines causes a sliding motion between the loaded teeth when the splines are rotated. Even minor misalignment causes most of the load to be carried by just a few teeth,which then wear quickly. In practice, some misalignment is inevitable. It is important to understand that with the vibration present in aircraft, fretting occurs even if the spline coupling is not rotating to transmit power.

In the case discussed here,[19] steel splines (male and female surfaces) were coated with various thicknesses of softer metals in an attempt to improve grease-lubricated service life. The time to failure was determined by testing the splines on a spline testing machine built by the Southwest Research Institute in which the splines are purposely misaligned and then oscillated at 4400 cpm. The female spline is held fixed and the male spline gyrates within it without rotation. A torque is applied to the spline coupling by means of a deadweight. The downward movement of the deadweight as detected by a linear variable differential transducer (LVDT) is a measurement of wear in the spline. When the deadweight has dropped a certain distance, corresponding to heavy wear on the teeth, the splines are judged to have failed and the test is stopped.

The failed splines were prepared for ferrographic analysis by washing them in 100 ml of 50% MIL-L-23699 synthetic polyester jet oil and 50% hexane using an ultrasonic bath. Wooden toothpicks were used to pry grease loose from between spline teeth. The grease was dry and well adhered to the spline, but ultrasonic agitation was effective in breaking up the dried grease to free the metal wear particles. The resulting wash was then diluted by as much as 2000:1 to obtain ferrograms on which the number of particles was low enough so that microscopic examination was not difficult due to piling up of particles.

Ref. 18. Loker, A. "Aircraft Engine Driven Accessory Shaft Coupling Improvements Using High-Strength, Low Wear Polyimide Plastic", Report No. TM76-1 SY, Naval Air Test Center, Patuxent River, Maryland.

19. Saka, N., Sin, H., Suh, N.P. "Prevention of Spline Wear by Soft Metallic Coatings", Report to the Office of Naval Research, Contract No. N00014-76-C-0068 (Jul 1980).

Ferrographic analysis revealed that the wear particles from all the failed splines, regardless of coating thickness or material (Cd, Ni, Ag, and Au were used), are similar. The particles are all quite thick, are large compared to benign wear debris from rolling or sliding contacts, ar. ! are heavily covered with surface oxides, both red and black.

Figure 2.7.1 shows some of these particles near the entry at 1000x magnification. Cracks in the particles are not unidirectional, which is consistent with the equiaxed or chunky shape of the particles. In terms of reporting, these particles are classified as dark metallo-oxides and as fatigue chunks since they fi either category. Quite a bit of red oxide is also present, and that category must be included as well. **Figure 2.7.2** shows a black oxide particle with gold adhered to it. Observe how cracks run in several different directions across and into the particle. **Figure 2.7.3** is the same view as seen by the SEM. **Figure 2.7.4** shows some of these fretting wear particles in polarized reflected light which highlights the oxide coating which is a non-stoichiometric compound. See paragraph 1.7 on Ferrous Oxides. Another characteristic of these particles is that the small particles look identical to the larger particles, which is an indication that they are all produced by the same wear mechanism.

One feature of the failure mode for these splines is that practically no wear occurs for most of the test, but once wear is initiated, it proceeds very rapidly. **Figure 2.7.5** shows wear versus time curves for splines tested under various conditions. The slopes of the curves are virtually identical once the rapid wear mode begins. This is consistent with the observation that the wear particles from all the failed splines are the same.

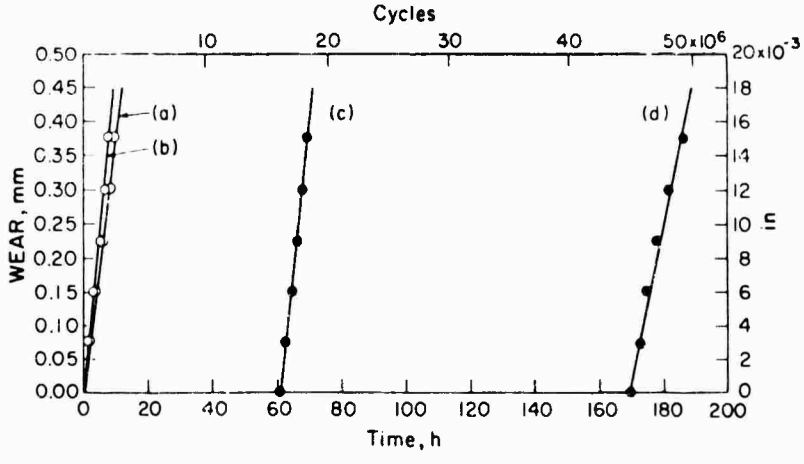

Total wear of unlubricated and lubricated splines as a function of test time. (a) unlubricated and uncoated, (b) unlubricated and gold-coated (10 um), (c) lubricated and uncoated, and (d) lubricated and gold-coated (10 um). (From the work of Saka, et al[19]).

Figure 2.7.5 Spline Wear Curves

The test for one gold-coated spline was stopped before the high wear rate failure mode was reached. This spline was washed in the same manner as the other splines, but in this case, the wash had to be diluted only by a factor of 10:1 to make a ferrogram with proper particle density. Therefore, the particle concentration for the unfailed spline was on the order of 200 times less than the particle concentration for the failed splines. Figure 2.7.6 shows strings of particles from the unfailed spline at 400x magnification. In this case, most of the particles are unoxidized free metal platelets such as would be found in moderate to severe lubricated sliding wear. However, fretting wear chunks are also present. In the center of **Figure 2.7.6** a large fretting wear particle is seen out of focus. **Figure 2.7.7** shows this particle in focus, but the rubbing wear platelets in the background are out of focus. This gold-coated spline was run for 209 hours which statistically is longer than the average lifetime for similarly coated splines. The presence of some fretting wear particles indicates that the final, high wear rate failure mode is just beginning.

For these splines, the onset of the high wear rate failure mode appears to correspond to failure of the lubricant. The many millions of low-amplitude oscillations, with attendant heat generation, probably oxidizes the grease until it is dry. Once that occurs, the friction coefficient increases dramatically, cracks propagate deeper into the material because of higher tractive stress, chunks break out, and the particles oxidize because of high temperature and availability of oxygen. Whenever particles of this type are encountered, a highly abnormal wear mode may be assumed to be occurring.

2.8 BALLSCREWS

The effect of ball material on wear was studied in a bench test designed to simulate the relative motion and operating conditions of a ballscrew assembly in fueling machine heads.

The tests were initiated due to a rash of ballscrew failures that were attributed to the balls. The balls were broken up or suffered damage (chipping, exfoliation) which resulted in ram failures. It was later established that the problem had originated due to sintered powder metallurgy balls being substituted for the normal cast load balls.

Ballscrews are used to convert rotary motion to translational motion to drive fueling machine rams. A ballscrew consists of a helically threaded shaft and nut with balls which run in the grooves formed by the threads. After rotating a number of times around the shaft, the balls are fed back to the initial position by means of a deflector and return tube.

This continuous circulation of the balls reduces the friction between the shaft and the nut, and as well, transfers the load. When the ballscrew assembly is lubricated with oil, it is known that the friction is so low that the wear is insignificant. However, when run in water, as it is in a nuclear application, the conditions are severe. The materials used

Fig. 2.5.2 Opt. M. 1000X ⊢20μm⊣

Fig. 2.5.3 Opt. M. 1000X ⊢ 20μm ⊣

Fig. 2.5.4 Opt. M. 1000X ⊢ 20μm ⊣

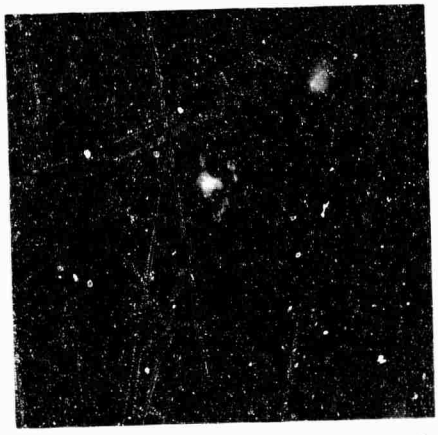

Fig. 2.5.5 Opt. M. 1000X ⊢ 20μm ⊣

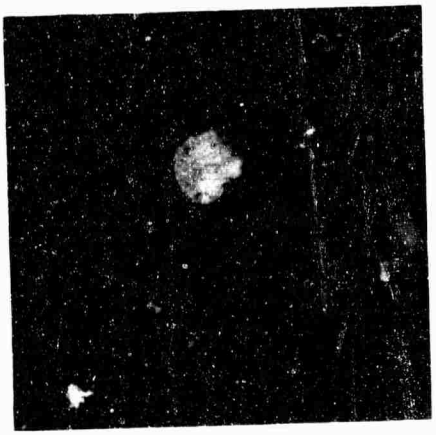

Fig. 2.5.6 Opt. M. 1000X ⊢ 20μm ⊣

Fig. 2.5.7 Opt. M. 1000X ⊢ 20μm ⊣

Fig. 2.7.1 Opt. M. 1000X ⊢ 20μm ⊣

Fig. 2.7.2 Opt. M. 1000X ⊢ 20μm ⊣

Fig. 2.7.3 S.E.M. 1000X. ⊢ 20μm ⊣

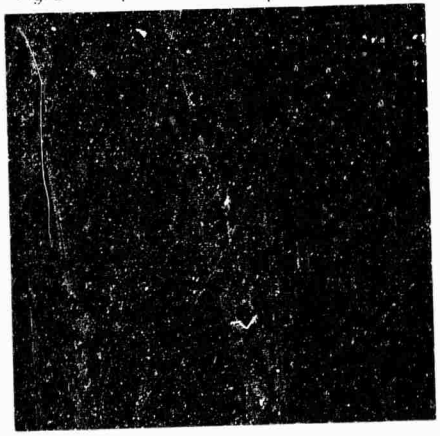

Fig. 2.7.4 Opt. M. 400X ⊢ 50μm ⊣

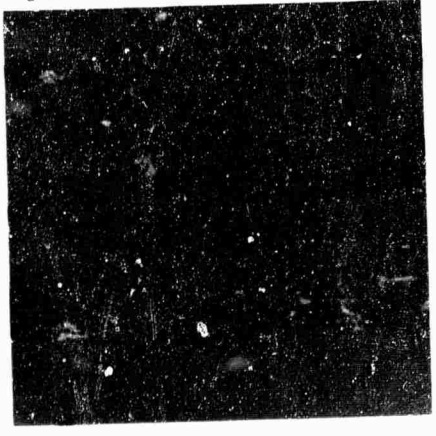

Fig. 2.7.6 Opt. M. 400X ⊢ 50μm ⊣

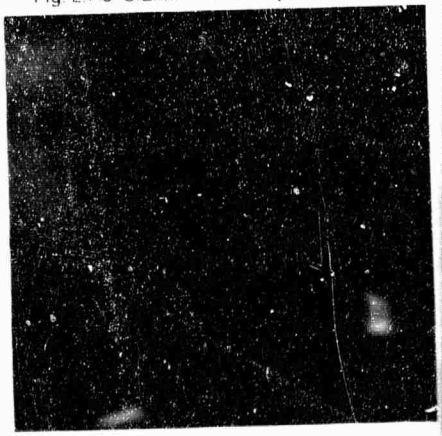

Fig. 2.7.7 Opt. M. 1000X ⊢ 20μm ⊣

must also be impervious to hydrogen embrittlement and to corrosive attack by alkaline water.

The specifically designed test rig used an axially loaded/water lubricated radial bearing whose inner and outer races were modified to a gothic arch configuration to simulate the contact geometry in the ballscrew assembly. The gothic arch thread minimizes skidding which damages ball surfaces. The test load was applied axially to simulate the thrust load experienced by the balls in the ballscrew assembly.

The outer diameter of the stainless steel bearings was 76 mm. Twenty-two ball bearings were used. The eleven load balls, 6.350 mm in diameter, were cast from Stoody 2, a CoCrW alloy. The remainder were spacer balls, 6.248 mm in diameter, and manufactured from an acetal resin.

The tests were conducted at a constant rotational speed of 240 rpm and in the particular test discussed here, an axial load of 294 N/ball. This load condition is very drastic since, in the field, the ram would not be moving while the force was being exerted. The direction of rotation and load application were reversed every 1200 revolutions. An axial clearance increase of 0.6 mm was used as a shutdown condition for the wear test rig as this is well beyond what a field assembly could tolerate. Under this condition, the deflector would contact the screw, causing the ram to stall so that it would subsequently need to be replaced.

Ferrograms were prepared at the following operating times: 2.4, 7.4, 11.4, 33.3, and 40.0 hours. A_L and A_S were determined using the ferrogram reader, A_L at the entry and A_S at the 50 mm position using the 10x objective.

The severity of wear calculated from these is as follows:

Operating Time (Hours)	$A_L^2 - A_S^2$
2.4	5.3
7.4	70.7
11.4	23.0
33.3	41.8
40.0 Test Stopped	238.7

The increase in severity of wear at 7.4 hours is attributed to break-in wear since the index decreases thereafter. Many spheres are noted at 11.4 hours, forecasting bearing fatigue. Cutting wear particles are also present, a result of abrasive wear caused by hard particles circulating in the unfiltered water.

At 33.3 hours, cutting wear and spheres are again observed. The wear situation deteriorates significantly thereafter. Fatigue chunks indicating spalling predominate in the sample at 40 hours, the shutdown condition.

2.9 TAPERED ROLLER BEARING

Ferrographic analysis of oil from a double reduction low-speed gearbox, of a type used for agitation in the process industries, revealed severe wear particles, many normal rubbing wear particles, and friction polymers. The ferrogram analysis report sheet, presented as **Figure 2.9.1,** shows that in addition to the above named particles, nonmetallic crystalline debris, cutting wear particles, and dark metallo-oxides were also present, but to a lesser extent. **Figure 2.9.2** shows the entry at low magnification in bichromatic illumination. An abnormal wear mode is immediately recognized by the many large wear particles present. **Figure 2.9.3** is a SEM photograph of the entry. The predominately blue temper color, **Figure 2.9.4,** subsequent to heat treatment of the ferrogram to 330° C/625° F for 90 seconds shows that most of the wear particles are low alloy steel, although a few smaller cast iron particles are present. **Figures 2.9.5, 2.9.6, and 2.9.7** show some of the larger severe wear particles at the entry. Notice the striation marks on some of these particles indicating severe sliding wear, although other large steel particles have smooth surfaces and irregularly shaped circumferences typical of fatigue spall particles. A few steel particles have a low enough aspect ratio (<5) to be classified as fatigue chunks. **Figures 2.9.8 and 2.9.9** show some of the many friction polymers found on this ferrogram. Although a moderate amount of nonmetallic crystalline particles were present, these seem not to have had a tremendously adverse effect since not that much cutting wear is present.

The main conclusion from this ferrogram is that low alloy steel components are in an abnormal wear mode. The fact that more than one abnormal particle morphology is represented argues that more than one part is in trouble. The presence of friction polymers suggests overload on the lubricant.

Discussion with the manufacturer, subsequent to the analysis, revealed that the gearbox in question was operated in an explosion-proof nitrogen environment which helps to explain the wear mode. It has been known for some time, especially from lubrication problems solved during various space efforts,[20] that special problems arise in oxygen free environments. A thin iron oxide surface film, which forms automatically in air, greatly reduces the coefficient of friction in nonlubricated contacts. If a test is conducted in vacuum, adhesive wear (metal-to-metal welding) will occur much more rapidly than in air where relatively weak oxides form that break away to prevent metal-to-metal contact. In fact, work done by Reda, et al,[5] on the regimes of sliding wear for lubricated contacts show that when conditions are made more adverse than those which produce severe wear particles, first the red oxide of iron forms on the wear particles and then, when conditions are harsher still, the black oxide forms on the wear

---

Ref 20 Bisson, E E. "Lubrication Problems in Space for Exposed Mechanisms and for Power Generation Equipment", Chapter 45, Standard Handbook of Lubrication Engineers (1968)

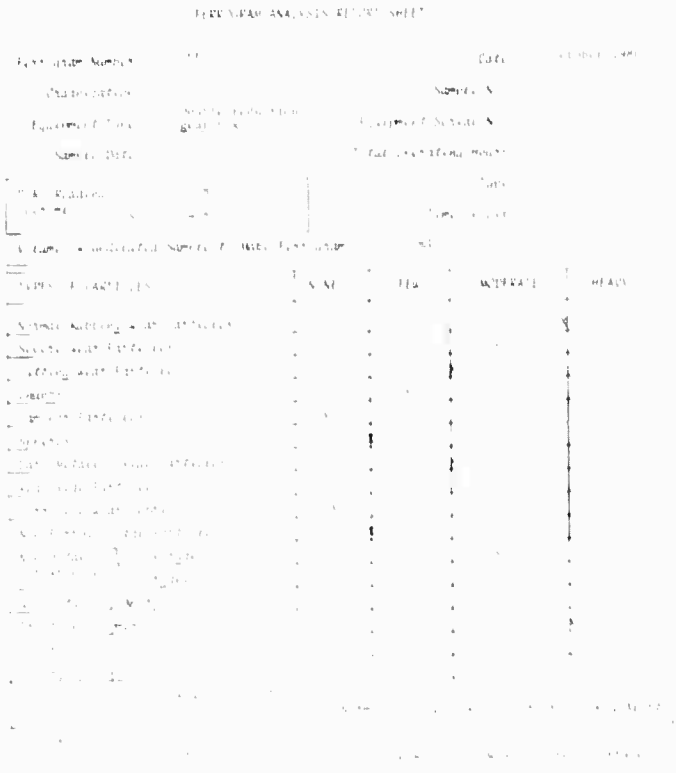

Figure 2.9.1 Ferrogram Analysis Report Sheet, Ferrogram 0566

particles. The latter, black oxide coated particles, are categorized as dark metallo-oxides. When load is increased even further, catastrophic wear ensues where very large free metal particles are generated and adhesive (welding) wear occurs.

This phenomena, of red oxide forming under less adverse conditions than those which give rise to dark metallo-oxides, is probably governed by the speed of the reaction. The red oxide of iron is the final reaction product of iron and oxygen; dark metallo-oxides are generated more rapidly so that the reaction does not go to completion. In practice, fretting wear is virtually the only wear mode that produces a lot of red oxide other than when water gets in the oil. The black oxide as found on dark metallo-oxides is much more commonly encountered in oil lubricated wear.

Disassembly of the gearbox revealed heavy damage to the tapered roller bearings supporting the various gear shafts. **Figure 2.9.10** shows one roller obtained from this gearbox. The end shows clear signs of metal-to-metal smearing as would occur in catastrophic (adhesive) wear. The rolling surface shows signs of a combined sliding and galling wear mode that could be expected to generate particles of various morphology such as were found in this oil sample. It is hypothesized that the nitrogen atmosphere suppressed the formation of oxides when severe wear conditions were exceeded, causing the wear mode to go directly to adhesive (gailing) wear, thus resulting in rapid deterioration of the surfaces.

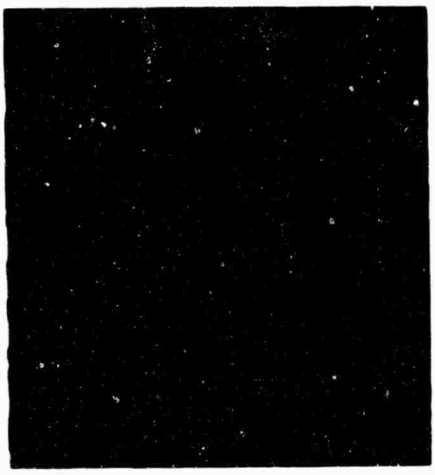

Fig 2 9 2 Opt M 200X ⊢— 100μm —⊣

Fig 2 9 3 S E M 200X ⊢— 100μm —⊣

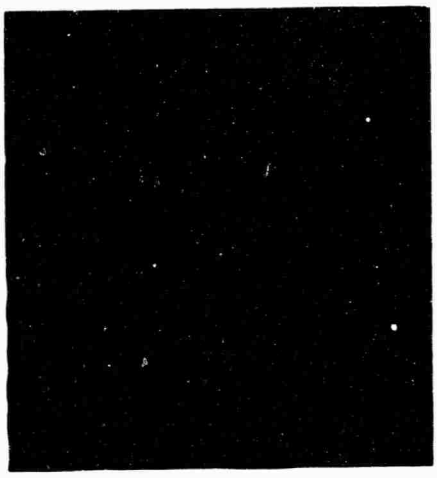

Fig 2 9 4 Opt M 200X ⊢— 100μm —⊣

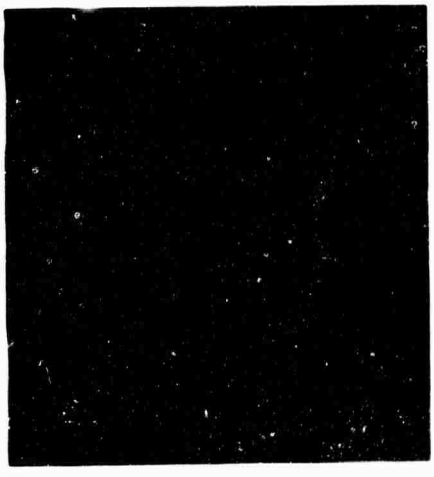

Fig 2 9 5 Opt M 400X ⊢— 50μm —⊣

Fig 2 9 6 S E M 400X ⊢— 50μm —⊣

Fig 2 9 7 S E M 1000X ⊢— 20μm —⊣

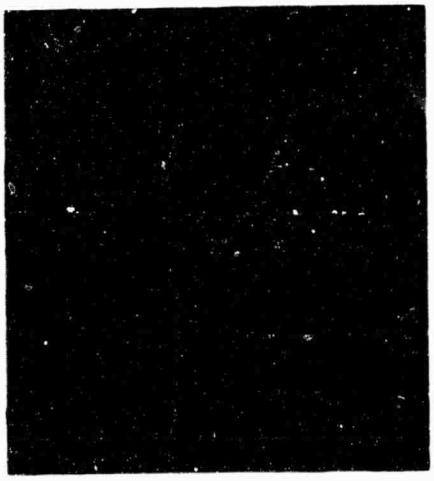

Fig 2 9 8 Opt M 1000X ⊢— 20μm —⊣

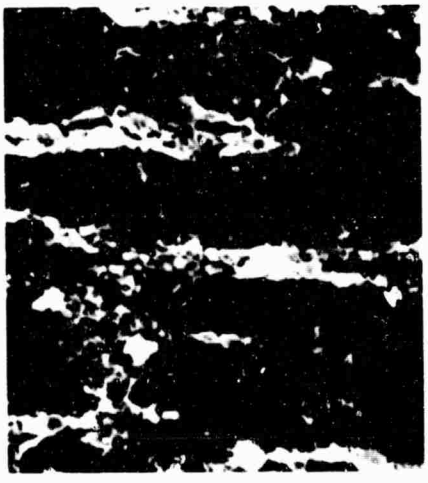

Fig 2 9 9 Opt M 1000X ⊢— 20μm —⊣

Fig 2 9 10 Lifesize

3. OPERATIONAL PROCEDURES

3.1 OBTAINING A REPRESENTATIVE SAMPLE

Before a ferrogram is prepared for wear particle analysis, careful consideration must be given to obtaining a representative sample. In order to appreciate the importance of obtaining a representative sample, paragraph 3.1.1 is presented which deals with the behavior of particles in a machine. As will be explained, particle concentration achieves a dynamic equilibrium such that samples taken the same way over a period of time will have the same quantity of particles. If the sample is not taken properly, however, the concentration and size distribution of the particles can vary dramatically, giving false indications regarding machine condition.

3.1.1 Particle Behavior in a Machine

The underlying reason that quantitative information can be used to signal a changing wear situation is that the particle concentration for normally operating equipment reaches a dynamic equilibrium. Experience has shown this to be true for diverse equipment. Data showing this have appeared in the literature for jet engines,[21] diesel engines,[6] and helicopter gearboxes.[15]

A mathematical model, given a few simplifying assumptions, has been constructed which demonstrates how equilibrium concentration is reached. **Figure 3.1.1.1** shows a diagram of a hypothetical machine that, at given operating parameters such as load, speed, fluid inlet temperature, etc., generates X particles per unit volume of oil that passes through it. Here it is assumed that oil flow rate is constant.

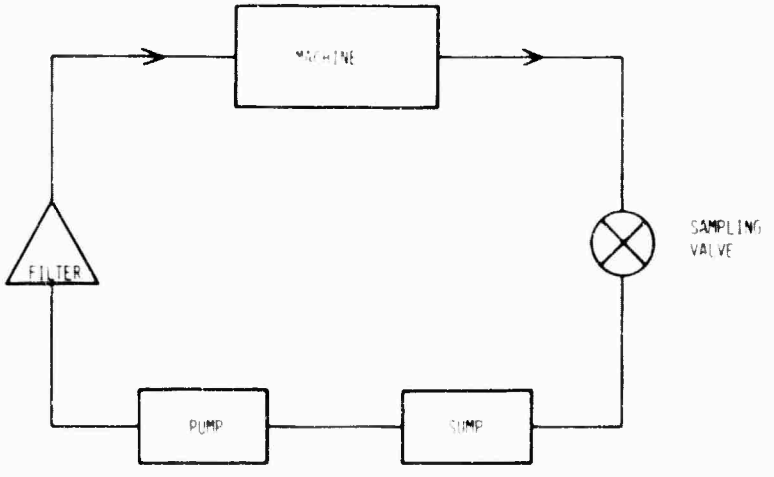

Figure 3.1.1.1 Simplified Oil Path

Ref 21. Scott, D., McCullagh, P.J., and Campbell, G.W. "Condition Monitoring of Gas Turbines —An Exploratory Investigation of Ferrographic Trend Analysis". Wear, 49 (1978) 373-389.

The sampling valve is located immediately downstream of the machine so that if a cycle is begun with clean oil in the sump, the oil at the sampling valve for the first cycle of the oil through the machine (cycle here refers to the time for all the oil to pass through the system once) contains X particles per unit volume.

Now, during passage of the oil through the system, there are various mechanisms for the removal of the particles. These are:

(1) filtration
(2) settling
(3) impaction and adhesion (sticking to solid surfaces)
(4) comminution (the grinding up of particles)
(5) dissolution (oxidation or other chemical attack)
(6) magnetic separation (as occurs in electric machinery).

For purposes of developing this model, it is assumed that these mechanisms are all proportional to the number of particles present which is reasonable if the particle dispersion is sufficiently dilute; that is, if particles do not interact with other particles to form agglomerates or that particles are mutually repelled. Oil loss will not be considered in this model. Clearly, these removal mechanisms are a strong function of particle size, density, and shape.

For the first cycle of oil through the system, the concentration, N, is

$$N(a_i, 1) = X \tag{1}$$

where a_i refers to the removal efficiency for particles of size i. The second term in parenthesis, which is 1, refers to the number of cycles the oil has gone through the system.

After the second cycle of oil through the system, a fraction, a_iX, of the particles generated during the first cycle are removed, the fraction left is $(1-a_i)$ and another X particles are generated so that after 2 cycles the concentration is

$$N(a_i,2) = X + X(1-a_i). \tag{2}$$

After three cycles, the term from the first cycle becomes $X(1-a_i)(1-a_i)$ and the term from the second cycle is $X(1-a_i)$ so that

$$N(a_i,3) = X + X(1-a_i) + X(1-a_i)(1-a_i). \tag{3}$$

For the fourth cycle, each term in equation (3) is multiplied by $(1-a_i)$ and another X particles are generated so that

$$N\,(a_i,4) = X + X\,(1-a_i) + X\,(1-a_i)^2 + X\,(1-a_i)^3. \tag{4}$$

A pattern is seen to emerge and for n cycles the concentration is

$$N\,(a_i,n) = X + X\,(1-a_i) + X\,(1-a_i)^2 + \ldots + X\,(1-a_i)^{n-1}. \tag{5}$$

To sum this series, let $y = (1-a_i)$, then

$$N\,(1-a_i) = X\,(1 + y + y^2 + y^3 + \ldots + y^{n-1}) \tag{6}$$

which equals

$$X\sum_{r=1}^{n} y^{r-1} = X\left(\frac{1-y^n}{1-y}\right). \tag{7}$$

Replacing $(1-a_i)$ for y, the concentration now is

$$N\,(a_i,n) = X\left(\frac{1-(1-a_i)^n}{1-(1-a_i)}\right) = X\left(\frac{1-(1-a_i)^n}{a_i}\right). \tag{8}$$

For equilibrium condition, $n = \infty$, the term $(1-a_i)^n$ becomes zero, and the simple result emerges that

$$N\,(a_i,\infty) = X\left(\frac{1}{a_i}\right) \tag{9}$$

which says that concentration is inversely proportional to removal rate.

Figures 3.1.1.2 and 3.1.1.3 give a numerical example of the establishment of equilibrium particle concentration for a production rate of 500 particles for each millimeter of oil flowing through a machine with a removal efficiency of 40%. If particle free oil is introduced into the machine, the first cycle of that oil through the machine results in a concentration of 500 particles/ml. As the oil passes through the filter (or is acted upon by other removal mechanisms), 40% or 200 particles/ml will be removed. The second cycle adds 500 particles to the 300 particles remaining from the first cycle. Cycle 3

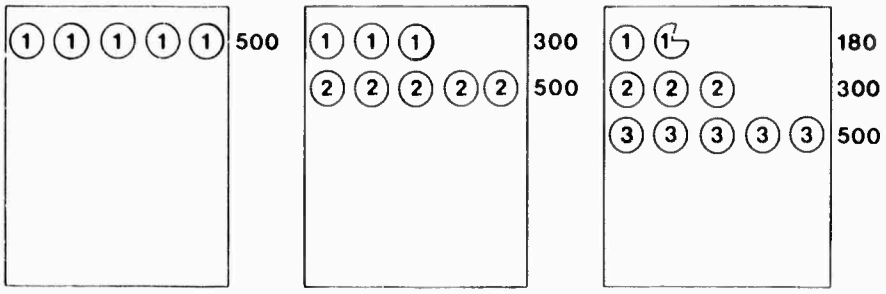

PRODUCTION RATE = 500 PARTICLES/ML

REMOVAL EFFICIENCY = 40%

Figure 3.1.1.2 Establishing Equilibrium Particle Concentration

		PARTICLES LEFT	PARTICLES REMOVED LAST CYCLE
1	1	2	1.2
2	1	3	2
3	1	5	3
4	1	8	6
5	1	14	9
6	1	23	16
7	1	39	26
8	1	65	43
	9 1	108	72
	10 1	180	120
	11 11 11	300	200
	12 12 12 12 12	500	
		1247	498.2

Figure 3.1.1.3 Establishing Equilibrium Particle Concentration

removes 40% of the 300 remaining from cycle 1 and 40% of the 500 particles/ml from cycle 2, leaving 180 particles/ml from cycle 1 and 300 from cycle 2. Another 500 particles/ml are added during cycle 3. After 12 cycles (**Figure 3.1.1.3**), only 2 particles remain from the first cycle. If the particles remaining from each of the 12 cycles are added, a concentration of 1247/ml results which is close to the equilibrium concentration of

$$N(a_i,\infty) = X\left(\frac{1}{a_i}\right) \text{ which equals 1250 particles/ml for}$$

X = 500 particles/cycle

and $a_i = 0.4$ (40%).

If the particles removed during the last cycle are added, the result is 498.2 particles/ml which shows that as equilibrium is approached the removal rate equals the production rate.

Of the most interest to the oil analyst is the number of oil cycles which must occur before the concentration approaches its equilibrium value so that a representative oil sample may be taken. The term β is introduced here so that after R cycles the situation is

$$\frac{N(a_i,R)}{N(a_i,\infty)} \geq 1-\beta \qquad (10)$$

where $\beta << 1$. For example, if β is chosen to equal 0.01, equation (10) says that after R cycles the concentration has reached $1-\beta$, or (1 - .01) = 99%, of its equilibrium value which is close enough to the final equilibrium concentration for obtaining a representative sample.

To evaluate equation (1) for R, when a_i and β are specified, equations (8) and (9) are used;

$$\frac{X\left(\frac{1-(1-a_i)^R}{a_i}\right) \geq 1-\beta}{X\left(\frac{1}{a_i}\right)} \qquad (11)$$

simplifying,

$$1-(1-a_i)^R \geq 1-\beta \qquad (12)$$

$$(1-a_i)^R \leq \beta \qquad (13)$$

and taking logs,

$$R \ln (1-a_i) \leq \ln\beta \tag{14}$$

the result is

$$R \geq \frac{\ln\beta}{\ln (1-a_i)} \tag{15}$$

where R is taken as the smallest integer value to make equation (15) valid.

In **Table 3.1.1.1** values of the quantity $N(a_i,n)$ are given for various values of n and a, and it is seen as expected that this series is less convergent the smaller a is. At the middle of **Table 3.1.1.1**, the values of $N(a_i,\infty)$ are listed for the various a's used in **Table 3.1.1.1**. Also, at the bottom of **Table 3.1.1.1** the number of cycles, R, needed for the particle concentration to reach 99% (β = 0.01) of its equilibrium value is listed.

TABLE 3.1.1.1

VALUES OF $N(a_i,n)$ for X = 1

n	a_i = 0.8	a_i = 0.1	a_i = 0.05	a_i = 0.01	a_i = 0 001
2	1.2	1 9	1.95	1.99	1.999
5	1.2496	4.095	4.524	4.901	4.990
100	1.25	9.9997	19.88	63.49	95.21
*	1.25	10.0	20.0	100.0	1000.0
3*	1.24				
44*		9.903			
90*			19.802		
459*				99.007	
4603*					990.0

* These numbers of cycles are for when the particle concentration has reached 99% of its equilibrium value.

dynamic equilibrium during normal wear, but the spectrometer readings increase linearly. This is consistent with the foregoing particle equilibrium concentration model when it is considered that the spectrometer reading integrates the metal content from the molecular level to the largest particle size that can be vaporized. Very fine metal particles have decreasing removal efficiency as size decreases until molecular size is reached when the dissolved metal becomes one with the carrier fluid and the removal efficiency equals zero. The contribution of the dissolved metal to the spectrometer reading will increase with time as long as the oil is unchanged, but the concentration of large particles, measured by the ferrograph, will stay in dynamic equilibrium. **Figure 3.1.1.4** shows that ferrography measures wear rate whereas spectroscopy measures total wear. The fundamental premise of machine condition monitoring by wear particle analysis is that an abnormal wear mode causes an increase in the concentration and size distribution of wear particles above a previously established baseline.

Other authors have come to the same conclusion,[22,23] that an equilibrium particle concentration is established, by means of differential equations based on a material balance; namely,

$$\frac{dC_i}{dt} = \frac{P_i k C_i}{V} \qquad (16)$$

where

C_i = Concentration of particles of a certain size i (mg/l)
P_i = Production rate of particles of a certain size i (mg/l)
k = Removal rate constant (l/h)
V = Volume of oil (l)
t = Time (h).

Assumptions are the same as for the other model: Wear rate is constant and rate of removal is proportional to particle concentration.

If equation (16) is integrated with initial time and concentration equal to zero, the result is

---

Ref 22. Fitch, E.C., and Tessman, R.K. "Practical and Fundamental Descriptions for Fluid Power Filters", Paper No. 730796, SAE Trans., Society of Automotive Engineers, New York (1974).

23. Kjer, T. "Wear Rate and Concentration of Wear Particles in Lubricating Oil", submitted to Wear for publication.

dynamic equilibrium during normal wear, but the spectrometer readings increase linearly. This is consistent with the foregoing particle equilibrium concentration model when it is considered that the spectrometer reading integrates the metal content from the molecular level to the largest particle size that can be vaporized. Very fine metal particles have decreasing removal efficiency as size decreases until molecular size is reached when the dissolved metal becomes one with the carrier fluid and the removal efficiency equals zero. The contribution of the dissolved metal to the spectrometer reading will increase with time as long as the oil is unchanged, but the concentration of large particles, measured by the ferrograph, will stay in dynamic equilibrium. **Figure 3.1.1.4** shows that ferrography measures wear rate whereas spectroscopy measures total wear. The fundamental premise of machine condition monitoring by wear particle analysis is that an abnormal wear mode causes an increase in the concentration and size distribution of wear particles above a previously established baseline.

Other authors have come to the same conclusion,[22,23] that an equilibrium particle concentration is established, by means of differential equations based on a material balance; namely,

$$\frac{dC_i}{dt} = \frac{P_i k C_i}{V} \qquad (16)$$

where

C_i = Concentration of particles of a certain size i (mg/l)
P_i = Production rate of particles of a certain size i (mg/l)
k = Removal rate constant (l/h)
V = Volume of oil (l)
t = Time (h).

Assumptions are the same as for the other model: Wear rate is constant and rate of removal is proportional to particle concentration.

If equation (16) is integrated with initial time and concentration equal to zero, the result is

---

Ref 22. Fitch, E.C., and Tessman, R.K. "Practical and Fundamental Descriptions for Fluid Power Filters", Paper No. 730796, SAE Trans., Society of Automotive Engineers, New York (1974).

23. Kjer, T. "Wear Rate and Concentration of Wear Particles in Lubricating Oil", submitted to Wear for publication.

$$C_i = \frac{P_i}{k}\left(1-e^{\frac{-kt}{V}}\right) \qquad (17)$$

which indicates that concentration is directly proportional to wear rate and inversely proportional to removal rate and that the equilibrium concentration will be approached exponentially as drawn on **Figure 3.1.1.4** when the oil is changed. Also, this equation shows that the time to equilibrium is dependent upon the removal rate but independent of particle generation rate. For a circulating system where most of the particle removal is due to filtration,

$$k = EQ \qquad (18)$$

where

E = filter collection efficiency (dimensionless)
Q = flow rate (l/h).

3.1.2 Oil Sampling Techniques

In consideration of the previous section, that both particle generation and particle loss mechanisms affect the particle equilibrium level in lubricating fluids, the following recommendations are made.

a) If samples are to be taken while a system is operating, it is desirable to do so during known operating conditions. It has been observed that the particle concentration in the lubricating oil of gas turbines, for example, varies significantly between high and low power settings.

b) If samples are to be taken after machine shutdown, the effect of particle settling rates and the location of the sampling point must be considered.

c) The effect of an oil change must be considered because of the time to regain the equilibrium particle concentration. Each material will have a characteristic operating time to return to its normal equilibrium level which is governed by the particle removal mechanisms.

   Factors which influence the operating time to equilibrium are:

   - Filtration, i.e., the number of times a particle of a given size and material may, on the average, pass through the filter. The better the filter, the shorter the time to equilibrium.
   - The oil pumping cycle rate. This rate is the pumping rate expressed in volume per unit time divided by the volume of lubricant in the system. On

some systems, the volume of oil is circulated as much as five times per minute, while on others once per hour or longer may be normal. This factor applies principally to losses in the filter.

- Even systems that do not circulate the lubricant, such as a gearbox in which the gears are partially submerged in oil, reach an equilibrium concentration due principally to settling and comminution although the time to achieve this is long compared to circulating systems.
- Dispersive qualities of the lubricant. In systems where the fluid contains detergent additives, these additives prevent agglomeration of the particles and also discourage their adhering to surfaces, thus increasing their life. Diesel engine lubricants usually contain such additives to prevent deposits on cylinder walls.

d) Samples should be taken from a single location in a system. The different parts of any one system may have different particle concentrations, e.g., before and after a filter. Since large particles are so important in incipient failure detection by ferrography, every effort should be made to take a sample before an in-line filter.

An oil filter can profoundly modify the particle distribution in the machine's lubricant. The filter changes the particle population in two ways. First, the filter lowers the concentration of the particles in the oil. The average particle which remains in the oil of a filtered system was generated more recently than in the case of a system with no filter.

Secondly, the filter will remove large particles more effectively than the small ones so that the concentration of the larger particles is reduced. This may aid or hinder the detection of the onset of severe wear. If the sample is taken before the filter, the presence of quantities of large particles is an indication that their generation rate is high, i.e., they are being produced here and now and detection of severe wear is aided. It will be hindered when the oil sample is taken after the filter

Sampling from Pipes

The sampling technique which gives the most representative sample is one in which the sample is taken from a pipe carrying oil scavenged from the wearing parts and before filtering. Clearly, it is necessary for the machine to be operational to do this. Care must be taken that the sample is representative of the complete system, i.e., that the scavenged oil has passed through all the wearing parts.

If the pipe is large and the flow velocity is low, sampling from the bottom of the pipe should be avoided.

Valves should always be flushed when taking a sample since the valve may be a particle deposition site as well as contributing particles from its opening and closing.

Sampling from Oil Tanks

There are two principal sources of error in oil tank sampling, both related to the natural tendency of the particles to settle.

- If the sample is removed from the bottom of a tank, there is the possibility of obtaining a high particle concentration as a result of sedimentation.
- If a sample is taken from the main body of the fluid after machine shutdown, too low a particle concentration may be obtained due to settling of the debris.

The classical way in which particle sinking rates are calculated is to apply Stokes Law to spherical shapes. The fluid viscosity and density along with the particle diameter and density are used to calculate the sinking speed, assuming gravity to be the only force. The calculated speeds reveal the potential for losing the larger particles. **Figure 3.1.2.1** shows settling rates for particles of various sizes. In reality, the sinking rates may be much lower. Factors which reduce the sinking rate are:

- There are convection currents in the fluid medium. On shutdown, many machines are hotter than the ambient. This results in convective stirring of the oil, thus delaying the settling of the particles.
- Most wear particles are not spherical in shape. They generally have a larger projected area-to-weight ratio than spherical particles. Consequently, the particles sink more slowly than spherical particles of the same weight.
- Wear particles are frequently enveloped by a gel. These gels, which have densities comparable to the oil, lower the effective density and cause the particle to sink more slowly than they otherwise would.

Figure 3.1.2.1 Settling Rate of Spherical Particles in Oil

Taking into account the above discussion, the following recommendations for sampling oil tanks are made:

(1) It is considered preferable to remove a sample while the system is operational. If this is not possible, the sample should be obtained as soon as possible after machine shutdown. For the case of sampling oil from jet engines, the following rule is suggested: The sampling tube should dip into the oil a depth of at least 2 inches. If the sample is not to be influenced by the sampling time, add 1 inch for each hour of delay after shutdown. For example, if it is determined that the maximum delay in taking a sample is two hours, then the depth should be:

$$D = 2 + 2 \times 1 = 4 \text{ inches}$$

If the sampling time were less than two hours after shutdown, the excess depth would be conservative. These considerations naturally lead to the thought that the best procedure might be to take the sample from the bottom of the tank. As pointed out earlier, this is not so, because any sludge or large particles which might be lying on the bottom of the tank may be sucked up. Therefore, the sampling tube should not be inserted so far that there is a chance of touching the bottom or the walls. This is understandably a crude guide as variation in viscosity and system type are not considered. Because of the possibility of losing large particles, it is unwise to take a sample more than two hours after shutdown.

(2) If the system contains a permanently installed sampling line such as a pipe into the tank, then the sampling line should be flushed prior to sample removal. Since any oil in a sample line entered that pipe when the previous sample was taken, it must be removed in order to obtain a current sample. The dead volume of oil in the sampling system should be estimated and approximately twice that volume extracted before the actual sample is taken.

Sample Bottles and Caps

If the oil samples are to be analyzed for particle content, the use of plastic bottles should be avoided. Plastic materials in contact with oils, particularly the polyester oils, may contribute particles of plastic, gels, and corrosive liquids. For example, the plasticizer in polyvinyl chloride tubing may leach out and cause corrosion of metal wear particles. Further, a gel-like compound is generated and this gel gathers on wear particles to make agglomerates which float in the oil. The most prevalent difficulty with plastic bottles is that they may become sticky and hold the wear particles on their inner surface so that the oil sample is no longer representative after storage in the bottle. Metal can be used, but there is danger that particles from the can, particularly metal plating, may be confused with wear particles. It is best to use glass sample bottles.

It is recommended that the sample bottle hold at least 15 ml and be made of clear glass. The advantage of clear glass is that the sample may be visually examined. Visual examination can yield important information concerning:

- Color — oxidation due to overheating or lubricant degradation generally darkens the oil.
- The degree of sludge formation after sample storage.
- Very severe wear cases — frequently large individual wear particles may be seen in the oil.
- The detection of foreign liquids in the oil. For example, in one case a large fraction of the liquid was found to be a detergent which was heavier than the oil.

These conditions may be missed if the bottles are not clear.

Glass bottles are often fitted with plastic screw-on caps. The caps have liners which are designed to provide a sealing surface against the lip of the bottle. Many cap designs employ fibrous backing material with a thin plastic coating on the surface. The polyester oils will often attack the coating and release sticky material and fibrous particles into the oil. Also, the papers used contain clay particles which may enter the oil.

Although such particles are easily distinguished from wear particles, they may distort information regarding the contamination level of the oil. Teflon cap liners solve these problems. Teflon, however, may creep under the compressive stress of the seal and the cap may loosen. Consequently, if the sample is to be shipped or stored, it is advisable to lock the cap, using shrink tubing, for example.

Frequency of Sampling

The appropriate sampling frequency is determined by the nature of the machine, its use, and how important early warning is to the user.

Experience has shown that in many failures abnormal wear particles were present in the lubricant, indicating that the machine was defective from the start. The reasons for this are easy to see. Many failures are the result of improper assembly, a defective part, or poor design. Such difficulties result in abnormal wear debris from the beginning.

Many other failures result from operation of a machine beyond its intended specifications. Excessive speed, load, shock, overloading air filters, etc., can lead to premature failure of oil-wetted parts. If such conditions were known to occur, sampling some time after corrective action has been taken can reveal if the concentration and size distribution has returned to baseline.

If a system is new or has just been overhauled, it is desirable to sample the system more frequently to ensure a normal break-in.

Once a normal break-in has been established, then, depending upon the degree of reliability of failure prediction required, the sampling interval can be increased. The following sample times are suggested as a guideline for various systems:

aircraft gas turbines*	50 hours
airborne hydraulic systems	50 hours
aircraft derivative gas turbines	50 hours
diesel engines	200 hours
heavy transmissions/gears	200 hours
surface hydraulic systems	200 hours
heavy duty gas turbines	250 - 500 hours
steam turbines	250 - 500 hours
large bore reciprocating engines	250 - 500 hours

*For established military programs, guidelines for sampling frequency should be followed. These frequencies are often shorter than 50 hours.

3.1.3 Sample Preparation and Sample Dilution

Gravimetric settling of wear particles from lubricating oil commences immediately after a sample is left to stand. Therefore, to obtain a representative sample from a larger sample, the particles in the larger sample must be dispersed and homogenized. To obtain a homogeneous mixture, the following procedure as proposed by A.S.T.M. D811-48 is recommended.

Heat the sample of oil to 65° C ± 5° C and vigorously shake the sample in the original container to mechanically agitate and disperse debris agglomerations until all sediment is homogeneously suspended in the oil. If the original container is of opaque material, or if it is more than 3/4 full, transfer the entire sample to a clear glass bottle having a capacity at least 1/3 greater than the volume of the sample. Transfer all traces of sediment from the original container to the bottle by vigorous agitation of portions of the sample in the original container.

Before taking each further portion for testing, reheat and thoroughly mix tl e oil.

Sample Dilution

Some oil samples result in ferrograms with a dense pileup at the entry with heavy deposits further downstream from the entry because the concentration of particles is too high. This causes the following difficulties:

- Individual particles are not easy to observe.
- The size distribution will be distorted. A ferrogram with 90% of the entry area covered with ferrous particles will appear to consist of particles less than about

10 or 15 μm. Yet, if the same sample is diluted 100 to 1, the corresponding ferrogram may reveal particles as large as 200 μm. While running a ferrogram, an initial heavy deposit can cause local intensification of the magnetic field, resulting in early precipitation of the remaining smaller particles. These smaller particles pile up on and subsequentiy hide the majority of the larger particles Samples from reciprocating machines, with their inherent high generation rate of fine rubbing wear debris, are particularly susceptible to this problem.

- Percent area covered readings (see paragraph 3.2.2, Ferrogram Readings) are nonlinear above 40% area covered due to the pileup of particles. In order to eliminate these effects, it is recommended that samples with a high particle concentration be diluted to give entry area coverages of between 10 and 40%.

  Dilution is normally done on a logarithmic basis, i.e., 10:1, 100:1, or 1000:1. Due to the forementioned pileup process, a 10:1 dilution of a sample originally giving a 90% area coverage does not result in a new ferrogram with a 9% coverage. The coverage will be substantially greater. A dilution of 10:1 in this instance means the concentration of particles becomes 10% of the original sample, i.e., the new sample is made up of 9 parts clean oil per 1 part of the original sample. A 100:1 sample should be similarly made from a 10:1 sample and so on. **Figure 3.1.3.1** illustrates this procedure.

  Whenever possible, the oil used to dilute the sample should be fresh filtered oil of the same specification. One should be wary of attempting to assess the particle concentration of a given sample by its visual appearance. The eye cannot discern particles below about 40 μm. The presence of contaminants, such as carbon in the case of internal combustion engines, can make it a very hazardous procedure.

Figure 3.1.3.1 Dilution Procedure

3.2 FERROGRAPHIC TECHNIQUES

3.2.1 Optical Examination of Ferrograms

The most readily available information about particle type and composition is obtained by optical examination using a bichromatic microscope. The basic requirements for this type of microscope are that it have both reflected and transmitted light sources which may be used simultaneously and that it employ dry metallurgical objectives. The highest magnification objective should have a numerical aperture of at least 0.85. The numerical aperture is the sine of the half angle of the cone of incident light that the lens accepts. If the angle is not large enough, spheres and particle surface characteristics cannot be properly identified.

Figure 3.2.1.1 shows the light paths for a bichromatic microscope. Transmitted light comes from beneath the microscope stage, passes through the ferrogram, and proceeds straight up through the 2-way mirror to the eyepieces. Reflected light passes down

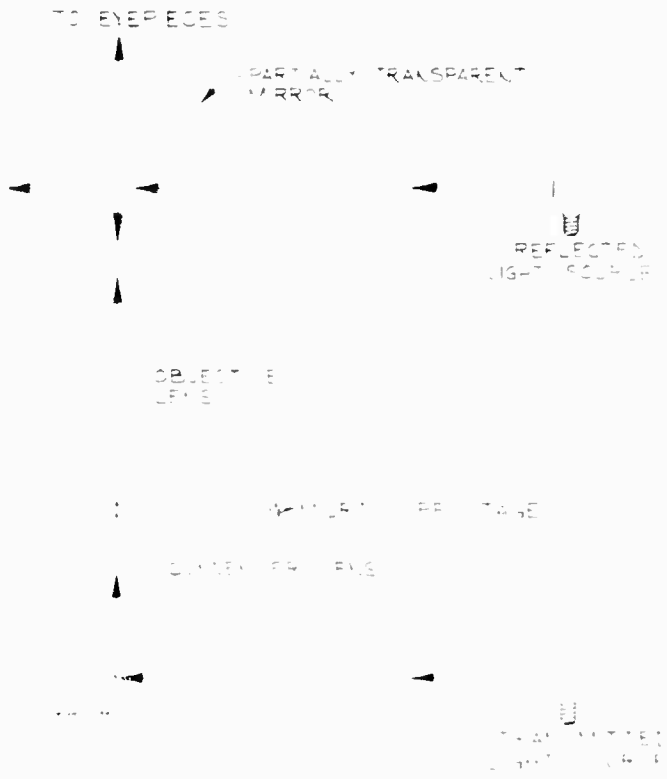

Figure 3.2.1.1 Light Path of Bichromatic Microscope

through the objective lens, is reflected from the objects being viewed, passes back up through the objective lens, and through the 2-way mirror to the eyepieces. Transmitted

light microscopes have traditionally been used mostly for biological specimens which are transparent in thin sections. Reflected light microscopes are used for examining opaque specimens such as polished and etched metal samples to reveal metal microstructure. Reflected light microscopes are, therefore, frequently called metallurgical microscopes.

Wear particles are examined using a bichromatic microscope because distinctions can be made that would be difficult with either a transmitted or reflected light microscope used singly. A useful arrangement for quickly determining if particles are metal or compounds is to use red reflected and green transmitted light, which is called bichromatic illumination. Free metal particles appear bright red while nonmetals and compounds appear green to yellow, depending on the degree of light attenuation. Thick nonmetal particles, which have blocked most of the green transmitted light from below the microscope stage, may appear cloudy red, but they do not appear bright red as do the highly reflective surfaces of free metal particles. Bichromatic illumination is used principally to allow easy detection of the more important metal particles. This illumination is particularly useful for examining polymeric or amorphous particles on ferrograms. Free metal particles embedded in an amorphous matrix are difficult to observe with any other illumination.

Reflected white light is used for further examination of the surfaces of particles. The principal advantage of using white light is that colors may be observed with this illumination. Copper alloys appear yellow or reddish brown, while most other free metals appear silver white. Ferrous particles display yellow to blue color if, during their formation, they are subjected to any significant heating. These colors are light interference effects due to formation of thin surface oxides. See paragraph 3.2.6, Heating of Ferrograms, for more information about this subject. Lead/tin alloys, used extensively for bearings, show various colors, depending upon the thermal and chemical environment they have been subjected to, which permits their identification. See paragraph 1.6 on Nonferrous Metals.

Examination under transmitted white light ascertains whether a particle is transparent, translucent, or opaque. The attenuation of light in free metal particles is such that they will be opaque even to submicron thicknesses. In consequence, free metal particles appear black when examined with this illumination. On the other hand, most other elements and all compounds appear translucent or transparent, the color displayed being characteristic of the material. Hematite, Fe_2O_3, for instance, will transmit red light through a thickness of several micrometers depending on the crystal size. It can often be ascertained whether an oxide particle has a free metal core or not because free metal is opaque.

The use of polarized light to examine particles has proven to be quite useful, quick, and convenient as an aid in identifying the materials of nonmetal particles, particularly oxides, plastics, and various solid contaminants in the oil. Briefly stated, most nonmetallic crystals and polycrystalline clusters and many plastics and biological materials will depolarize polarized light, but amorphous materials, such as glass and liquids, will not. A more detailed explanation is given in paragraph 3.2.10 for those who wish to better characterize nonmetallic particles using the optical microscope with polarized light.

Ferrogram Readings

A ferrogram reading is an electromechanically determined optical extinction measurement which quantifies the percent of the area under examination covered by particles The reading is obtained by using a 10x objective lens with reflected light. The power source for the light is regulated so that power line fluctuations will not cause the light intensity to vary. To take a reading, (1) the area of interest is brought into focus; (2) the reader is zeroed on a clean ferrogram area (just outside the non-wetting barrier is recommended); (3) the area of interest is brought back into view maintaining lengthwise position; and (4) the area of interest is scanned transversely to maximize the reading (minimize the light intensity) corresponding to the field of view that has the most area covered by particles. For entry readings, the ferrogram is scanned in both directions, that is, lengthwise and transversely; but for readings at locations downstream from the entry, such as at the 50 mm location, the ferrogram is scanned in only the transverse direction, care being taken to exclude large extraneous particles such as clumps of fibers which are not representative of the wear particles at that location.

At first it may appear counter-intuitive to use reflected light to obtain a measurement of the area covered by particles since many of the particles are shiny, but this is done to eliminate inaccuracies that will be caused by smudges or dirt underneath the ferrogram or on the glass slide which supports the ferrogram on the microscope stage. **Figure 3.2.1.2** illustrates this situation. If an unequal amount of dirt is under the ferrogram where it is zeroed, compared to where the reading is taken, the measurement will be biased. The reason that reflected light can be used is that the low magnification lens is so far from the ferrogram that all but the largest metal particles will appear dark. The numerical aperture (NA) of the 10x objective commonly used for examining ferrograms is 0.25. The NA is the sine of the half angle of the cone of light that the lens accepts. For a NA of 0.25, the angle is 14° . Under these circumstances, a particle must be large and flat to reflect light back up to the lens. For the high magnification lens, the NA is high. For the commonly used 100x objective, the NA is 0.9 and the half angle is 64° which is why particles reflect back a great deal of light at high magnification. **Figure 3.2.1.3** shows that the high magnification lens is very near to its object. Ferrogram readings cannot be made with a high NA lens because the particles reflect back light.

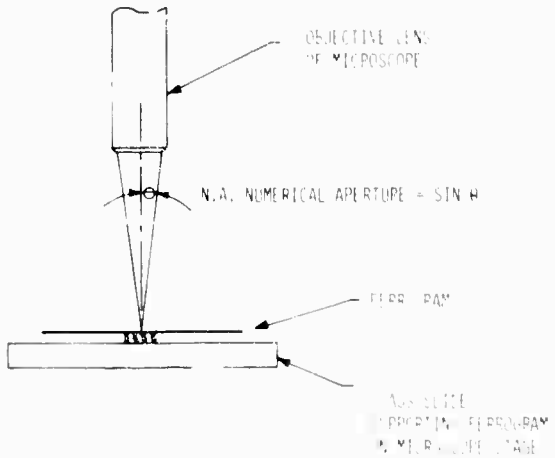

Figure 3.2.1.2 Taking a Ferrogram Reading

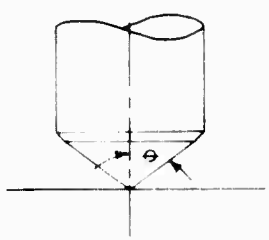

Figure 3.2.1.3 High Magnification Objective Lens

3.2.2 Ferrogram Analysis Report Sheet

Figure 3.2.2.1 shows a Ferrogram Analysis Report Sheet. At the top of the sheet is space for various data connected with the sample and the preparation of the ferrogram. Identification of the various types of particles listed on the sheet is the subject of much of the Atlas. Some comments follow.

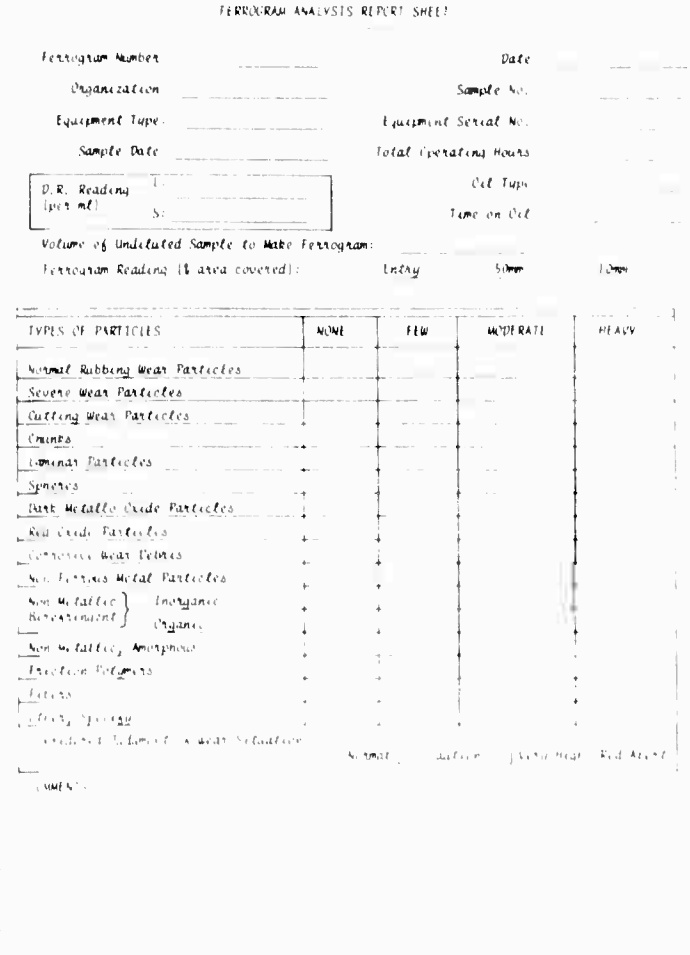
FERROGRAM ANALYSIS REPORT SHEET

Ferrogram Number _____ Date _____

Organization _____ Sample No. _____

Equipment Type _____ Equipment Serial No. _____

Sample Date _____ Total Operating Hours _____

D.R. Reading (per ml) L: _____ S: _____ Oil Type _____ Time on Oil _____

Volume of Undiluted Sample to Make Ferrogram: _____

Ferrogram Reading (% area covered): Entry _____ Sump _____ Comp _____

TYPES OF PARTICLES	NONE	FEW	MODERATE	HEAVY
Normal Rubbing Wear Particles				
Severe Wear Particles				
Cutting Wear Particles				
Chunks				
Laminar Particles				
Spheres				
Dark Metallic Oxide Particles				
Red Oxide Particles				
Corrosive Wear Debris				
Non Ferrous Metal Particles				
Non Metallic Contaminant — Inorganic				
Non Metallic Contaminant — Organic				
Non Metallic, Amorphous				
Fiber Formations				
Fibers				
Fibers, Cotton				

Normal Severe Cutting Red Oxide

COMMENTS:

Figure 3.2.2.1 Ferrogram Analysis Report Sheet, Blank

The judgment of none/few/moderate/heavy should be roughly based on the percent area covered by each particle type. Few corresponds to 1 - 5%, moderate to 5 - 25%, and heavy to greater than 25%. A mark on the line between none and few would indicate less than 1% of the area covered. This judgment is usually made with as low a magnification as possible (10x objective).

Often there exists confusion on the distinction between some of the various free metal particles; namely, between normal rubbing wear particles, severe wear particles,

chunks, and laminar particles. As a convention for completing the Ferrogram Analysis Report Sheet, it is recommended that only size and shape be considered criteria for assigning a particle into one of these categories. **Table 3.2.2.1** lists the essential differences. Shape factor is the ratio of major dimension to minor dimension which can also be considered "length-to-thickness ratio". Length can be determined using a calibrated reticle in the ocular lens of the microscope. Thickness can be determined by measuring the stage travel between focus on the top of a particle and focus on the plane of the surface of the ferrogram.

TABLE 3.2.2.1

DISTINCTION BETWEEN FREE METAL PARTICLES

Particle Type	Size (major dimension)	Shape Factor (major dimension ÷ thickness)
Normal Rubbing Wear	$< 15\ \mu m$ in major dimension $< 5\ \mu m$	~ 10:1 no regard to Shape Factor
Severe Wear Particles	$> 15\ \mu m$ in major dimension	> 5:1 but < 30:1
Chunks	$> 5\ \mu m$ in major dimension	< 5:1
Laminar Particles	$> 15\ \mu m$ in major dimension	> 30:1

Table 3.2.2.1 is meant as a guide. Clearly, the $15\ \mu m$ cut between severe wear particles and normal rubbing wear particles is generalized. For example, there is a substantial difference between a particle population of normal rubbing wear particles all less than $5\ \mu m$ and another population, which covers the same area on a ferrogram, that has particles ranging in size up to $15\ \mu m$. Yet both these populations would be described as normal rubbing wear following **Table 3.2.2.1**.

The category "chunks" has in the past been called "fatigue chunks", which was something of a misnomer because fatigue particles from rolling contact fatigue are often large flat platelets with shape factors of about 10:1. See paragraph 1.3.

These would be classified as severe wear particles following **Table 3.2.2.1**. Sliding wear may be distinguished from rolling contact fatigue wear in that sliding wear particles have surface striations and straight edges, whereas rolling contact wear particles have smooth surfaces and jagged edges. It is, however, true that rolling contacts generaliy produce thicker particles than sliding contacts.

Dark metallo-oxides are typically produced in highly loaded, poorly lubricated contacts, whereas red oxides are most likely due to ox. 'ative attack from water in the oil. Black oxides, paragraph 1.7.2, are included in the dark metallo-oxide category since both will usually be present in the same sample. Corrosive wear debris is generated by acidic attack at wearing contacts and results in extremely fine particles being generated. Corrosive wear debris is most often found in diesel engines where the ring/cylinder contact produces most of the debris. Corrosive wear is different from the rusting that attacks all parts of a machine when water is present and which generates red oxides. The ability to distinguish between these three oxidative wear modes will allow choice of the proper corrective measure.

Nonferrous metals are easily recognized by their paramagnetic deposition patterns. Copper alloys are easily recognizable by their distinctive yellow/orange color (gold is not likely to be in most machines). Distinction can be made between white nonferrous metals by heat treating of the ferrogram and by wet chemical tests done on the ferrogram (see paragraph 1.6, Nonferrous Metals). Austenitic stainless steel, which also deposits in a nonferromagnetic manner, can be identified by heat treatment as described in **Table 3.2.6.1**, Identification of Particles by Heat Treating Ferrograms. Molybdenum disulfide, which looks like metal, is easily recognized by its dull gray appearance and the presence of multiple cleavage planes. See paragraph 1.8.3.

Nonmetallic birefringent particles may be categorized whether they are organic or inorganic if that information is desired. The organic particles will respond to heat treating by charring, melting, or vaporizing. If a photograph is taken in polarized light of a certain field of view, a second photograph taken after heat treating will show a decrease in brightness for those birefringent particles which are organic. Analysis time can be saved by skipping this exercise if so little birefringent debris is present that distinction between organic/inorganic is unimportant.

Nonmetallic amorphous particles are distinguished from friction polymers. The latter are typically quite flat and contain wear particles.

A line is left for other particles, which may be carbon flakes (seal wear), oxidized Pb/Sn alloys, molybdenum disulfide, black agglomerates, or some other less encountered particle type.

In several situations, it is appropriate to check off more than one particle category for a certain particle type. For example, aluminum severe wear particles fall into the "severe wear particles" and the "nonferrous metal particles" categories. Fretting wear particles, as described in paragraph 2.7, can be classified as "chunks", "dark metallo-oxide particles", and "red oxides" since they are equiaxed particles covered with a mixture of red and black oxides. Use the space left for "comments" on the Ferrogram Analysis Report Sheet for particles that are difficult to classify such as those that show on more than one line of the report sheet.

Table 3.2.2.2 is offered as a suggested procedure for the sequential steps to follow when examining a ferrogram. It contains information about which objective lens is proper for different circumstances. The individual analyst should feel free to modify this procedure according to specific case needs.

3.2.3 The Direct Reading (DR) Ferrograph

Experience with analytical ferrography, where optical densitometer readings of particle deposits are taken in conjunction with the bichromatic microscope, indicated that the entry point of the oil sample onto the ferrogram (where the largest particles are deposited) and a position some 5 mm down from the entry (where 1-2 μm size particles are deposited) are the most sensitive locations for detecting a changing wear situation. Accordingly, the direct reading (DR) ferrograph was designed to quantify particles in these two size ranges.

As shown in **Figure 3.2.3.1**, oil from a sample is siphoned through a precipitator tube, where a magnet assembly located beneath the tube precipitates the wear particles according to size. Virtually all unwanted carbon dirt particles are not precipitated, but

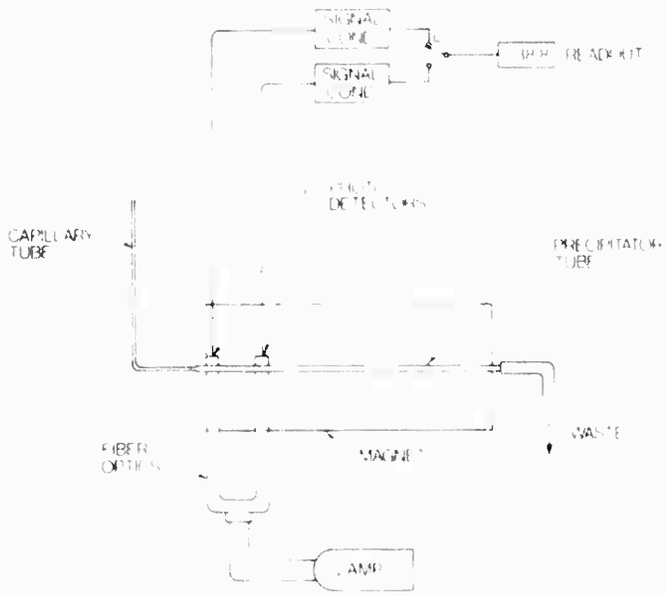

Figure 3.2.3.1 Schematic of DR Ferrograph

are carried away by the oil. The large particles are deposited first, then the smaller ones further down the tube. Two light beams pass through the precipitator tube. The first beam is located near the tube's entry where the larger (L) particles (>5 μm) are

deposited, and the second beam crosses the tube where the smaller (S) particles (1 to 2 μm) are deposited. The reduction in light intensity indicates the amount of wear particles deposited at each location. The level of light is sensed, amplified, and displayed in terms of units on a digital meter. The digital meter has a range of 0 to 190 units, where a reading of 100 units, which corresponds to approximately one-half of the area covered, is the recommended upper limit because, for readings greater than 100, the instrument response is nonlinear due to coincidence effects; that is, particles pile on top of one another so that less light is attenuated. A reading of 190 corresponds to complete blockage of light. A switch allows selection of either the L reading or the S reading. The instrument is zeroed just after the sample covers the two optical channels upon entering the glass precipitator tube. This eliminates any effect that variations in oil opacity would have upon the readings. After zeroing, the sample flows through and magnetic particles are deposited along the bottom of the precipitator tube. The readings increase as light is blocked by the deposited particles. If the readings are seen to increase by several units and then decrease, it is an indication that large, weakly magnetic particles are passing by the sensor location. The readings are recorded when flow stops and the readings stabilize.

The DR ferrograph may be used with opaque oil samples such as the black oil samples obtained from diesel engines. This is accomplished by first zeroing the instrument with fixer, which is clear, then running the dark oil through the precipitator tube and finally flushing the dark oil away with fixer. Left in the precipitator tube are fixer and the particles precipitated from the dark oil. Tests at Foxboro Analytical showed that the opaque oil technique gives better repeatability for the same sample than does the usual method. This is probably due to the fact that the entire 1 ml sample, as delivered by pipette, is run through the DR ferrograph when using the opaque oil procedure, whereas inaccuracy is introduced by the zeroing process when the translucent oil is stopped after passing the optical channels. Users may elect to run translucent samples using the dark oil technique. Refer to the operating instructions[24] for further details.

If a sample contains only small particles, the readings at the L and S channels will be about equal. **Figure 3.2.3.2** illustrates why this occurs. When particles enter the precipitator tube and are influenced by the magnetic field, vectors of motion can be used to describe their trajectory within the precipitator tube. The vector of motion in the flow direction will be equal for large and small particles. However, the vector of motion in the downward direction will be greater for large particles because the magnetic force is proportional to volume (proportional to the diameter cubed), whereas flow resistance in the downward direction is proportional to surface area (proportional to the diameter squared). Large particles move so rapidly to the bottom of the

Ref. 24 Foxboro Analytical, "Sample Processing with the Model 7067 Direct Reading Ferrograph", MI 612-101 (Jun. 1980)

TABLE 3.2.2.2

Step	Mag.	Ref.	Trans.
1	100	Red	Green
2	400	White	Green
3	1000	White	Green
4	100	OFF	POL
5	400	POL	OFF
6		As Required	
7		—	
8		As Required	
9		—	

SUGGESTED PROCEDURE FOR ANALYSIS OF A FERROGRAM

Comments

Look for severe wear particles at entry by presence of bright red. Normal rubbing wear particles are too small to be resolved at this magnification and will appear black. Therefore, if only normal rubbing wear particles are present on the ferrogram, no red particles will be observed. Scan length of ferrogram looking for severe nonferrous wear particles, nonmetallic particles, or a heavy deposit at the exit typical of corrosive wear.

Examine the entry deposit making a preliminary judgment as to the specific types of wear particles present such as severe wear, normal rubbing wear, chunks, etc. A preliminary judgment of dark metallo-oxides must be confirmed at 1000x magnification because particles that are not flat will appear dark. Scan the length of the ferrogram looking for nonferrous metal particles and other distinctive features such as nonmetallic particles, friction polymers, etc.

Most particle types can be recognized at 400x, but 1000x provides critical details necessary to complete the analysis. Spheres, fine cutting wear particles, and small spots of temper color on the surface of particles indicative of high heat during generation can be distinguished only at high magnification. Because of the high numerical aperture of the 100x lens (good light gathering ability), jagged free metal particles may be distinguished from dark metallo-oxides. Nonmetallic amorphous particles do not contain fine metal particles whereas friction polymers are recognized by the presence of fine metal particles in the amorphous matrix. Bichromatic light (red reflected and green transmitted) is useful for identifying friction polymers because of the greater contrast provided. When using the 100x objective it is recommended that one hand be used for the fine focus control so that the stage may be easily racked up or down. When viewing particles that are not perfectly flat, continually move the stage so that focus scans up and down, forming a more complete impression of the particles.

Use polarized transmitted light to identify nonmetallic particles. These will appear bright in an otherwise dark field.

Use polarized reflected light to determine surface characteristics of particles. Oxidized surfaces of metal particles will depolarize the light. Small nonmetallic particles, which may not have been seen at 100x magnification can now be detected. Use 1000x magnification with polarized reflected light if surface characteristics are of particular interest.

Take photos prior to heat treating ferrogram. A polarized light photo may be appropriate if it is desired to distinguish between organic and inorganic birefringent particles. The organic particles will not be as bright after heat treatment. A second photo exposed for the same time will show this difference. It may also be desirable to photograph strings of ferrous particles prior to heat treatment as well as any suspected Pb/Sn alloy particles.

Heat treat ferrogram. See paragraph 3.3.7, Heating of Ferrogram.

Reexamine ferrogram after heat treating. Take photos as necessary.

Heat treat to higher temperature if required.

precipitator tube that all magnetic particles larger than about 5 μm are deposited at the first sensor location. Small particles which migrate much more slowly to the bottom of the precipitator tube penetrate much further along the tube being deposited. As a sample enters the precipitator tube, small particles are dispersed throughout the volume of the tube so that some small particles are near the bottom of the tube and will be pulled down over the first sensor location. Other small particles, however, which enter the tube higher up from the bottom will travel further along the tube before being deposited. Therefore, if the L and S readings are equal, only small particles are present and a true indication of large particles is L minus S.

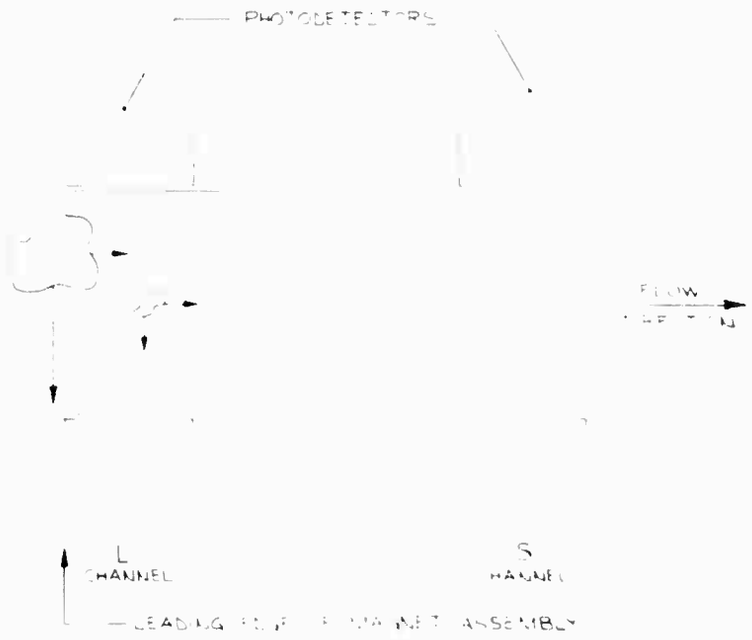

Figure 3.2.3.2 Particle Deposition in the DR Ferrograph

Flow rate through the precipitator tube has some effect on particle deposition efficiency. Experiments showed that for a certain sample, decreasing the flow rate by a factor of 2 caused about 15% more particles to be deposited. The capillary tubing portion of the precipitator tube assembly controls the flow rate through the precipitator tube. To ensure constant flow rate, the capillary tubing section is trimmed during manufacture so that the pressure drop of air flowing through the precipitator tube assembly is within certain limits. This ensures that sample flow will be nearly the same for any precipitator tube assembly. The other important factor controlling flow rate is sample viscosity. Operating instructions call for the addition of an equal amount of solvent (fixer) to each sample before processing, which breaks up gels and lowers sample viscosity. More solvent may be used for high viscosity oils, such as heavy-duty-gearbox oil, but

the proportion must remain constant when resampling so that flow rate effects do not bias the readings.

Two neutral density filters are included with the instrument to allow periodic calibration checks. By inserting one of the filters in the light path, without the precipitator tube in place, a reading within a certain range will result if the instrument is functioning properly.

3.2.4 Quantifying a Wear Situation

As presented in paragraph 3.1.1, Particle Behavior in a Machine, the number of particles in lubricating oil will reach a dynamic balance because the number of particles generated will equal the number lost. The time it takes before a particle is lost is a function of particle size; the larger particles will be lost sooner. If a machine operates normally, not only will the concentration remain the same, but the size distribution will remain the same. Abnormal wear modes, except perhaps for corrosive wear, will generate larger particles. The normal wear process, that is, the wear mode associated with smooth stable surfaces (see paragraph 1.1) generates particles with a maximum dimension of about 15 μm, the majority of which are 2 μm or less. Abnormal wear modes, those that significantly reduce the potential life of a wear surface, generate particles with a maximum size greater than 15 μm. The actual maximum size (and shape) is dependent on the wear mode.

Quantitative information obtained by ferrography signals a changing wear situation. Readings may be obtained from ferrograms via analytical ferrography which indicate the percent area covered by particles at selected ferrogram locations. The DR ferrograph provides two readings which correspond to the concentration of large and small particles in the sample and the on-line ferrograph gives the wear particle concentration (WPC) and the percentage of large particles.

The data obtained from these three instruments can be processed in several ways to allow easy identification of an abnormal wear mode. Three such ways are briefly described.

(1) A Severity of Wear Index — If the L reading, or the sum of the L and S readings, is used as an indication of concentration, and if the difference, L - S, between the readings is used as an indication of size distribution, the product of these terms, either

$$L\,(L - S) \text{ or}$$
$$(L + S)\,(L - S) = L^2 - S^2$$

may be used as a severity of wear index. If the severity of wear index is plotted as a function of operating time, it will respond in a more volatile manner than would a plot of either the L reading versus time or the S reading versus time.

(2) Cumulative Plots — A cumulative plot may be used where each new reading is added to the sum of all the previous readings. This will result in a straight line if the readings are the same and the interval which they are plotted is the same. The Eastern Airlines data (paragraph 2.2.2), is presented in this manner. A variation of this method is presented in reference 21 in which cumulative concentration $\Sigma (L + S)$, and cumulative size distribution $\Sigma (L - S)$ are plotted on the same graph. A normally operating machine will produce two straight, divergent lines, but a machine in distress will cause both plots to increase in slope.

(3) WPC and Percentage Large — This method was developed for the on-line ferrograph although it is equally applicable to DR readings or ferrogram readings. The wear particle concentration (WPC) is calculated as L + S and the percentage large is calculated as

$$\frac{L - S}{L + S}$$

An increase in both WPC and percentage large signals an abnormal wear mode.

3.2.5 Establishing a Condition-Monitoring Program

There are two requisites aside from logistical arrangements, method of taking the sample, reporting, etc., for establishing a condition-monitoring program. These are:

(1) Determining length of time between samples, and
(2) Establishing a baseline.

The time between samples will be determined primarily by the warning period before failure. Ideally, the sampling period will be less than the warning time although in practice this may not be possible due to either logistics or that certain failures proceed so rapidly that only an on-line method will provide adequate warning. For any real machine, many different failures are possible; it may be that anything less than an on-line detection method may be nearly futile for some of these failure types. Clearly, extensive secondary damage or major inconvenience, such as loss of an aircraft jeopardizing the pilot or shutdown of a production line, will argue for briefer sampling intervals. In many cases, the logistics of the situation will determine the minimum sampling interval, such as when a truck or locomotive returns to the depot.

A baseline of normal wear may be established either by taking a number of samples from the same machine or by taking one sample from a number of similar machines.

The following ferrographic analysis report (**Figure 3.2.5.1**) is presented in its entirety to show how a baseline was established for a one-of-a-kind machine (for that operator) by taking samples as the machine broke in

Figure 3.2.5.1 Report for Solvay in its Entirety

Figure 3.2.5.1 Report for Solvay in its Entirety (Continued)

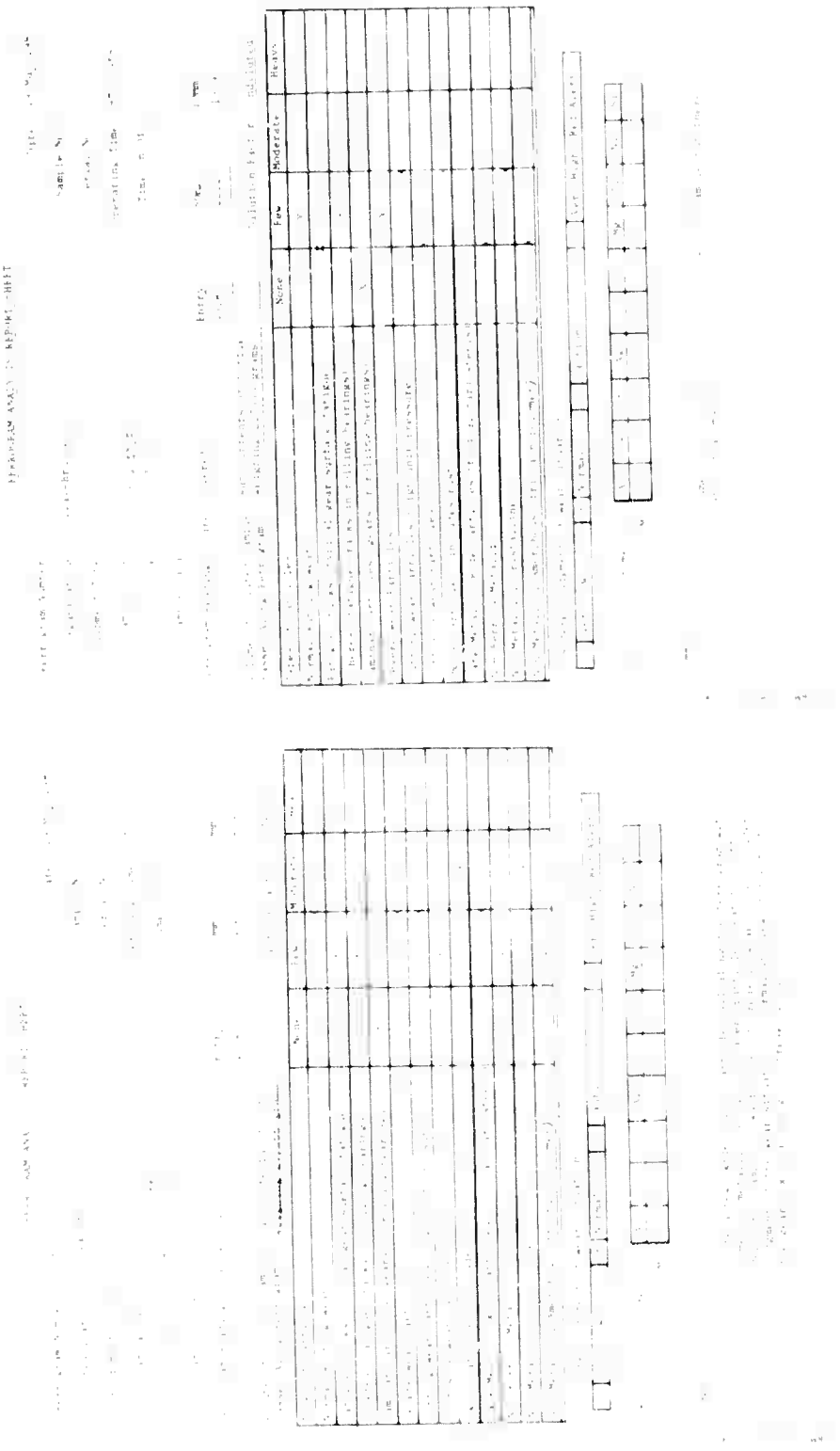

Figure 3.2.5.1 Report for Solvay in its Entirety (Continued)

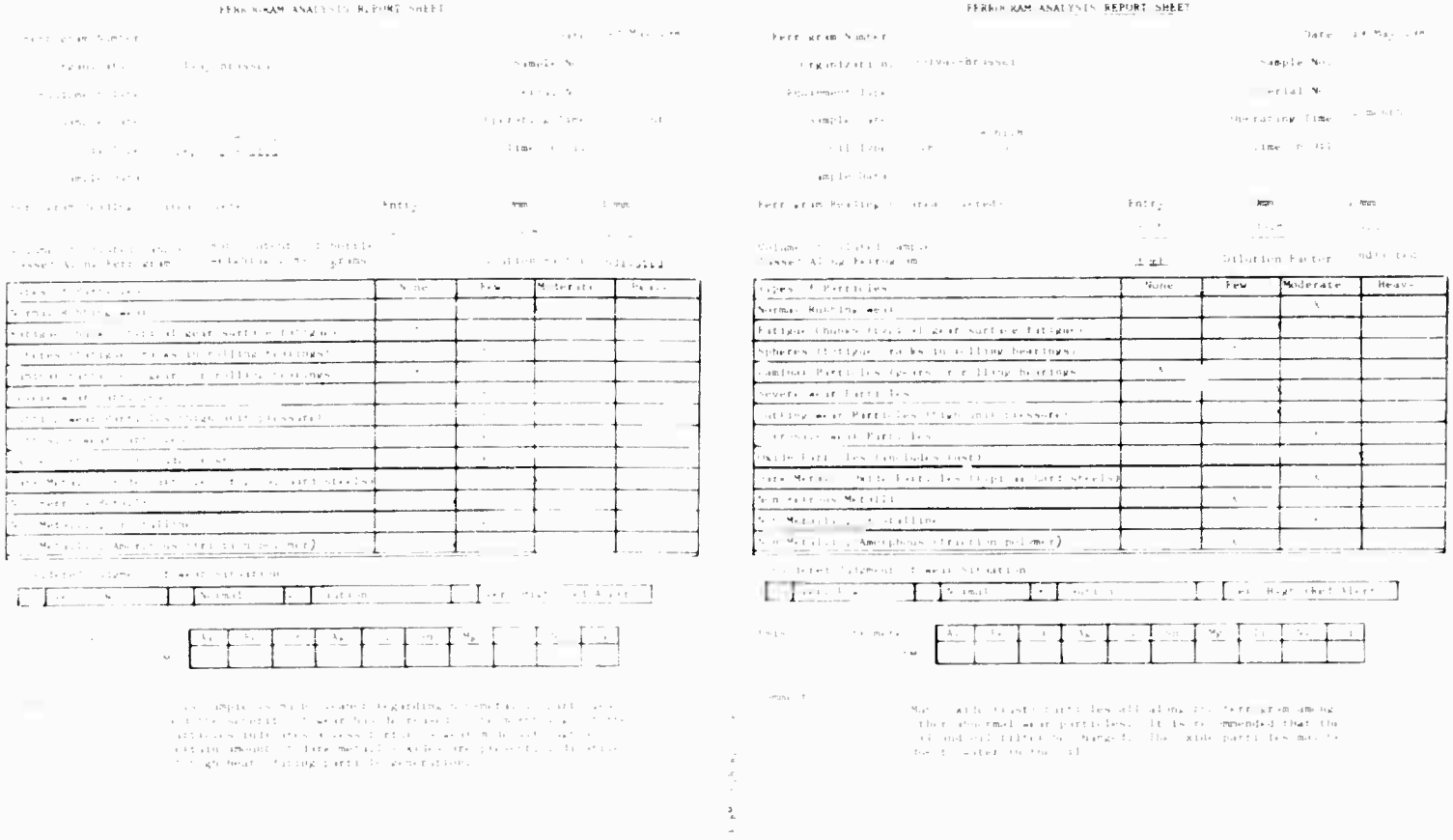

Figure 3.2.5.1 Report for Solvay in its Entirety (Continued)

PHOTO NO. [illegible] DATE [illegible]

MAGNIFICATION [illegible]

LOCATION ON FERROGRAM: Entry

SAMPLE IDENTIFICATION

OPERATING HISTORY:

24 hours

REMARKS:

Low magnification view of the entry deposit shows strings of ferrous particles and some nonmetallic crystalline debris, viewed with white reflected and green transmitted light.

PHOTO NO. P0354-3 DATE 5/20/80

MAGNIFICATION: 400x

LOCATION ON FERROGRAM: Entry

SAMPLE IDENTIFICATION:

OPERATING HISTORY:
24 hours

REMARKS:

A photomicrograph of the entry deposit showing dark metallo-oxide particles, rust particles, and some non-metallic particles, which all indicate an abnormal wear mode.

PHOTO NO. [illegible] DATE [illegible]

MAGNIFICATION [illegible]

LOCATION ON FERROGRAM [illegible]

SAMPLE IDENTIFICATION

OPERATING HISTORY
24 hours

REMARKS

A photomicrograph of the entry deposit showing dark metallo-oxide particles, rust particles, and some non-metallic particles, which all indicate an abnormal wear mode.

PHOTO NO. P0354-4 DATE 5/22/80

MAGNIFICATION: 400x

LOCATION ON FERROGRAM: Entry

SAMPLE IDENTIFICATION:

OPERATING HISTORY

24 hours

REMARKS

Same view as above after heat treating to 130°C on a laboratory hotplate, showing a straw temper color for particles at entry. This indicates the ferrous particles are medium alloy steel or cast iron.

Figure 3.2.5.1 Report for Solvay in its Entirety (Continued)

PHOTO NO. [illegible] DATE [illegible]

MAGNIFICATION [illegible]

LOCATION ON
FERROGRAM [illegible] mm

SAMPLE IDENTIFICATION

OPERATING HISTORY
[illegible] hours

REMARKS
Two break-in wear particles [illegible] attached to string of ferrous particles further down from the [illegible]

PHOTO NO. P0354-7 DATE 5/21/80

MAGNIFICATION: 1000x

LOCATION ON
FERROGRAM: 54.0 mm

SAMPLE IDENTIFICATION:

OPERATING HISTORY:
24 hours

REMARKS:
A large break-in wear particle attached to a string of ferrous debris. Taken with white reflected and green transmitted light.

PHOTO NO. [illegible] DATE [illegible]

MAGNIFICATION [illegible]

LOCATION ON
FERROGRAM [illegible] mm

SAMPLE IDENTIFICATION

OPERATING HISTORY
[illegible]

REMARKS
A large severe wear particle [illegible] [illegible] severe [illegible] wear. [illegible] taken with white [illegible] green transmitted light.

PHOTO NO. DATE

MAGNIFICATION:

LOCATION ON
FERROGRAM:

SAMPLE IDENTIFICATION:

OPERATING HISTORY:

REMARKS:

Figure 3.2.5.1 Report for Solvay in its Entirety (Continued)

PHOTO NO. P0355-1 DATE 5/20/80

MAGNIFICATION: 400x

LOCATION ON FERROGRAM: Entry

SAMPLE IDENTIFICATION:

OPERATING HISTORY: 48 hours

REMARKS:

Overall view of the entry deposit showing possible stator wear in the 24 hours sample except that the concentration is lower

PHOTO NO. P0355-3 DATE 5/20/80

MAGNIFICATION: 400x

LOCATION ON FERROGRAM: entry

SAMPLE IDENTIFICATION:

OPERATING HISTORY: 48 hours

REMARKS:

High magnification view of the entry deposit reveals break-in wear, cutting wear, and some dark metallo-oxides. Photo taken with white reflected and green transmitted light.

PHOTO NO. P0355-2 DATE 5/20/80

MAGNIFICATION: 400x

LOCATION ON FERROGRAM: entry

SAMPLE IDENTIFICATION:

OPERATING HISTORY: 48 hours

REMARKS:

Same view as above after heat treatment to 330°C/625°F. Blue temper color indicates low alloy steel.

PHOTO NO. P0355-4 DATE 5/22/80

MAGNIFICATION: 400x

LOCATION ON FERROGRAM: entry

SAMPLE IDENTIFICATION:

OPERATING HISTORY: 48 hours

REMARKS:

Same view as above after heat treatment to 330°C/625°F. Blue temper color indicates low alloy steel.

Figure 3.2.5.1 Report for Solvay in its Entirety (Continued)

PHOTO NO. P0355-5 DATE 5/23/80

MAGNIFICATION: 1000x

LOCATION ON FERROGRAM: S1

SAMPLE IDENTIFICATION:

OPERATING HISTORY:
48 hours

REMARKS:

Two large severe wear particles with a sphere and a cutting wear particle on the same string of particles

PHOTO NO. P0356-1 DATE 5/20/80

MAGNIFICATION: 100x

LOCATION ON FERROGRAM: entry

SAMPLE IDENTIFICATION:

OPERATING HISTORY:
120 hours

REMARKS:

The entry deposit taken at low magnification revealing rubbing wear particles in white reflected and green transmitted light.

PHOTO NO. P0355-6 DATE 5/23/80

MAGNIFICATION: 1000x

LOCATION ON FERROGRAM: S1

SAMPLE IDENTIFICATION:

OPERATING HISTORY:
48 hours

REMARKS:

Heat treatment of the particles above shows majority of the particles ranging from a blue temper color, indicating low alloy steel. The severe wear particle shown by the arrow ranged to a straw temper color, indicating medium alloy steel such as 4340.

PHOTO NO. P0356-2 DATE 5/20/80

MAGNIFICATION: 400x

LOCATION ON FERROGRAM: entry

SAMPLE IDENTIFICATION:

OPERATING HISTORY:
120 hours

REMARKS:
Higher magnification view of the entry deposit shows that dark amorphous oxides are present in the entry which indicates an abnormal wear mode.

Figure 3.2.5.1 Report for Solvay in its Entirety (Continued)

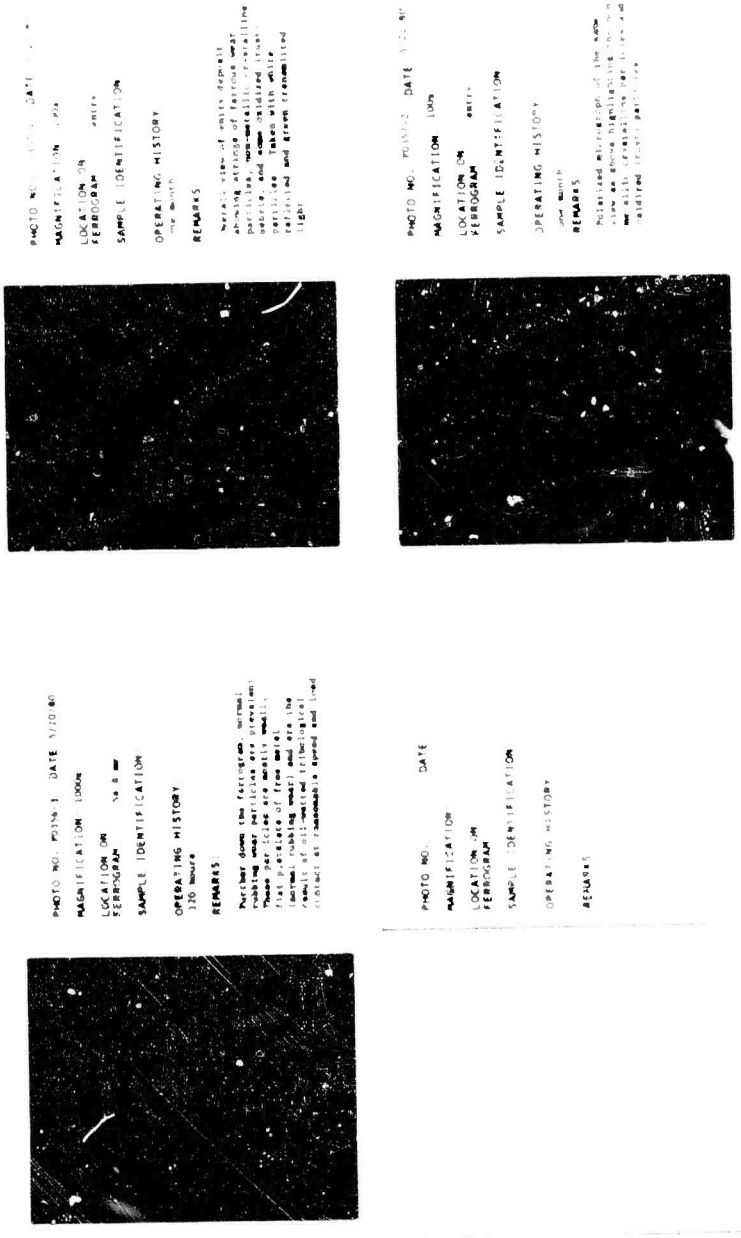

Figure 3.2.5.1 Report for Solvay in its Entirety (Continued)

PHOTO NO. [illegible] DATE [illegible]

MAGNIFICATION [illegible]

LOCATION ON
FERROGRAM entr-

SAMPLE IDENTIFICATION

OPERATING HISTORY
one month

REMARKS
Higher magnification view of the entry shows dark metall[illegible] oxide particles along with some rubbing wear. The shape of these particles is more equiaxed (chunky) which is typical of fatigue wear particles.

PHOTO NO. P0357-5 DATE 5/21/80

MAGNIFICATION: 1000x

LOCATION ON
FERROGRAM 51.6 mm

SAMPLE IDENTIFICATION

OPERATING HISTORY:
one month

REMARKS:

A large cutting wear particle attached to several strings of rubbing wear particles. Taken with white reflected and green transmitted light.

PHOTO NO. [illegible] DATE [illegible]

MAGNIFICATION 600x

LOCATION ON
FERROGRAM entry

SAMPLE IDENTIFICATION

OPERATING HISTORY
one month

REMARKS
Same view as above after heat treating [illegible] for [illegible] seconds. Large bright particle in the center [illegible] above, now shows a [illegible] temper [illegible] characteristic [illegible] steel [illegible] particles, however [illegible] consistent with the behavior [illegible] steel as evidenced [illegible]

PHOTO NO. P0357-6 DATE 5/21/80

MAGNIFICATION: 1000x

LOCATION ON
FERROGRAM 49.3

SAMPLE IDENTIFICATION

OPERATING HISTORY
one month

REMARKS

A large copper alloy particle weakly attached to strings of ferrous particles.

Figure 3.2.5.1 Report for Solvay in its Entirety (Complete)

The following DR readings, obtained for six samples from the gearboxes of six oil-free screw compressors, illustrate establishing a baseline for a number of similar machines:

	L	S
1	18.6	3.7
2	1.6	0.7
3	1.0	0.7
4	2.4	1.6
5	15.4	3.1
6	6.3	0.8

Ferrograms were prepared for each of the six samples with the following summary of their analysis:

Sample	Summary
1	Excessive cutting wear; bad wear situation. Recommend change of oil and oil filter.
2	Machine appears to be operating satisfactorily.
3	Machine appears to be operating satisfactorily
4	Some cutting wear but not nearly as bad as Sample 1.
5	Appears that oil is either heavily contaminated or there is a corrosive wear mode, or both. Recommend change of oil and oil filter. Resample after running for a few days.
6	Sample appears similar to Sample 5; same recommendations apply.

Samples #2 and #3 had no large ferrous wear particles. The few large particles that are present are nonmetallic and most of those are organic, having no significance regarding the wear situation. From the Sample #2 and Sample #3 ferrograms which are almost clean, it may be assumed that these gearboxes, when operating properly, produce only a small amount of wear debris. Samples #2 and #3 may be taken as baseline. Paragraph 2.3.4 shows two photomicrographs of the Sample #1 ferrogram which is highly abnormal compared to baseline.

The following recommendations are offered as a guideline toward establishing a condition-monitoring program.

1. Coordinate with the right people
   a) machine operators

b) machine maintenance men
c) machine servicemen
d) management

2. For each individual involved
   a) document each person's role
   b) use their knowledge to improve program
   c) establish a chain of authority
   d) educate all personnel involved

3. Establish a data base before program startup
   a) machine specifications
   b) fluid system schematics and specifications
   c) operator, service, and repair manuals
   d) lubricant type
   e) filter specifications
   f) wear components, especially material s ey data
   g) prior service and maintenance reports to identify problem areas

4. Establish sampling and sample handling procedures
   a) design and document sampling methods such as in-line valve, modified drain plug, suction tube etc.
   b) ensure cleanliness of sample containers — run some blank ferrograms with filtered oil
   c) take sample from system while it is operating if possible
   d) take sample at the same location and machine operating conditions each time
   e) coordinate sampling with operator or maintenance personnel
   f) provide sampling kits
   g) document handling or shipping

5. Data base after startup
   a) program normally should be quantitative -- plot DR graphs for each machine
   b) initially generate ferrograms for all samples to establish machine signature
   c) document all ferrograms with ferrogram analysis sheets
   d) store oil samples and ferrograms for possible retrospective analysis

6. Program administration
    a) communication — make sure results and recommendations reach the appropriate people
    b) ensure that the analyst's role within the organization is understood
    c) document all substantive work
    d) establish contacts with equipment manufacturer personnel

3.2.6 Heating of Ferrograms

Significant information about the composition of wear particles may be obtained by heat treating ferrograms and observing the change in appearance of the particles. Ferrous alloy particles may be categorized into broad alloy classes by the temper colors formed by heating. Lead/tin particles will be grossly affected because of the low melting temperature and susceptibility to oxidization of both these metals. Other white nonferrous metals commonly used in oil-lubricated wear contacts are aluminum, chromium, silver, and titanium. These are unaffected by heat treatment up to 550°C except for titanium which will tan slightly at 400°C. At lower temperatures, titanium is unaffected. Magnesium, molybdenum, and zinc are not easily distinguished from the other white nonferrous metals but then they would not normally be part of an oil-wetted path. Copper alloy particles, which are readily identified by their color without heating (gold is the only other yellow metal), will form temper colors upon heating, but these reactions so far have eluded practical use since there are a large variety of alloys and each alloy can have various responses depending on the stress state and crystal orientation. See paragraph 1.6 for details on identifying nonferrous metals.

Heat treatment of the ferrogram is accomplished using a hot plate and a surface thermometer. The ferrogram is placed, with the particles on the up side of the ferrogram, on the hot plate for 90 seconds at the chosen temperature. A flat-tipped forceps is recommended for manipulating the ferrogram on and off the hot plate.

Temper color is due to the growth of a uniformly thick oxide layer on metal when it is heated in air. Destructive interference gives rise to the appearance of colors depending on the thickness of the oxide layer. **Figure 3.2.6.1** illustrates how this occurs. If white light is incident on a heat treated ferrous alloy, some light will be reflected from the air/oxide interface and some will travel through the oxide and be reflected from the oxide/metal interface. If beam (2) lags behind beam (1) by a half wavelength, these light waves will cancel and the color corresponding to that wavelength will be absent from the complete spectrum which comprises white light. The first wavelengths for which this occurs are the short wavelengths, the blue/violet end of the visible spectrum (see **Figure 3.2.6.2**). The cancellation of blue/violet causes the alloy to appear red/orange. In practice, this is described as straw or tan color. As the oxide layer grows

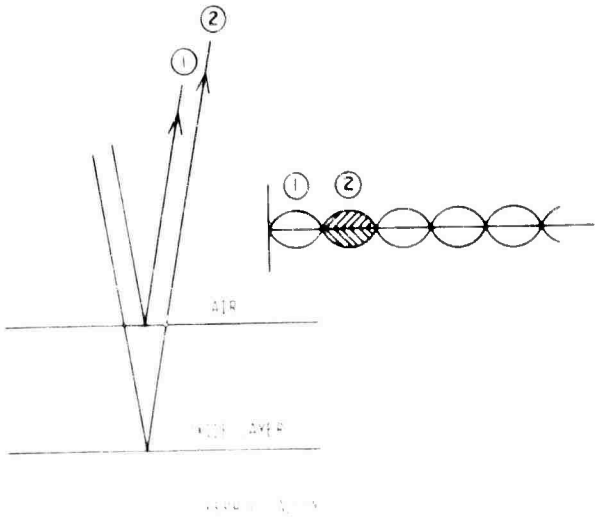

Figure 3.2.6.1 Formation of Interference Colors

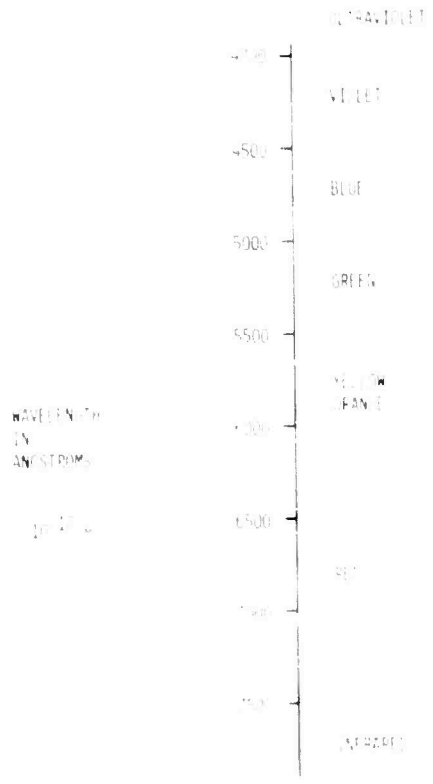

Figure 3.2.6.2 Visible Spectrum

thicker, the condition for destructive interference moves to the longer wavelength end of the spectrum. The red/oranges will be cancelled and the alloy will appear blue/violet. As the layer becomes still thicker, destructive interference occurs when the path difference equals odd integral half wavelengths, but the effect is less pronounced since the layer becomes less uniform and more light is attenuated as it passes through the oxide layer so that the beam reflected from the air/oxide interface is relatively more intense. In practice, as the oxide layer grows progressively thicker by heat treatment at successively higher temperatures, a ferrous metal will first appear light tan, straw, blue/violet, pale blue, and then grayish white without its original luster.

For ferrous alloys, the growth rate is retarded by alloying elements. Steel, which has relatively few alloying elements, has the quickest oxide layer growth rate. Cast iron, which typically has a much higher carbon content, has a slower oxide layer growth rate. High alloy steels, which are made with significant percentages of nickel, chrome, and other elements, are most resistant to the growth of the oxide layer.

The temper color phenomenon is exploited by first heating ferrograms to 330° C for 90 seconds which allows distinction of ferrous particles into three broad alloy classes: low alloy steel which turns blue, medium alloy steel (such as cast iron) which turns straw, and high alloy steel which is unaffected

Low alloy steel includes both mild steel and high hardenability steel such as is used for rolling-element bearings. Low alloy steel, as it is identified by its blue color subsequent to the above test, may have carbon contents up to about 1.5%. Medium alloy steel, as the term is used here, generally will be a cast iron with a carbon content of 2 to 4%, but steels with much lower carbon content may show straw temper color in this test if they contain other alloying elements such as chrome or nickel. High alloy steel has a substantial fraction of other alloying metals, typically chrome and nickel, and not much carbon.

The thickness of the oxide layer for blue/violet destructive interference which gives rise to straw temper color is:

$$\frac{\lambda}{4n}$$

where

λ = wavelength of light

and

n = index of refraction, which is the ratio of the speed of light in a vacuum divided by the speed of light in a given material.

Taking a wavelength of 450 nm and an index of refraction of 3 (Fe_2O_3 has a high index of refraction), the thickness is .0375 μm. The thickness of the oxide layer for blue/violet temper color is about .05 to .06 μm. This calculation indicates why even very fine rubbing wear particles show temper colors. For a 2 or 3 μm rubbing wear particle which typically may be a half micrometer thick, about 10% of the thickness will be oxidized. Only the very thinnest ferrous platelets will oxidize through their entire thickness in which case they will be translucent.

Table 3.2.6.1, after the work of Barwell, et al,[25] gives the recommended test procedure for categorizing ferrous particles into broad alloy classes.

Figures 3.2.6.3 and 3.2.6.4 show low alloy steel particles before and after heat treatment to the first heat challenge temperature (330° C/625° F). **Figures 3.2.6.5 and 3.2.6.6** show cast iron particles before and after heat treatment to the same temperature.

A word of caution to the wear particle analyst: Surface thermometers are often not accurate so it is prudent to check the reaction of particles of known metallurgy to be certain that heat treatment is being done at the proper temperature. A drill press can be used to conveniently generate wear particles. One piece of metal is held in the chuck and rotated with some downward load against a flat piece of the same metal clamped to the work table. Filtered oil is used to lubricate the wear contact. Some of this oil, collected after a few minutes of rotation, will provide a copious supply of wear particles. The contact should not be too heavily loaded to avoid generating dark metallo-oxides.

In the practical application of the heat treatment of ferrograms, the investigator will have knowledge of the materials in the oil-wetted path of the machine from which the sample came. In many cases, heat treatment to only the first challenge temperature of 330° C will be sufficient. At this temperature, cast iron may be distinguished from steel, which would, for example, be all that is needed for diesel engines which normally are made only with these common materials.

Heat treatment of ferrograms also allows easy distinction between organic and inorganic compounds. While both of these types of materials may appear similar when examined with polarized light, the organic material will char, melt, shrivel, or vaporize when exposed to heat. Heat treatment to the higher test temperatures (i.e., 540° C) will exacerbate these effects. Organic material will appear much less brilliant in polarized light after heat treatment. Inorganic compounds, because of their stronger chemical bonds, will be much less affected.

Ref. 25 Barwell, F. T., Bowen, E. R., Bowen, J. P., and Westcott, V. C. "The Use of Temper Colors in Ferrography", Wear, 44 (1977) 163-171

3.2.7 Scanning Electron Microscopy and X-Ray Analysis

Two functions can be performed using a scanning electron microscope (SEM). The first is to better study particle morphology, and the second, if the SEM is suitably equipped, is to determine particle composition. The SEM with its great depth of focus and high resolution is ideal to examine and photograph details of the shape of the particles. Because of the depth of focus, the SEM photographs are suitable for publications and other applications where a single photograph is desired to show the entire particle morphology. Although particles may be photographed in detail with an optical microscope, the particles are sometimes too large to bring the entire particle into focus. The SEM does not have this limitation.

A SEM, however, does not display the optical properties of the particles. The difference between an opaque particle and a transparent one is not observed nor is the color, behavior in polarized light, etc., available through the SEM. Since an average ferrogram contains thousands or millions of particles it is necessary to know the types of particles present to avoid unnecessary analysis. Consequently, it is necessary to examine the ferrogram optically prior to insertion in the SEM.

The recommended sequence for the preparation of a ferrogram for SEM analysis is as follows:

- Examine the ferrogram optically and note any particles of particular interest for examination in the SEM.
- Photograph the ferrogram under low magnification (100x) and mark out the particles of interest so that they may later be found with the SEM. Any desired optical photographs should be taken at this point.
- Coat the ferrogram in the coating apparatus (sputterer or evaporator) associated with the microscope so that the surfaces of the particles and the substrate are made electrically conductive. This is normally done with carbon or a metal, which should be chosen so that it will not interfere with the constituents of the particles. More on this subject appears below. The ferrogram must be made conductive to promote image quality and prevent particle charge-up. Otherwise, a static charge will build rapidly and individual particles will fly off. This sometimes occurs when a ferrogram is poorly coated.
- If the ferrogram is too long to fit into the specimen chamber of the available SEM, the ferrogram may be broken in two by scribing a light line on the upper surface. Place the ferrogram on a flat plate and, using a diamond tipped pencil and a metal ruler placed at an angle against the substrate, rule a single scratch across the width of the ferrogram. This scratch need not be deep but should be continuous. Cantilever the half of the ferrogram above the scratch over the edge of a supporting flat plate and break off.

TABLE 3.2.6.1
IDENTIFICATION OF PARTICLES BY HEAT TREATING FERROGRAMS

Test Material	Other Similar Materials	COLOR			
		Test 1 330° C/625° F	Test 2 400° C/750° F	Test 3 480° C/900° F	5
AISI 52100*	Carbon steels and low alloy steels	Blue	Light Grey		
3-1/2% carbon cast iron	Medium alloy steels, approximately 3-8% alloy	Straw to bronze	Deep bronze and some mottled bluing		
Type "A" nickel	High nickel alloy	No change	No change	Bronze with significant bluing on most particles	All blu blu
AISI 304‡ stainless steel	High alloy steels	No change	Generally no change; slight yellowing on some particles	Straw to bronze with slight bluing on some particles	Mo stil bro pa ing blu
Organic materials	—	Charring, contraction, vaporization, depending on mate			
Nonferrous metals	—	See Table 1.6.1 for white nonferrous metals See paragraph 1.6.2 for copper alloys See paragraph 1.6.3 for lead/tin alloys			

* AISI 52100: 0.98 - 1.10% C, 0.25 - 0.45% Mn, 0.025% P max, 0.025% S max, 0.20 - 0.35% Si, 1.30 - 1.6
† Nickel, commercial, 99% pure
‡ AISI 304: 0.08% C max, 2.00% Mn max, 1.00% Si max, 18.00 - 20% Cr, 8.00 - 10.50% Ni

TABLE 3.2.6.1
IDENTIFICATION OF PARTICLES BY HEAT TREATING FERROGRAMS

Other Similar Materials	COLOR			
	Test 1 330° C/625° F	Test 2 400° C/750° F	Test 3 480° C/900° F	Test 4 540° C/1000° F
arbon steels and w alloy steels	Blue	Light Grey		
edium alloy eels, approxi- ately 3-8% alloy	Straw to bronze	Deep bronze and some mottled bluing		
igh nickel alloy	No change	No change	Bronze with significant bluing on most particles	All particles blue or blue/grey
igh alloy steels	No change	Generally no change; slight yellowing on some particles	Straw to bronze with slight bluing on some particles	Most particles still straw to bronze; some particles showing mottled bluing
—	Charring, contraction, vaporization, depending on material			
—	See Table 1.6.1 for white nonferrous metals See paragraph 1.6.2 for copper alloys See paragraph 1.6.3 for lead/tin alloys			

- 1.10% C, 0.25 - 0.45% Mn, 0.025% P max, 0.025% S max, 0.20 - 0.35% Si, 1.30 - 1.60% Cr
cial): 99% pure
C max, 2.00% Mn max, 1.00% Si max, 18.00 - 20% Cr, 8.00 - 10.50% Ni

- When locating the particles in the SEM, set the magnification to approximately the same as the low magnification photograph, making sure that the photograph is viewed with the same orientation as the picture on the SEM screen. It is easy to get the photograph upside down with respect to the screen in which case locating the particles is much more difficult. Once the general area is located, increase the magnification, in steps, until the selected particle appears on the screen. Photography and analysis may then be performed.

X-ray analysis is possible because atoms of every element emit characteristic X-rays when they are ionized by high energy radiation. This occurs because vacancies in inner electron shells are created when atoms are bombarded with radiation that has enough energy to remove an electron from its normal energy level. After an inner shell electron is removed, an outer shell electron "relaxes" to the inner shell state. The electron relaxation results in X-ray emission of a certain energy level. The characteristic X-rays emitted by the atoms in a given target can be detected. The detected X-rays can then be electronically processed and computer analyzed to give qualitative and quantitative determination of the elements present in the target.

Elements below atomic number 11 (sodium) cannot be detected because the X-rays emitted from these lower atomic number elements have insufficient energy to penetrate the beryllium window commonly used in the X-ray detector.

If an X-ray analysis is to be conducted, attention should be given to the electron beam generating voltage. At higher voltages, the electrons penetrate deeper into the particle structure and the X-rays are therefore emitted further from the particle surface. Since most wear particles are less than 3 μm thick, emissions may be received from the glass substrate or from particles beneath the particle of interest. This can obviously result in incorrect quantitative and qualitative measurements. (The ferrogram glass typically contains Si, Na, K, Ti, Al, and Zn, but the composition is not consistent from substrate to substrate.)

For good SEM photomicroscopy, gold is the recommended coating for ferrograms. For X-ray analysis, however, carbon is the recommended material. Because of its low atomic number of 6, carbon will not contribute to the X-ray energy spectrum, whereas gold or other higher atomic number elements may have energy peaks that can be confused with elements present in the particle being analyzed. Also, carbon coatings are sufficiently translucent that not all optical information is lost if it is desired to examine the ferrogram by optical microscopy after electron microscopy has been performed.

Electrically conductive substrates eliminate the need for coating ferrograms. Pure metals may be used to make ferrogram substrates but that metal cannot then be detected in particles which are X-ray analyzed. Further, since higher atomic number metals have a more complicated X-ray spectra with more emission peaks, these are

usually a poor choice for substrate material; it is more likely that an emission peak will be close to a peak of one of the elements in the particle being analyzed.

Carbon filled plastic ferrograms are convenient for SEM work. The carbon makes them sufficiently conductive that they need not be coated. If the plastic is properly chosen, the resulting ferrogram will have no peaks in its X-ray emission spectra since it is composed entirely of hydrogen and carbon. A drawback of carbon-filled plastic ferrograms is that they are opaque so that they can be viewed in the optical microscope only with reflected light. However, light extinction is quite complete when viewed in polarized reflected light so that nonmetallic crystalline particles appear in bright contrast to the black background.

Carbon coated translucent plastic ferrograms combine the advantages of carbon filled plastic ferrograms with the ability to be examined in bichromatic illumination. Plastic ferrograms, of course, cannot be used for laboratory hot plate heat treatment tests.

3.2.8 Grease Analysis

In order to apply the techniques of ferrography to grease-lubricated bearings, it was necessary to develop a solvent system which would dissolve the grease sample so as to produce a fluid of suitable viscosity for ferrogram preparation and to demonstrate that the particles found in the grease are accurately represented in the fluid sample.

Because the ingredients used in grease formulations are diverse, the selection of a single solvent for all greases appears to be a difficult task. Solid additives incorporated in greases are insoluble. A wide variety of soaps or thickeners may be used by different manufacturers with the same liquid lubricant to comply with specific grease requirements and the same specifications. Further differences in greases from manufacturer to manufacturer may result from differences in manufacturing procedures. For example, one manufacturer may use a soap base to thicken a specific lubricating fluid, while another may incorporate the soap-making procedure in the grease manufacturing process. The concentration, distribution, and size of the solid phases may also vary.

It was therefore necessary to establish a reliable technique for sampling grease and to select solvents which could be used to dissolve greases of all types. It was also necessary to demonstrate that once a sample of grease had been treated with a suitable solvent, the same techniques of ferrography could be used as successfully applied to samples of lubricating oil.

In order to conduct solvating studies covering a range of combinations of ingredients in the more frequently used greases, unused samples were obtained of the nine greases listed in **Table 3.2.8.1**. The nine greases cover a range of fluid lubricants, soap phases, and solid additives.

TABLE 3.2.8.1

TYPES OF GREASE SELECTED FOR INVESTIGATION

Sample No.	Base Oil	Thickener (Soap)	Solids
1	Petroleum	Lithium Soap	.....
2	Petroleum	Lithium Soap	Molybdenum Disulfide
3	Synthetic Diester	Silica	Silica
4	Silicone	Lithium Soap	.....
5	Petroleum	Aluminum Complex Soap	.....
6	Petroleum	Mixed	Molybdenum Disulfide
7	Petroleum	Clay (Bentone)	Molybdenum Disulfide
8	Petroleum	Barium Complex Soap	.....
9	Petroleum	Calcium Soap	.....

Three solvent systems were initially chosen for solvation studies on the nine unused greases. As the solvency power of a solvent system on different materials cannot be accurately predicted, the three solvent systems chosen had varying balances of polar nonpolar, and aromatic or aliphatic constituents. The solvents were:

1. Grease Solvent #1
   (toluol/isopropanol)
   an aromatic/polar blend
2. Grease Solvent #2
   (toluol/methyl ethyl ketone (MEK)/isopropanol)
   an aromatic, highly polar blend
3. Grease Solvent #3
   (toluol/hexane)
   an aromatic, aliphatic, essentially nonpolar blend

Previous experience indicated that the use of glass beads considerably shortened the time of agitation required for grease solution. Therefore, ten 3 mm diameter glass beads were introduced into a sample bottle, the capacity of which is 1/2 U.S. fluid ounces (15 ml). A small amount of grease (the amount will vary depending upon particle concentration but 50 mg is a recommended starting amount) and 10 ml of the solvent to be tested were added. Then the bottle was sealed and well shaken by hand. Ultrasonic agitation is also useful in dissolving grease samples. The sample should be briefly hand shaken after ultrasonically agitating. The small scale oscillations of the ultrasonic bath will thoroughly mix the sample on a local level but the sample will become stratified with the largest particles settling to the bottom. After shaking, a ferrogram may be prepared following the usual operating instructions except that the grease solvent is substituted for fixer during the wash cycle.

Solvents #1 and #2 were found to be ineffective for lithium soap greases, but Solvent #3, containing less aromatic solvent (30% toluol) and more nonpolar aliphatic solvent (70% hexane), proved to be effective for the solution of lithium soap/petroleum oil type grease. This solvent was therefore used to treat the remaining grease samples.

The three greases found most difficult to dissolve for ferrographic analysis procedure, #4, #6, and #8, **Table 3.2.8.1**, were subjected to working in a test machine before being used for further solvation studies. The grease working test consisted of running an AISI 52100 steel race against a fixed AISI steel bearing ball under a load of 80 lb/in.^{2} for 2 minutes. A small quantity of grease was used for each test and treated with Solvent #3 after working. Satisfactory ferrograms were then prepared.

A background network of organic material was found on ferrograms prepared from unused barium soap base petroleum oil grease #8 and also on ferrograms prepared from worked samples of the same grease, but to a lesser extent. Heating of the ferrogram to 625° F for 90 seconds eliminated the organic material which enabled the examination and analysis of the metallic wear particles to be carried out more satisfactorily.

Observations on the movement and structure of grease in roller bearings[26] has shown that in a grease-lubricated roller bearing, only the small amount of grease between the rollers and races performed the lubrication. The pockets of grease held by the retainer were relatively inactive. The principal role of the grease in the pockets appeared to be to keep in position the small amount of material responsible for lubrication and to replenish the oil as it was lost by evaporation or degradation. Thus, in a correctly operating grease-lubricated bearing, a small amount of grease becomes severely worked and degraded whereas the bulk of the grease remains in an almost virgin state.

Ref. 26 Milne, A.A., Scott, D., and Scott, H.M., "Observations on the Movement and Structure of Grease in Roller Bearings", Proc. Conf. on Lubrication and Wear, 1957, 450-453 and 803, Inst. Mech. Engrs., London (1958)

The movement of wear particles in a grease-lubricated part is restricted to the region where the active grease is located. Therefore, a basic problem in monitoring grease-lubricated parts is that the sample measurement of the concentration of an element in the bulk grease provides no information regarding the wear rate; the concentration of wear particles is not uniform throughout the grease and varies with the place from which the grease was sampled.

The applicability of ferrography to the examination of grease-lubricated systems is therefore critically dependent on the possibility of obtaining representative samples and, in order to assess the feasibility of the application, a number of samples were taken from critical areas of fixed-wing aircraft and helicopters at the Naval Air Rework Facility (NAVAIREWORKFAC), San Diego, California. Analysis of these samples[27] indicated the critical nature of the sampling process as well as the risk of contamination of the grease from external sources.

A number of samples taken from the swash plate of an H53 helicopter serve to emphasize the critical nature of the sampling process. A sample taken from behind the spaces between the two rolling bearings revealed a surprising number of severe wear particles, whereas a sample taken from around the balls of the upper bearing showed heavy deposits of friction polymer.

The following is a list of recommendations and conclusions when using ferrography for greases:

1. Grease solvent #3 (toluol/hexane) was effective for use with the wide range of grease samples investigated. It appears to be potentially suitable as a general solvent for all greases. It should contain up to 50% of diester synthetic oil (MIL-L-23699) to suspend high-density large particle material and to prevent co-settling of wear particles.
2. Commonly used solid additive materials such as silicone and carbon black present no difficulty to ferrographic analysis if the foregoing procedure for grease analysis is used.
3. Insoluble organic materials present in greases if deposited on ferrograms may be eliminated by heating the ferrogram.
4. The use of glass beads to speed up the grease solvating process should be incorporated in any standard grease ferrogram preparation procedure.
5. Ferrograms made with samples from grease lubricated bearings are of a quality which is comparable with those made from oil-based samples.

Ref. 27 Bowen, E.R., Bowen, J.P., and Anderson, D.P. "Applications for Ferrography to Grease Lubricated Systems" presented at the 46th Annual Meeting of the National Lubricating Grease Institute, Hot Springs, Virginia (Oct. 29 - Nov. 1, 1978).

6. Results demonstrate the feasibility of obtaining satisfactory ferrograms from grease-lubricated bearings. The examination of such bearings is not, however, as straightforward as when oil is used as a lubricant for two reasons. Firstly, the distribution of wear particles within the grease in a bearing is very uneven; and secondly, because the physical configuration of most bearings precludes the extraction of grease without actually dismantling the bearing.

7. There will be many situations where condition monitoring using ferrography will be precluded by sampling difficulties. However, in systems where sampling can be carried out readily, similar techniques to those perfected for oil-lubricated systems can be applied. In many cases, however, it will not be possible to dismantle bearings for sampling and the role of ferrography will be restricted to diagnosis of failed bearings or of those which have been dismantled for one reason or another.

3.2.9 Precipitation of Nonmagnetic Particles

From discussions with military and industrial oil analysts, it transpires that some failures in hydraulic systems are not initially predictable by metallic wear particle monitoring, but are due to failure of seals and gaskets which are made from various synthetic organic materials, or from the ingression of other nonmetallic contaminants. Application of magnetizing solvents, which contain rare earth salts, developed to precipitate biological materials for medical ferrography,[28,29,30] have been successful in precipitating various organic materials from hydraulic oil.

Hydraulic oils fall into three primary categories, namely, water glycol, water-oil emulsions, and petroleum or synthetic fluids. It is feasibile to dissolve in these fluids magnetic metal cations which interact chemically with organic elastomers in the oil. In the case of glycol fluids, this is achieved by direct dissolution of the metal halide. With the oleophilic fluids, the use of transitionary fluids is required. These magnetizing fluids work as follows.

The trivalent cations of the lanthanide series are strongly paramagnetic due to the presence of unpaired f shell electrons. When these cations bind to negative sites on organic compounds in solution, the compounds are given a positive magnetic susceptibility. Erbium ions (Er^{3+}) are effective for this purpose although other magnetic cations in the lanthanide series work similarly.

Ref 28 Mears, D C , Hanley, E N , Rutkowski, R , and Westcott, V C , "Ferrographic Analysis of Wear Particles in Arthroplastic Joints" Journal of Biomedical Materials Research, 12 (1978) 867-875

29 Evans, C H , Mears, D C , and McKnight, J L , "A Preliminary Ferrographic Survey of the Wear Particles in Human Synovial Fluid" Arthritis and Rheumatism, 24 (1981) 912-918

30 Evans, C H , and Tew, W P , "Isolation of Biological Materials by use of Erbium III — Induced Magnetic Susceptibilities" Science 213 (1981) 653-654

While many plastics are not ionic in nature and thus cannot absorb metal cations by ion exchange, several of them have polar side chains. Examples of this are polyacrylamide, which has a polar amide side group, poly (methylmethacrylate) and polyvinyl acetate, which have polar carbon-halogen groups. Such structures are expected to interact electrostatically with metal cations.

Magnetizing solution has been used to prepare ferrograms from hydraulic oil samples which showed progressively more organic material until the equipment failed.[31] This material was identified as fluoroelastomer based on comparison with seal material used in that equipment.

For condition monitoring of hydraulic equipment, or other equipment with potential for nonmetallic component failure, it is recommended that seal or gasket material from the equipment to be monitored be artificially dispersed in filtered lubricant of the same specifications that its deposition efficiency and appearance under the microscope may be determined.

3.2.10 Polarized Light

The use of polarized light to examine particles allows the analyst to distinguish, in general, between crystalline and amorphous materials. As will be explained, there are some qualifications to this generalization regarding the behavior of cubic crystals, biological materials, plastics, and finely divided amorphous material. The light is polarized and analyzed by oriented molecular films (Polaroid)* having high absorption of the electric field perpendicular to the polarization direction. Since the polarizer and analyzer are identical, they will be referred to here as polarizers (Nichol prisms are obsolete for such applications).

In practice, a polarizer is placed between the light source and the object plane (ferrogram) and another polarizer, rotated 90° to the first polarizer, is placed between the object plane and the observer. **Figure 3.2.10.1** illustrates this arrangement. The electric fields of the light waves coming from the microscope light bulb radiate in all directions perpendicular to the direction of propagation of these light waves. Viewed from the side, a light ray can be thought of as sine waves oscillating in all directions perpendicular to the direction of propagation. **Figure 3.2.10.1** shows two such sine waves perpendicular to each other. Light can be resolved vectorally into two perpendicular components, one parallel with the polarizer and one perpendicular. The components that are parallel pass through the first polarizer resulting in linearly polarized waves. If nothing disrupts the light path, the second polarizer will block the light allowed through by the

* Trademark of Polaroid Corporation

Ref. 31 Anderson, D.P., Bowen, E.R., and Bowen, J.P. "Advances in Wear Particle Analysis" Report ONR-CR169-007-1F to the Office of Naval Research (1979).

first polarizer and the field of view will be dark. However, if certain materials are interposed, the light will be depolarized and some will pass through the second polarizer (see **Figure 3.2.10.2**).

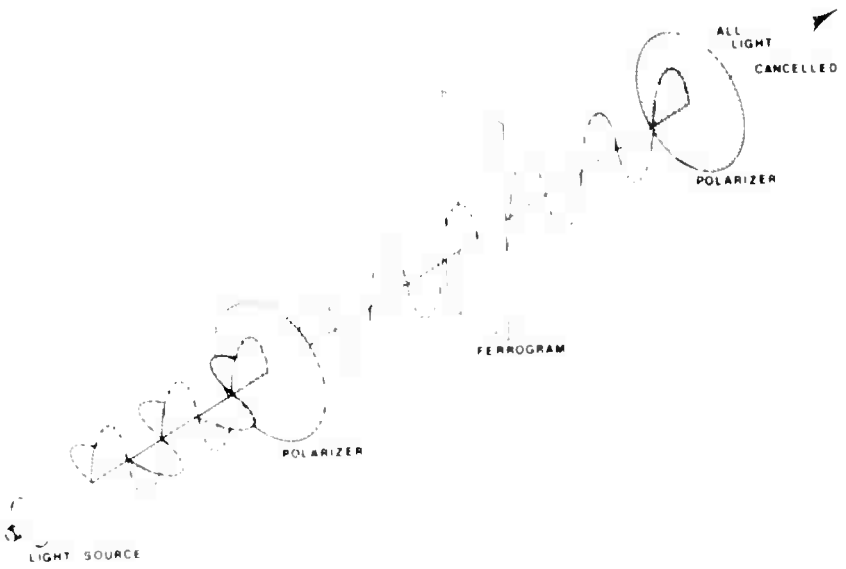

Figure 3.2.10.1 Polarizer Arrangement in the Optical Microscope

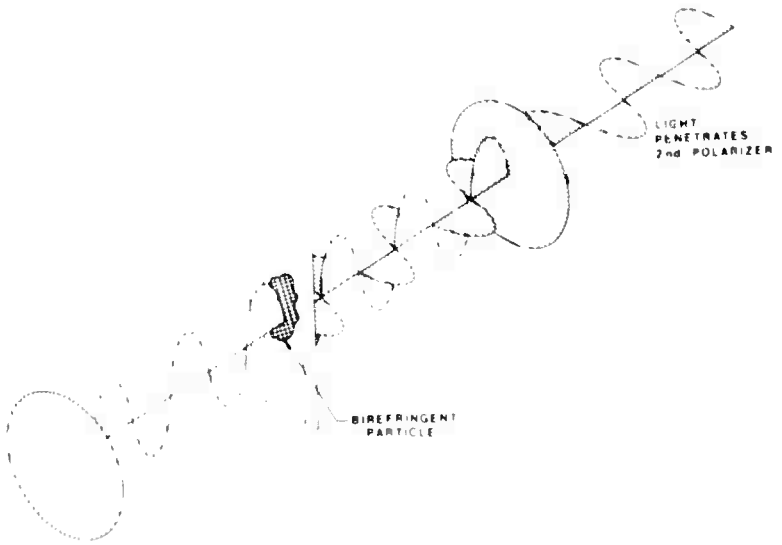

Figure 3.2.10.2 Birefringent Particle in Crossed Polarizers

Most nonmetallic crystalline particles will disrupt polarized light because they are birefringent; that is, the crystals have different indices of refraction along different crystal directions. This is because most crystals are anisotropic; there is different atomic spacing and strength of atomic bonding along different crystal axes. Consequently, light propagates at a different velocity along these axes. When plane-polarized light is incident upon an anisotropic crystal at an arbitrary angle, the components of light along the differing optic axes travel with different velocities such that a retardation of one component with respect to another occurs. The retardation causes a rotation of the plane of polarization of the light exiting the crystal with respect to the incident light. Upon emerging from the crystal, the light can be resolved into any two perpendicularly plane-polarized components so that some component will be parallel to the second polarizer and will pass through. Only when the plane of polarization of the incident light coincides with one of the optic axes of the crystal will the exit beam have the same plane of polarization as the incident beam.

Retardation is calculated as

$$\text{Retardation} = t\,(n_1 - n_2)$$

where t is the crystal thickness and n_1 and n_2 are two different refractive indices of the crystal. Retardation is measured in units of length since the refractive index is dimensionless (it is the ratio of the speed of light in a vacuum to the speed of light in a given material). Retardation determines the degree by which the emergent beam of light is rotated with respect to the incident beam of linearly polarized light. If the light coming from the microscope light bulb was monochromatic (light of the same wavelength and therefore the same color) and a wedge shaped anisotropic crystal was viewed so that the crystal thickness varied, alternating bright and dark bands would be seen on the crystal. The dark bands correspond to regions of the crystal where the thickness is such that the retardation is an integral number of wavelengths. In this case, the emergent light is in phase with the incident polarized light and will therefore be blocked by the second polarizer which is 90° to the first polarizer. The bright bands correspond to regions where the retardation is odd multiples of a half wavelength so that the emergent beam is polarized 90° to the incident beam and will pass through the second polarizer. This phenomena may be seen by putting a red filter over the first polarizer when viewing birefringent particles. Now, if one of the polarizers is rotated 90° so that both polarizers are aligned, rather than being crossed, the regions of the birefringent crystal that were dark will now be bright and the formerly bright regions will be dark (the background, of course, will be bright with parallel polarizers). The dark regions are where the retardation is an odd multiple of a half wavelength so that the light is polarized 90° to either polarizer.

When birefringent crystals are examined in white light with crossed polarizers, certain wavelengths (colors) of the full visible spectrum (which, when blended together

produce white light) will be deleted and brilliant bands of interference colors will be seen rather than light and dark bands as seen in monochromatic light. If a crystal wedge is viewed in crossed polarizers, the thinnest regions will be dark because the retardation is insufficient to rotate the emergent beam's plane of polarization enough to align much of the light with the second polarizer. Slightly thicker sections of the wedge will cause enough retardation to rotate the plane of polarization so that a substantial fraction of the light penetrates the second polarizer. This light will be white. At even thicker regions of the wedge, the retardation is equal to a full wavelength in the visible region and interference colors result. The first color produced is yellow, resulting from retardations of about 300 to 400 nanometers (10^{-9} m) removing blue/violet from the incident white light. As the wedge gets thicker, the color bands become paler and broader until it becomes milky white when the retardation is greater than about 5 times the wavelength of red light.

If, for a certain material, the difference between refractive indices is large, bands of interference colors may be seen on crystals as thin as 2 or 3 μm. For example, a 2 to 3 μm thick particle of calcite ($CaCO_3$ — calcium carbonate), with refractive indices of 1.658 and 1.486, will show interference colors. For the 2 μm thick region the retardation equals 2000 (1.658 - 1.486) = 344 nm which gives yellow interference color. However, for most materials, where the difference in refractive index is not great, the particles must be 10 μm or more in thickness before interference colors are seen. Consequently, many of the crystalline particles on ferrograms are too small to show interference colors, but will appear bright in crossed polarizers. The very smallest particles will be dark.

Crystals may be identified by interference colors, which is the subject of optical mineralogy or optical crystallography[32,33,34,35,36] but which is beyond the scope of ferrography.

Cyrstals of the cubic system are not birefringent because perpendicular crystalline directions are equivalent. However, small cubic crystals viewed in a microscope with crossed polarizers will appear bright although not as bright as birefringent crystals. The reason for this is that light is partially polarized whenever it is reflected from a surface. Upon reflection, some of the incident polarized light has its direction of polarization shifted from its original orientation, thus depolarizing the light. Edges of

---

Ref 32 Kerr, P.F. "Optical Mineralogy", McGraw-Hill, Third Edition (1959).

Ref 33 Phillips, W.R. "Mineral Optics", W.H. Freeman and Co. (1971).

Ref 34 Bloss, D.F. "An Introduction to the Methods of Optical Crystallography", Holt, Reinhart and Winston (1961)

Ref 35 Longhurst, R.S. "Geometrical and Physical Optics", Longmans, Green and Co., Ltd., 2nd Edition (1967)

Ref 36 Hecht, E., and Zajac, A. "Optics", Addison-Wesley Publishing Co. (1974)

cubic crystals appear bright in polarized light. The following experiment demonstrates that the depolarization is due to reflection. After first examining some cubic crystals (common salts such as NaCl or KCl will do) to observe their brightness in polarized light, put a drop of immersion oil with a comparable refractive index onto some of the crystals The field becomes completely dark because reflection cannot occur without a difference in refractive index.

If immersion oil is put on birefringent particles, an opposite effect is observed. **Figure 3.2.10.3** shows some sodium sulfate (Na_2SO_4) particles in transmitted polarized light at 100x magnification. **Figure 3.2.10.4** shows the same view after a drop of immersion oil of comparable refractive index was put on the particles. Both photographs were exposed for 1 second. The brightness of the crystals is greater with immersion oil because light is not scattered and reflected away from the direction of incidence because of the matching of refractive indices. This effect is most pronounced using the 10x objective (100x total magnification), rather than using higher power objectives, because the numerical aperture of the 10x lens is low and the angle of the cone of acceptance from the object plane is small.

Figure 3.2.10.5 shows potassium chloride (KCl) crystals in polarized transmitted light at 100x magnification. Exposure time was 20 seconds compared to the 1-second exposure time for the Na_2SO_4 crystals which gives an indication of the relative light intensity for depolarization by birefringent materials versus depolarization by reflection and/or scattering.

Amorphous materials in bulk do not depolarize light because they lack long-range internal structure. Therefore, their optical properties, as well as other physical properties, are isotropic. However, powdered amorphous materials, such as powdered glass, depolarize light due to multiple reflections from the surface of the particles. **Figure 3.2.10.6** shows particles of crushed glass at 100x in polarized transmitted light. Exposure time was one minute. As expected, powdered glass becomes dark in polarized light if a drop of immersion oil of matched index is put on the glass particles.

Plastics display birefringence according to the degree of crystallization or molecular orientation. Highly ordered plastics such as extruded nylon fibers appear very bright.

Polycrystalline clusters of crystallites smaller than 2 or 3 μm appear bright, snow-like, and do not change in intensity as the direction of polarization is changed. Because they are too thin to show birefringent colors (depolarization is due to scattering and reflection), the polycrystalline particles exhibit the color of the substance. The colors are much more saturated than when the particles are viewed with unpolarized light, permitting color distinctions which could not otherwise be made. Sometimes the color absorption of a substance is so great that in bulk it appears brown or black, whereas small particles of the same substance display brilliant colors.

Particles of biological origin often are quite bright in polarized light because of an ordered structure. Hair, cotton fibers, and paper are good examples.

Metal particles appear dark because their electronic structure prevents light from penetrating. The edges of metal particles when viewed in polarized transmitted light often appear bright due to depolarization by reflection. Surface layers of oxides or other substances may also cause metal particles to have bright edges.

When viewed in polarized reflected light, the surfaces of metal particles are dark except at steps or imperfections where a relatively thicker oxide/compound layer must be traversed or where some depolarization due to reflection can take place.

Fig. 3.2.6.3 Opt. M. 400X ⊢— 50μm —⊣

Fig. 3.2.6.4 Opt. M. 400X ⊢— 50μm —⊣

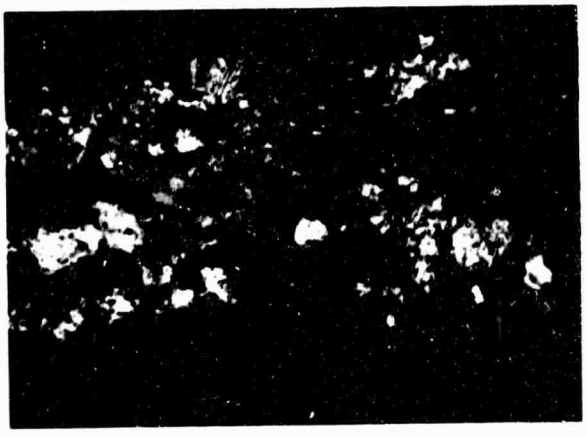

Fig. 3.2.6.5 Opt. M. 400X ⊢— 50μm —⊣

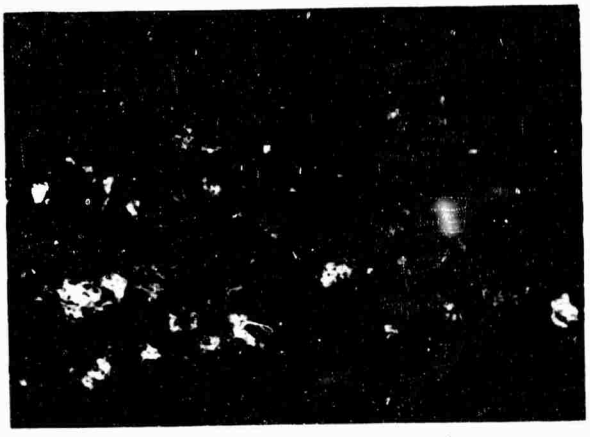

Fig. 3.2.6.6 Opt. M. 400X ⊢— 50μm —⊣

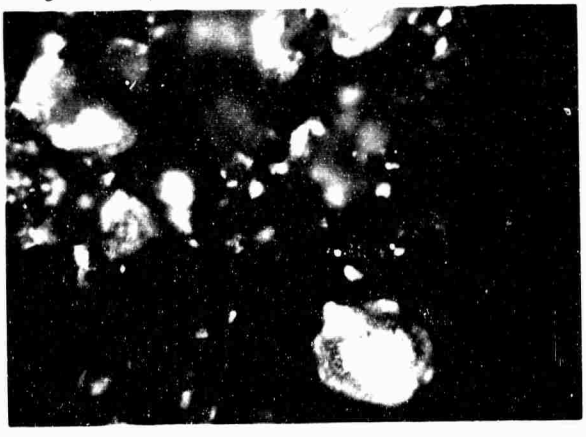

Fig. 3.2.10.3 Opt. M. 100X ⊢— 200μm —⊣

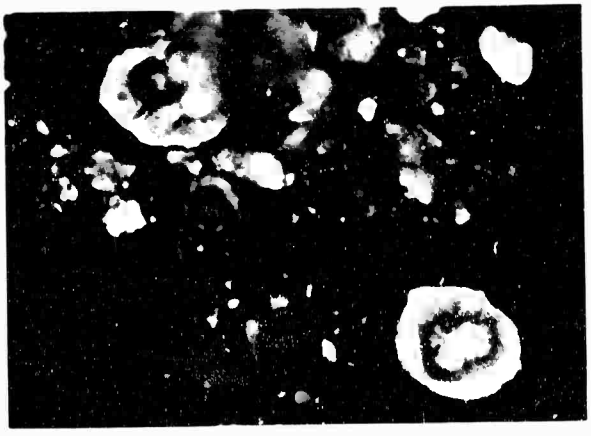

Fig. 3.2.10.4 Opt. M. 100X ⊢— 200μm —⊣

Fig. 3.2.10.5 Opt. M. 100X ⊢— 200μm —⊣

Fig. 3.2.10.6 Opt. M. 100X ⊢— 200μm —⊣

4. REFERENCES

1. Seifert, W.W., and Westcott, V.C. "A Method for the Study of Wear Particles in Lubricating Oil", Wear, 21 (1972) 22-42.
2. Bowen, E.R., Scott, D., Seifert, W.W., and Westcott, V.C. "Ferrography", Tribology International, 9 (3) (1976) 109-115.
3. Scott, D., and Mills, G.H. "Spherical Particles in Rolling Contact Fatigue", Nature (London), 241 (1973) 115-116.
4. Scott, D., and Mills, G.H. "Spherical Debris — Its Occurrence, Formation, and Significance in Rolling Contact Fatigue", Wear, 24 (1973) 235-242.
5. Reda, A.A., Bowen, E.R., and Westcott, V.C. "Characteristics of Particles Generated at the Interface Between Sliding Steel Surfaces", Wear, 34 (1975) 261-273.
6. Hofman, M.V., and Johnson, J.H. "The Development of Ferrography as a Laboratory Wear Measurement Method for the Study of Engine Operating Conditions on Diesel Engine Wear", Wear, 44 (1977) 183-199.
7. Jones, M.H. "Ferrography Applied to Diesel Engine Oil Analysis", Wear, 56 (1979) 93-103.
8. Davies, C.B. "Identifying Solid Particles in Used Lubricating Oils", Diesel and Gas Turbine Worldwide (Apr 1980).
9. Caterpillar Service Letter, Caterpillar Tractor Co. (8 May 1979).
10. Hoffman, J.G. "Crankcase Lubricants for Four-Cycle Railroad and Marine Diesel Engines", Lubrication Engineering. V. 35, No. 4 (Apr 1979) 189-197.
11. Scott, D., and Mills, G.H. "An Exploratory Investigation of the Application of Ferrography to the Monitoring of Machinery Condition from the Gas Stream", Wear, 48 (1978) 201-208.
12. Blyskal, E.P. "RB.211 Ferrographic Analysis Investigation Status Report No. 1", Eastern Airlines, Engineering Report No. E-954 (18 Jul 1977).
13. Eisentraut, K.J., Thornton, T.J., Rhine, W.E., Constandy, S.B., Brown, J.R., and Fair, P.S. "Comparison of the Analysis Capability of Plasma Source Spectrometers vs. Rotating Disc Atomic Emission and Atomic Absorption Spectrometry for Wear Particles in Oil: Effect of Wear Metal Particle Size", presented at the 1st International Symposium on Oil Analysis, Erding, Germany (4-6 Jul 1978).
14. "Standard Handbook of Lubrication Engineering" sponsored by the American Society of Lubrication Engineers (1968), McGraw-Hill Book Company.

15. Pocock, G., and Courtney, S.J. "Ferrography as a Health Monitor and a Design Aid for the Development of Helicopter Gearboxes", Paper 80-LC-6B-4, San Francisco (Aug 1980).

16. Fluid Power Research Center "Wear in Fluid Power Systems", Final Report to the Office of Naval Research, Contract No. N00014-75-C-1157 (Jun 1979).

17. Tessman, R.K., and Fitch, E.C. "Contaminant Induced Wear Debris for Fluid Power Components", Tribology 1978 — Materials Performance and Conservation, University College of Swansea, Wales (3-4 Apr 1978), Published by the I. Mech. E., Paper C45/78 (1978).

18. Loker, A. "Aircraft Engine Driven Accessory Shaft Coupling Improvements Using High-Strength, Low Wear Polyimide Plastic", Report No. TM76-1 SY, Naval Air Test Center, Patuxent River, Maryland.

19. Saka, N., Sin, H., Suh, N.P. "Prevention of Spline Wear by Soft Metallic Coatings", Report to the Office of Naval Research, Contract No. N00014-76-C-0068 (July 1980).

20. Bisson, E.E. "Lubrication Problems in Space for Exposed Mechanisms and for Power Generation Equipment", Chapter 45, Standard Handbook of Lubrication Engineers (1968).

21. Scott, D., McCullagh, P.J., and Campbell, C.W. "Condition Monitoring of Gas Turbines — An Exploratory Investigation of Ferrographic Trend Analysis", Wear, 49 (1978) 373-389.

22. Fitch, E.C., and Tessman, R.K. "Practical and Fundamental Descriptions for Fluid Power Filters", Paper No. 730796, SAE Trans., Society of Automotive Engineers, New York (1974).

23. Kjer, T. "Wear Rate and Concentration of Wear Particles in Lubricating Oil", submitted to Wear for publication.

24. Foxboro Analytical "Sample Processing with the Model 7067 Direct Reading Ferrograph", MI 612-101 (Jun 1980).

25. Barwell, F.T., Bowen, E.R., Bowen, J.P., and Westcott, V.C. "The Use of Temper Colors in Ferrography", Wear, 44 (1977) 163-171.

26. Milne, A.A., Scott, D., and Scott, H.M. "Observations on the Movement and Structure of Grease in Roller Bearings", Proc. Conf. on Lubrication and Wear, 1957, 450-453 and 803, Inst. Mech. Engrs., London (1958)

27. Bowen, E.R., Bowen, J.P., and Anderson, D.P "Applications for Ferrography to Grease Lubricated Systems", presented at the 46th Annual Meeting of the National Lubricating Grease Institute, Hot Springs, Virginia (Oct 29 — Nov 1, 1978).

28. Mears, D.C., Hanley, E.N., Rutkowski, R., and Westcott, V.C. "Ferrographic Analysis of Wear Particles in Arthroplastic Joints", Journal of Biomedical Materials Research, 12 (1978) 867-875.

29. Evans, C.H., Mears, D.C., and McKnight, J.L. "A Preliminary Ferrographic Survey of the Wear Particles in Human Synovial Fluid", Arthritis and Rheumatism, 24 (1981) 912-918.

30. Evans, C.H., and Tew, W.P. "Isolation of Biological Materials by use of Erbium III — Induced Magnetic Susceptibilities", Science, 213 (1981) 653-654.

31. Anderson, D.P., Bowen, E.R., and Bowen, J.P. "Advances in Wear Particle Analysis", Report ONR-CR169-007-1F to the Office of Naval Research (1979).

32. Kerr, P.F. "Optical Mineralogy", McGraw-Hill, Third Edition (1959).

33. Phillips, W. "Mineral Optics", W.H. Freeman and Co. (1971).

34. Bloss, D.F. "An Introduction to the Methods of Optical Crystallography", Holt, Reinhart and Winston (1961).

35. Longhurst, R.S. "Geometrical and Physical Optics", Longmans, Green and Co., Ltd., 2nd Edition (1967).

36. Hecht, E., and Zajac, A. "Optics", Addison-Wesley Publishing Co. (1974).

This page left blank
intentionally.

INDEX

Abrasive Particles 1.2
Adhesive Wear 2.9
Agglomerates 2.1.1
Aluminum 1.6
Arizona Road Dust 1.2, 1.9.3
Asbestos 1.9.5
Babbitt Metal 1.6.3, 2.5
Black Oxides 1.7, 1.7.2
Break-In Wear 1.1
Calcium 2.1.1
Carbon 1.9.8, 2.1.1, 3.2.3
Cast Iron 2.1.2, 3.2.6
Cellulose 1.9.7
Chip Detectors 2.2.1, 2.2.3
Coal Dust 1.9.4
Contaminant Particles 1.2, 1.6.3, 1.9.1, 1.9.2, 1.9.3, 1.9.6, 2.1.5, 2.3.4, 2.6
Copper 1.6.2, 1.6.3, 2.1.6, 2.5
Corrosive Wear 1.8.1, 2.1.4, 3.2.2
Cutting Wear Particles 1.2, 2.1.5, 2.3.4
Cylinder Scoring 2.1.1, 2.4
Dark Metallo-Oxides 1.7.3, 2.1.1, 2.2.3
Diesel Engine 1.3, 2.1
Dilution 1.8.3, 2.7, 3.1.3
DR Ferrograph 2.2.1, 3.2.2
Fatigue Spall Particles 1.3, 1.4, 2.5, 2.3.1, 2.9, 3.2.2
Ferrogram Deposition Pattern 1.0
Fibers 1.9.5, 1.9.7
Filters 1.9.7, 2.1.5, 3.1.2
Fretting Wear 2.7
Friction Polymers 1.8.2, 1.8.3
Gas Turbines 2.2
Gears 1.4, 2.3, 2.9, 3.2.5
Grease 1.6.2, 1.9.2, 2.7, 3.2.8
Heat Treatment of Ferrograms 1.6.3, 1.7.3, 1.8.2, 1.8.3, 1.9.2, 2.1, 2.1.2, 2.1.3, 2.3.2, 2.4, 2.9, 3.2.6

Hydraulic Systems 2.6, 3.2.9
Jet Engines 2.2
Journal Bearings 1.6.3, 2.5
Laminar Particles 1.3, 3.2.2
Lead/Tin Alloy 1.6.3, 2.5
Microscope 3.2.1
Molybdenum Disulfide 1.8.3
Nonferrous Metal Particles 1.6
Numerical Aperture 1.3, 3.2.1
Organic Particles 3.2.2, 3.2.6, 3.2.8, 3.2.9
Overload 1.8.2, 2.3
Oxides 1.7, 3.2.1, 3.2.6
Particle Concentration 3.1.1, 3.2.4
Pitch Line 1.4
Polarized Light 3.2.10
Red Oxides 1.7, 1.9.3, 2.3.3, 2.9, 3.2.5
Rubbing Wear Particles 1.1, 3.2.2, 3.2.6
Rust 1.7.1
Sampling 3.1.1, 3.1.2, 3.2.5
Sand 1.1, 1.2
Scanning Electron Microscope 1.0, 3.2.7
Scuffing 1.4
Severe Wear Particles 1.5, 2.3.2, 2.9, 3.2.2
Severity of Wear 2.8, 3.2.4
Shear Mixed Layer 1.1
Silica 1.9.3, 1.9.4
Sliding Wear Particles 1.5, 2.3.2, 3.2.2
Solid Lubricant 1.8.3
Spalling 1.3
Spectrometry 2.2.3, 2.3.5, 3.1.1
Spherical Particles 1.3, 2.2.3
Splines 2.7
Stainless Steel 1.9.2, 3.2.6
Striations 1.4, 1.5, 2.3.2, 2.9
Temper Colors 1.4, 1.5, 1.6.2, 1.7.3, 2.1.3, 2.2.3, 3.2.6
Water in Oil 1.7.1, 2.3.3, 3.2.5
X-Ray Analysis 1.8.1, 3.2.7

DISTRIBUTION LIST

JOAP-TSC Director (1)
Building 780
Naval Air Station
Pensacola, FL 32508

Air Force Program Manager/Oil Analysis Program (1)
San Antonio Air Logistics Center/MMETP
Kelly AFB, TX 78241

Army Program Manager Oil Analysis Program (1)
Commander
US Army DARCOM Material Readiness Support Activity
Attn: DRXMD-MS
Lexington, KY 40511

Navy Program Manager/Oil Analysis Program (1)
Commanding Officer
Naval Air Rework Facility (440)
Naval Air Station
Pensacola, FL 32508

Commander (1)
Naval Air Development Center
Code 60612 Lubrication Section Head
Attn: L. Stallings
Warminster, PA 18974

Commander (1)
Naval Aviation Logistics Center
Naval Air Station
Patuxent River, MD 20670

Commanding Officer
Naval Air Propulsion Center (1)
Code PE72
Attn: A. D'Orazio
P.O. Box 7176
Trenton, NJ 08628

National Bureau of Standards (1)
Metallurgy Division
Attn: Dr. W. Ruff
Institute for Materials Research
Washington, DC 20234

DISTRIBUTION LIST (CONTINUED)

Office of Naval Research
Attn: Dr. R.S. Miller (432) (1)
Dr. K. Ellingsworth (430) (1)
800 North Quincy Street
Ballston Tower #1
Arlington, VA 22217

Commanding Officer
Naval Research Laboratory
Washington, DC 20375 (1)

Commander
David W. Taylor Naval Ship Research & Development Center
Bethesda, MD 20084 (1)

Commander
Air Force Wright Aeronautical Laboratories
Attn: Materials Laboratory MLBT (1)
POSL Branch Chief (1)
Wright-Patterson Air Force Base
Ohio 45433

Director
Applied Technology Laboratory
US Army Research and Technology Labs (AVRADCOM)
Attn DAVDL-ATL-ASR (Mr D P Lubrano)
Fort Eustis, VA 23604 (1)

US Army Mobility Equipment R&D Command
Energy and Water Research Laboratory
Attn M E. LePera
Fort Belvoir, VA 22060 (1)

Army Office of Research
Attn: Dr F Schmiedeshoff
Raleigh-Durham Research Triangle
North Carolina (1)

DISTRIBUTION LIST

NAVAIRENGCEN
1114 (2)
1115
9011
92A1C
92A3
92713

NAVAIRSYSCOM
AIR-00D4 (2)
AIR-340E (2)
AIR-411
AIR-417
AIR-552
AIR-55232D

DTIC (12)

DISTRIBUTION CONTINUED ON PAGES

193 and 194

REVISION LIST

REVISION	PAGES AFFECTED	DATE OF REVISION